Sun and Nesbitt (1978) confirmed the latter view in a study of komatiites from Archaean terranes the world over. These authors discounted crystal fractionation as a viable mechanism for the formation of STPK and high magnesium GBK types and suggested a significant melting (> 50%) of mantle peridotite at depths of > 400 km as being necessary for their formation. In order to explain the LIL(*) element depletion of certain STPK (relative to its suggested source), these authors suggested a process whereby a small degree of LIL-enriched melt must first be removed from the source region. This melt would subsequently enrich higher portions of the mantle in the LIL elements, subsequent melting of which was considered to result in the formation of the basaltic komatiite series.

That the LIL element depletion of peridotitic komatiites represents a problem in their petrogenesis is reflected in the fact that other theories for their origin have been put forward. Bickle et al. (1977) have suggested, on the basis of high-pressure melting experiments, that neither accumulation of olivine phenocrysts, fractional crystallization or partial melting could account for the chemical characteristics of STPK. As an alternative they suggested that near-complete melting of garnet lherzolite, together with the polybaric assimilation of harzburgitic or dunitic residues, would best account for the high CaO and MgO contents of the STPK. It was envisaged that the entrained residue would undergo melting as the result of adiabatic decompression during the initial upward movement of the magma. These ideas have been confirmed in a recent, detailed, study on the geochemistry of mafic and ultramafic lavas of the lower Onverwacht Group by Smith and Erlank (1978), who suggested that the mechanical mixing model of Bickle et al.(1977) best explained the composition of the Barberton rocks. Smith and Erlank (1978) also confirmed the importance of the process of crystal fractionation subsequent to extrusion and referred to it as an important mechanism in modifying the internal composition of flows in the Komatiite type area.

It is clear from this resumé, that the ultimate source of the komatiite series is related to processes whereby partial melting of mantle material (either peridotite, or garnet lherzolite) is accompanied by the entrainment of hig sidues that are responsible for the concomitantly high MgO contents of the STPK. Crystal fractionation appears to be important only locally and once extrusion of the lavas has taken place. A genetic link between komatiites and tholeiites is difficult to envisage in that the latter appear, at least in the Barberton succession, to be

---

(*) Footnote : LIL is used in this thesis as an abbreviation for large-ion lithophile

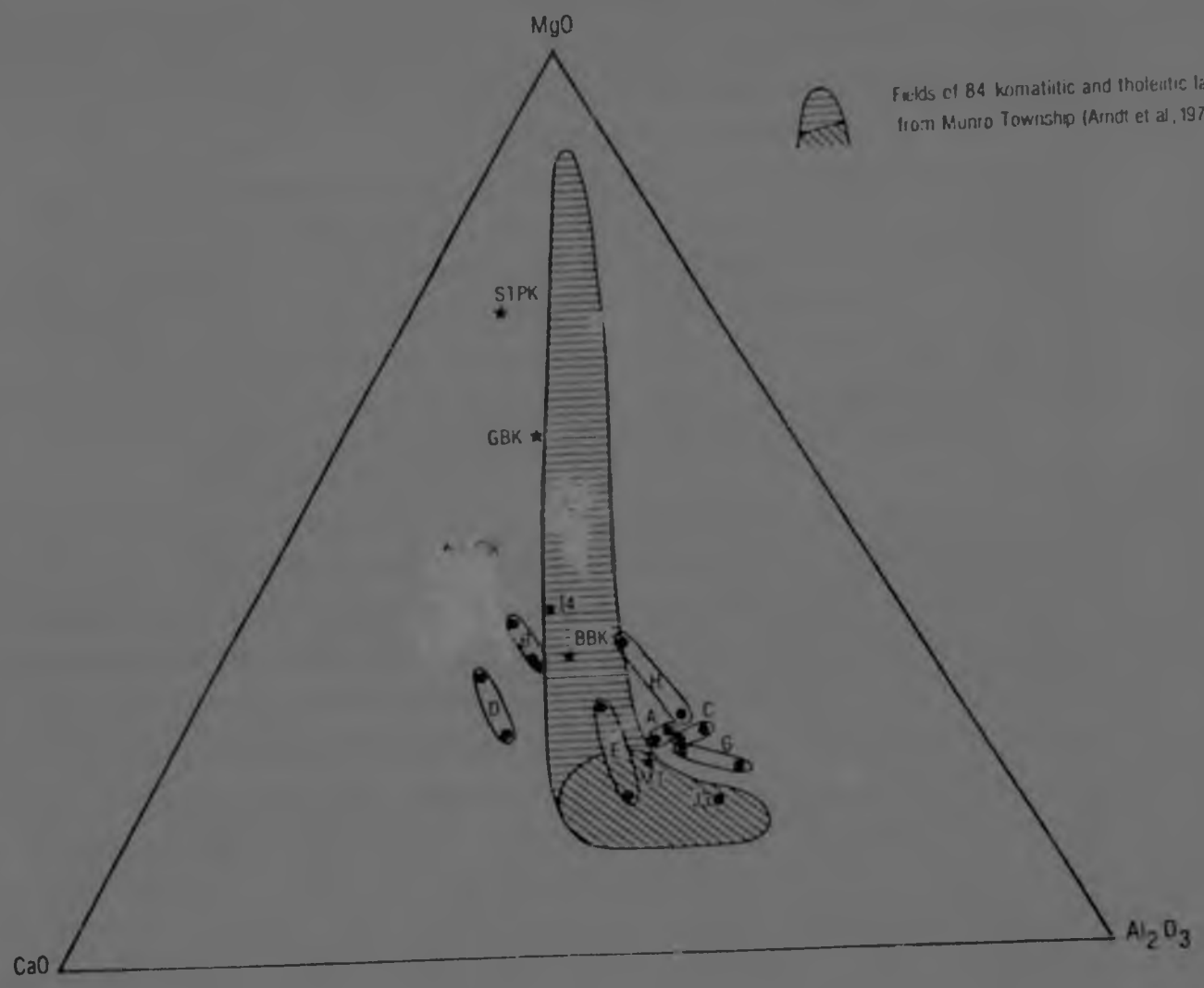

Figure 29 : Ternary $MgO-CaO-Al_2O_3$ plot of amphibolites from the migmatite outcrops described in Chapter 2. Individual samples for A, B, C, D, E, G, H, I and J outcrops are plotted from data in Tables 1-10. Average compositions of spinifex-textured peridotitic komatiites (S1PK), Geluk-type basaltic komatiites (GBK), Badplaas-type basaltic komatiites (BdBK), Barberton-type basaltic komatiites (BBK) and meta-tholeiites (MT) are taken from Viljoen and Viljoen (1969c). Fields of komatiites (horizontal hatch) and tholeiites (diagonal hatch) from the Abitibi greenstone belt (Munro Township locality) are after Arndt et al. (1977).

relatively late in the extrusive succession. It is possible, therefore, that the relationship between komatiites and tholeiites lies in processes of crystal fractionation rather than partial melting. In the Barberton context, the cumulus-enriched layered ultramafic sills that intrude the Onverwacht Group may have formed as the result of crystal fractionation from a peridotitic komatiite lava with the residue representing a differentiated liquid with a tholeiitic composition. This suggestion is considered again in a later section.

4.3. Chemical characteristics of amphibolites from the migmatite outcrops

The purpose of this section is to compare the chemistry of amphibolitic rocks from the various migmatite outcrops described in Chapter 2, with that of basaltic komatiites from the Barberton greenstone belt and also to assess the significance of differences in the composition of the amphibolites from one outcrop to another.

The composition of all the migmatite-related amphibolitic rocks are plotted on a ternary MgO - CaO - Al_2O_3 diagram in Figure 29. Two broad clusters are seen to emerge from this diagram; the first, consisting of B, D and I samples centres around the average composition of a Barberton-type basaltic komatiitic (BBK), whereas the second, with generally lower CaO and MgO contents, is more consistent with the average meta-tholeiite composition (MT) from the Barberton greenstone belt. The komatiitic group was described above as being generally more mafic than the remainder of the amphibolites and often contained clinopyroxene, a factor which contributes to their higher calcium contents. The tholeiitic amphibolites, which represent both greenstone xenoliths as well as dykes, are occasionally characterized by biotite as well as hornblende and have higher Al_2O_3 contents than the komatiites. Although the E samples generally have higher CaO values than the average meta-tholeiite (again due to the presence of minor clinopyroxene) and a sample from outcrop H is higher in MgO, it is suggested, on the basis of this diagram, that a clear distinction between basaltic komatiites (B, D and I) and meta-tholeiites (A, C, F, G, H and J) can be made in the amphibolitic rocks from the migmatite outcrops.

It is interesting to compare the fields of komatiitic and tholeiitic lavas from the Abitibi greenstone belt in Canada with average compositions from the Barberton area (Figure 29). With respect to the komatiitic field, it is seen that the average peridotitic and basaltic komatiites from Barberton are higher in CaO for any value of MgO, than their counterparts at Munro Township. As Arndt et al. (1977) have pointed out, this is the reason for the anomalously high CaO/Al_2O_3 ratios in the Barberton komatiites and they stress the fact that, in a general sense, $CaO/Al_2O_3 > 1$ is not a pre-requisite for the identification of a komatiite. However, in the Barberton area it is still valid to identify komatiites on the basis of a CaO/Al_2O_3 ratio > 1, even though Smith and Erlank (1978) have demonstrated that a rigorous definition, even in this area, does not apply. These authors have shown that CaO/Al_2O_3 varies between 0,85 - 2,5 in basaltic komatiites and between 0,66 - 0,85 in tholeiitic lavas and, hence, a marked distinction between the two rock types is still discernible.

It is noticeable in Figure 29 that the most mafic of the samples analysed from the migmatite outcrops (namely sample 14) has a composition with only approximately 14% MgO (Table 4). As the amphibolites plotted in this figure are considered reasonably representative of the migmatite outcrops from the study area, it is clear that a distinct lack of high-magnesian basaltic komatiites and peridotitic komatiites is preserved in the migmatitic terrane. This feature has been noted before (C.R. Anhaeusser, personal communication) and is somewhat difficult to reconcile in view of the fact that an abundance of these rocks occurs in the greenstone belt itself. One possible explanation for this paucity is that the high magnesium basalts, which probably represent greater proportions of partial melt of the mantle (and, hence, higher liquidus temperatures) are more out of equilibrium in a lower pressure and temperature environment than are the low magnesium basaltic komatiites and tholeiites and may not, therefore, have survived the effects of alteration to the same extent. It should be noted, however, that highly altered ultramafic remnants are not particularly evident in the migmatite terranes, and this apparent discrepancy remains, therefore, something of a problem. A final point that warrants mention is the fact that the tholeiite field from Munro Township is characterized by MgO contents that are slightly lower than the tholeiites analysed from the Barberton migmatites. The reasons for this are not at all clear, but may be related to fundamental differences between the basalts from the Abitibi greenstone belt and those of the Barberton area.

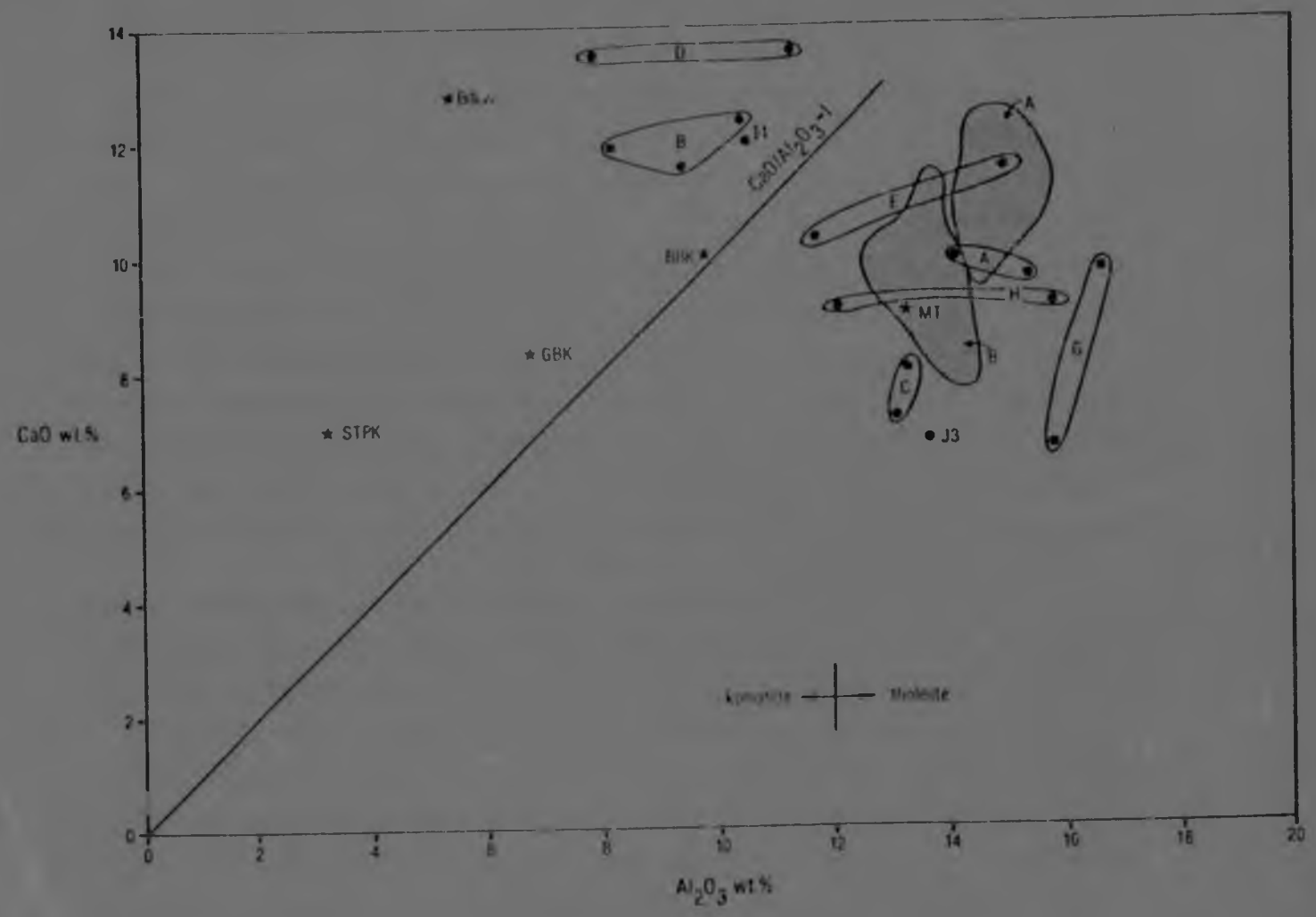

Figure 30 : Plot of CaO v Al_2O_3 for amphibolites from the migmatite outcrops described in Chapter 2. Symbols used are the same as those in Figure 29. Compositional fields A and B represent the Ameralik dykes from the Isua and Godthaabsfjord areas, West Greenland, respectively (after Gill and Bridgwater, 1979).

The high CaO/Al_2O_3 ratios of the Barberton komatiites is again emphasized in Figure 30 where both basaltic and peridotitic komatiites are seen to have a CaO/Al_2O_3 ratio > 1. The average meta-tholeiite composition, however, has a CaO/Al_2O_3 ratio of significantly less than unity. Smith and Erlank (1978) have pointed out that high CaO/Al_2O_3 ratios in the Barberton rocks are due, not so much to the CaO contents of the komatiites, but rather to their low Al_2O_3 contents. As a result, they choose to define komatiites, not on the basis of a CaO/Al_2O_3 ratio, but in terms of an Al_2O_3 content < 12%, a figure which coincides well with the cut-off between komatiites and tholeiites from the migmatite outcrops (Figure 30). These authors also suggest that tholeiites from the upper portions of the Onverwacht Group (i.e. Geluk Subgroup) have Al_2O_3 contents generally in excess of 13,5%, which also broadly coincides with the subdivision placed on the migmatite amphibolites.

It is pertinent, in Figure 30, to compare the compositional fields of Ameralik dykes from West Greenland with the amphibolitic dykes from the migmatite outcrops (i.e. G, H and possibly J). It is clear that the two suites have similar characteristics in terms of this diagram and this point is referred to again later. In Figure 31, it is interesting to note that the CaO/Al_2O_3 ratio of migmatite-related amphibolites is broadly proportional to the Mg number (i.e. 100.Mg/(Fe + Mg)) of these rocks. This suggests an inverse relationship between the alumina and magnesium contents of the amphibolites. It is again evident in this diagram that the amphibolitic dykes have compositions that are similar to the Ameralik swarm in West Greenland (Figure 31).

It is apparent from Figures 29 - 31 that the composition of the B, D and I magmatite-related samples are all very similar to that of the average Barberton-type basaltic komatiite from the greenstone belt itself. On the other hand, whereas certain of the tholeiites are seen to have a composition that is similar to the average Barberton meta-tholeiite, others have certain chemical traits that are not similar to the latter. This is particularly noticeable in cases where the tholeiitic dykes have undergone a significant degree of alteration and contamination (e.g. from outcrops G and H, see Tables 7 and 8). In Figure 32 these differences are emphasized when CaO/Al_2O_3 is plotted against K_2O and it becomes apparent that certain of the samples are enriched in K_2O by comparison with unaffected tholeiites.

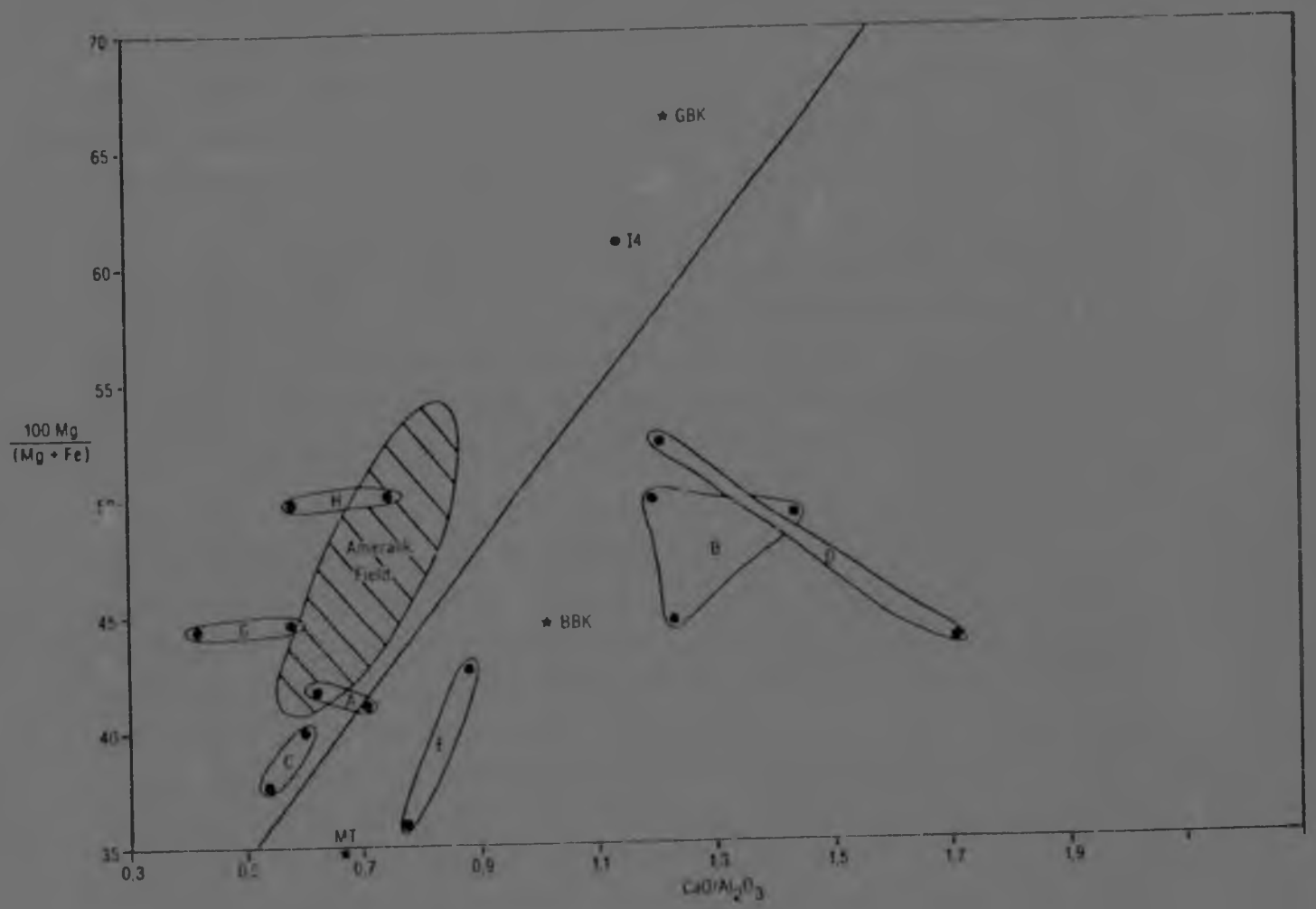

Figure 31 : Plot of Mg number against CaO/Al_2O_3 for amphibolites from the migmatite outcrops described in Chapter 2. Symbols used are the same as those in Figure 29. The Amerallik field is after Gill and Bridgwater (1979). The Mg number is calculated here as $100.Mg^{2+}/(Fe^{2+} + Mg^{2+})$ where $Fe_2O_3^*/0,75 = FeO$, and may, therefore be slightly different to the Mg number obtained in the case where actual analyses for FeO have been undertaken.

In the case of the dyke at outcrop C, which contains about 3,5% K_2O, the high potash content is related to the abundance of biotite which, as mentioned previously, appears to be a primary constituent of the rock. However, the dykes at outcrops G and H probably owe their relatively high potash contents to a combination of "residence" contamination (Fratta and Shaw, 1974) and the effect of migmatization of the dykes by anatectic melts formed during and after the emplacement of the former.

Residence contamination was first defined by Fratta and Shaw (1974) as a phenomenon resulting from the intrusion of a "hot" dyke into "cold" granitic rock. They envisaged that chemical constituents probably diffused along a thermal (and possibly chemical) gradient between the intruding dyke and enveloping granite, and noted that, along an individual dyke, contamination of LIL elements such as K, Rb and Li was greater in the dyke when it intruded granitic rock, than when it intruded basic volcanics of similar composition to the dyke itself. Gill and Bridgwater (1979) have pointed out that the extent of residence contamination probably depends on the nature (more specifically, the temperature) of the rocks being intruded. As such, it becomes a question of semantics whether the dyke is merely contaminated or whether it has been affected by mechanical interaction with rocks which may themselves have been partly mobile (or liquid). Gill and Bridgwater (1979) have shown that the Ameralik dykes of West Greenland exhibit a range between 1,5 - 5,5% K_2O where they intrude the quartzo-felspathic gneisses of the Isua region. By comparison, in the case where the same dykes intrude mafic supracrustals the range in potash content is only between 0,88 - 1,00%. This pronounced increase in K_2O (which is the only element, besides trace elements such as Ba and Rb, which exhibits these effects to any marked degree) is similar to the effects seen in the G and H tholeiitic dykes from the Barberton migmatite terrane (Figure 32). It is also interesting to note that the Amitsoq gneisses, into which the Ameralik dykes intrude, are very similar in composition to the trondhjemite gneisses intruded by the G and H dykes of the study area. In view of the fact that both the Ameralik dykes and the tholeiitic dykes from the migmatite terrane are both described as having been "migmatized" to a certain extent, it is suggested that contamination *(sensu stricto)* is not the correct way of referring to the chemical changes that have taken place. Rather, the term "assimilation", which implies the physical involvement or mixing of a liquid component with a pre-existing rock, is considered to more accurately

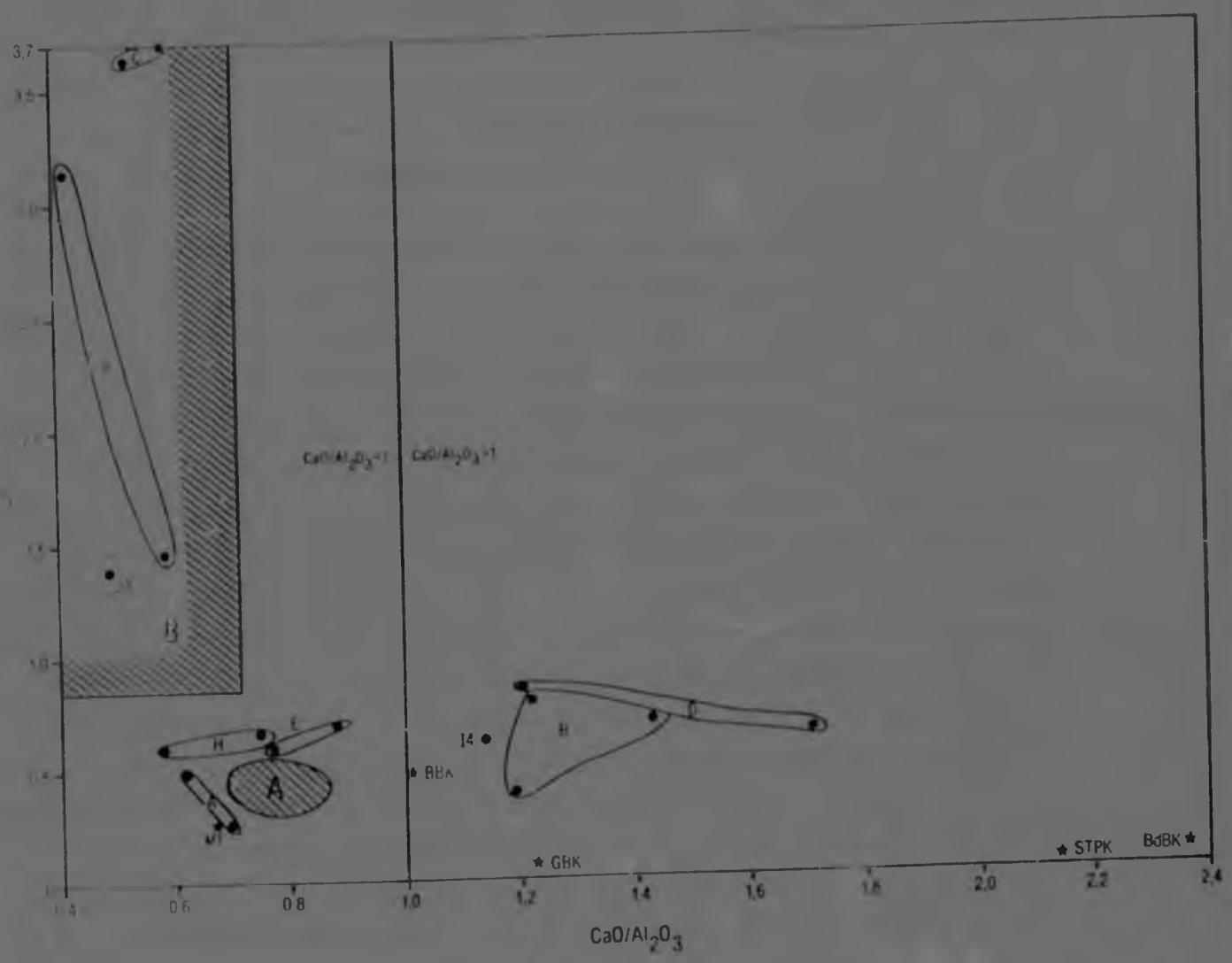

Figure 31 : Plot of K_2O against CaO/Al_2O_3 for amphibolites from the migmatite outcrops described in Chapter 2. Symbols used are the same as those in Figure 29. Also shown are the fields of well-preserved Ameralik dykes (A, hatched) and altered/ contaminated Ameralik dykes (B, hatched) from West Greenland (after Gill and Bridgwater, 1979).

reflect the processes being described in the present study. Both sets of dykes may well have been affected by anatectic components which, as previously mentioned, appear to have formed both during and after dyke emplacement.

The similarities in tectonic style and setting, characteristics of assimilation or contamination, and mineralogical aspects (i.e. the presence of biotite), as well as the gross compositional similarities between the Ameralik dykes and the amphibolitic dykes of the migmatite terrane being studied, suggests that they may be secular equivalents. The Ameralik dykes have been referred to as representing one of the earliest magmatic events in geologic history (i.e. they are older than 3,0 b.y.) to have been emplaced into an existing sialic crustal environment (Gill and Bridgwater, 1979). These particular dykes are not considered, however, to act as feeders to adjacent greenstone belts such as the Isua supracrustals and, likewise, in the Barberton region there is no evidence that the tholeiite dykes were feeders to any of the assemblages in the Onverwacht Group. These tholeiite dykes are, however, considered to possibly represent a phase of intrusive magmatism that was coeval with the extrusion of tholeiitic magmas that took place during the deposition of the dominantly tholeiitic Geluk Subgroup of the Upper Onverwacht volcanic sequence.

A final consideration in terms of the chemical characteristics of the migmatite-related amphibolites concerns their trace element contents. The Rb, Sr and Ba concentrations in the komatiitic amphibolites are generally low and this fact is considered again in later sections. Their abundances in the tholeiitic amphibolites, however, are much higher, but usually variable (Tables 1 - 10) indicating inconsistencies and mobility of these elements in the more altered rock types. The rare-earth elements, on the other hand, exhibit consistent patterns and these are illustrated in a chondrite normalized plot in Figure 33. In this figure, amphibolitic komatiites (Samples B14, D2 and I4) are characterized by relatively low ΣREE contents and flat patterns reflecting the primitive nature of these magmas. The tholeiitic greenstone remnants (i.e. samples A4 and E3) have slightly higher ΣREE contents, but, likewise, have flattish patterns with Ce_N/Yb_N ratios of approximately unity. The tholeiite dykes in Figure 33 (in particular sample G1), have Ce_N/Yb_N ratios that are, on average, slightly greater than one, as well as having slighly higher ΣREE contents. These features may reflect either, the more evolved nature of the original

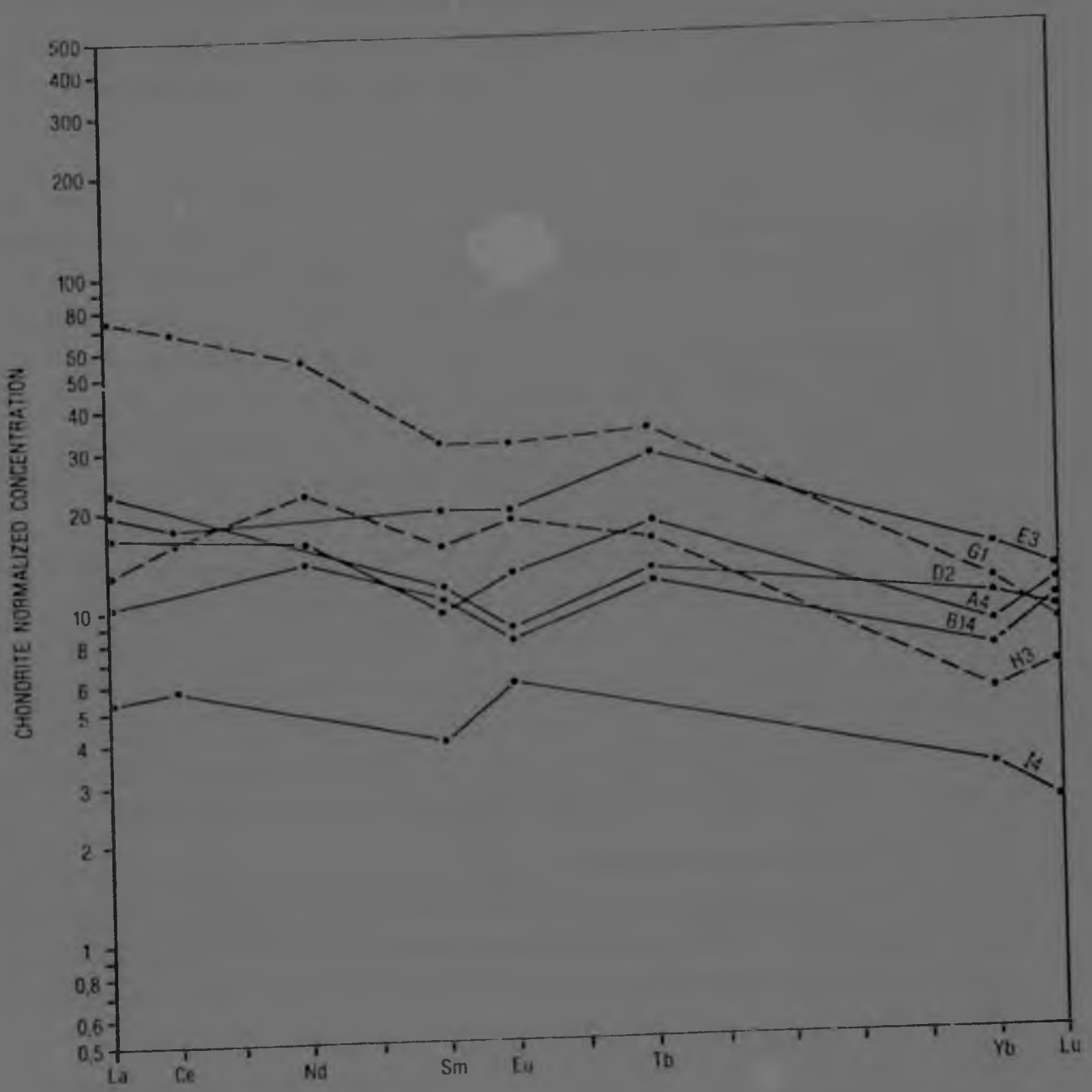

Figure 33 : Chondrite normalized rare-earth element plot for the amphibolites from the migmatite outcrops described in Chapter 2. The data for the individually plotted samples is presented in Tables 1-10. Solid lines represent amphibolitic greenstone xenoliths whereas dashed lines are amphibolite dykes.

magma or the altered and migmatized nature of the dykes in their present form. In the following section brief consideration is given to the petrogenesis of the amphibolitic tholeiites in the study area, which, unlike Archaean komatiites, have not, to date, received much attention in the published literature.

4.4. Petrogenesis of tholeiitic magmas in the migmatite study area

The origin of significant volumes of tholeiitic magma that characterize the upper formations of typical greenstone belt successions, such as, for example, the Yellowknife greenstone belt and the upper portions of the Onverwacht Group, is poorly understood. This aspect has been considered by Arth et al. (1977), who studied the tholeiites and closely-related komatiites of Munro Township in the Abitibi greenstone belt. They suggested that the LIL-enriched character of the tholeiites could be explained by considering them as the first formed melts that were tapped and emplaced prior to the more mafic komatiite lavas and which, therefore, represented small degrees of fusion of a probable garnet peridotite parent. It is difficult, however, to reconcile this suggestion with the appearance of tholeiites at the top of greenstone successions, the latter having presumably been derived after the more mafic, lower portions of the pile. An alternative suggestion, namely that of considering the tholeiites as differentiated liquids resulting from the fractionation of phases such as olivine, clinopyroxene and orthopyroxene, is considered below.

In the Barberton greenstone belt the lower Onverwacht Group in particular, is characterized by the presence of semi-contemporaneous differentiated sills which clearly represent cumulus-enriched assemblages of olivine (dunites) orthopyroxene plus olivine (harzburgites) and clinopyroxene (websterites). On the basis of major element-mineral control lines, it has been suggested that fractionation of these phases can lead to a differentiated liquid of tholeiitic composition (Anhaeusser, 1977). Consequently, in terms of trace elements, fractionation of olivine, followed by orthopyroxene and then clinopyroxene, from a peridotitic komatiite liquid, should also result in the enriched LIL element contents that generally characterize Archaean tholeiitic basalts.

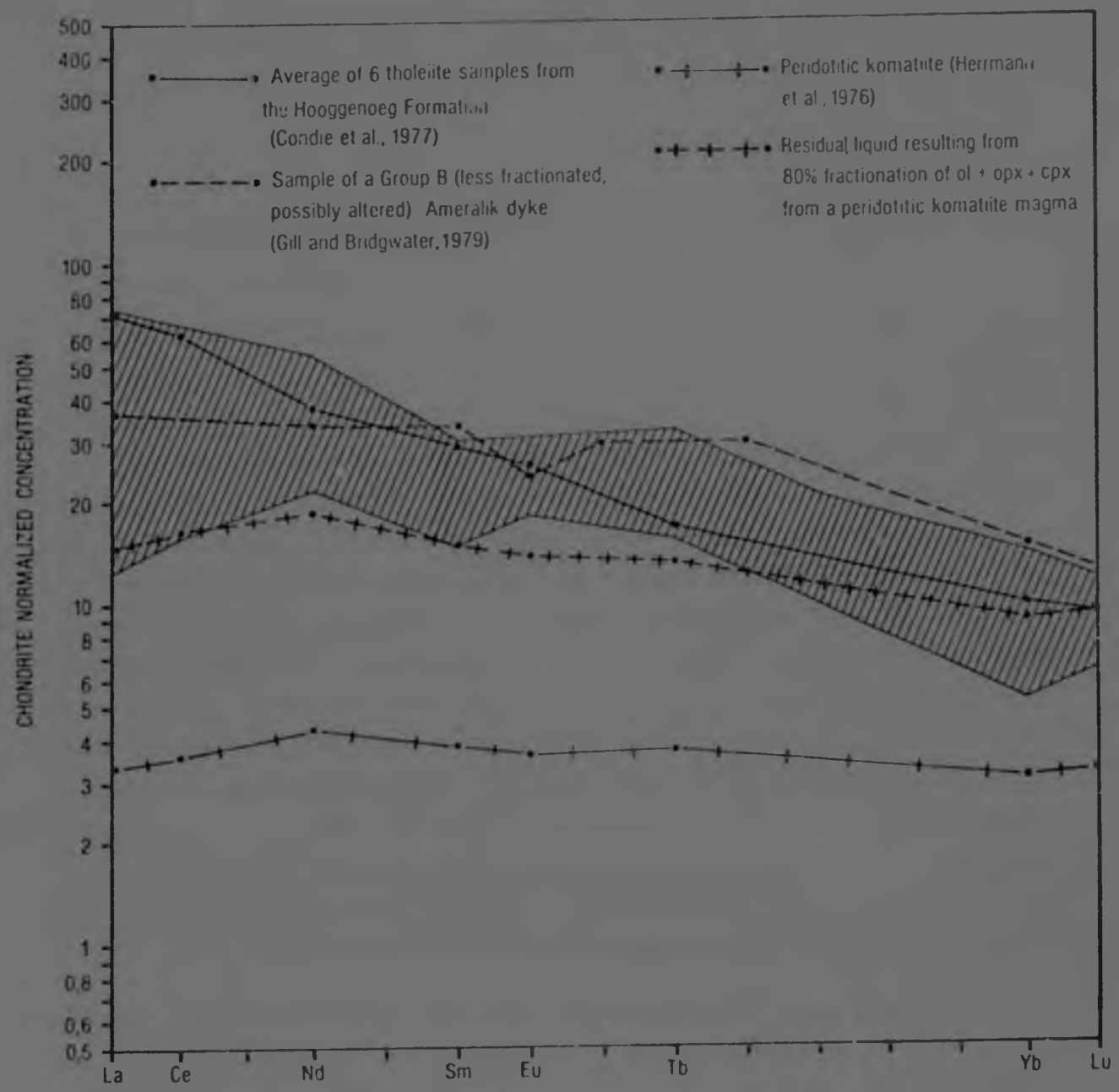

Figure 34 : Chondrite normalized rare-earth element model plot for the generation of tholeiitic magmas by differentiation of a peridotitic komatiite magma. The hatched field represents the envelope of tholeiitic xenoliths and dykes from the migmatite-related amphibolites plotted in Figure 33. The model curve represents a residual liquid resulting from 80% fractional crystallization of an olivine + orthopyroxene + clinopyroxene assemblage from a peridotitic komatiite magma.

This process can be tested for the REE as follows :-

The bulk partition coefficients for an assemblage consisting of equal proportions of olivine + clinopyroxene + orthopyroxene are as follows :-

	La	Ce	Nd	Sm	Eu	Tb	Yb	Lu
K_D	0,06	0,06	0,11	0,17	0,17	0,22	0,32	0,33

In Table 14, below, the composition of a residual liquid (Cℓ) after 80% crystal fractionation of the above assemblage, is compared with that of a parental magma (Co) having the composition of a peridotitic komatiite.

TABLE 14

RARE-EARTH ELEMENT MODEL CONSIDERATIONS FOR THE FORMATION OF A THOLEIITIC MAGMA BY FRACTIONATION OF A PERIDOTITIC KOMATIITE

	La	Ce	Nd	Sm	Eu	Tb	Yb	Lu
*Co (ppm)	0,8	2,3	2,1	0,6	0,21	0,14	0,49	0,08
+Cℓ (ppm)	3,6	10,4	8,8	2,3	0,80	0,49	1,46	0,23

* after Herrmann et al. (1976)

\+ Fractional crystallization equations used, see Appendix 2.

When plotted on a chondrite normalized diagram the composition of this residual liquid is very similar to the envelope of REE traces for tholeiitic xenoliths and dykes from the migmatite outcrops (Figure 34). It is feasible, therefore, that most, if not all, the tholeiitic magmas in the Barberton Mountain Land owe their origin to processes of crystal fractionation, direct evidence for which is observed in the cumulus-enriched intrusives in the area. These brief considerations, however, require a much more detailed assessment before this process can be emphatically attributed to the entire tholeiitic component of the Barberton greenstone belt.

In summary, the following general points can be made concerning the amphibolites related to the migmatites in the study area :-

(i) amphibolitic meta-basalts of komatiitic composition occur in the migmatites as remnants and xenoliths that can be correlated with similar lithologies in the Barberton greenstone

belt. The ultimate origin of these volcanic rocks is a study that is beyond the scope of the present thesis, but appears to be related to partial melting of mantle-derived material;

(ii) amphibolites of tholeiitic composition occur both as greenstone xenoliths and discrete dykes in the migmatites. Tholeiitic volcanics predominate in the upper successions of the Onverwacht Group although they also occur in the earlier-developed, predominantly komatiitic, sequences;

(iii) the tholeiitic dykes associated with the migmatite outcrops probably represent the intrusive equivalents of volcanics that were extruded in adjacent greenstone depositories. The dykes show no evidence for having fed the volcanics and, in this sense as well as in a number of other likenesses, closely resemble the pre-3,0 b.y. Ameralik dykes of West Greenland; and

(iv) the origin of tholeiitic magmas in the Barberton area may be related to the fractional crystallization of phases such as olivine, orthopyroxene and clinopyroxene from a peridotitic komatiite parent, leaving a differentiated liquid relatively enriched in the large-ion lithophile elements.

5. THE GENETIC RELATIONSHIP BETWEEN QUARTZ-DIORITE VEINS AND TONALITE-TRONDHJEMITE GNEISSES FROM THE MIGMATITES SOUTHWEST OF THE BARBERTON GREENSTONE BELT

Medium-fine grained quartz-diorite dykes and veins are found in a number of the migmatite outcrops examined in Chapter 2 (e.g. samples A2, B1, F1, F7, H5 and I6). These rocks are always intrusive into tonalite or trondhjemite gneisses and, like the anatectites, are invariably syn-tectonic with respect to the deformation that characterizes the development of the migmatites. In outcrop B, for example, the dykes are generally conformable with the foliation in the younger trondhjemite gneiss and are characterized by gentle, open folds (Figure 8), whereas in outcrop F, the dykes have been severely deformed by at least two fold episodes (Figure 14).

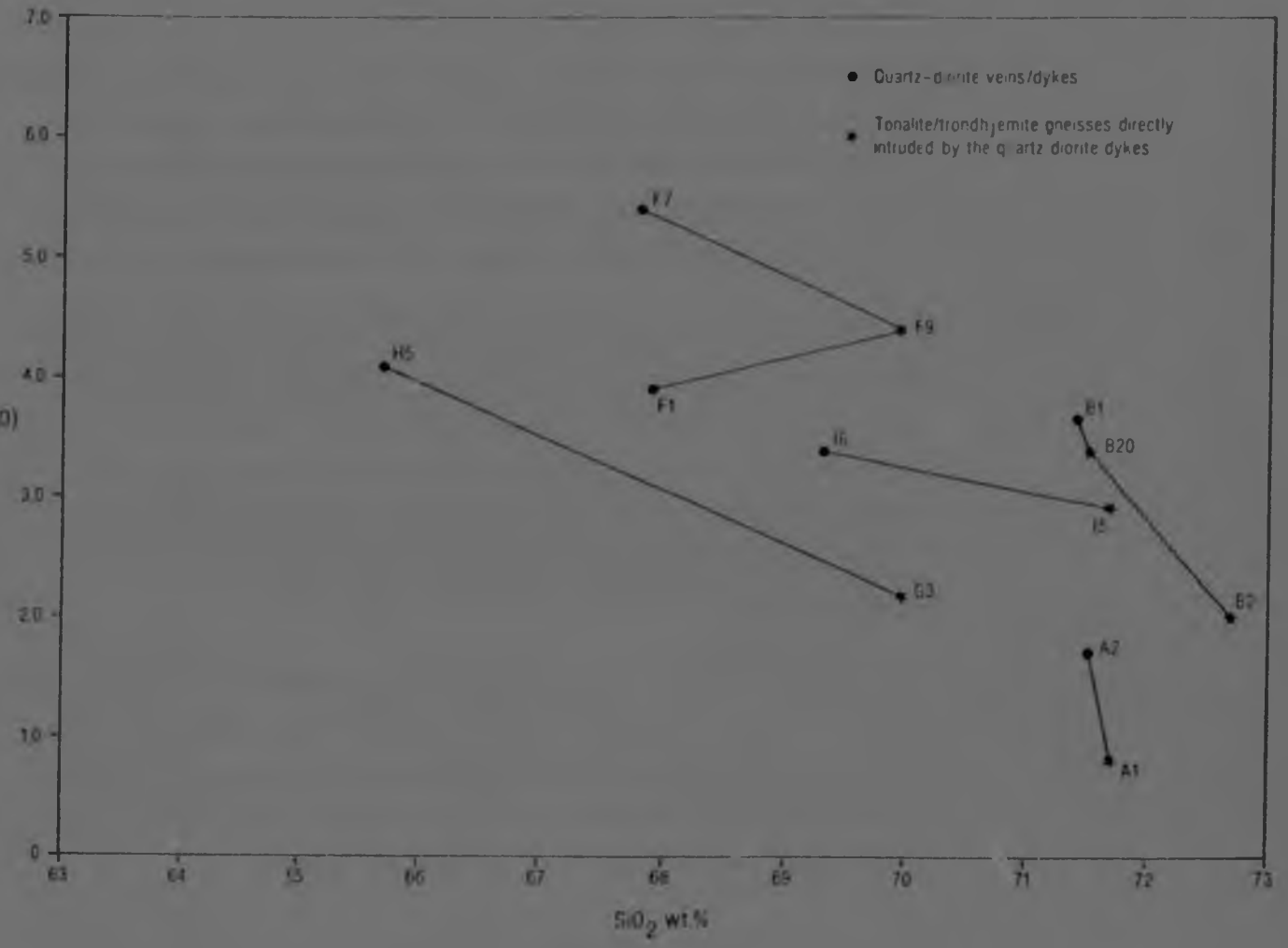

Figure 35 : Plot of $Fe_2O_3{}^* + MgO$ against SiO_2 for quartz-diorite veins and dykes and tonalite-trondhjemite gneisses from the migmatite outcrops described in Chapter 2. The data is derived from Tables 1-10. Tie-lines join quartz-diorite dykes with their host tonalitic or trondhjemitic gneisses (Note, $Fe_2O_3{}^*$ refers to the total iron content of the rock analysed as Fe_2O_3).

Although the quartz-diorite dykes have compositions that are broadly similar to their host tonalite and trondhjemite gneisses, they are invariably finer-grained and contain more abundant mafic minerals, in particular biotite. The chemical characteristics of the quartz-diorite are shown in a plot of SiO_2 v $Fe_2O_3^*$ + MgO (Figure 35) where tie-lines between coexisting quartz-diorite dykes and the tonalite/trondhjemite gneisses in their immediate vicinity, indicate that in almost all cases the dykes have a higher ferromagnesian content than the gneisses which they intrude. In terms of their trace elements, both rock types have similar Rb, Sr and Ba concentrations (Tables 1 - 10) and it is interesting to note, particularly with respect to Rb, that where concentrations in the tonalite-trondhjemite gneisses are low, so too are the quartz-diorite dykes characterized by similarly low values. This parity is emphasized in Table 15, below.

TABLE 15

RUBIDIUM CONTENTS IN SPATIALLY RELATED QUARTZ-DIORITE VEINS AND TONALITE-TRONDHJEMITE GNEISSES

SAMPLE	Rb (ppm) QUARTZ-DIORITE	SAMPLE	Rb (ppm) TONALITE-TRONDHJEMITE
A2	48	A1	61
B1	49	B2	52
		B20	60
F1	21	F9	18
F7	18		
H5	19	G3 (*)	15
I6	20	I5	14

(*) Trondhjemite gneiss sample closest to H5
Data taken from Tables 1 - 10, Chapter 2.

Factors such as these, together with the intimate relationship that exists between quartz-diorites and tonalite/trondhjemite gneisses, suggests that the two rock types may be cogenetically related and that the dykes were intruded into recently emplaced, and probably still hot, tonalites or trondhjemites. In this regard it is important to note that besides the similarity in the Rb contents between the dykes and the gneisses, both units

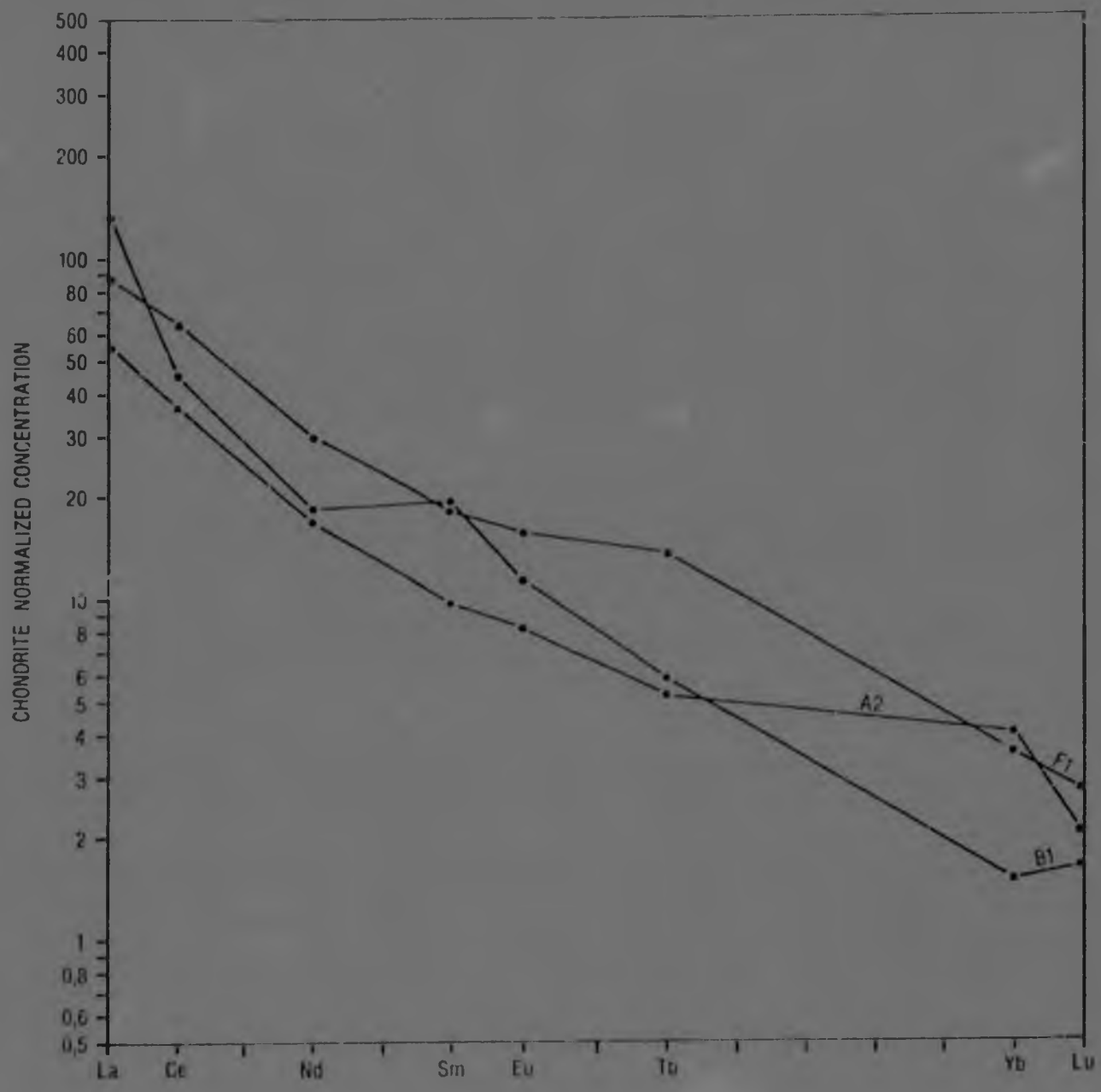

Figure 36 : Chondrite normalized rare-earth element plot of quartz-diorite dykes from the migmatite outcrops described in Chapter 2. Data is from Tables 1-10.

have comparable REE traces when plotted on a chondrite-normalized diagram (Figure 36). Besides the similarity in shape and lack of Eu anomaly, it is nevertheless clear that the quartz-diorites are slightly enriched in ΣREE content over the gneisses (Figure 37). This enrichment of the REE, together with the ferromagnesium-enriched character of the quartz-diorites suggests that the latter may have been derived by the crystal fractionation of a dominantly quartz + plagioclase + K-felspar assemblage from a tonalitic magma, leaving behind a residue of somewhat similar composition, but slightly enriched in mafic phases. If the degree of fractionation was high (i.e. ≈70%) and a small amount of biotite was included in the crystal extract, it is unlikely that Rb contents in the differentiated liquid would be significantly different from the parent, as observed above. In terms of the REE however, where biotite has little, or no, influence on the bulk partition coefficient, it will be expected that ΣREE contents in the residual liquid will be higher than those in the parent. This suggestion can best be tested by modelling the REE contents of the relevant phases :-

If the trondhjemite gneiss in Figure 37 (sample A1) is taken as representative of the composition of a typical parental magma, i.e.

	La	Ce	Nd	Sm	Eu	Tb	Yb	Lu	
ppm	9	17	5,7	0,9	0,28	0,12	0,3	0,02	(from Table 1)

then the bulk partition coefficients for a crystallizing assemblage consisting of 47% quartz, 40% plagioclase, 10% K-felspar and 2% biotite, are as follows :-

	La	Ce	Nd	Sm	Eu	Tb	Yb	Lu
K_D	0,13	0,15	0,11	0,07	1,11	0,03	0,04	0,03

If one considers the equilibrium crystallization of this assemblage from the above trondhjemitic parent (using the equation provided in Appendix 2), then the composition of a residual liquid ($C\ell$) after 70% crystallization of this assemblage is as follows :-

	$C\ell_{La}$	$C\ell_{Ce}$	$C\ell_{Nd}$	$C\ell_{Sm}$	$C\ell_{Eu}$	$C\ell_{Tb}$	$C\ell_{Yb}$	$C\ell_{Lu}$
ppm	23	42	15,1	2,6	0,26	0,37	0,91	0,06

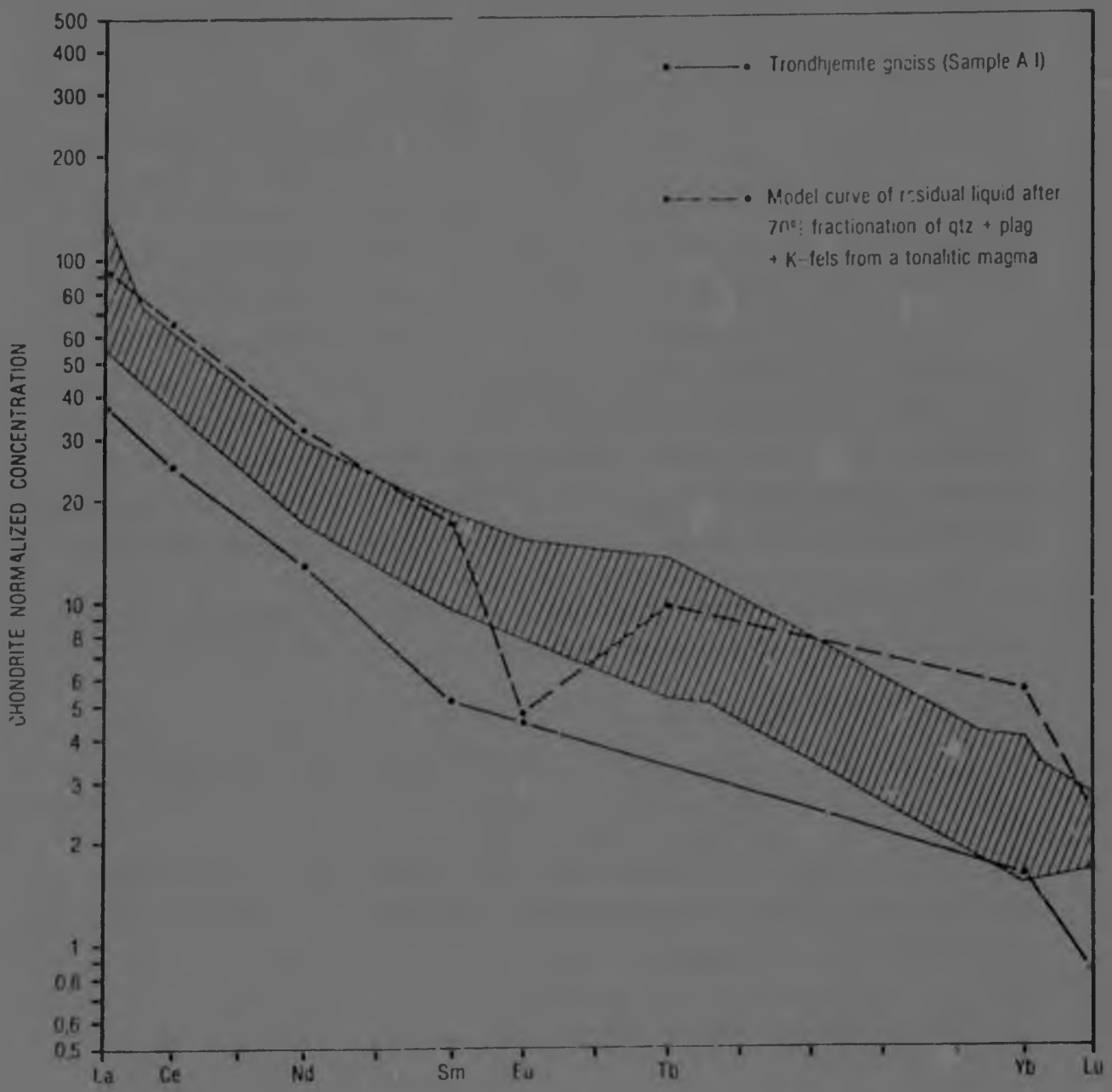

Figure 37 : Chondrite normalized rare-earth element model plot for the generation of quartz-diorite liquid from the fractionation of a tonalite. The envelope of quartz-diorite samples from Figure 36 (hatched) is compared with a typical trondhjemite gneiss from one of the migmatite outcrops (i.e. sample A1, Table 1).

When plotted on a chondrite normalized diagram (Figure 37) the composition of this residual liquid is not dissimilar to the envelope of samples representing the quartz-diorite dykes, with the exception of Eu, which has a slight negative anomaly in the model trend. This anomaly is not reflected in the empirical trends and may be due to an over-estimation in the model of the partition coefficient of Eu into both plagioclase and K-felspar.

In conclusion, it is suggested that the subtle, yet systematic, differences in chemistry of the quartz-diorite dykes and their host tonalite-trondhjemite gneisses indicates a probable cogenetic link between the two rock types. The observed differences can best be explained by the effects of crystal fractionation in the original tonalitic or trondhjemitic magmas and the generation of differentiated liquids slightly enriched in ferromagnesian and ΣREE content, and depleted in silica. This liquid, now represented by the quartz-diorite dykes, was probably intruded into the, still hot, fractionated tonalites and trondhjemites by processes such as filter pressing.

6. POSSIBLE ORIGINS OF THE PLAGIOGRANITES FROM THE MIGMATITES SOUTHWEST OF THE BARBERTON GREENSTONE BELT

6.1. Characteristics and major element chemistry

During the mapping of migmatites in the area southwest of the Barberton greenstone belt, two separate occurrences of highly siliceous felsic veins with "plagiogranitic" (Coleman and Peterman, 1975) compositions were encountered. Both samples (i.e. A9 and B10(A), Tables 1 and 2) are characterized by SiO_2 in excess of 77%, low Fe_2O_3* + MgO (<0,5%), low K_2O (~0,5%) and very low Rb (~20 ppm) contents. The plagiogranitic veins are found as deformed bodies occurring *within* amphibolite, either from the greenstone belt itself (in the case of A9), or from a greenstone remnant (in the case of B10(A)) related to a migmatite outcrop. These small veins often gave the impression of representing a mesostasis fraction, possibly genetically related to the amphibolites themselves.

When plotted on a diagram of K_2O v SiO_2 (after Coleman and Peterman, 1975), the plagiogranites fall very close to a field representing

When plotted on a chondrite normalized diagram (Figure 37) the composition of this residual liquid is not dissimilar to the envelope of samples representing the quartz-diorite dykes, with the exception of Eu, which has a slight negative anomaly in the model trend. This anomaly is not reflected in the empirical trends and may be due to an over-estimation in the model of the partition coefficient of Eu into both plagioclase and K-felspar.

In conclusion, it is suggested that the subtle, yet systematic, differences in chemistry of the quartz-diorite dykes and their host tonalite-trondhjemite gneisses indicates a probable cogenetic link between the two rock types. The observed differences can best be explained by the effects of crystal fractionation in the original tonalitic or trondhjemitic magmas and the generation of differentiated liquids slightly enriched in ferromagnesian and REE content, and depleted in silica. This liquid, now represented by the quartz-diorite dykes, was probably intruded into the, still hot, fractionated tonalites and trondhjemites by processes such as filter pressing.

6. POSSIBLE ORIGINS OF THE PLAGIOGRANITES FROM THE MIGMATITES SOUTHWEST OF THE BARBERTON GREENSTONE BELT

6.1. Characteristics and major element chemistry

During the mapping of migmatites in the area southwest of the Barberton greenstone belt, two separate occurrences of highly siliceous felsic veins with "plagiogranitic" (Coleman and Peterman, 1975) compositions were encountered. Both samples (i.e. A9 and B10(A), Tables 1 and 2) are characterized by SiO_2 in excess of 77%, low Fe_2O_3* + MgO (<0,5%), low K_2O (<0,5%) and very low Rb (<20 ppm) contents. The plagiogranitic veins are found as deformed bodies occurring *within* amphibolite, either from the greenstone belt itself (in the case of A9), or from a greenstone remnant (in the case of B10(A)) related to a migmatite outcrop. These small veins often gave the impression of representing a mesostasis fraction, possibly genetically related to the amphibolites themselves.

When plotted on a diagram of K_2O v SiO_2 (after Coleman and Peterman, 1975), the plagiogranites fall very close to a field representing

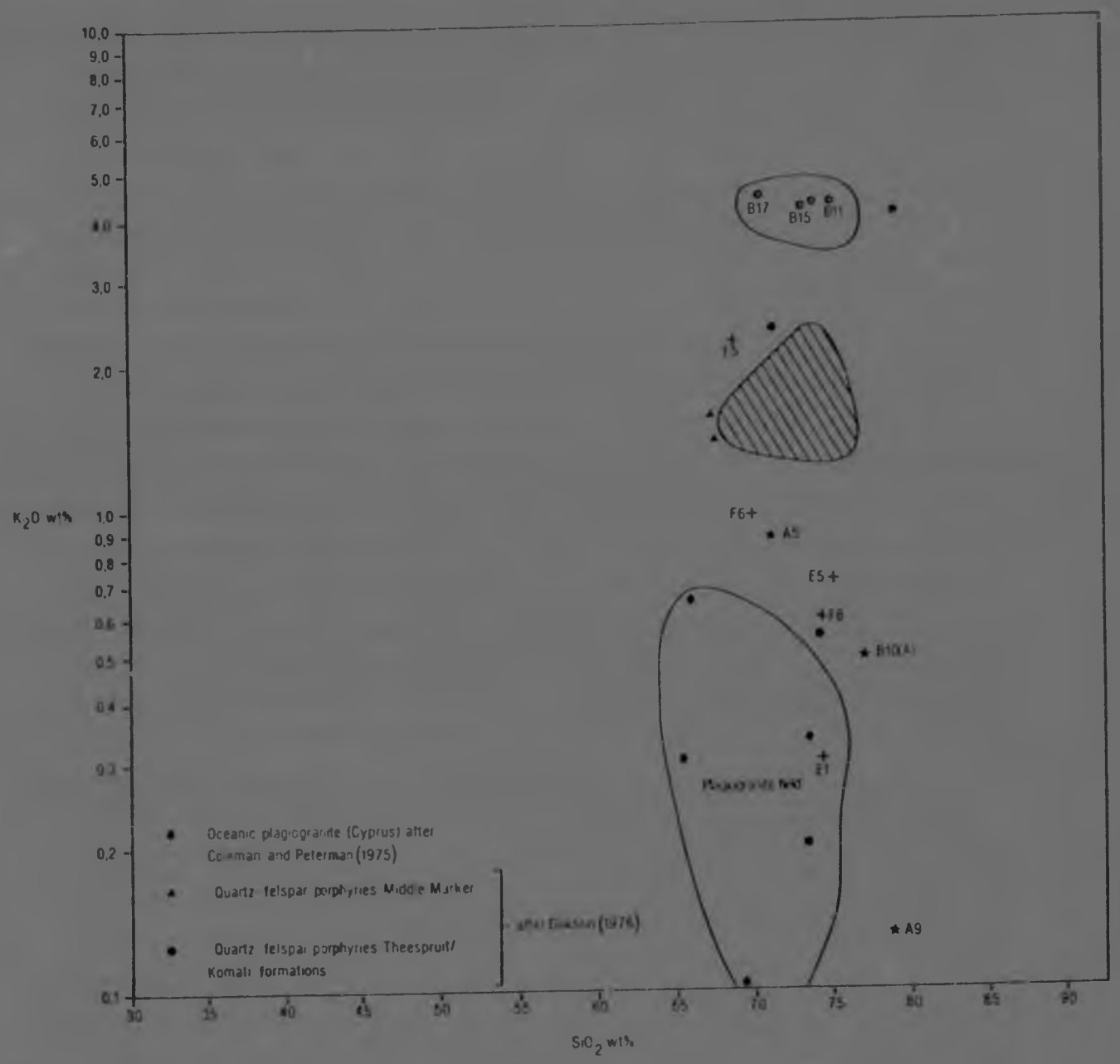

Figure 38 : Plot of SiO_2 against K_2O used by Coleman and Peterman (1975) to define the characteristics of plagiogranites. The field of ophiolite-related oceanic plagiogranites is shown in relation to the migmatite-related plagiogranites from the present study (i.e. A9 and B10(A) from Tables 1 and 2). Also plotted are quartz-felspar porphyries from the Onverwacht Group (after Glikson, 1976a) and a similar rock-type from the Bockenhoutrand outcrop (A5. Sample types E and F (Tables 3 and 6) are Or-depleted anatectites; cotectic anatectites are represented by the field encircling the B samples. The hatched field represents the compositions of migmatite-related tonalite and trondhjemite gneisses.

oceanic plagiogranites from the Troodos ophiolite complex in Cyprus (Figure 38). It is also interesting to note that certain acid porphyry bodies (more specifically, acid tuffs and porphyries from the Theespruit and Komati formations, Glikson, 1976a) also plot in the vicinity of the field of oceanic plagiogranites as defined by Coleman and Peterman (1975). The latter rocks are similar to the migmatite-related plagiogranites and have low K_2O and Rb and high SiO_2; they are, however, characterized by a higher ferromagnesian contents and occur at a variety of stratigraphic localities in the Barberton greenstone belt, with the bodies occurring above the Middle Marker unit invariably having higher amounts of potash and rubidium. A quartz-felspar porphyry dyke exposed in the Boekenhoutrand outcrop (sample A5) also plots close to the plagiogranitic field in Figure 38. Like the acid volcanics it, too, has a higher $Fe_2O_3^* + MgO$ content than the migmatite-related plagiogranites, but is also characterized by high silica and low potash and rubidium values.

The migmatite-related plagiogranites are very similar in both texture and appearance to the anatectites described previously; they are syn-tectonic and have been deformed during the development of the migmatites (see Figure 5). They are, however, chemically different in that they have significantly higher SiO_2 contents and noticeably lower $Fe_2O_3^* + MgO$. Although the major element composition of the plagiogranites may, in some instances resemble that of the Or-depleted anatectites described in section 3 of this chapter (see Figure 38), certain of their chemical attributes militate against their having also been derived by partial melting of a tonalitic-trondhjemitic precursor. As is shown below, the REE contents of the plagiogranites are significantly different from both Or-depleted and Or-rich anatectites and, in this light, they are considered as having a different origin to both the latter.

6.2. Petrogenesis of the migmatite-related plagiogranites

A consideration of the petrogenesis of the plagiogranites in terms of their major, trace and rare-earth element contents is provided below. Because of the similarities between the chemistry of the migmatite-related plagiogranites and certain acid porphyries, particularly those located in the lower portions of the Onverwacht Group, it is suggested that the latter may have a similar origin to that suggested for the plagiogranites below.

These acid porphyries have been studied by Glikson (1976a) who analysed 6 samples of quartz-felspar porphyry from the Theespruit and Komati formations, as well as from the vicinity of the Middle Marker unit. His analyses showed a wide range of both major and trace element compositions such that it was difficult to consider only a single mode of origin for these rock types. He concluded that some of them could be derived by low degrees of partial melt (~1%) of a metatholeiite, but pointed to the fact that such low melt factions are not geologically realistic. It was suggested, alternatively, that certain of the more fractionated acid porphyries and volcanics (with high Rb and ΣREE contents) could be produced by fractional crystallization of a tonalitic magma. Neither of these processes is relevant to the plagiogranites in the present study and the characteristics of the latter are considered in a different light below.

A petrologic mixing programme makes it possible to test the feasibility of suggested origins for the plagiogranites in terms of their major element composition. In terms of Glikson's (1976a) previous considerations and also their geological setting, two possibilities present themselves; the first is that the plagiogranites represent a residue resulting from the partial melting of a trondhjemitic precursor. This is not considered to be feasible, however, as such a residue will probably be enriched in mafic phases, a feature that is incompatible with the plagiogranitic compositions. A second possibility is that the plagiogranites represent a mesostasis resulting from the fractional crystallization of a mafic or ultramafic crystal assemblage from a komatiitic parent magma (alternatively, a very small degree of partial melt of the same parent would have the same effect, as, in fact suggested by Glikson, 1976a). This suggestion is considered to be feasible in terms of the discussion on the petrogenesis of komatiites where it was mentioned that, on a localized scale, fractional crystallization plays an important role in changing the composition of individual flows. Thus, the likelihood of generating small quantities of felsic mesostasis during the crystallization of the mafic and ultramafic volcanics is a realistic one.

Petrologic mixing considerations suggest that this process may be feasible if large quantities of olivine, orthopyroxene, clinopyroxene and magnetite are fractionated from an initial peridotitic komatiite liquid, such

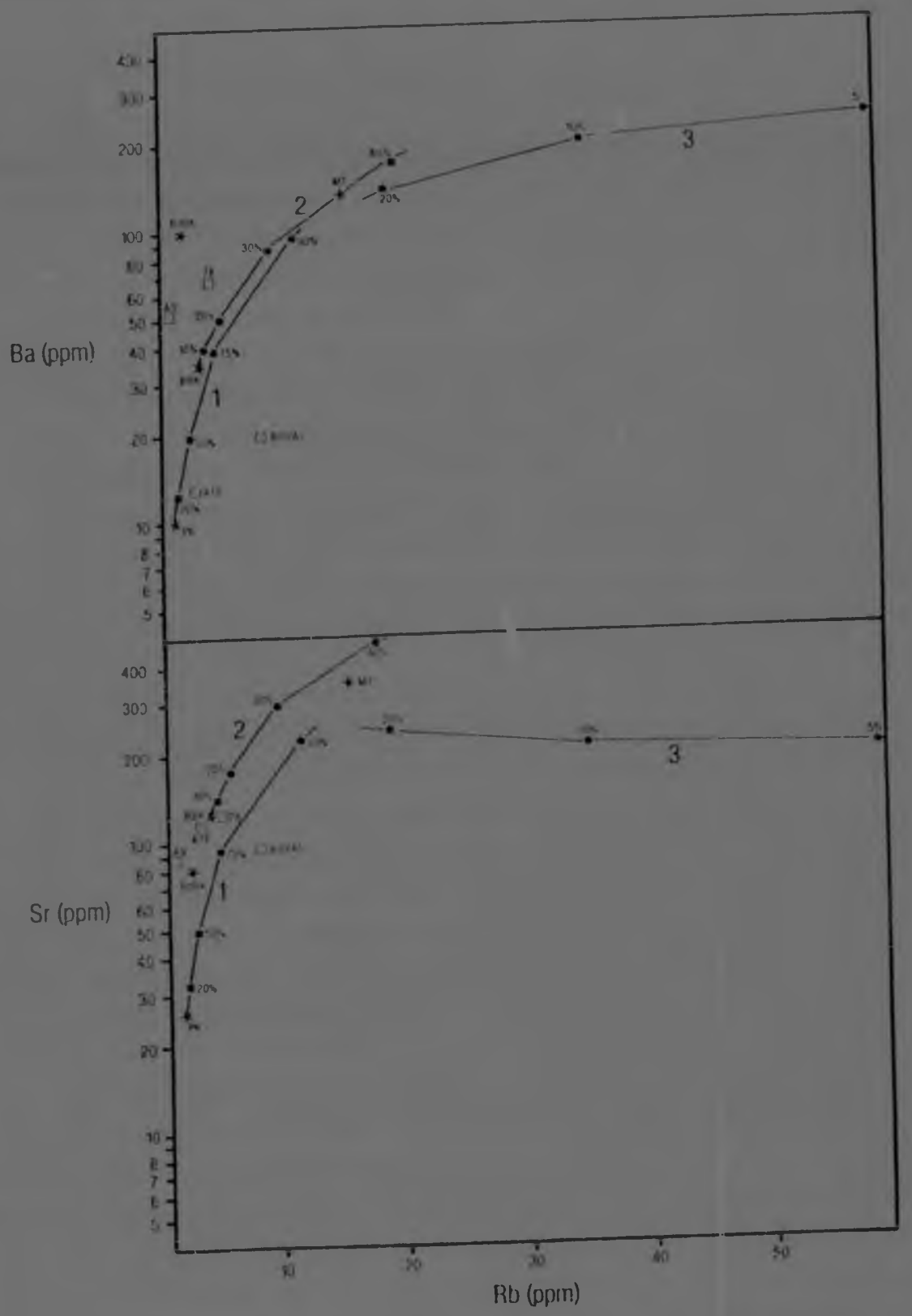

Figure 39 : *Rb v Sr and Rb v Ba model plots for the possible origin of plagiogranites; Curve 1 represents a differentiated liquid arising from the fractionation of a peridotitic komatiite (PK) and Curve 2 a differentiated liquid from the fractionation of a Barberton-type basaltic komatiite (BBK). Curve 3 represents small degrees of partial melt (5-20%) from an amphibolitic BBK. MT is a metatholeiite and BdBK is a Badplaas-type basaltic komatiite. A9 and B10(A) are migmatite-related plagiogranites (Tables 1 and 2), 7E is a quartz-felspar porphyry from the Theespruit Formation (after Glikson, 1976a) and ATP is an average Troodos plagiogranite (after Coleman and Peterman, 1975).*

that a small plagiogranitic residue remains. The least squares solution for the relative proportions of these phases are presented in Table 16 below.

TABLE 16

LEAST SQUARES PETROLOGIC MIXING SOLUTION(*) FOR THE DERIVATION OF A PLAGIOGRANITE BY FRACTIONAL CRYSTALLIZATION OF A PERIDOTITIC KOMATIITE

A.	peridotitic komatiite	-	parental magma	100%
B.	olivine	-	extracted phases	27,6%
	orthopyroxene			21,5%
	clinopyroxene			42,7%
	magnetite			0,0%
C.	plagiogranite	=	mesostasis (residue)	8,2%

Although the sum squares of errors on the above solution are relatively high (possibly due to the arbitrary mineral compositions selected for the problem) this table indicates that it is possible to derive a small quantity of highly felsic differentiated liquid by this process. The following sections try to confirm this suggestion in terms of the expected trace element content of such a mesostasis.

6.2.1. *Rubidium, strontium and barium considerations*

The trace element concentrations of plagiogranitic and quartz-felspar porphyry samples A5, A9 and B10(A) are compared with those of peridotitic and basaltic komatiites from the Barberton greenstone belt in Figure 39. In addition, the model trends for the fractionation of a

(*) Footnote : The considerations of petrologic mixing in this thesis are based on the least-squares mass balance calculations devised by Wright and Doherty (1970). These procedures are available in a standardized form in a computer programme which was made available to the writer by Dr. R.G. Cawthorn, Department of Geology, University of the Witwatersrand. In simple terms, this programme will indicate the statistically most suitable combination of crystalline phases that must be removed to form a particular liquid composition from another more primitive composition.

peridotitic komatiite magma and also, the partial melting of a basaltic komatiite are plotted. These comparisons are made bearing in mind the fact that it has been shown that alteration can be responsible for the re-mobilization of trace elements such as Rb, Sr and Ba (Condie et al., 1977) and caution should, therefore, be taken in the over-emphatic interpretation of the resulting genetic models.

Figure 39 shows the typical trace element compositions of peridotitic komatiite, Badplaas- and Barberton-type basaltic komatiite and basaltic tholeiite; all four points are characterized by low Rb (< 20 ppm) contents and Sr and Ba values that increase with decreasing MgO in the rock. In the following models, fractionation of equal proportions of olivine, clinopyroxene and orthopyroxene is considered, firstly from an average peridotitic komatiite liquid and secondly, from an average Barberton-type basaltic komatiite liquid. The bulk partition coefficients for the crystal extract are as follows :-

Rb - 0,01
Sr - 0,07
Ba - 0,02

The compositions of the respective parental magmas are taken as :-

Peridotitic komatiite

Rb - 1,2 ppm
Sr - 26 ppm
Ba - 10 ppm

Barberton-type basaltic komatiite

Rb - 4 ppm
Sr - 125 ppm
Ba - 35 ppm

(from data after Herrmann et al., 1976 and Glikson, 1979b)

If solidification of these magmas takes place by fractional crystallization (equations provided in Appendix 2) then the compositions of differentiated liquids ($C\ell$) remaining after a number of increments of fractionation can be calculated and are listed in Table 17 below :-

TABLE 17

TRACE ELEMENT CONTENTS OF LIQUIDS REMAINING AFTER FRACTIONAL CRYSTALLIZATION FROM PERIDOTITIC AND BASALTIC KOMATIITE MAGMAS

Parent	Increments of fractionation	$C\ell_{Rb}$	$C\ell_{Sr}$	$C\ell_{Ba}$
peridotitic komatiite	20%	1,5	32	12,4
	50%	2,4	49	19,7
	75%	4,7	94	39
	90%	11,7	221	95
basaltic komatiite	10%	4,4	138	59
	30%	5,7	174	50
	60%	9,9	293	86
	80%	20	558	169

When plotted on the Rb v Sr and Rb v Ba diagrams in Figure 39, the changing composition of the residual liquids form sub-parallel trends which increase only slightly in Rb, but more markedly in Sr and Ba as the liquid becomes more differentiated. It is seen that the samples of komatiites and tholeiites as well as the migmatite-related plagiogranites and the quartz-felspar porphyry (78) from the lower portions of the Onverwacht Group (after Glikson, 1976a) fall on, or near, the model trends of differentiated liquids.

By comparison, the model compositions of successive partial melts from a Barberton-type basaltic komatiite (i.e. BBK in Figure 39) are also plotted on the Rb v Sr and Rb v Ba diagrams. In this instance the model trends are derived using the following considerations :-

The bulk partition coefficients for a plagiogranite comprising 34% quartz, 65,5% plagioclase and 0,5% biotite are as follows :-

Rb - 0,05
Sr - 1,86
Ba - 0,27

The K_D's for a basaltic komatiite which consists of a mesonormative

assemblage comprising 9% quartz, 17% plagioclase, 54% hornblende and 20% clinopyroxene are as follows :-

Rb - 0,02
Sr - 0,70
Ba - 0,11

Considering the same parental basaltic komatiite composition as previously and using the batch melt equations provided in Appendix 2, the melt compositions ($C\ell$) of various melt increments are provided in Table 18 below.

TABLE 18

TRACE ELEMENT CONTENTS OF LIQUIDS DERIVED BY THE PARTIAL MELTING OF A BARBERTON-TYPE BASALTIC KOMATIITE

Parent	Increments of melt	$C\ell_{Rb}$	$C\ell_{Sr}$	$C\ell_{Ba}$
basaltic komatiite	5%	59	190	239
	10%	35	204	192
	20%	19	237	138
	30%	13	283	106

When plotted on Rb v Sr and Rb v Ba diagrams these melt compositions form a sub-horizontal trend (Figure 39, curve 3) at right-angles to the trends of crystal fractionation discussed above. It is also clear that a small degree of partial melt from a basaltic komatiite parent will *not* produce the trace element compositions of the migmatite-related plagiogranites. These diagrams suggest that it may also be feasible to derive certain of the quartz-felspar porphyries in the Barberton greenstone belt (more specifically, those related to the lower Onverwacht, such as sample 78 in Figure 39) in the same fashion as that considered for the plagiogranites.

The trace element models considered above suggest that the plagiogranites that intrude the amphibolites in certain of the migmatite outcrops described in Chapter 2 may be genetically related to komatiitic magmas from the basal portions of the Onverwacht Group. It is feasible that the plagiogranites, as well as certain acid porphyries in the area, which together represent a volumetrically insignificant constituent of the

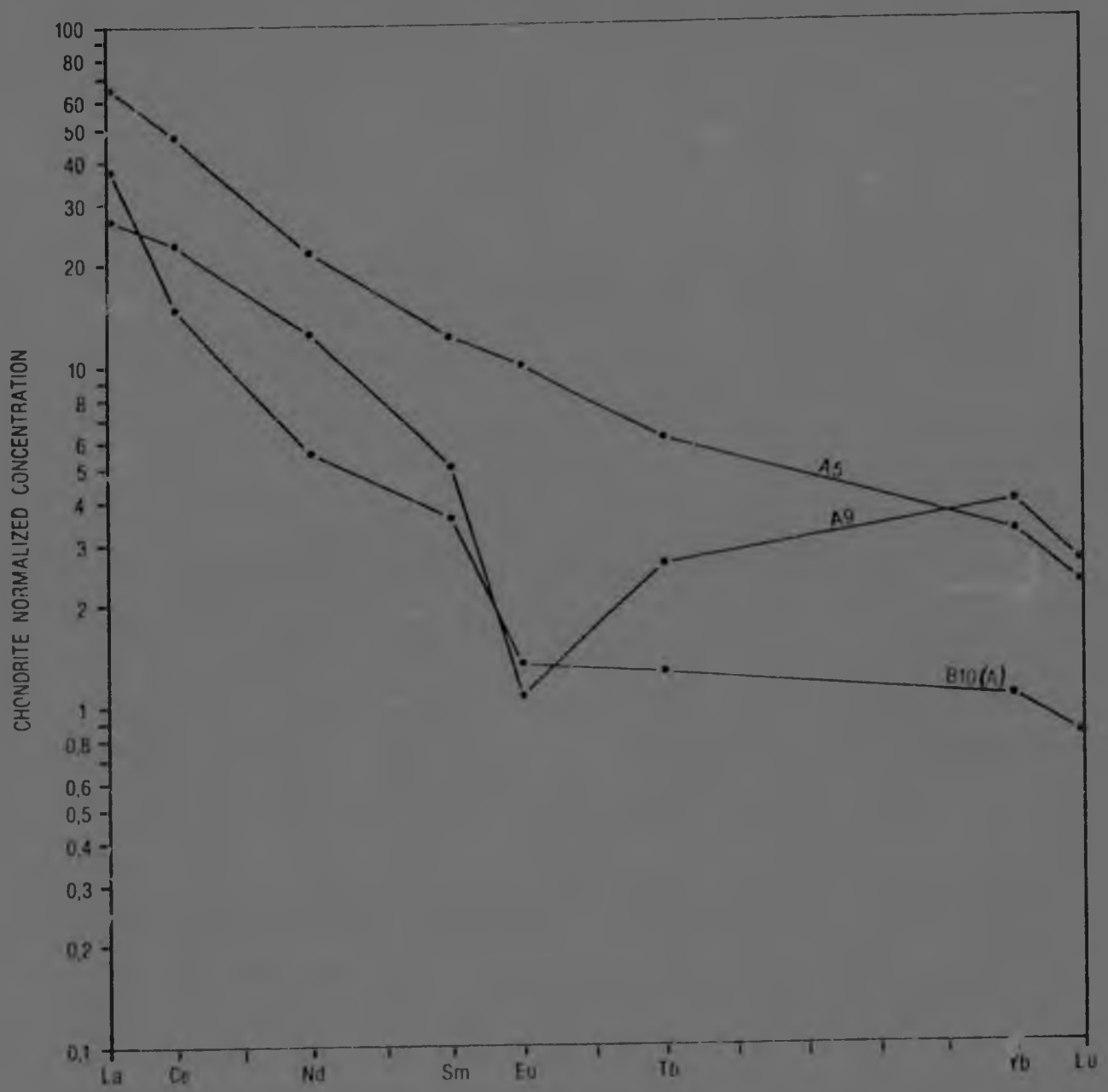

Figure 40 : Chondrite normalized rare-earth element plots of plagiogranites (A8, B10(A)) and a quartz-felspar porphyry dyke (A5) from the migmatite outcrops described in Chapter 2. Data is from Tables 1 and 2.

greenstone pile, represent a mesostasis remaining after significant fractionation (of olivine, orthopyroxene and clinopyroxene) of the mafic and ultramafic volcanics has taken place. The mesostasis may have been subsequently emplaced by a filter-pressing action related to the regional tectonism accompanying the intrusion of early tonalite/trondhjemite plutons in the area.

6.2.2. Rare-earth element contents of the plagiogranites

The migmatite-related plagiogranites are characterized by a distinctive REE trace when plotted on a chondrite normalized diagram (Figure 40). They have a high La_N/Eu_N ratio (≈25) but contrastingly low Eu_N/Lu_N ratio (≈1); this unusual L-shaped pattern reflects a slight enrichment in the LREE and uniform, relatively depleted HREE. The quartz-felspar porphyry (A5) from the Boekenhoutrand outcrop does not have this pattern and is characterized by a greater ΣREE content and a linear trend.

The REE content of the plagiogranites can be reasonably well modelled in terms of a high degree of fractionation of a peridotitic komatiite magma, in a similar fashion to the considerations for Rb, Sr and Ba above. The following parameters apply to the REE model :-

Parental composition of a peridotitic komatiite (after Herrmann et al., 1976) :-

	La	Ce	Nd	Sm	Eu	Tb	Yb	Lu
ppm	0,8	2,3	2,1	0,58	0,21	0,14	0,49	0,08

The bulk partition coefficients for the crystal extract are calculated for approximately equal proportions of olivine, clinopyroxene and orthopyroxene, as well as a small amount of plagioclase (~10%):-

	La	Ce	Nd	Sm	Eu	Tb	Yb	Lu
K_D	0,15	0,18	0,43	0,72	0,73	0,72	1,02	0,91

The small amount of plagioclase included in the REE model was considered necessary in order to obtain the low Eu contents characteristic of the plagiogranites (Figure 40). If one considers a high degree of fractional crystallization (i.e. 92%, as indicated in the petrologic mixing considerations)

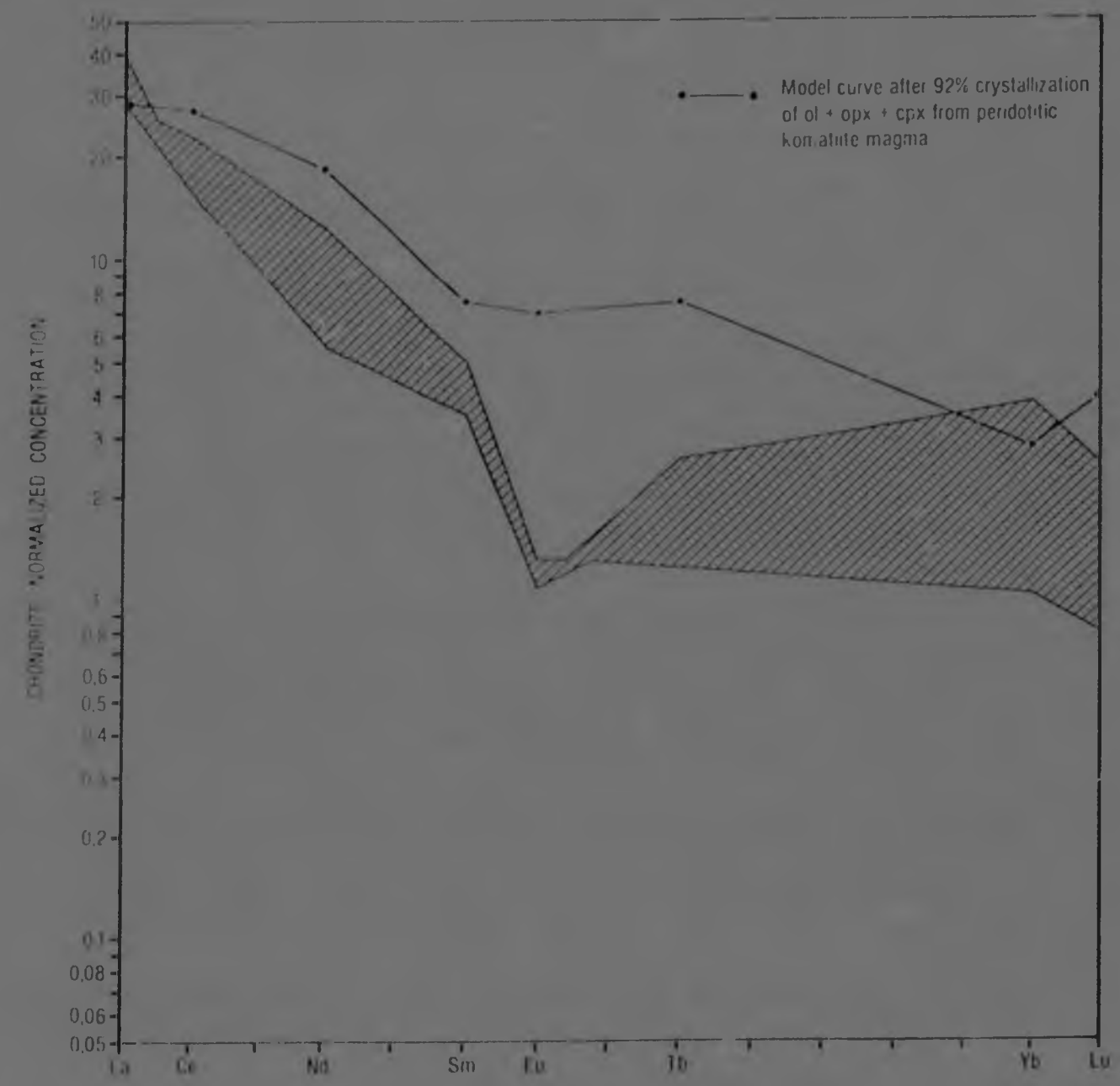

Figure 41 : Chondrite normalized rare-earth element model plot for the derivation of a plagiogranite by fractionaction of a peridotitic komatiite magma. The hatched area represents the envelope of the two plagiogranite samples plotted in Figure 40 (i.e. A9 and B10(A)).

then the REE content of the differentiated liquid ($C\ell$) or mesostasis is given below :-

	$C\ell_{La}$	$C\ell_{Ce}$	$C\ell_{Nd}$	$C\ell_{Sr}$	$C\ell_{Eu}$	$C\ell_{Tb}$	$C\ell_{Yb}$	$C\ell_{Lu}$
ppm	7,05	18,43	8,79	1,18	0,41	0.28	0,46	0,10

When plotted on a chrondite normalized diagram (Figure 41) the composition of this model mesostasis is not dissimilar to the envelope of migmatite-related plagiogranites and is characterized by a La_N/Eu_N ratio of 4,1 and a Eu_N/Lu_N ratio of 1,7. The La_N/Eu_N ratio is lower than that of the empirical trend because the model Eu content is too high, in spite of the fact that a small amount of plagioclase was included in the crystal extract. This indicates that during the latter stages of fractionation, plagioclase may have been more dominant than envisaged in calculating the K_D for Eu and, hence, the residual liquid might be more depleted in Eu than predicted in the model. The REE data, however, is not incompatible with the suggestion that the plagiogranites may represent a mesostasis resulting from the fractionation of ultramafic (or mafic) lavas. Irrespective of whether this model is correct or not, it is clear that the plagiogranites reflect a liquid composition that is strongly depleted in Eu. This characteristic is in marked contrast to the Or-depleted anatectites discussed in a previous section, which have significant positive Eu anomalies. Although both the plagiogranites and the Or-depleted anatectites have similar bulk compositions, they cannot have been derived in the same way, with the latter differing from the former in that they represent a plagioclase-enriched "cumulate" assemblage.

7. A COMPARISON BETWEEN THE PROCESSES OF PARTIAL MELTING AND SUB-SOLIDUS METAMORPHIC DIFFERENTIATION IN THE STUDY AREA, WITH PARTICULAR REFERENCE TO THE WEERGEVONDEN OUTCROP

7.1. Introduction

The migmatite outcrop at Weergevonden was described earlier (Chapter 2) as consisting essentially of a heterogeneous (migmatized) meta-tuffaceous unit that had been intruded by, and subsequently deformed together with, a tonalitic gneiss. It was suggested that variations in the texture and appearance of the meta-tuffaceous unit at this outcrop were

dependent on the nature of the deformation in that unit; as seen in section A of Figure 13, minor Z folds occur in a region where felsic veinlets, occurring within the meta-tuff, are easily recognizable as individual units (Plate 4A and B). In Section B of the same figure, where symmetrical, minor structures are indicative of a fold hinge, the felsic veins form a complex, anastomosing network (Plate 4 C and D) giving the rock the appearance of a complex banded gneiss.

The purpose of this section is to examine the processes of migmatization within the heterogeneous meta-tuffaceous unit, in the light of the following two textural observations :-

(i) that the felsic veins are rimmed by a mafic (biotite/ chlorite-rich) selvedge, and

(ii) that the felsic veins are preferentially concentrated in the low-pressure hinge zone of a fold.

As mentioned in the introduction to this chapter, the genesis of migmatites can usually be attributed to one (or more) of four possible mechanisms, namely, *in situ* anatexis, sub-solidus metamorphic differentiation, metasomatism and the introduction of an externally derived magma. In the case of migmatization processes at the Weergevonden outcrop, the latter two mechanisms are not applicable for reasons that are relatively obvious. Metasomatism is a process which involves the introduction into a rock of a pore fluid that has been derived from an external source with which it has previously equilibrated. As a result it is likely that chemical gradients between components of the fluid and that of the rock will exist and that reaction and changes in bulk composition will occur. Mineral reaction rims do *not* occur in the migmatized tuffaceous unit, nor do significant compositional changes appear to have taken place from one portion of the unit to another; it is unlikely, therefore, that metasomatism can have significantly contributed to migmatization in this instance. The introduction of an externally derived magma has a possible application in view of the fact that the meta-tuffaceous unit as a whole has been intruded by a tonalitic magma. However, the presence of a mafic selvedge bordering the felsic veinlets within this unit (Plate 4B) as well as the fact that the latter do not have a tonalitic composition (compare columns 4 and 5, Table 5) is sufficient evidence to discount this mechanism as having contributed to the migmatization *within* the heterogeneous meta-tuffaceous unit.

Migmatization of the meta-tuffaceous unit would appear, therefore, to be related to a process that operated *in situ* and involved either sub-solidus metamorphic differentiation or anatexis. Numerous studies have been undertaken in attempts to differentiate between these two mechanisms (e.g. von Platen, 1965; White, 1966; Misch, 1968; Hedge, 1972; Amit and Eyal, 1976; Ashworth, 1976 and Yardley, 1978) and the following points are considered to be important in distinguishing between them :-

(i) during metamorphic differentiation (where a melt phase is not present), no change in the bulk composition of the system is expected and solid solution minerals such as the plagioclases should have similar compositions throughout;

(ii) during anatexis, a system will retain its original composition only if the anatectic component remains strictly *in situ* and does not migrate even for short distances;

(iii) anatectites that are formed from small degrees of partial melting will invariably have bulk compositions that approximate minimum-melt or eutectic compositions in the granite system (i.e. Qtz-Ab-An-Or-H_2O) and will also tend to be enriched in incompatible elements;

(iv) anatectites will normally be enriched in the lower temperature phases of solid solution minerals (for example, preferentially enriched in the albite molecule with respect to plagioclase solid solution) except where subsequent re-equilibration has taken place.

The above points indicate that a detailed evaluation of the process of migmatization in the meta-tuffaceous unit requires that the original composition of the parent rock be known. In Chapter 2, it was suggested that the migmatized unit may originally have been a felsic tuff because some of the larger greenstone xenoliths in the region, as well as in the immediate vicinity of the outcrop, contain a significant felsic schist component that has a recognizably tuffaceous or agglomeratic origin (Anhaeusser, 1980). In addition, it is apparent when comparing the bulk compositions of the migmatized meta-tuff at the Weergevonden outcrop with those of the felsic schists from nearby greenstone remnants (Table 19), that the two suites have very similar chemical characteristics. The most

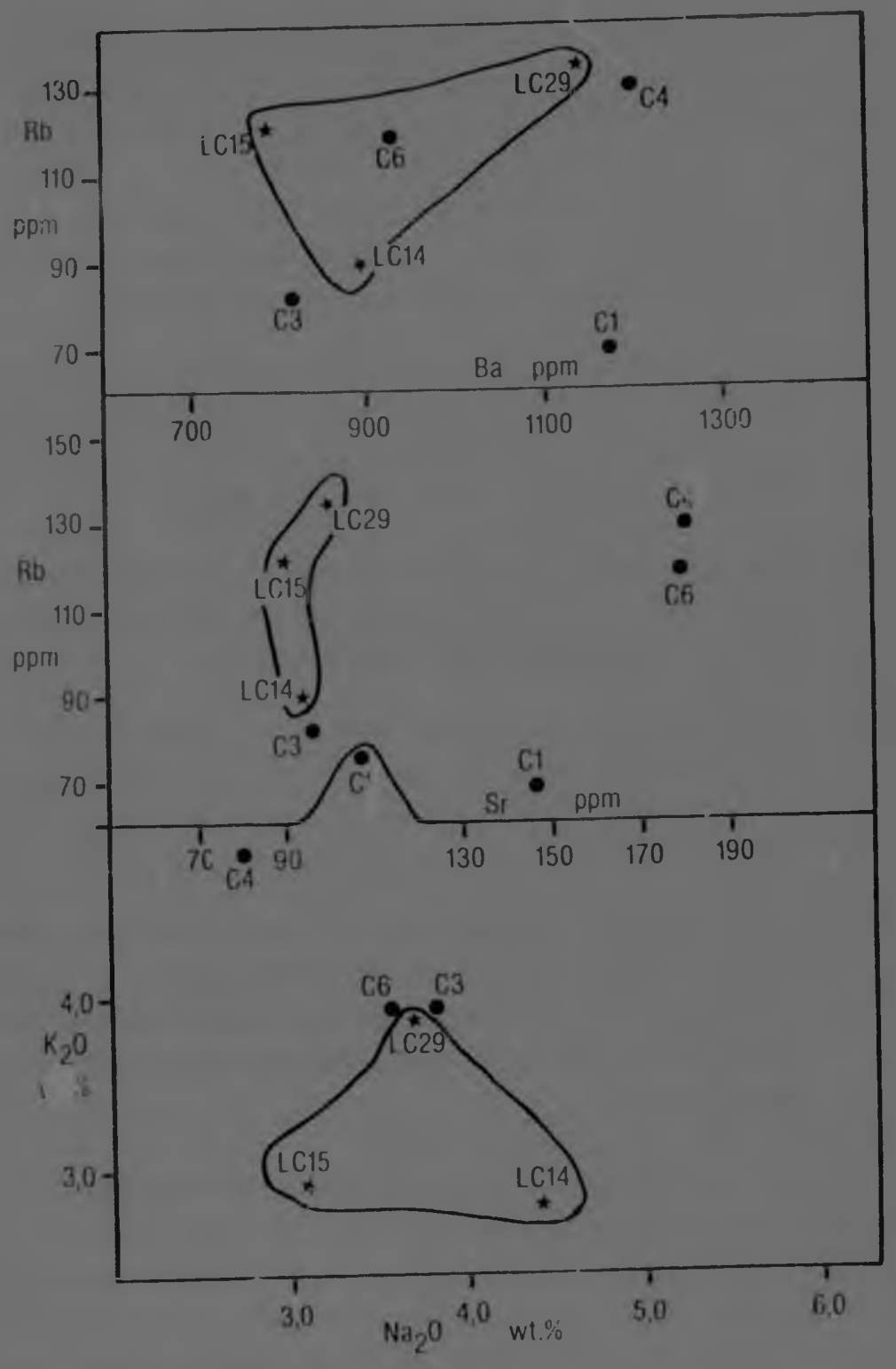

Figure 42 : Plots of Rb v Ba, Rb v Sr and K_2O v Na_2O for components of the migmatite outcrop at Weergevonden as well as felsic schists possibly representing the precursors to the migmatites. Data is from Tables 5 and 19.

TABLE 19

COMPARISONS BETWEEN FELSIC SCHISTS FROM THE WEERGEVONDEN SCHIST BELT AND THE FELSIC META-TUFFACEOUS UNIT FROM MIGMATITE OUTCROP C

		1	2	3	4	5	6
		C1	C3	C4	LC14	LC15	LC29
Wt.%	SiO_2	72,65	74,29	71,39	76,08	73,14	75,68
	TiO_2	0,21	0,20	0,26	0,20	0,25	0,15
	Al_2O_3	13,45	12,66	14,91	12,80	12,95	12,79
	Fe_2O_3*	2,18	2,18	2,99	1,47	2,40	1,54
	MnO	0,03	0,01	0,08	0,03	0,06	0,04
	MgO	1,01	0,78	0,87	0,62	0,97	0,62
	CaO	0,68	0,87	1,04	0,78	2,46	0,54
	Na_2O	3,37	3,77	2,73	4,38	3,08	3,72
	K_2O	5,36	3,86	4,77	2,79	2,87	3,93
	P_2O_5	0,08	0,06	0,07	0,03	0,05	0,03
	L.O.I.	0,47	0,49	1,12	0,81	1,71	0,99
	TOTALS	99,49	99,17	100,23	99,99	99,94	100,03
ppm	Rb	69	83	128	89	121	135
	Sr	148	95	180	93	90	101
	Ba	1170	817	1193	896	789	1138

(Fe_2O_3* - Total iron as Fe_2O_3)

Columns 1 - 3 - Samples of the felsic meta-tuff from the Weergevonden outcrop (descriptions in section 7., Chapter 2).

4 - 6 - Felsic schists (metamorphosed tuffs and agglomerates) from the Weergevonden schist belt (analyses from Anhaeusser, 1980).

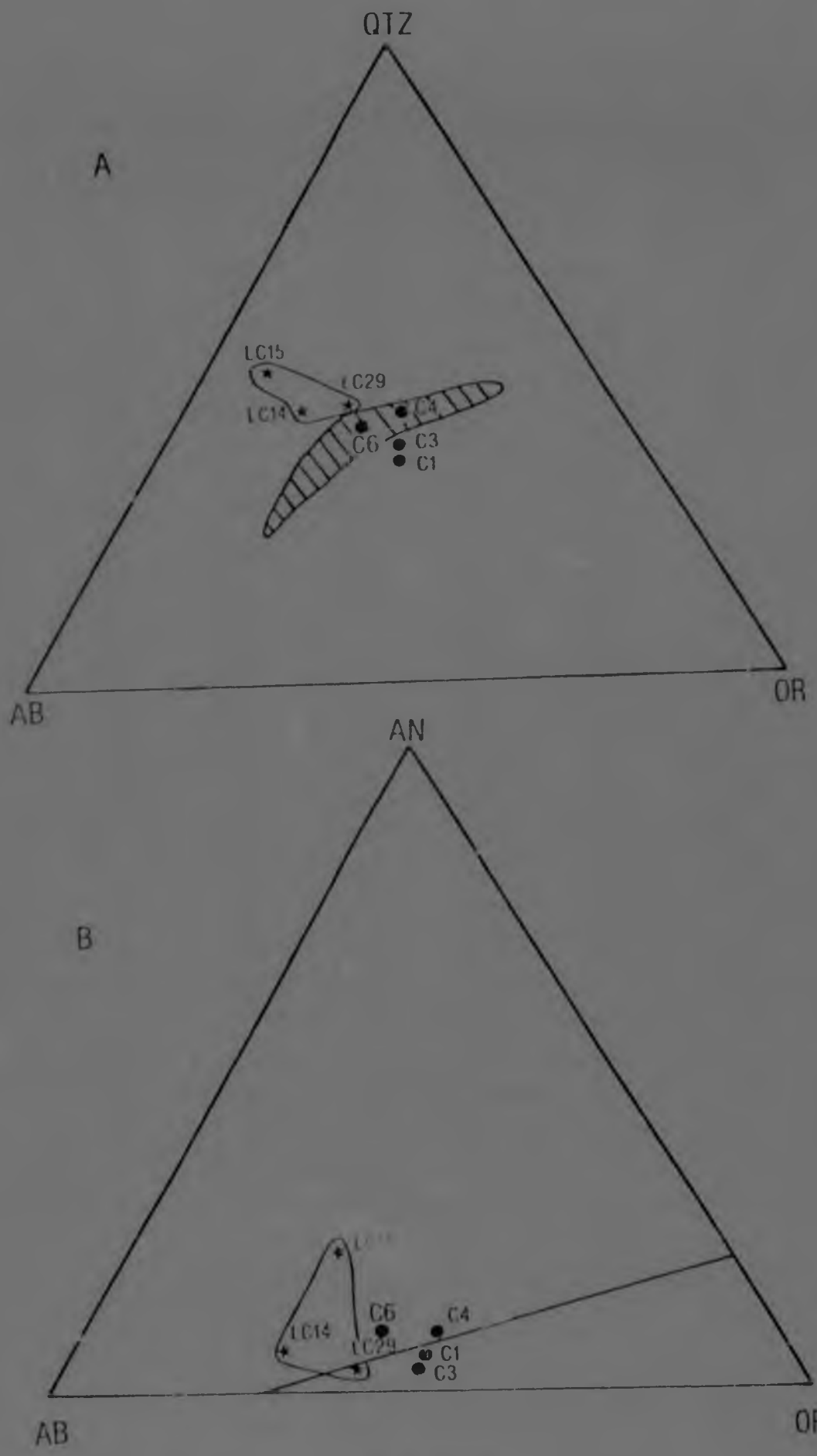

Figure 43 : *Ternary Qtz-Ab-Or (A) and An-Ab-Or (B) plots of the components from Figure 42. The hatched field in (A) represents projected eutectic and minimum-melt compositions for a variety of $^{1}H_2O$ and Ab/An ratios (see Figure 22); the K-felspar-plagioclase tie-line in (B) is taken from Figure 23.*

severely migmatized sample (C4) has a slightly higher alumina and potash content than the suggested precursors, but in general the migmatized rocks appear to have remained isochemical. Thus, a reasonable estimation of the original composition of the migmatized unit at the Weergevonden outcrop is available. It is also of interest to compare the REE contents of the non-migmatized meta-tuff with those of pristine dacitic volcanics. In Figure 45 a dacite from the Yellowknife greenstone belt in Canada compares favourably with the Weergevonden material suggesting again that migmatization at this outcrop has been an isochemical, relatively isochemical, process.

7.2. Migmatitic whole-rock compositions

The whole-rock compositions of components of the migmatized meta-tuff are compared with probable parental compositions (i.e. felsic schists from the Weergevonden schist belt) in Table 19 and Figures 42 and 43. Samples C1 and C3 represent the non migmatitic meta-tuffaceous unit from the Weergevonden outcrop, whereas the samples with an LC prefix are the felsic tuffs and agglomerates from the Weergevonden schist belt. Sample C4 is an intensely migmatized (leucosome-enriched) meta-tuffaceous unit from the fold hinge zone (Figure 13 B) at the Weergevonden outcrop and C6 is a sample of a discrete felsic veinlet, the locality of which is shown in Figure 13A. In Figure 42, samples C4 and C6 have higher K_2O values than the suggested parental material, whereas the non-migmatized meta-tuffaceous samples have variable potash contents with C1 appearing anomalously high. The Rb contents of C4 and C6 are systematically higher than those of the non-migmatitic meta-tuff, but are not significantly enriched with respect to the three samples of felsic schist, which represent a range of possible parental compositions. Although the pattern is not systematically diagnostic, the migmatitic leucosomes (or portions of the meta-tuff enriched in leucosomes) appear to be slightly enriched in those elements (i.e. K, Rb) which tend to be enriched in anatectic/partial melt fractions. This view is reinforced when comparing the REE contents of C4 and C1 (Figure 44) where it is apparent that the leucosome-enriched sample (i.e. C4) is slightly enriched in both LREE and HREE content compared to the sample which contains no quartzo-felspathic veins or segregations. In view of the points mentioned previously, this suggests that migmatization may have been derived by partial melting rather than sub-solidus processes.

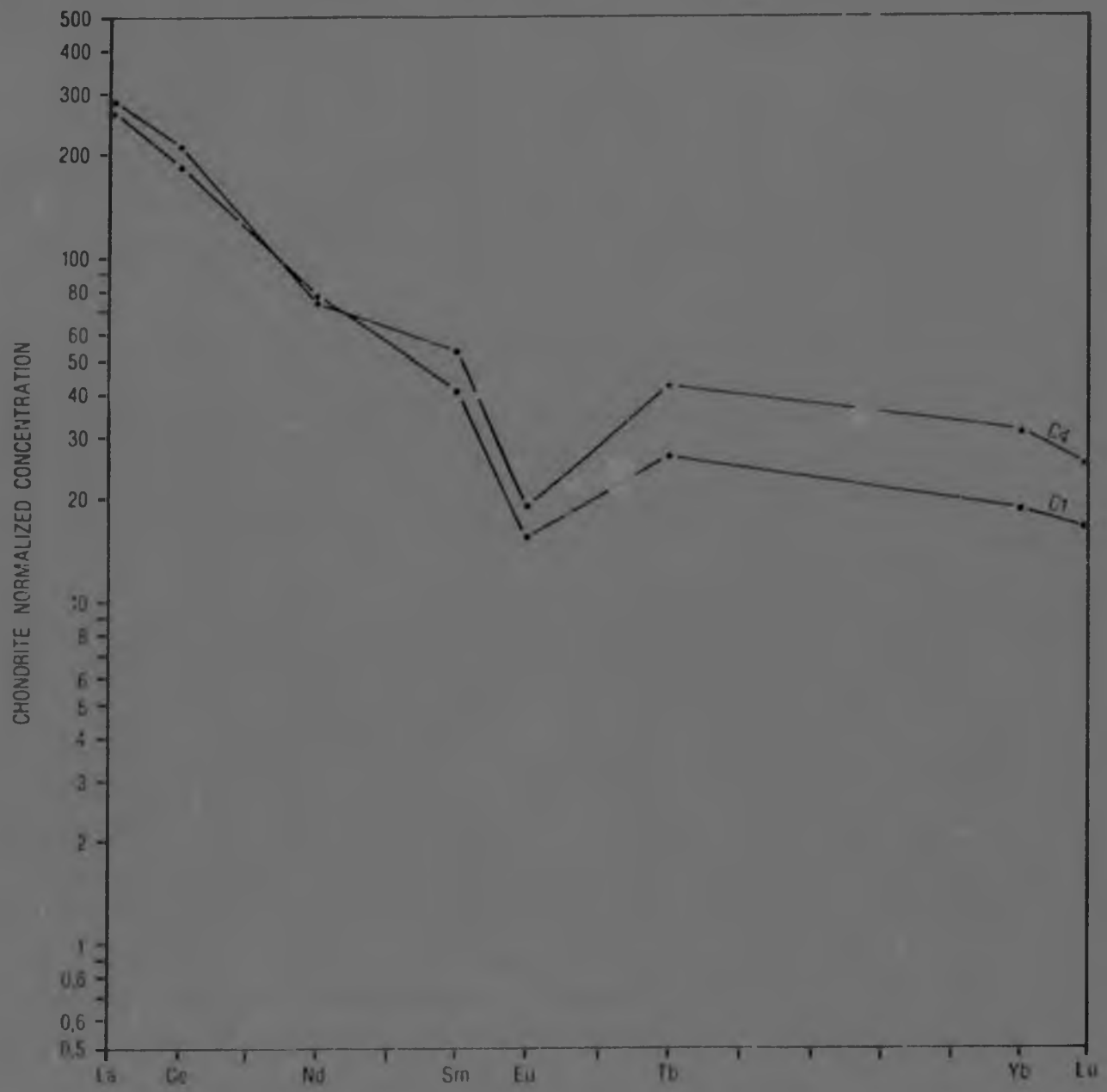

Figure 44 : Chondrite normalized rare-earth element plots for the non-migmatized meta-tuff (C1) and the leucosome-enriched, intensely migmatized meta-tuff (C4) from the Weerg vonden outcrop. Data is from Table 5.

The mesonormative compositions of the migmatite constituents at Weergevonden as well as their probable precursors are plotted on Qt-Ab-Or and An-Ab-Or ternary diagrams in Figure 43 A and B. In these diagrams samples C3 and C6 plot in close proximity to projected minimum melt or eutectic compositions in the granite system (i.e. Qtz-Ab-Or-An-H_2O) whereas the felsic schists plot in a position that is somewhat removed from the latter. In Figure 43 A, samples C1 and C3 have a different normative composition on the Qtz-Ab-An projection to the felsic schists because of the slightly higher SiO_2 and lower K_2O values characteristic of the latter. In general, however, these diagrams confirm the fact that the leucosomes (C6) and leucosome-enriched samples (C4) at the outcrop have eutectic or minimum-melt compositions, a factor which is consistent with their having been derived by partial melting.

7.3. Plagioclase compositions in the migmatitic components

Major element analyses of plagioclases from the various constituents of the meta-tuffaceous unit at the Weergevonden outcrop are presented in Table 20 and their characteristics with respect to the plagioclase solid-solution series are presented on a CaO v Na_2O plot in Figure 46. Both Table 20 and Figure 46 illustrate the fact that the plagioclase from the meta-tuff are stoichiometrically imperfect, a feature that is probably related to the sericitization of these grains. In spite of this, plagioclase compositions in four analysed units are seen to vary between approximately An_{10} and An_{25}. Zonation in the plagioclases is poorly developed with only very small differences in either Na_2O or Ca_2O between the core and rim of the same grain (see samples C3 and C6, Figure 46). Similarly, in any one sample, individual grains do not appear to vary by more than 1% Na_2O and a negligible amount of CaO, indicating that disequilibrium effects are likely to have been negligible.

In contrast to the plagioclase analyses from the meta-tuffaceous unit at the Weergevonden outcrop, the single plagioclase analysis from a felsic schist (sample C15) possibly representing the precursor to the meta-tuffaceous unit, is characterized by a stoichiometrically near-perfect composition (Table 20 and Figure 46). As mentioned in Chapter 2, the meta-tuff at the Weergevonden outcrop is characterized by a recrystallized texture comprising a quartz-microcline-plagioclase-biotite assemblage as opposed to

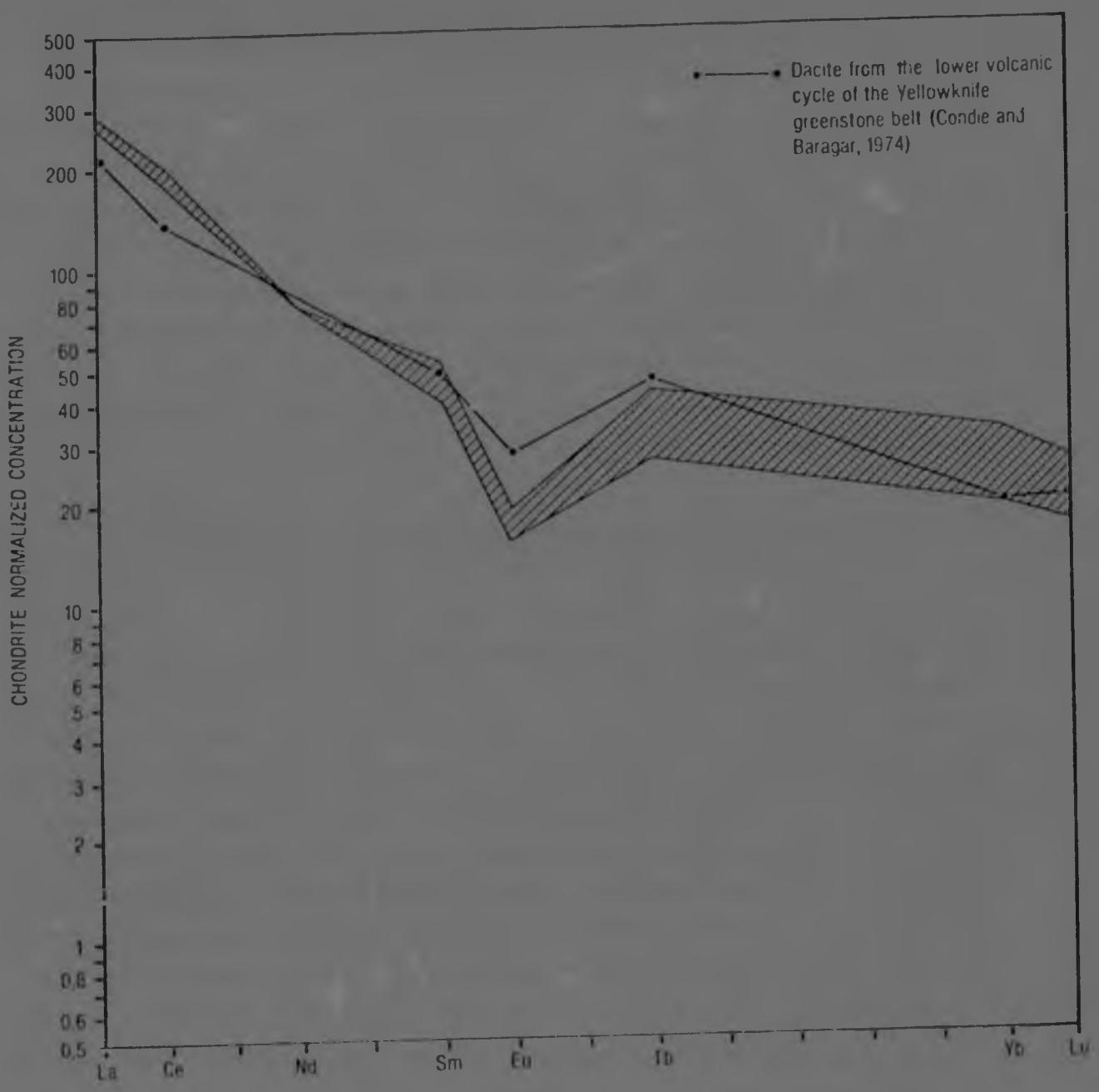

Figure 45 : Chondrite normalized rare-earth element plot showing the similarities between the meta-tuff from the Weergevonden outcrop (hatched envelope) and a typical dacite from the Yellowknife greenstone belt in Canada (after Condie and Baragar, 1974).

TABLE 20

ANALYSES OF PLAGIOCLASES FROM THE MIGMATIZED FELSIC META-TUFF AT THE WEERGEVONDEN OUTCROP

		1	2	3	4	5	6	7	8	9	10
		C1	C1	C3	C3	C4	C4	C6	C6	LC15	STANDARD
Wt.%	SiO_2	69,28	71,08	64,52	64,07	69,07	67,23	68,78	68,12	64,12	44,43
	TiO_2	0,00	0,00	0,02	0,00	0,00	0,00	0,00	0,03	0,00	0,00
	Al_2O_3	21,84	21,55	24,37	24,20	22,51	23,41	22,22	22,83	23,21	35,38
	FeO	0,00	0,00	0,00	0,01	0,00	0,06	0,02	0,01	0,07	0,39
	MnO	-	-	-	-	-	-	-	-	-	-
	MgO	-	-	-	-	-	-	-	-	-	-
	CaO	1,27	1,04	4,23	4,28	2,20	2,43	1,48	1,76	3,44	19,07
	Na_2O	7,76	8,96	7,86	8,92	6,36	7,72	8,02	7,93	9,82	0,60
	K_2O	0,11	0,10	0,22	0,18	0,17	0,09	0,08	0,12	0,14	0,20
	P_2O_5	-	-	-	-	-	-	-	-	-	-
	TOTALS	100,26	100,72	101,22	101,66	100,31	100,94	100,66	100,80	101,30	99,84
Structure*											
	Si	11,91	11,78	11,26	11,13	11,85	11	11,81	11,74	11,26	8,23
	Ti	0,00	0,00	0,00	0,00	0,00	0,00	0,00	0,00	0,00	0,00
	Al	4,43	4,48	4,92	4,98	4,55	4,71	4,51	4,58	4,77	7,73
	Fe	0,00	0,00	0,00	0,00	0,00	0,01	0,00	0,00	0,01	0,06
	Mn	-	-	-	-	-	-	-	-	-	-
	Mg	-	-	-	-	-	-	-	-	-	-
	Ca	0,24	0,27	0,78	0,78	0,41	0,45	0,27	0,32	0,64	3,78
	Na	2,59	2,90	2,51	2,94	2,11	2,56	2,67	2,62	3,32	0,22
	K	0,03	0,02	0,05	0,04	0,04	0,02	0,02	0,03	0,03	0,00
	P	-	-	-	-	-	-	-	-	-	-
	TOTALS	19,20	19,45	19,94	19,87	18,96	19,35	19,28	19,29	20,03	20,02

(* Calculated on the basis of 32 oxygens)

Columns 1 - 2 - Analyses of two separate grains of plagioclase from sample C1.

3 - 4 - Analyses of the core (3) and margin (4) of a single plagioclase grain from sample C3.

5 - 6 - Analyses of the core (5) and margin (6) of a single plagioclase grain from sample C4.

7 - 8 - Analyses of two separate grains of plagioclase from sample C6.

9 - Analysis of plagioclase from a felsic schist (LC15) in the Weergevonden schist belt.

10 - Reference plagioclase analysed as a standard.

(All analyses carried out on the ARL Electron Microprobe at the University of the Witwatersrand by G. Davies).

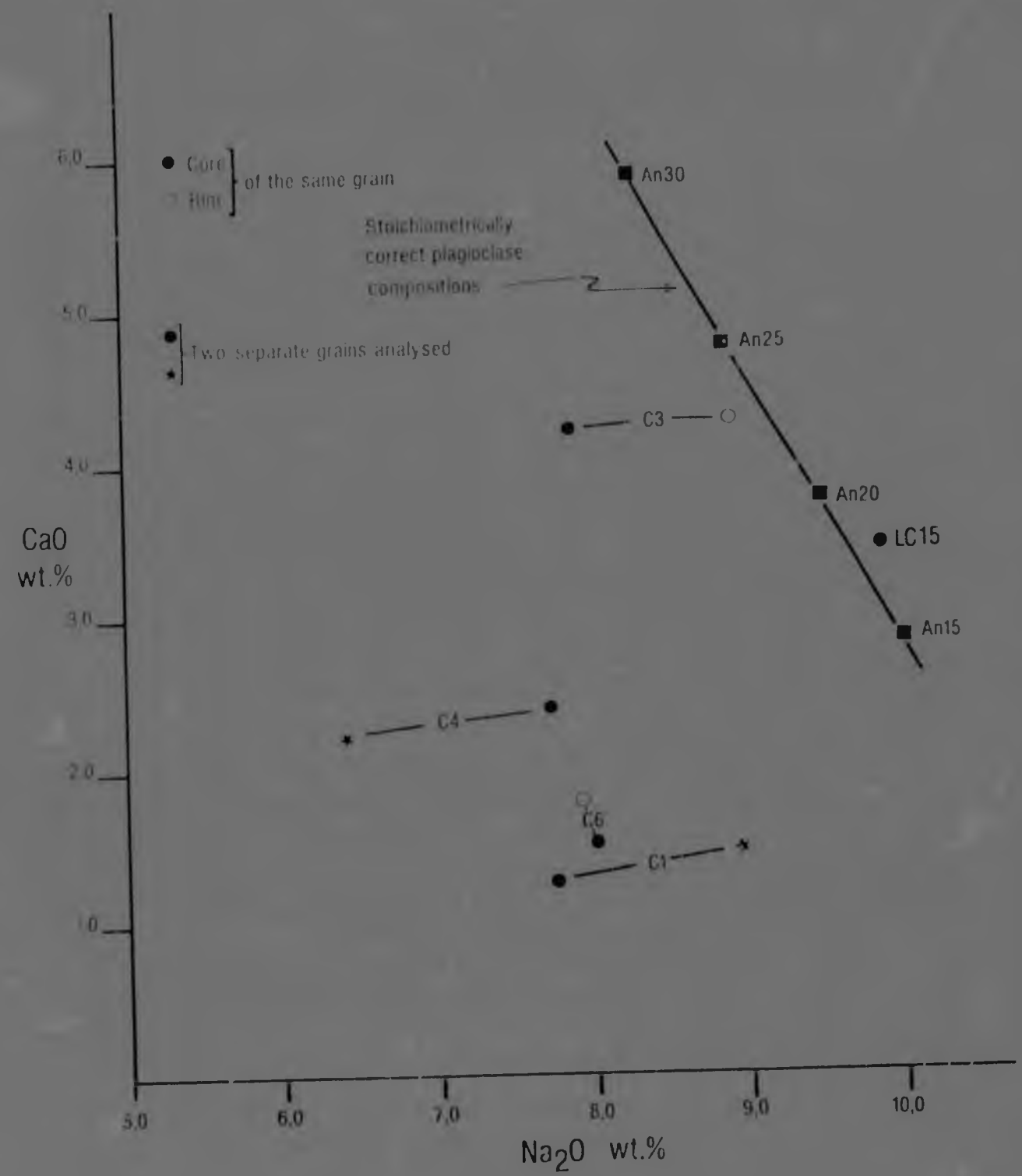

Figure 46 : Plot of CaO against Na_2O showing the composition of plagioclases from various components of the meta-tuffaceous unit at the Weergevonden outcrop. The data is from Table 20. LC15 is an analysis of a plagioclase grain from a sample of felsic schist from the Weergevonden schist belt. This plagioclase has a stoichiometrically correct composition (i.e. compare to the curve plotted for the range An15-An30 of correct plagioclase compositions) by comparison with the various plagioclase compositions from the meta-tuffaceous unit, the latter having been altered and sericitized.

the quartz-sericite-potash felspar assemblage in the possible felsic schist precursors. The recrystallized textures, together with the effects of migmatization, are evidently responsible for the stoichiometric defects in the former and it is perhaps relevant to the argument that the suggested precursor material has not been affected in the same manner. It is also relevant to note that the leucosome-enriched samples (C4 and C6) in Figure 46 have plagioclase compositions that are slightly more albite-enriched than the plagioclases in the possible precursor material (i.e. C15). However, these differences are probably not meaningful in terms of the range of plagioclase compositions exhibited by the non-migmatized meta-tuffaceous units (i.e. C1 and C3). Thus, systematic differences in plagioclase compositions between suggested parental and anatectic components do not occur and this may be related to re-equilibration subsequent to the metamorphic or melting episodes.

7.4 The preferred mechanism of migmatization in the meta-tuffaceous unit

In the light of the evidence presented above it is clear that an unequivocal distinction between *in situ* metamorphic differentiation and anatexis in the migmatized meta-tuffaceous unit at Weergevonden, is difficult. Features such as the presence of a mafic restite adjacent to the neosomes are consistent with an origin by both mechanisms. Similarities in the plagioclase compositions generally indicate a metamorphic origin although anatectic processes may be masked if later re-equilibration took place. Likewise, the presence of microcline in the neosomes and neosome-enriched samples is not conclusive evidence for an anatectic origin as the adjacent material (i.e. the non-migmatized meta-tuff) also contains significant amounts of K-felspar. Finally, even the preferential concentration of felsic veinlets in the low-pressure hinge zone of the fold at Weergevonden is not a diagnostic feature for either mechanism in the light of a recently developed stress-induced theory for metamorphic differentiation. Robin (1979) has suggested that migmatitic layering may form under sub-solidus conditions in response to a principal stress that is orientated at right angles to that layering. As a result, solid-state diffusion processes will react to differential pressures in exactly the same way as an incipient melt will, with a tendency for the mobile constituents (i.e. silica etc.) to migrate to areas of low stress.

In spite of this apparently conflicting evidence, however, three factors definitely tend to be more consistent with an anatectic, rather than a metamorphic, origin. These points are :-

(i) that leucosome-enriched samples have eutectic compositions by comparison with the samples considered to represent the possible parental material (i.e. the felsic schists);

(ii) the presence of a dominantly quartz-muscovite-sericite assemblage in the possible precursor material, in contrast to the microcline-bearing migmatized equivalents, a factor suggesting that the incongruent melting of muscovite may have taken place (see Chapter 2); and

(iii) that leucosome-enriched samples are marginally enriched in incompatible elements such as the REE and Rb.

Thus, when viewed in the light of the combined evidence, these factors indicate that the generation of the migmatized meta-tuffaceous unit at Weergevonden is weighted towards an anatectic origin. As such, it appears that the quartzo-felspathic leucosomes at this outcrop were originally melts and did not result from sub-solidus segregation processes. This conclusion places constraints on the lower limits of temperature and P_{H_2O} that prevailed during the formation of these rocks, and these are consistent with findings from other migmatite outcrops where discrete anatectic components were identified. These points are discussed again in the concluding section to this chapter.

8. THE EFFECTS OF ASSIMILATION IN THE GENERATION OF MIGMATITES IN THE STUDY AREA

A variety of petrological processes have been described in this section in order to account for the mechanisms whereby the migmatites in the study area have formed. Such mechanisms include *in situ* anatexis and palingenesis as well as the introduction of externally derived magmas of varying composition. Most of the components described in the migmatitic outcrops have so far been ascribed to one or more of these processes. In some instances, however, hybridized rocks have been described, the latter

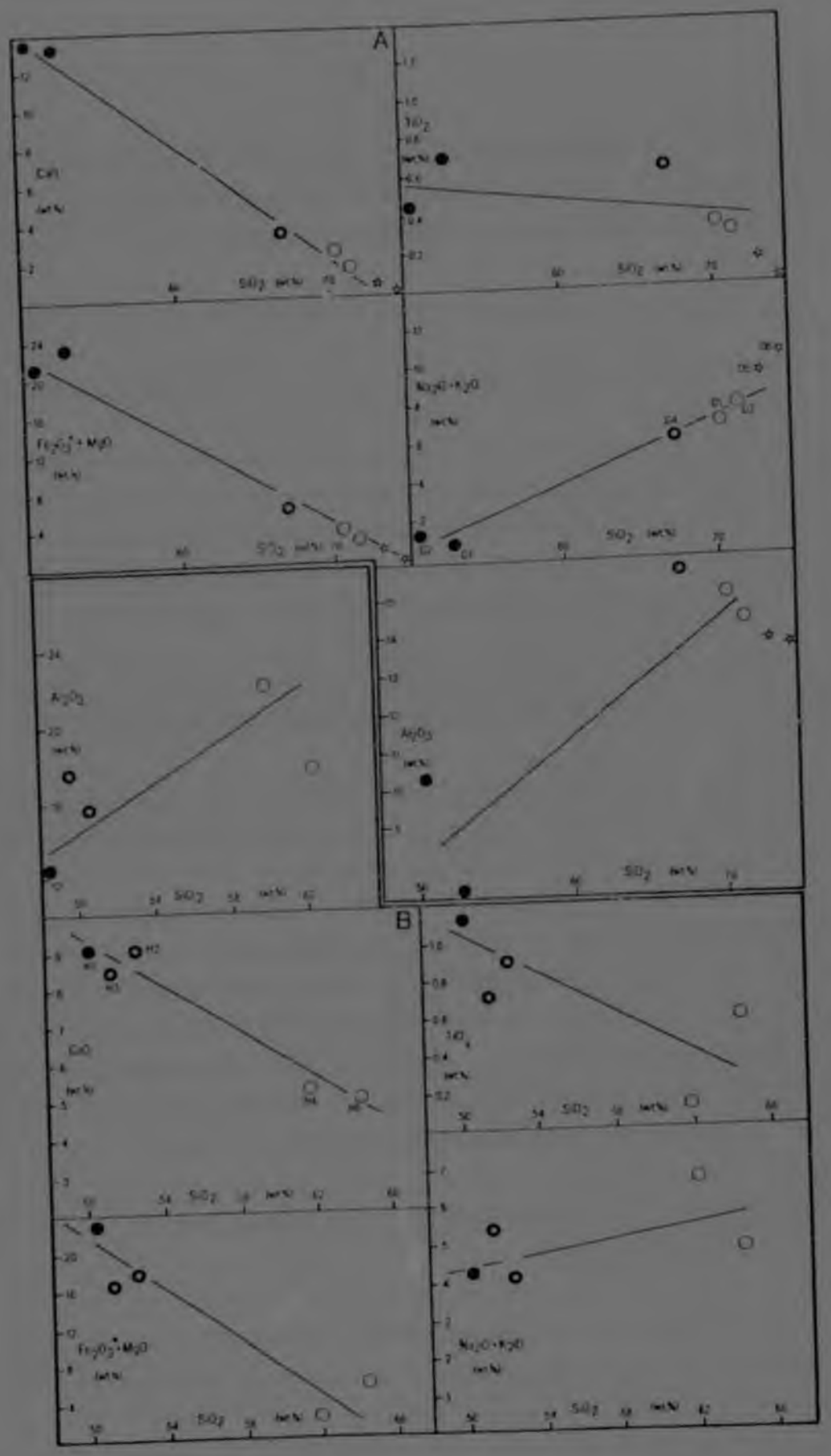

Figure 47 : *Harker-type variation diagrams showing the relationships between various chemical components of (i) the Mara outcrop (part A; D samples) and, (ii) outcrop H from the Batavia section (part B; H samples). Samples plotted represent those components of the outcrops that have been involved in the process of assimilation. Data is from Tables 8 and 10. In each case, the closed circles represent the unaltered mafic precursors with the open circles being the assimilant; encircled stars are the hybridized products that result from mixing of the assimilant with unaltered mafic precursor. In part A, the open stars represent pegmatitic dykes that intrude the Mara outcrop.*

possibly owing their origin to the process of assimilation. Assimilation, contamination or hybridization is defined here as ".... the process of incorporating solid or fluid foreign material into magma" (Glossary of Geology, 1977) and has no genetic connotation, implying, therefore, a variety of mechanisms of formation and no specified end product.

Hybridized rocks from two of the outcrops studied in the immediate vicinity of the Barberton greenstone belt, were described and samples collected in order to test the possibility of their being products of assimilation. At the Mara outcrop a quartz-diorite is believed to have formed by the contamination of remnants of basaltic komatiite by potash-rich magma. In the Batavia section, outcrop H was described earlier as consisting of an amphibolitic dyke, portions of which have been hybridized by quartzo-felspathic (possibly palingenetic) magma. In both outcrops a range of rock-types exists which are represented by the parental (mafic) material, the felsic magma which intrudes the parent and the assimilated product. In this context, the process of assimilation can best be tested by assuming that simple physical mixing takes place between the parent and the assimilant during the production of a range of hybridized by-products.

In Figure 47, major element mixing curves for both the Mara and Batavia outcrops have been constructed. In the case of the Mara outcrop (Figure 47A) linear mixing curves exist between the potash-rich gneiss (i.e. the assimilant) which forms the dominant constituent in the outcrop, remnants of relatively unaltered basaltic komatiite and the quartz-diorite xenolith (Figure 18). This indicates that the quartz-diorite composition, which generally plots in an intermediate position between that of the gneiss and unaltered basalt, may have formed by contamination of the basalt by the granite (sensu lato). In the case of most of the major elements, this process appears to have taken place in a relatively closed system, with the exception of Al_2O_3 where the quartz-diorite is enriched with respect to the potassic gneiss constituents (Figure 47A).

As described earlier, the Mara outcrop is intruded by three discrete phases of pegmatite veins, at least two of which are post-tectonic (see Chapter 2). These pegmatite dykes, which are abundant in the outcrop (Figure 18), are also plotted in Figure 47A in view of the fact that they might have contributed directly to the formation of the quartz-diorite by assimilation. In this diagram, the compositions of two pegmatite veins are

plotted, and it is seen that in most cases (with the exception of CaO and Fe_2O_3* + MgO plots) they do not fall on the mixing curve defined by the other three rock types. As a result, it is considered that these pegmatite veins did not contribute significantly to migmatization and assimilation at the Mara outcrop, but were emplaced after these processes were terminated.

At the Batavia outcrop, portions of an amphibolitic dyke appear to have been differentially hybridized by a palingenetically intruded quartzo-felspathic magma. In this case, sample H1 (Figure 16) represents the pristine, unaltered dyke material, whereas samples H2 and H3 appear to have been progressively assimilated by the intruding magma, which is represented by samples H4 and H6. As in the case of the Mara outcrop, the relevant components of the Batavia outcrop form linear mixing curves confirming that parts of the mafic dyke have in fact been contaminated by the felsic magma (Figure 47B). Although some scatter is observed it is clear that the process of mixing has been such that the system has remained relatively closed, at least with respect to the major elements. This implies that the mechanism of hybridization involves fragmentation of the mafic precursor by a permeating felsic assimilant without a significant loss of the constituents from the system; this is reflected both on a macro-scale (Figure 18) as well as microscopically, where individual grains are themselves fragmented, altered and assimilated (Plate 6 C and D).

Two fundamental points with respect to the process of assimilation can be gauged by comparing each of the respective plots in Figure 47 A and B. At both the Mara and Batavia outcrops, the pristine mafic remnants that were assimilated are characterized by broadly similar compositions, although the amphibolite at Mara is komatiitic (with a lower TiO_2 concentration and a higher CaO/Al_2O_3 ratio) in comparison with that at Batavia, which is tholeiitic. In contrast, the felsic magmas which intrude these mafic remnants, are different in composition and the slopes of the resultant mixing curves are also, therefore, different. For example, the intrusive tonalitic (or anatectic) magma at Batavia has a higher CaO content than the intrusive adamellitic magma at Mara, so that the slope of the CaO v SiO_2 mixing curve at Batavia is, therefore, less steep (compare CaO v SiO_2 in Figure 47 A and B). It is also clear when comparing Figure 47A with Figure 47B that the composition of the assimilated rocks

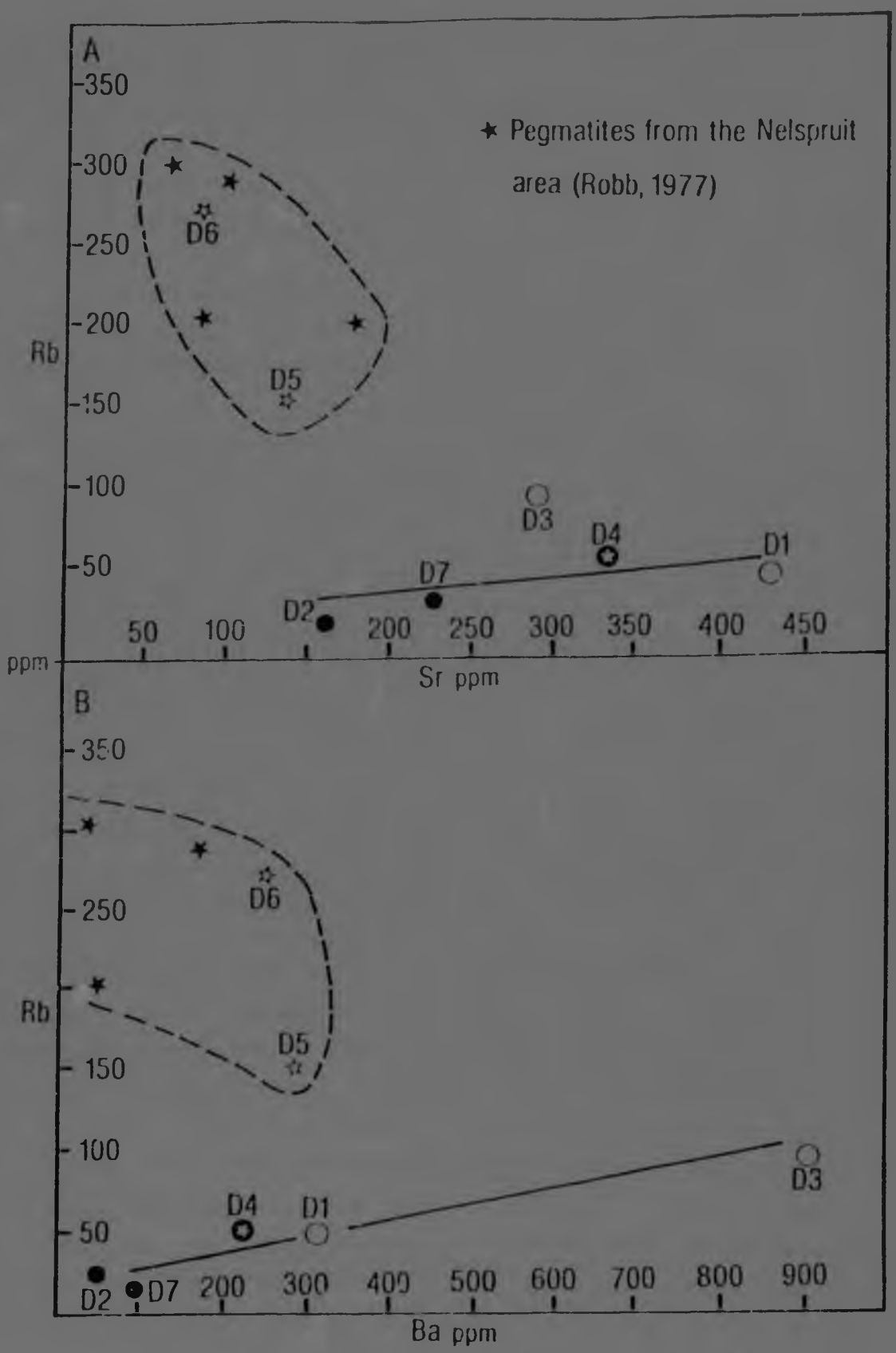

Figure 48 : Plots of Rb v Sr and Rb v Ba for the components of the Mara outcrop that have been involved in the processes of assimilation. Samples D2 and D7 are relatively unaltered basaltic komatiite remnants, D1 and D3 are components of the potash-rich gneissic assimilant and D4 is the hybridized quartz-diorite body. D5 and D6 are discrete pegmatite veins that include the Mara outcrop. Data is from Table 10.

at the two outcrops are also different. The quartz-diorite at Mara is distinctly more felsic than the hybridized mafic units at Batavia and this is obviously a function of the degree of assimilation that has taken place. At Batavia, for example, the hybridized dyke samples plot relatively closely to the pristine dyke composition, so that the degree of assimilation cannot be as great as in the Mara example. An estimation of the extent to which the pristine mafic remnants have been assimilated by the intruding felsic magmas can, therefore, be gauged by the proximity of the assimilated rocks to either of the components at each end of the mixing curves.

Although certain trace elements such as Rb, Sr and Ba may sometimes be remobilized during metamorphic and tectonic processes, their distribution in terms of the assimilation process has also been assessed. In Figure 48 plots of the Rb v Sr and Rb v Ba indicate that at the Mara outcrop, the distribution of these trace elements defines a linear mixing curve such that the quartz-diorite occupies an approximately intermediate position between the amphibolitic parent and felsic assimilant. It is also apparent that the pegmatitic veins at the outcrop (which are similar in composition to other pegmatite veins analysed from the Nelspruit batholith) cannot have contributed to the distribution of trace elements in the outcrops during the assimilation process, this confirming the general view obtained from the major element mixing curves. The distribution of trace elements at the Batavia outcrop is less systematic (although a regular increase in Sr between parent amphibolite and quartzo-felspathic assimilant is observed, Table 8) and in this case the alkali and alkali-earth elements appear to have been more mobile than at the Mara outcrop. The reason for this is possibly related to the higher temperature (and/or pressure) conditions that are considered to have prevailed in the case of the Batavia migmatite outcrops (see section 9 of this chapter).

The various components of the Mara outcrop have also been analysed for the REE and these are plotted in chondrite normalized form in Figure 49. This diagram is not diagnostic of the hybridization processes that have occurred and simple mixing of the REE is not apparent. The mafic (komatiitic) parent (sample D2) has a characteristic flat REE trace whereas the potassic gneiss components (D1 and D3) are LREE enriched and HREE depleted with respect

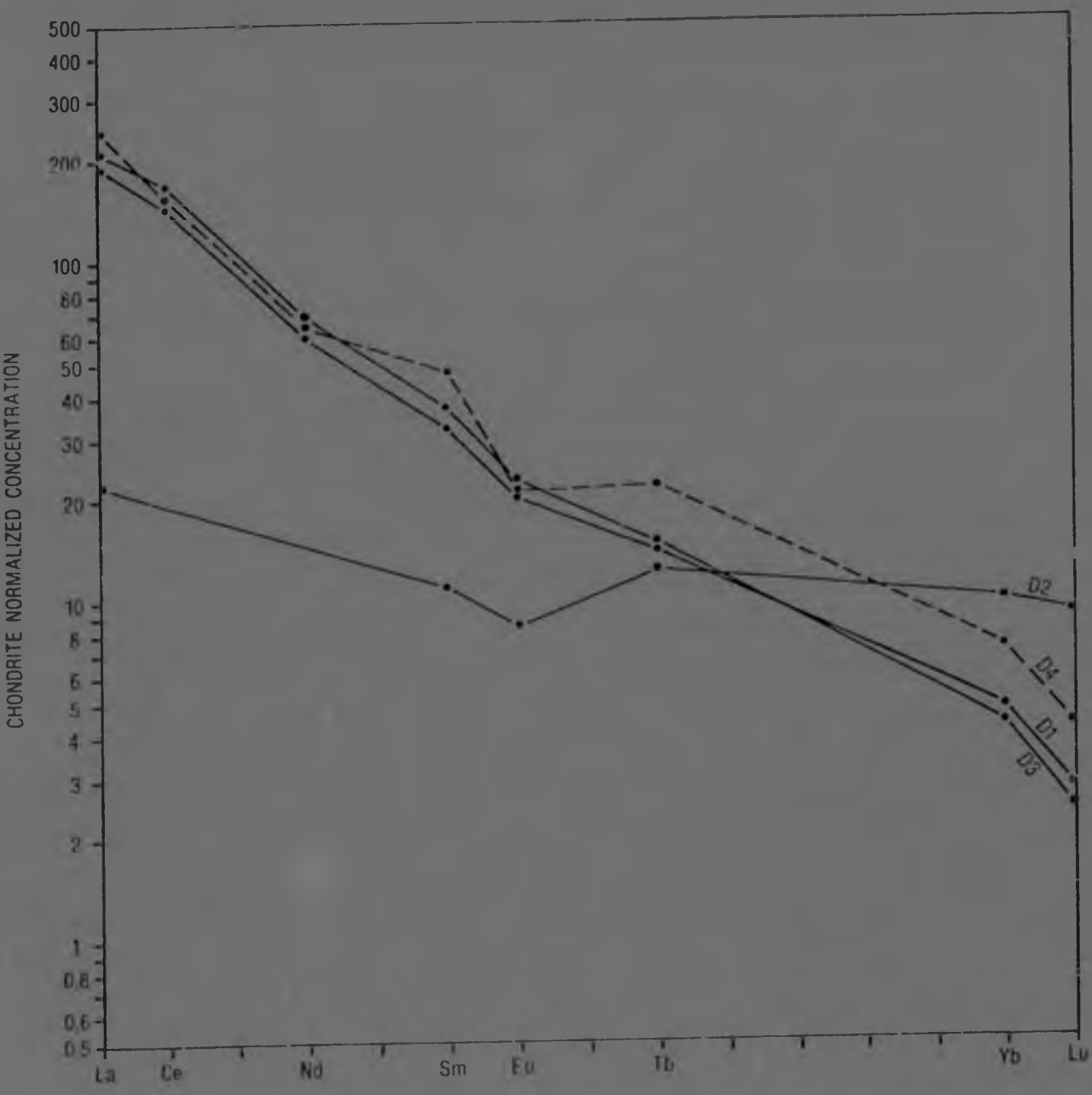

Figure 49 : Chondrite normalized rare-earth element plot of components from the Mara migmatite outcrop. Sample descriptions are the same as those in Figure 48. Data is from Table 10.

to the mafic xenolith. The quartz-diorite hybrid (sample D4) has an essentially indistinguishable LREE content from that of the gneiss and only the HREE are intermediate in abundance between parent and assimilant. As mentioned earlier, the quartz-diorite at Mara appears to have been affected by a high degree of assimilation and this is probably the reason why the rare-earth elements do not reflect contamination in this body.

In summary, the above section demonstrates that the process of assimilation can be adequately explained by assuming that simple physical mixing takes place between a parent rock and an introduced assimilant (magma). The discussion deals mainly, however, with the chemical characteristics of the components in question and, as such, little acccunt is taken of the actual mechanisms by which hybridization occurs. If one assumes that the assimilant is a liquid or magma, then mixing probably involves the partial dissolution and fragmentation of previously solidified parental material. Alternatively, if the assimilant is a vapour or pore-fluid (i.e. metasomatism is taking place), then bulk changes in the composition of the system might occur without significant disruption of the pre-existing material. In either event, a detailed assessment of the mechanisms of assimilation is likely to be a complex affair involving a more detailed approach than that taken above. Assimilation is best regarded as the end product of, possibly extensive, externally derived, processes of migmatization (i.e. either metasomatism or the introduction of a foreign magma) but which must be recognized by both petrographic means as well as systematic chemical changes. In this light, its extent is not likely to be restricted only to the margins of plutonic masses, but will, rather, cover a wide variety of rock types in metamorphic terranes with deep-seated origins.

9. DISCUSSION AND CONCLUSIONS

Much of the discussion and many of the conclusions derived from the detailed mapping of migmatite outcrops in the Barberton Mountain Land, described in the preceding sections, can best be carried out within a framework that encompasses the regional geology of the area. Following a recent reappraisal of the granitic rocks of the eastern Transvaal and Swaziland, it is possible to allocate the various migmatite outcrops mapped to one of three major subdivisions. Anhaeusser and Robb (1980b) defined

three major magmatic cycles within this Archaean granitic terrane and have allocated most of the identifiably discrete granitoid units into one of these three episodes (Figure 1). In brief the three cycles are represented, in order of broadly decreasing age, by :-

(i) the emplacement of soda-rich tonalite and trondhjemite magmas and the formation of complex bimodal gneisses and migmatites;

(ii) the intrusion of large, multi-component, potash-rich batholiths that have enveloped large areas previously occupied by components of the first cycle; and

(iii) the emplacement of late, post-tectonic granitic (*sensu stricto*), adamellitic and syenitic plutons into components of either of the above two cycles, or the greenstone belt itself.

Because the rationale behind the study of migmatitic rocks in this thesis was an attempt to elucidate the primary relationships between the earliest granitic (*sensu lato*) episodes and the greenstones, it is obvious that most of the migmatites examined fit, in terms of the above framework, into the first magmatic cycle. This is true of nine out of ten of the migmatite outcrops described and these can, therefore, be broadly described as representing the nature of complex interactive processes between an early ensimatic (greenstone) crust and the initial phases (i.e. tonalite and trondhjemite magmatism) of a progressively developing sialic crust.

Principally for comparative purposes, a tenth migmatite exposure (i.e. the Mara outcrop) was examined from the point of view of contrasting the processes relating to the evolution of the first magmatic cycle, with those operative during the second magmatic cycle mentioned above. As stated by Anhaeusser and Robb (1980b), the intrusion of large, multi-component, potash-rich batholiths is invariably characterized by complex marginal effects (i.e. around the peripheries of the intrusions) which usually involve the assimilation and granitization of pre-existing material. The latter processes are responsible for the formation of complex migmatitic gneisses which are genetically related to the emplacement of these batholiths. The present study did not examine any aspects related to the emplacement of

granites associated with the third magmatic cycle,as the latter event is not responsible for the production of migmatitic rocks and represents the final event in the evolution of the granitic crust in the study area.

As a result of the detailed mapping of the various outcrops described above, migmatites in the study area can be described as having formed in response to *four* processes, more than one of which may have applied to the formation of any one outcrop. These processes include :-

(i) the physical intrusion of tonalitic/trondhjemitic magmas into pre-existing mafic or felsic remnants which are correlatable with recognized greenstone lithologies;

(ii) anatexis and palingenesis, where both tonalitic/trondhjemitic and greenstone components are intruded and disrupted by material considered to have been derived by the partial melting of tonalitic or trondhjemitic gneisses;

(iii) assimilation, where a felsic contaminant (be it either tonalitic/trondhjemitic magma, anatectite or potash-rich magma) is responsible for the hybridization and contamination of a pre-existing, usually mafic, component; and

(iv) the physical intrusion of basic magma (dykes) into pre-existing tonalitic or trondhjemitic gneisses.

These four points summarize the processes applicable in all the migmatite outcrops examined. All can, furthermore, generally be described as being *arteritic* in nature with one or more of the migmatitic components having been derived externally and subsequently introduced into the system. In general, therefore, *venitic* processes such as *in situ* sub-solidus metamorphic differentiation do not appear to have taken place. One possible exception is where anatectic material appears to have been locally derived and remained relatively *in situ* , as, for example, in the Weergevonden outcrop. In most cases, however, although anatectites appear to have originated locally, migmatites can nevertheless be viewed as arteritic as this material is usually re-emplaced into a different environment from its source. As mentioned previously, the entire range of processes related to the formation of migmatites in the study area is best observed in the Batavia section (Figure 2) which can be regarded as a type-area for migmatites related to the first magmatic cycle in the Barberton Mountain Land.

Although the above, mainly arteritic, processes are considered to account, petrogenetically, for the formation of the migmatite outcrops studied, a fifth, structurally-related, factor has also played a major role in the formation of these rocks. Structural deformation is a factor, which, although not directly affecting the petrogenesis of the migmatites, is responsible for complicating the recognition of primary relationships (often magmatic) between the various components in these rocks. Certain migmatites, for example, have formed by the intrusion of mafic dykes into pre-existing tonalite-trondhjemite gneisses. These amphibolitic dykes are, themselves, deformed and characterized by residence contamination and assimilation by palingenetically-intruded anatectites. As such, their recognition is dependent on the preservation of a discordancy between the dyke and an earlier-formed planar fabric in the host gneisses. If the discordancy does not occur, or deformation has been so intense that primary angularities are made parallel, then it may be impossible to differentiate between amphibolitic greenstone remnants and amphibolitic dykes. Although the mafic dykes in the study area are volumetrically insignificant, many amphibolitic bodies may, on this basis, have been misinterpreted in the past.

Structural deformation at the Theeboom exposure is also responsible for the uncertainty that exists in the interpretation of sections of this outcrop. As described previously, a discordancy exists between compositionally banded trondhjemite gneisses and an amphibolitic meta-basalt of komatiitic composition. Whether this feature is a primary relationship or merely the result of boudinaging with a rotational aspect, is not clear, so that the relative ages of trondhjemite and amphibolite are uncertain.

The influence of structure on the development of migmatitc rocks has a further ramification at the Weergevonden exposure. At this outcrop, locally derived anatectic melts have been concentrated into the low-pressure hinge zones of folds giving the latter a complex, heterogeneous texture that differs markedly from identical rock types represented on the fold limbs. It is clear, therefore, that rock deformation has played an important role in the development of migmatites in the study area, the nature of which is particularly important in the detailed interpretation of these complex rocks.

The recognition of dominantly arteritic processes behind the formation of migmatites in the study area places certain constraints on the dynamo-thermal conditions that prevailed in the crust during this period. Particularly relevant in this regard is the ubiquitous presence of anatectically-derived intrusions which indicate that pressures and temperatures were high enough to intersect the solidus of certain mineral phases associated with components of the migmatites. In contrast, sub-solidus processes such as metamorphic differentiation were not encountered in the present study, although it is possible that this mechanism applies to certain banded trondhjemite gneisses in the area. Although it is difficult to quantify the minimum pressure and temperature conditions that may once have prevailed, anatexis requires that P, T and P_{H_2O} were such that at least the near-solidus mineral phases were melted. At best, conditions of load pressure and P_{H_2O} are difficult to quantitatively assess, but a measure of the equilibration temperature of a coexisting garnet-biotite assemblage associated with the migmatites is available and these results are discussed below.

Tonalite gneisses in the Batavia section (i.e. section H-E-F-G, Figure 2) contain minor amounts of garnet which is commonly juxtaposed with biotite in the same rock (Plate 6F). Thompson (1976) and Ferry and Spear (1978) have demonstrated that the partitioning of Fe and Mg between coexisting garnet and biotite is a temperature dependent process and, as long as the two minerals have attained equilibrium and the system has remained closed, mineral analyses will provide an indication of the equilibration temperature of that system. Appendix 3 presents electron-microprobe analyses of biotite and garnet from a tonalite gneiss (sample F2) from the Batavia section, as well as an assessment of the equilibration temperature of these two minerals. The latter value, which is calculated at an average of 733°C in Appendix 3, is an indication of the temperature to which the rock was raised during the formation of the metamorphic garnet constituent and also points to the severity of the later dynamo-thermal imprint on the rocks of the area.

Experimental work has shown that, in the presence of excess H_2O (i.e. water not trapped in the lattice structure of hydrous minerals such as biotite) the solidus curves of granite (*sensu stricto*), as opposed to tonalite, vary by only a few degrees (Merrill et al., 1970; Stern et al., 1975; Wyllie et al., 1976). In contrast, the liquidus curve for tonalite

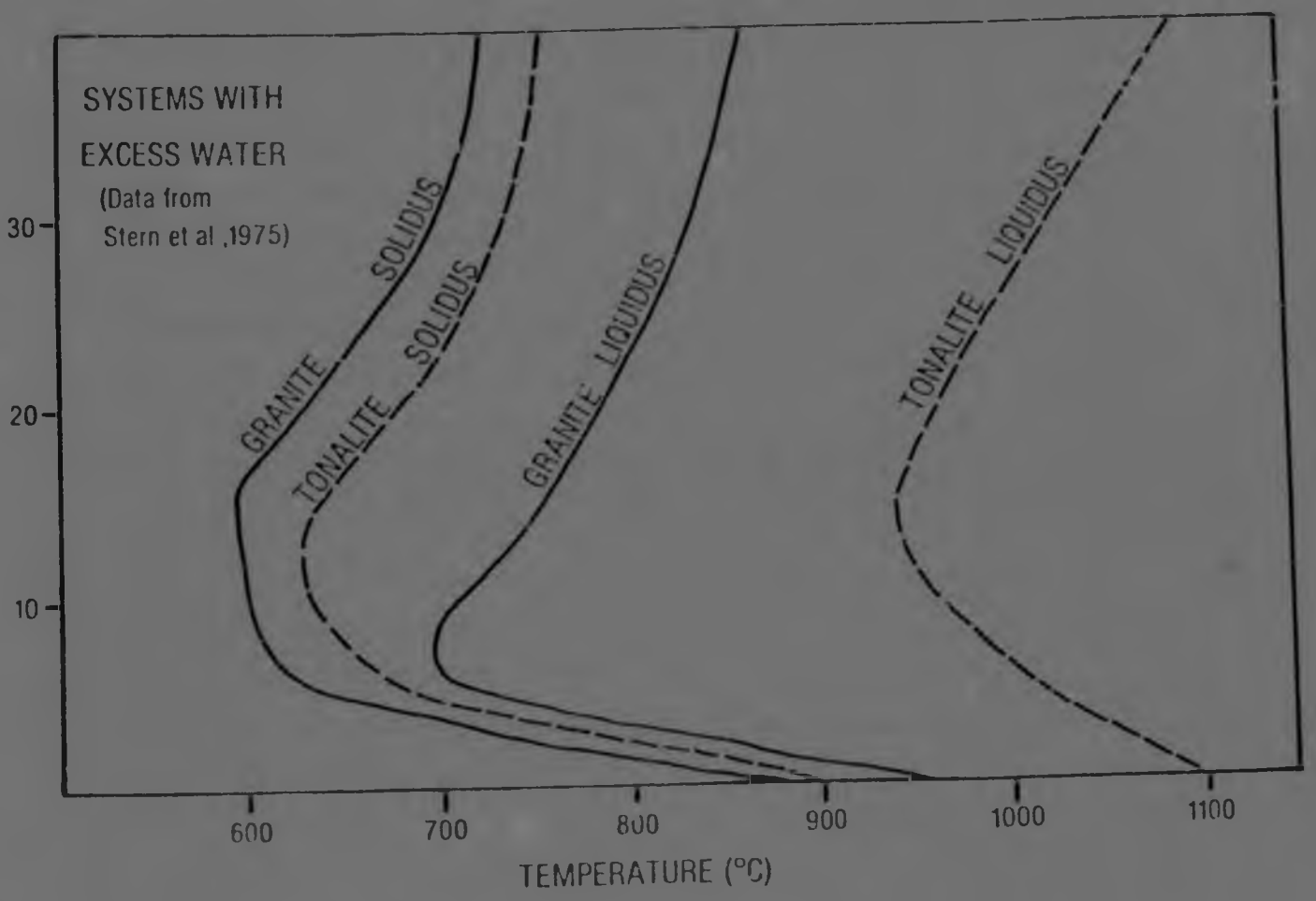

Figure 50 : Diagram showing the relative liquidus and solidus temperatures of granite (sensu stricto) and tonalite in the presence of excess H_2O. The melt interval for a granitic rock is seen to be considerably less than that for a tonalite.

is considerably higher (by 200 - 300°C) than that for granite, which means that for any temperature within this melt interval, tonalites will undergo a smaller degree of partial melting than that experienced by a granite at that temperature. These points are illustrated in Figure 50 where it is apparent that at temperatures in the vicinity of 750°C and in the presence of even small amounts of excess H_2O, tonalitic rocks will undergo partial melting. It is also seen that, whereas near-total fusion of granitic material may be accomplished at these temperatures, the tonalite liquidus is not attained for another 200°C and, hence, only the low-temperature components of the latter will melt. As such, the conclusion mentioned above, namely that many of the migmatitic rocks have been formed through the introduction of anatectic material probably derived from tonalitic or trondhjemitic precursors, is quite feasible in the light of the equilibration temperature obtained from the garnet/biotite geothermometer.

Indispensable, however, to the above argument and, therefore, to the mechanism of anatexis in the migmatitic zones, is the presence of excess water in these rocks, in order that incipient fusion can occur. Without the presence of such a volatile phase, temperatures concomitant with granulite metamorphism are likely to be reached before the tonalite solidus is intersected (Stern et al., 1975; Collerson and Fryer, 1978) and sub-solidus processes such as metamorphic differentiation might, therefore, be expected to prevail. As neither of these conditions exist in the study area, the presence of excess water vapour in this environment is inferred. Two possible sources of volatiles (i.e. CO_2, S and halogens as well as H_2O) are likely in the prevailing circumstances; firstly as the result of the dehydration of xenolithic greenstone material (Glikson, 1979a) and, secondly, under conditions of high geothermal gradient (~100°C/km) where the degassing of lower crustal granulitic material has taken place (Collerson and Fryer, 1978). The second process is described as having been very extensive and one that is likely to have prevailed during a process of the magnitude envisaged during the emplacement of, for example, the second magmatic cycle. Anatexis during the formation of the migmatites is, in contrast, a process that is spatially linked with remnants of greenstone material and excess water is more likely to have been derived from the dehydration of the latter. In this case, a likely source of water is that derived from the breakdown of hornblende in the, now dominantly, amphibolitic greenstone remnants. Contrary to expectation, however, the large-scale

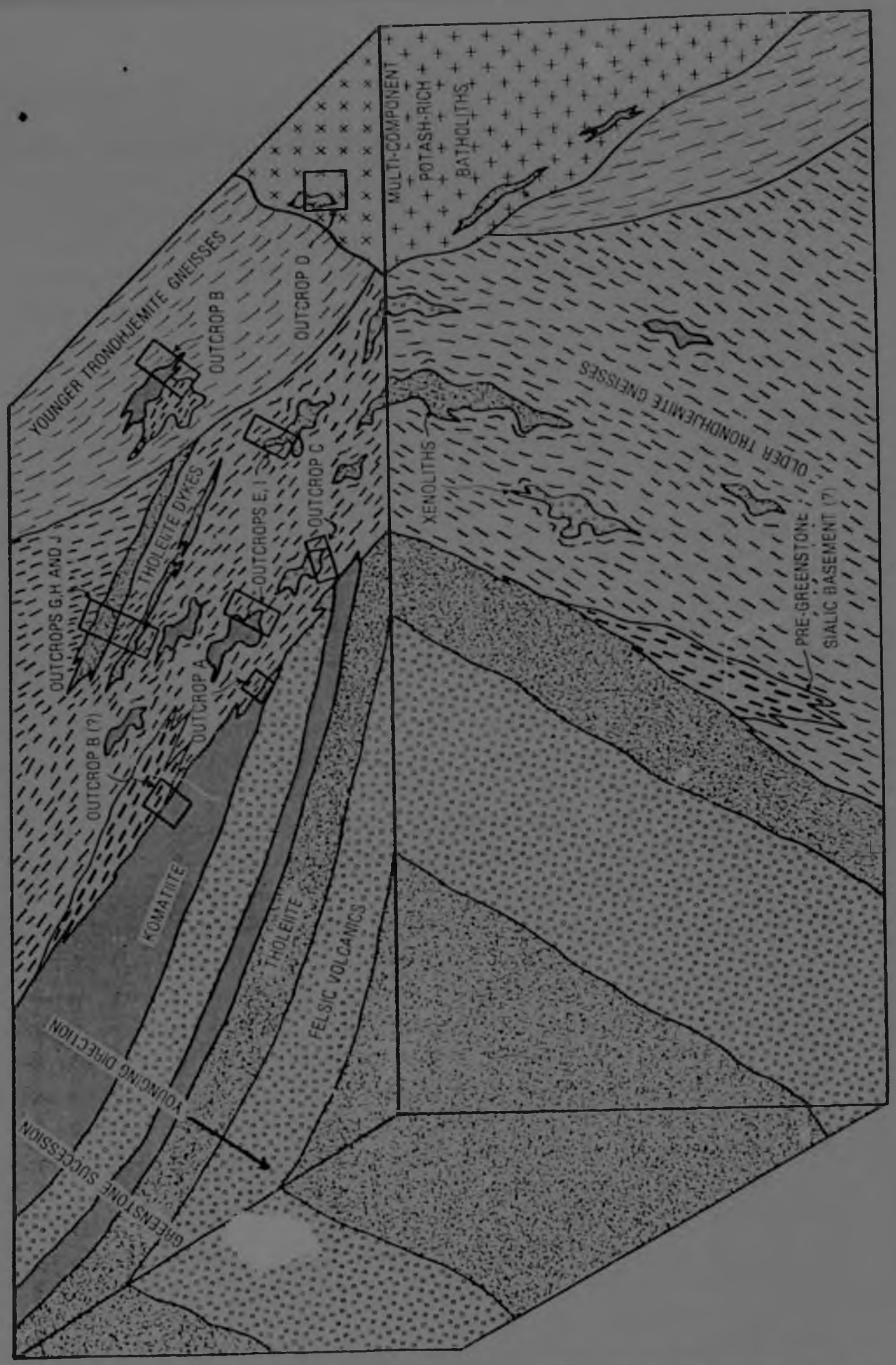

Figure 51 : *Schematic diagram showing the relationship of the migmatite outcrops to the major lithological components of the granite-greenstone terrane in the study area. All the components portrayed in this model represent realistic analogues in the field, with the possible exception of the "pre-greenstone sialic basement", which is inferred from the equivocal evidence available at the Theeboom outcrop.*

alteration of this mineral has not taken place and a readily available source of excess water is not, therefore, present. In the Barberton Mountain Land, however, one enigma that has been noted by numerous workers (C.R. Anhaeusser, personal communication) is the absence of widespread ultramafic (serpentinitic) xenoliths within the gneisses and migmatites in the region, in spite of the fact that this material is relatively abundant in the Tjakastad Subgroup. The complete breakdown of these ultramafic assemblages, which are likely to be out of equilibrium in an amphibolite facies, or incipient anatectic, environment, may well, therefore, have provided much of the excess water that was available during the formation of the migmatites.

In summary, the detailed study and resultant understanding of migmatitic rocks in the Barberton Mountain Land clearly provides certain additional insight into the evolution of the Archaean crust in the region. These conclusions are briefly described below in terms of a simplified block diagram which attempts to schematize the tectonic and magmatic setting of the various migmatite outcrops described (Figure 51) :-

(i) The emplacement of tonalite/trondhjemite plutons in the area southwest of the Barberton greenstone belt was a process that was regionally, neither cogenetic (see Chapter 6), nor coeval and was an event that probably spanned some 300 - 500 m.y. (Barton, et al., 1981). A number of different, discrete tonalitic-trondhjemitic bodies were emplaced during the first magmatic cycle so that younger plutons may intrude (either magmatically or structurally) into older ones (as shown in Figure 51). Direct evidence for this is available from the Theeboom outcrop (outcrop B in Figure 51) where older and younger trondhjemite gneiss phases are juxtaposed. The older gneiss is characterized by compositional banding and also preserves indications of higher strain (i.e. a more pronounced foliation), in contrast to the younger more homogeneous phase. This clearly indicates that the former recorded dynamo-thermal events not witnessed by the latter. In the light of evidence such as this it is envisaged that the emplacement of the first magmatic cycle is represented by a continuum of events that marked the development of a

protocraton. An unstable form of dominantly vertical tectonics (diapirism) is considered to have been active during this era (Anhaeusser and Robb, 1980b) and it is likely that younger phases were responsible for the deformation of, as well as intrusion into, older phases.

(ii) The study of migmatites did not reveal unequivocal evidence indicating that any of the numerous greenstone remnants to the southwest of the Barberton greenstone belt were deposited on top of (or intruded into) pre-existing sialic material. However, at the Theeboom outcrop (schematically shown as "outcrop B(?)", Figure 51) structural relationships indicate that the older gneissic unit may pre-date the exposed remnant of amphibolitic meta-basalt. These relationships, which include discordancies between the amphibolite and foliation/gneissocity/compositional banding in the gneiss (Figure 6), as well as a xenolith of gneiss partially enveloped by the amphibolite (Figure 7), have been affected by boudinaging and must, therefore, be viewed as contentious evidence for pre-existing sial. The intrusion of numerous younger tonalite/trondhjemite plutons into the greenstone successions and the dominance of gravity inversion (diapirism) during their emplacement, suggests that the presence of any pre-greenstone sial in the study area is likely to be preserved immediately juxtaposed with the, now vertical, amphibolitic remnants (Figure 51). In this sense too, therefore, the sliver of older banded gneiss at Theeboom also fits the criterion for possible candidacy as a remnant of sialic material that existed prior to the development of the greenstone successions. However, the doubt that is attached to this interpretation means that it is impossible to decide whether the greenstones were developed *entirely* in an ensimatic environment or whether, at least in certain areas where the migmatites are developed, they were extruded onto a sialic basement.

(iii) Certain migmatites examined in the study area preserve relationships indicating that they have formed by the intrusion of tonalitic/trondhjemitic magma into pre-existing greenstone lithologies (schematically shown as outcrops E, I and C, Figure 51). In terms of the regional geological framework mentioned above, the first magmatic cycle (i.e. events coincident with protocratonization) is considered to have been intrusive, at least

in the study area, into an ensimatic crust and these migmatites, therefore, represent the relics of interaction between the latter and these early granitic (*sensu lato*) magmas. As such, it must be expected that the early tonalitic magmas interacted with greenstones of variable composition and the study has documented examples where migmatites are related to felsic, as well as mafic, remnants, both of which can be correlated with greenstone lithologies.

(iv) In addition to documenting the interactive processes between early greenstones and the first magmatic cycle, one of the migmatite outcrops was studied specifically to assess the nature of the interaction between granites of the second magmatic cycle and the largely sialic crust that existed prior to their emplacement. Within the regional geological framework of the area, the emplacement of large, multi-component, K-rich batholiths is viewed as being largely responsible for the stabilization of the craton. The margins of these batholiths are characterized by extensive zones of migmatites and potash-rich gneisses, the nature of which reflect the pre-existing crustal material that existed prior to the development of these rocks. The study of this migmatite outcrop (schematically shown as outcrop D, Figure 51) points to the effects of granitization and assimilation that accompanied the emplacement of the large, syn- to post-kinematic batholiths of the second cycle.

(v) Dynamo-thermal metamorphism has variably affected the entire Barberton Mountain Land, most of the smaller greenstone remnants in the study area can be broadly described as having attained an amphibolite grade of metamorphism whilst the tonalites/trondhjemites are ubiquitously characterized by a penetrative mineral fabric. The majority of the migmatitic rocks examined, however, have been intruded by an anatectic component that is considered to have formed as the result of partial melting of a tonalitic or trondhjemitic precursor. Because very high temperatures (> 1000^{o}C) are not reflected in the metamorphic grade, partial fusion must have been facilitated by the intersection of the local geotherm with a water-saturated tonalite solidus. In such a situation,

temperatures as low as 750°C will have resulted in the partial fusion of tonalitic rocks. Progressive melting of these rocks is evidenced by a range of anatectite compositions, with the latter varying from minimum melt to more sodic varieties. As Brown (1970) has demonstrated, the effect of melt compositions becoming more sodic (and hence tending towards the bulk precursor composition) is explained either in terms of slight temperature increases or, the availability of greater amounts of excess water-vapour. In broad terms, therefore, the formation of migmatites in the study area did not involve sub-solidus processes such as metamorphic differentiation.

(vi) Finally, migmatitic rocks in the study area have formed as the result of the intrusion of mafic dykes into pre-existing, well-foliated tonalite/trondhjemite gneisses (schematically shown as outcrops G, H and J, Figure 51). These dykes, which are generally tholeiitic in composition, have been involved in a major part of the dynamo-thermal metamorphic history of the region and, as a result, reflect the effects of crustal residence contamination and migmatization. Thus, although the dykes cannot be shown to have directly fed younger greenstone successions (for example, the dominantly tholeiitic Geluk Subgroup) it is likely that they represent an intrusive magmatic event that was coeval with the extrusion of these lavas into adjacent oceanic settings. This suggests that the younger greenstone lithologies were developed in the presence of a locally-situated sialic basement and this may also be reflected in the calc-alkaline chemistry of these younger lavas, as opposed to the komatiitic characteristics of the older greenstones. Considerations such as these, together with the frequency of occurrence of greenstone belts on the Kaapvaal craton, suggest that the sizes of Archaean oceans, as well as the areas (or volumes) of early sialic nuclei occurring adjacent to these oceans, were considerably smaller than those of more recent times.

PART 2

TONALITE AND TRONDHJEMITE PLUTONS IN THE BARBERTON MOUNTAIN LAND

CHAPTER 4

THE KAAP VALLEY TONALITE PLUTON

–ITS GEOLOGY, CHEMISTRY AND MODE OF FORMATION

THE KAAP VALLEY TONALITE PLUTON - ITS GEOLOGY, CHEMISTRY AND MODE OF FORMATION

1. INTRODUCTION

The Kaap Valley tonalite is the largest and most distinctive of the numerous tonalite and trondhjemite gneiss plutons in the vicinity of the Barberton greenstone belt. In spite of this, and although it has been examined on a number of occasions, mainly on a regional basis, it has never received the detailed attention warranted by its prominent position. The Kaap Valley pluton is almost totally flanked by mafic and ultramafic rocks of the Onverwacht Group and is situated between the east-west trending Jamestown Schist Belt and the most westerly portion of the Barberton greenstone belt (Figure 52, inset locality map). The tonalite body is roughly elliptical in plan and has a surface area of approximately 430 km^2.

The Kaap Valley pluton was first described by Hall (1918) who distinguished between two granite types in the Barberton area, viz., the "Nelspruit Type" and the "De Kaap Type". More recently, however, van Eeden (1941) and Visser, compiler (1956) referred to the body specifically as the "Kaap Valley Granite" and recognized its unusual mineralogical trait with respect to other bodies of similar composition in the region, namely that hornblende constitutes the dominant mafic phase. Because of its proximity to the, then recognized, "Jamestown Plutonic Complex" these authors considered that the Kaap Valley Granite was actually the acid phase of the former and that the two together, represented a miniature prototype of the Bushveld Igneous Complex.

A subsequent re-examination of the Kaap Valley tonalite was carried out by Anhaeusser (1969) who recognized that the latter was intrusive into the enveloping greenstone supracrustal sequences and was, therefore, directly responsible for their deformation. He also recognized the sodic nature of this granite (*sensu lato*) and was the first to suggest that it be called a "tonalite". Although Anhaeusser (1969) genetically divorced the Kaap Valley tonalite from the supracrustals in the Jamestown Schist Belt, he attributed its mafic character (relative to trondhjemites of somewhat similar composition in other parts of the Barberton Mountain Land) to stoping and assimilation of

significant amounts of the mafic and ultramafic supracrustal rocks through which it apparently intruded. Thus the amphibole component of the rock was assumed to have been derived directly from mafic and ultramafic rocks with which the intruding acid magma had interacted.

A U-Pb isotope study on zircons from the Kaap Valley tonalite was carried out by Oosthuyzen (1970). This yielded an age of 3310 ± 40 m.y. for the body and placed it amongst the oldest granitic events in the region.

Prior to the present study, therefore, the Kaap Valley pluton was considered as one component of the tonalite and trondhjemite gneiss suite which represents the dominant unit in the first granitic magmatic cycle envisaged in the Barberton Mountain Land. In terms of crustal evolution, the body was considered to form one of the earliest components of sialic crust probably derived by down-sagging and anatexis of earlier developed simatic material (Anhaeusser, 1973). The object of this study is to consider in detail the geology, chemistry and mode of formation of the Kaap Valley pluton, in the light of these thoughts.

2. GEOLOGICAL AND CHEMICAL CHARACTERISTICS

2.1. Geology and petrography

This study was initiated when the Kaap Valley body was mapped on a regional scale with the aid of 1:30 000 aerial photographs. This process was accompanied by petrographic examination and chemical analysis of samples collected systematically across the pluton. Details of the geology and the distribution of sample localities are presented in Figure 52. This map shows the significant geological features of the area as well as the newly recognized sub-divisions within the Kaap Valley tonalite pluton itself.

For the most part, the Kaap Valley tonalite is underlain by terrain that is flat and featureless except for occasional ridges demarcating the outcrops of Proterozoic diabase dykes. Likewise, the tonalite itself has a remarkably homogeneous texture and appearance with the only discernible variations being due to fluctuations in the mafic content of the rock (see later). A topographically distinct diabase dyke, known as the Devils Knuckles dyke, trends in a northwesterly direction (from just north of

Figure 52 : Geological map of the Kaap Valley tonalite pluton.

sample locality LKV24 in Figure 52) and forms a resistant buttress with respect to the tonalite that outcrops to its southwest. As a result, this region is up to 750 m higher in elevation than the remainder of the pluton to the northeast of the dyke. Initially it was hoped that this topographic step might facilitate a three-dimensional view of this granite body, but the tonalites on either side of the dyke are indistinguishable both compositionally and texturally.

Mapping in the Kaap Va egion has led to the recognition of four granitic subdivisions, three of which are considered to constitute the Kaap Valley tonalite per se, and the fourth which is probably not correlatable with the latter. The Kaap Valley tonalite is subdivided into a hornblende-bearing phase and a hornblende + biotite-bearing phase; in addition the body contains numerous dykes and veins of medium-to-fine-grained tonalite which possess similar mineral constituents to the granite which they intrude (Plate 7D). As illustrated in Figure 52 the main development of hornblende tonalite occurs in a discrete crescentic zone centred around the town of Barberton, whereas the more abundant hornblende + biotite tonalites dominate the remainder of the area. Two smaller areas of hornblende tonalite also occur in the northwest quadrant of the pluton (Figure 52). In the field the distinction between these two subdivisions is not easily discernible on the basis of mineralogy alone, but, rather, by the overall mafic content of the rock. The hornblende tonalites are decidedly more mafic than the hornblende + biotite tonalites and had it not been for the presence of biotite in the latter phase, a colour index could have been used to distinguish them.

The fourth subdivision referred to above has been named the Goede Hoop trondhjemite (Figure 52). This body occurs in a poorly exposed region in the far west-central portion of the map area, where a pronounced embayment of the Transvaal Supergroup cover rocks is developed. The Goede Hoop trondhjemite does not contain hornblende nor is it as mafic as the Kaap Valley tonalite. It is also intruded by numerous aplite-like veins with a similar composition to the host rock but which bear no physical resemblance to the fine-grained tonalite dykes that are associated with the Kaap Valley pluton.

The Kaap Valley pluton, therefore, consists dominantly of a homogeneous tonalite which can be categorized into hornblende- and hornblende

+ biotite-bearing phases. The former phase is considerably more mafic than the latter. Finer-grained tonalitic veins intrude the Kaap Valley tonalite over a widespread area (Figure 52) but these are volumetrically insignificant. A poorly exposed area in the west-central part of the pluton contains trondhjemitic rocks which are probably genetically unrelated to the Kaap Valley tonalite.

The hornblende-tonalite phase contains an average of 21,5% normative mafic minerals (data from Table 21) and consists principally of plagioclase, euhedral hornblende and quartz (Plate 7A) with no biotite present except in sample SKV18 (Figure 52) where a small amount of this mineral is found. The plagioclase generally occurs as euhedral laths which are extensively sericitized and zoned. The calcic interiors of the plagioclase (see later) are often preferentially sericitized but oscillatory zoning is commonplace. Hornblende invariably occurs as euhedral grains which are commonly poikilitic, with small inclusions of quartz and felspar (Plate 7B). Occasionally, hornblende grains appear to have grown around smaller grains of quartz and plagioclase suggesting a mineral paragenesis whereby the latter two minerals started crystallizing somewhat before the hornblende. An examination of the tonalitic phase relationships presented in Figure 63 shows that plagioclase may crystallize before hornblende at pressures less than 4,5kb. However, according to this diagram it is unlikely that quartz will do the same, so that it is uncertain whether the textures in Plates 7 A-C reflect a real mineral paragenesis or an optical illusion caused by two dimensional effects. Some samples of the hornblende tonalite, particularly those that occur close to the sheared margins of the pluton, are extensively altered. Alteration manifests itself in the total sericitization of plagioclase and the breakdown of hornblende to epidote or chlorite and magnetite. In addition, incipient micro-fractures in the rock are occasionally filled with calcite which may be derived from the breakdown of hornblende in the presence of CO_2. In unaltered samples, small amounts of interstitial microcline may occur; accessory minerals usually include apatite, sphene and magnetite.

The less mafic hornblende + biotite tonalites contain an average of 15,5% normative mafic minerals (data from Table 21). These rocks have identical petrographic characteristics to those described above with the exception that the majority of them contain variable quantities of primary

PLATE 7

A. Photomicrograph showing the typical interstitial nature of twinned, euhedral hornblende (hbl*de) surrounded by quartz (qtz) and plagioclase (plag) grains in the Kaap Valley tonalite. The photograph was taken under crossed polars; the bar represents a length of 0,5 mm. The same conditions and scale apply to the photomicrographs in B and C below.

B. Euhedral hornblende crystal from the Kaap Valley tonalite showing typical poikilitic texture with inclusions of quartz.

C. Large subhedral hornblende (hbl*de) grain that appears to have grown around slightly smaller grains of quartz (qtz) and sericitized plagioclase (plag). Although it is feasible for plagioclase to crystallize before hornblende at pressures less than 4-5 kb (see phase relationships in Figure 63) it is not likely that quartz will do so, suggesting that the relationship seen in B and C may be the result of a two-dimensional illusion.

D. Photograph showing a fine-grained tonalitic dyke intrusive into coarser-grained Kaap Valley tonalite at locality SKV30 (Figure 53); the dyke is approximately on metre in width.

E. Sheared contact between the Kaap Valley tonalite and chloritic schists of the Barberton greenstone belt in the vicinity of sample locality LKV33 (Figure 52). No direct evidence exists at this locality for the igneous intrusion of the tonalite into the greenstone belt assemblage.

F. Amphibolitic xenolith enveloped by Kaap Valley tonalite at sample locality LKV5 (Figure 52). It is not certain whether remnants of this nature represent greenstone xenoliths or entrained cognate xenoliths from the tonalitic source region.

PLATE 7

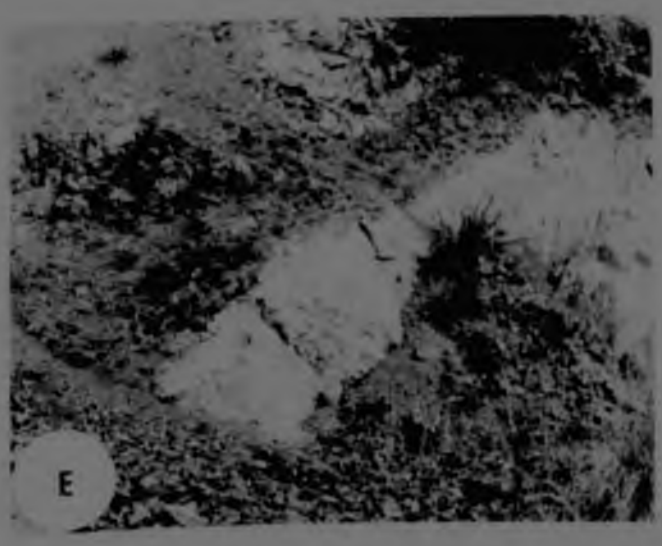

biotite. A few samples (SKV1, LKV 30, SKV 26, SKV6) do not contain biotite but have lower mafic contents, which justifies their inclusion in the hornblende + biotite phase (see later). The hornblende + biotite tonalites contain plagioclase, quartz, hornblende, biotite and minor microcline as their dominant assemblage; the ratio hornblende/biotite varies and in some instances (i.e. samples LKV 11, LKV 15A, LKV 10 and LKV 21) biotite exceeds hornblende. Generally however the reverse is true. Hornblende is significantly less abundant in the hornblende + biotite tonalites and generally occurs as smaller grains; it is still markedly poikilitic and invariably occurs interstitially with respect to plagioclase. Primary hornblende and biotite often appear juxtaposed. The outlines of hornblende grains in both phases are invariably euhedral-to-subhedral and there is absolutely no indication that they have been derived from a mafic precursor as the result of assimilation. The latter process is usually characterized by corroded grain boundaries and reaction rims suggesting equilibration of high-temperature mineral phases with felsic magma (see Chapter 3).

As mentioned above, the finer grained tonalitic dykes and veins are mineralogically similar to the tonalites that they intrude. Most of the tonalite dykes contain hornblende and biotite with the exception of LKV 9 which contains no hornblende; it is the only sample from the Kaap Valley tonalite suite that is characterized by the presence of biotite *without* hornblende.

The Goede Hoop trondhjemite consists dominantly of plagioclase and quartz with minor biotite that has been extensively altered to chlorite. This rock contains no hornblende and, as such, cannot be correlated with the Kaap Valley pluton. Where exposed the trondhjemite contains numerous anastomosing finer-grained, pinkish veins which contain similar constituents, and have similar compositions, to the host rock.

The Kaap Valley tonalite is characterized in most places, by a moderately well-developed mineral fabric which is undoubtedly more pronounced along the margins of the body than in the centre (Figure 52). A mineral lineation is also occasionally present, the orientation of which is usually sub-parallel to lineations observed in schistose rocks from adjacent greenstone successions (Anhaeusser, 1969; 1976b). In general, foliations

in the Kaap Valley tonalite are sub-parallel to the granite-greenstone contact (see Figure 52), suggesting that both units have been penecontemporaneously deformed during at least part of their structural histories. In the centre of the pluton, deformation fabrics are weakly developed or apparently non-existent and have random orientations. Another major structural fabric in the area is the dominantly northwesterly orientation of Proterozoic dykes and shear zones over the pluton. Dykes and shear zones are commonly juxtaposed (Figure 52) suggesting that the emplacement of the former may have been related to a regional stress inherent in the crust at that time. The orientation of dyke swarms at right-angles to the dominant axes of greenstone belts is a feature commonly commented upon. Halls (1978) has suggested that this orthogonal relationship may be explained by horizontal crustal compression such that the orientation of maximum principal stress is parallel to the direction of preferred dyke emplacement.

The Kaap Valley tonalite contains many mafic and ultramafic xenoliths, only the larger ones being illustrated in Figure 52. These are generally serpentinitic or amphibolitic in nature and can readily be related to similar lithologies within the greenstone belt. Numerous smaller mafic remnants also occur, however, and these are usually amphibolitic and appear to have undergone various degrees of assimilation (Plate 7F). One such xenolith (LKV 31) consists dominantly of poikilitic hornblende (as in the Kaap Valley tonalite) with lesser amounts of interstitial plagioclase and quartz. This sample, as with many similar ones within the tonalite, could possibly represent cognate xenoliths (i.e. residual material from the source region) rather than remnants merely rafted off from the adjacent supracrustal rocks.

The contact of the Kaap Valley pluton with the surrounding Barberton greenstone belt is generally not well-exposed; in the past a limited amount of evidence has indicated that the body was magmatically intruded into the greenstones and discrete felsic veins have been observed in the latter (Anhaeusser, 1966). However, most contacts are highly sheared (Plate 7E) and show no evidence of magmatic intrusion, suggesting that the emplacement of the Kaap Valley tonalite, at least to its present position, was accomplished in the solid state. Thus, minor felsic veining could be attributed to filter-pressing during emplacement, whilst contact metamorphic effects might be the result of the combined action of shear stresses and the

heat emitted from a, still hot, solid plutonic body. Effects such as these have been attributed to diapirism (*sensu stricto*) in the Archaean terranes of Canada (Drury, 1977; Fyson, et al., 1978; Schwerdtner, 1978; Schwerdtner et al., 1978, 1980 in press) and are discussed again in a later section of this chapter.

2.2. Major element chemistry

A total of 51 samples of the Kaap Valley pluton and related phases, were collected and analysed for major elements as part of this study. These analyses were carried out using X-ray fluorescence techniques and a description of the relevant procedures, together with an evaluation of the analytical uncertainties, is presented in Appendix 1. The major element data is presented in Table 21.

It is evident, from the position of certain sample localities (Figure 52), that many of the analyses presented here may be subject to contamination resulting from the proximity of, either mafic dykes, or shear zones. Dykes may be expected to influence the magnesium and iron contents of granitic rocks in their immediate vicinity and many workers have noted significant changes in SiO_2 and K_2O contents of granitic material subjected to shearing/mylonitization (Visser and Verwoerd, 1960; Beach and Fyfe, 1972; Robb, 1978). It is important, therefore, to assess the likelihood of such changes in the case of certain Kaap Valley tonalite samples.

The effect of shearing on these tonalites can be gauged by comparing an analysis of sample LKV 30 (an unaltered tonalite) with that of LKV 30A, which was collected from the vicinity of a shear zone. The latter sample was collected from within 50 metres of the unaltered tonalite outcrop and is characterized by a glassy mylonitic texture. A comparison of these two analyses in Table 21 shows that small chemical differences do occur (particularly in CaO and Na_2O) but these are insignificant by comparison with inter-sample variation. The trace elements Rb, Sr and Ba, likewise, appear to have remained relatively immobile during shearing. The effects of contamination by mafic dykes in the Kaap Valley tonalite appear, however, to be slightly more pronounced and these are demonstrated by comparing samples SKV 33 and SKV 34 in Table 21. The former sample is taken from within 2 metres of the Devil's Knuckles dyke whereas the latter is considerably removed from its influence. Although SKV 33 contains

TABLE 21

CHEMICAL ANALYSES OF SAMPLES FROM THE KAAP VALLEY TONALITE PLUTON AND RELATED PHASES

		ψ	ψ	*	*	*	*	fg	*	*
		LKV 1	LKV 2	LKV 3	LKV 4	LKV 5	LKV 6	LKV 9	LKV10	LKV11
Wt.%	SiO_2	64,11	63,63	64,12	66,94	65,07	68,37	72,71	65,25	66,98
	TiO_2	0,52	0,58	0,49	0,44	0,48	0,36	0,22	0,47	0,43
	Al_2O_3	15,90	15,03	15,98	15,25	15,47	15,12	14,41	16,41	16,18
	Fe_2O_3*	4,81	5,28	4,09	3,86	4,03	3,15	1,70	3,91	3,49
	MnO	0,02	0,06	0,09	0,01	0,01	<0,01	<0,01	0,09	0,10
	MgO	3,14	3,12	2,36	2,22	2,14	1,81	0,78	2,25	1,98
	CaO	4,67	5,04	4,48	3,61	4,23	3,04	2,18	4,56	4,30
	Na_2O	4,62	4,72	5,79	5,06	5,52	5,85	6,04	5,38	4,63
	K_2O	1,12	1,71	1,26	1,74	1,37	1,90	1,70	1,42	1,30
	P_2O_5	0,18	0,21	0,18	0,18	0,15	0,13	0,10	0,18	0,17
	L.O.I.	1,91	1,52	1,58	1,76	1,25	1,12	1,32	1,01	0,81
	TOTALS	101,00	100,90	100,42	101,07	99,72	00,86	101,17	100,66	100,08
ppm	Rb	53	74	50	73	64	51	55	66	63
	Sr	574	576	628	573	609	467	534	659	621
	Ba	327	479	424	466	390	148	259	424	401
Wt.%	Qtz	21,6	14,7	13,0	22,7	15,9	18,7	23,9	16,5	26,9
	Ab	39,5	40,3	49,5	43,0	47,4	49,5	52,8	45.6	39,2
	Or	0,0	9,5	7,2	5,2	7,9	10,2	10,0	6,7	0,2
	An	17,7	6,8	7,7	11,7	7,7	5,4	4,7	10,8	19,7
	Hblde	6,6	24,9	19,9	7,5	18,4	13,0	6,3	15,6	0,8
	Biot	10,0	3,0	0,4	7,7	0,4	1,6	0,0	2,6	11,3
	Opx	2,1	0,0	0,0	0,0	0,0	0,0	1,3	0,0	0,0
	Mgt	2,2	2,4	1,9	1,8	1,8	1,4	0,8	1,8	1,6
	Ap	0,3	0,4	0,3	0,3	0,3	0,2	0,2	0,3	0,3

(Analyst: L.J. Robb

Fe_2O_3* - Total iron as Fe_2O_3)

ψ Hornblende tonalites
* Hornblende + biotite tonalites
fg Fine-grained tonalite dykes

Sample localities presented in Figure 52

TABLE 21 (Continued)

		*	fg	st	*	fg		*	*	*
		LKV12	LKV13	LKV14	LKV15A	LKV15B	LKV16	LKV17	LKV18	LKV20
Wt.%	SiO_2	63,95	63,70	67,01	69,59	67,85	63,45	66,36	63,59	68,51
	TiO_2	0,59	0,42	0,40	0,32	0,36	0,53	0,47	0,47	0,45
	Al_2O_3	15,53	17,50	15,69	15,66	15,95	16,19	15,30	16,49	15,20
	Fe_2O_3*	4,76	3,10	3,59	2,80	2,77	4,70	3,62	4,28	3,65
	MnO	0,09	0,01	0,10	0,06	<0,01	0,06	<0,01	0,06	0,09
	MgO	2,47	2,08	2,10	1,46	0,97	2,92	2,15	2,44	2,18
	CaO	4,35	3,74	3,74	3,46	3,78	4,77	4,18	4,14	4,01
	Na_2O	5,56	6,43	5,24	5,79	6,61	4,87	5,23	5,17	4,89
	K_2O	2,03	0,79	0,98	0,67	0,98	0,91	0,71	1,23	1,70
	P_2O_5	0,19	0,14	0,13	0,14	0,15	0,23	0,18	0,20	0,17
	L.O.I.	1,26	2,04	2,19	1,43	1,18	1,63	1,91	1,55	0,65
	TOTALS	100,78	99,95	101,17	101,29	100,06	100,26	100,11	99,62	101,50
ppm	Rb	81	5	46	39	46	41	31	29	47
	Sr	511	760	706	639	731	734	616	631	551
	Ba	369	196	212	261	178	457	389	386	219
Wt.%	Qtz	11,0	14,7	24,8	26,4	17,0	19,8	23,8	20,2	23,4
	Ab	47,4	55,4	44,8	48,2	56,2	41,8	45,0	44,6	41,0
	Or	12,1	0,0	0,0	0,0	5,8	0,0	0,0	0,0	6,7
	An	4,6	16,7	15,5	14,9	8,7	18,3	13,8	18,3	10,9
	Hblde	21,5	1,8	3,5	2,0	7,9	6,2	8,8	1,9	11,2
	Biot	0,0	7,1	8,8	5,9	0,0	8,2	6,4	11,1	4,9
	Opx	0,0	2,4	0,9	1,2	0,0	3,1	0,2	1,5	0,0
	Mgt	2,2	1,4	1,6	1,3	1,3	2,2	1,7	2,0	1,6
	Ap	0,4	0,3	0,2	0,2	0,3	0,4	0,3	0,4	0,3

st - sheared tonalite

TABLE 21 (Continued)

		*	*	*	*	fg	GHT	GHT	*	*
		LKV21	LKV23	LKV24	LKV25	LKV27	LKV28	LKV28A	LKV29	LKV30
Wt.%	SiO_2	64,40	66,24	64,20	61,75	64,99	72,07	68,98	68,74	65,53
	TiO_2	0,49	0,42	0,42	0,64	0,16	0,12	0,26	0,39	0,47
	Al_2O_3	16,27	15,90	14,98	15,34	15,74	15,16	14,79	15,18	15,15
	Fe_2O_3*	4,47	3,52	3,86	5,46	4,07	0,94	1,70	3,38	2,91
	MnO	0,06	<0,01	0,14	0,12	0,06	0,02	0,03	0,08	0,08
	MgO	2,50	1,75	2,26	3,61	2,02	0,60	0,83	1,87	2,26
	CaO	4,67	3,72	2,86	4,37	4,33	1,39	1,72	3,87	4,14
	Na_2O	5,18	5,73	6,86	4,10	6,53	6,34	6,77	5,10	5,29
	K_2O	1,50	0,77	1,23	1,81	1,19	2,26	1,48	1,42	1,28
	P_2O_5	0,20	0,14	0,20	0,28	0,15	0,07	0,09	0,14	0,16
	L.O.I.	1,01	1,48	1,64	2,21	1,31	1,01	2,40	1,12	1,67
	TOTALS	100,75	99,67	98,55	99,69	100,55	99,98	99,05	101,29	99,32
ppm	Rb	51	23	35	67	42	47	52	40	59
	Sr	654	614	529	536	579	436	421	533	601
	Ba	423	216	259	795	173	286	246	247	241
Wt.%	Qtz	16,7	22,0	10,2	21,6	11,5	24,6	20,5	24,0	19,2
	Ab	43,9	49,3	60,9	40,0	55,8	53,8	59,0	43,0	45,9
	Or	5,4	0,0	7,6	0,0	7,1	11,1	8,0	5,7	6,4
	An	12,5	14,3	0,1	17,0	6,3	6,5	4,1	11,2	9,4
	Hblde	13,8	5,1	18,3	5,3	12,7	0,0	5,9	10,3	15,5
	Biot	5,2	6,9	0,0	16,6	0,0	3,4	1,5	4,0	2,0
	Opx	0,0	0,0	0,0	0,4	4,4	0,0	0,0	0,0	0,0
	Mgt	2,0	1,6	1,8	2,6	1,9	0,4	0,8	1,5	1,3
	Ap	0,4	0,3	0,4	0,5	0,3	0,1	0,2	0,2	0,3

GHT - Goede Hoop trondhjemite phase

TABLE 21 (Continued)

		st	ACX	*	*	*	*	*	*	ψ
		LKV30A	LKV31	SKV 1	SKV 2	SKV 5	SKV 6	SKV 8	SKV 9	SKV12
Wt.	SiO_2	64,76	53,60	64,83	63,87	68,96	66,68	65,76	63,22	62,96
	TiO_2	0,46	0,42	0,45	0,45	0,36	0,42	0,43	0,51	0,56
	Al_2O_3	15,30	11,69	15,96	15,28	14,98	15,27	15,52	15,10	15,29
	Fe_2O_3*	3,68	11,30	3,91	3,85	3,11	3,59	4,29	4,38	4,61
	MnO	0,01	0,18	0,09	0,08	0,05	0,01	0,12	0,01	0,12
	MgO	2,22	9,27	2,20	1,65	1,64	1,94	2,09	2,98	3,24
	CaO	3,07	9,53	4,30	3,54	2,93	3,59	4,35	3,72	4,03
	Na_2O	4,73	3,12	4,60	6,53	5,29	5,52	4,86	5,42	4,70
	K_2O	1,60	1,18	1,80	1,65	2,36	1,96	1,89	1,72	0,65
	P_2O_5	0,16	0,01	0,18	0,19	0,14	0,13	0,18	0,17	0,18
	L.O.I.	3,89	0,70	2,12	1,96	1,40	1,64	1,79	1,80	2,44
	TOTALS	99,88	101,00	100,44	99,25	101,22	100,75	101,28	99,03	98,78
ppm	Rb	65	49	68	62	83	65	74	70	39
	Sr	297	129	615	628	438	635	564	523	615
	Ba	223	116	494	468	403	453	393	354	157
Wt.	Qtz	25,9	-	21,9	10,5	22,0	17,0	18,9	15,3	20,9
	Ab	42,1	-	39,6	57,0	44,7	47,1	41,4	47,1	41,8
	Or	1,0	-	5,3	10,0	11,4	11,2	9,3	6,4	0,0
	An	14,9	-	15,6	3,5	7,5	6,1	10,4	7,3	19,5
	Hblde	0,0	-	7,2	13,7	8,9	16,1	14,8	15,5	9,3
	Biot	13,4	-	[illegible],3	0,0	3,8	0,6	2,9	6,1	6,1
	Opx	0,0	-	0,0	3,1	0,0	0,0	0,0	0,0	0,0
	Mgt	1,7	-	1,8	1,8	1,4	1,6	1,9	2,0	2,2
	Ap	0,3	-	0,03	0,4	0,2	0,2	0,3	0,3	0,3

ACX - Amphibolitic cognate xenolith

TABLE 21 (Continued)

		ψ SKV13	ψ SKV14	ψ SKV15	ψ SKV18	ψ SKV20	ψ SKV21	SKV22	ψ SKV25A	ψ SKV26
Wt.%	SiO_2	68,50	62,57	64,75	63,18	60,51	59,98	63,13	62,07	65,64
	TiO_2	0,51	0,54	0,52	0,50	0,57	0,60	0,45	0,55	0,50
	Al_2O_3	16,09	15,44	15,41	16,03	16,31	15,75	14,00	15,82	15,50
	Fe_2O_3*	4,43	5,04	4,56	4,38	4,56	5,28	3,95	5,28	4,47
	MnO	0,05	0,05	0,08	0,05	0,06	0,14	<0,01	0,12	0,01
	MgO	2,61	3,15	2,94	2,27	3,27	3,25	2,28	3,42	2,46
	CaO	4,26	4,79	4,67	4,53	4,32	5,12	4,63	5,24	4,27
	Na_2O	6,24	4,91	4,44	6,04	5,31	5,63	5,17	4,80	5,59
	K_2O	1,90	1,65	1,48	0,86	1,20	1,62	1,43	1,12	0,93
	P_2O_5	0,18	0,22	0,18	0,18	0,19	0,24	0,16	0,21	0,16
	L.O.I.	1,81	1,87	1,14	1,95	3,47	1,81	5,34	1,89	1,41
	TOTALS	100,58	100,23	100,17	99,97	99,61	99,42	100,54	100,52	100,94
ppm	Rb	78	58	65	47	48	61	50	57	45
	Sr	503	506	571	634	570	610	332	660	598
	Ba	405	390	308	193	191	534	258	227	182
Wt.%	Qtz	6,5	14,7	21,5	11,5	14,6	5,3	16,2	15,5	18,2
	Ab	53,5	42,3	38,2	52,6	47,0	49,3	46,0	41,6	47,5
	Or	11,4	6,7	3,5	5,2	0,0	9,9	8,9	2,5	2,9
	An	3,8	9,6	13,7	7,5	14,7	4,4	6,3	12,3	9,6
	Hblde	20,6	19,1	12,6	20,4	9,4	26,4	15,9	18,9	15,5
	Biot	0,0	4,8	8,0	0,0	11,1	0,0	0,0	6,4	3,9
	Opx	1,8	0,0	0,0	0,3	0,7	0,0	4,6	0,0	0,0
	Mgt	2,0	2,3	2,1	2,0	2,2	2,5	1,9	2,4	2,0
	Ap	0,3	0,4	0,3	0,3	0,4	0,5	0,3	0,4	0,3

TABLE 2: (Continued)

		*	*	fg	*	*	ψ
		SKV28	SKV29	SKV30C	SKV33	SKV34	SKV38
Wt.%	SiO_2	65,55	66,30	66,49	65,39	64,00	62,06
	TiO_2	0,46	0,44	0,46	0,46	0,44	0,51
	Al_2O_3	15,50	15,61	16,07	15,61	15,66	15,08
	Fe_2O_3*	3,85	3,63	3,63	4,09	3,99	4,66
	MnO	0,10	0,04	0,01	0,04	0,06	0,06
	MgO	2,14	2,00	2,08	2,43	1,89	2,84
	CaO	3,58	3,84	4,05	4,28	4,18	5,19
	Na_2O	6,17	4,58	5,33	5,88	6,44	4,89
	K_2O	1,03	1,21	0,96	0,56	1,28	1,60
	P_2O_5	0,16	0,16	0,17	0,20	0,20	0,21
	L.O.I.	2,32	1,39	1,45	1 65	1,57	2,59
	TOTALS	100,86	99,20	100,70	100,59	99,71	99,69
ppm	Rb	49	53	54	42	64	69
	Sr	635	611	637	613	574	750
	Ba	214	457	294	204	307	358
Wt.%	Qtz	15,5	27,5	23,1	18,1	10,4	12,6
	Ab	43,4	39,9	45,3	50,3	56,0	43,0
	Or	4,5	0,0	0,0	0,7	7,8	9,8
	An	6,5	18,5	16,2	10,1	5,4	7,3
	Hblde	15,4	0,0	4,3	14,7	14,5	22,5
	Biot	2,5	11,0	8,5	4,0	0,0	0,0
	Opx	0,0	0,9	0,6	0,0	3,7	2,0
	Mgt	1,8	1,7	1,6	1,9	1,9	2,2
	Ap	0,3	0,3	0,3	0,4	0,4	0,4

TABLE 21 (Continued)

		*	*	fg	*	*	ψ
		SKV28	SKV29	SKV30C	SKV33	SKV34	SKV38
Wt.%	SiO_2	65,55	66,30	66,49	65,39	64,00	62,06
	TiO_2	0,46	0,44	0,46	0,46	0,44	0,51
	Al_2O_3	15,50	15,61	16,07	15,61	15,66	15,08
	Fe_2O_3*	3,85	3,63	3,63	4,09	3,99	4,66
	MnO	0,10	0,04	0,01	0,04	0,06	0,06
	MgO	2,14	2,00	2,08	2,43	1,89	2,84
	CaO	3,58	3,84	4,05	4,28	4,18	5,19
	Na_2O	6,17	4,58	5,33	5,88	6,44	4,89
	K_2O	1,03	1,21	0,96	0,56	1,28	1,60
	P_2O_5	0,16	0,16	0,17	0,20	0,20	0,21
	L.O.I.	2,32	1,39	1,45	1,65	1,57	2,59
	TOTALS	100,86	99,20	100,70	100,59	99,71	99,69
ppm	Rb	49	53	54	42	64	69
	Sr	635	611	637	613	574	750
	Ba	214	457	294	204	307	358
Wt.%	Qtz	15,5	27,5	23,1	18,1	10,4	12,6
	Ab	43,4	39,9	45,3	50,3	56,0	43,0
	Or	4,5	0,0	0,0	0,7	7,8	9,8
	An	6,5	18,5	16,2	10,1	5,4	7,3
	Hblde	15,4	0,0	4,3	14,7	14,5	22,5
	Biot	2,5	11,0	8,5	4,1	0,0	0,0
	Opx	0,0	0,9	0,6	0,0	3,7	2,0
	Mgt	1,8	1,7	1,6	1,9	1,9	2,2
	Ap	0,3	0,3	0,3	0,4	0,4	0,4

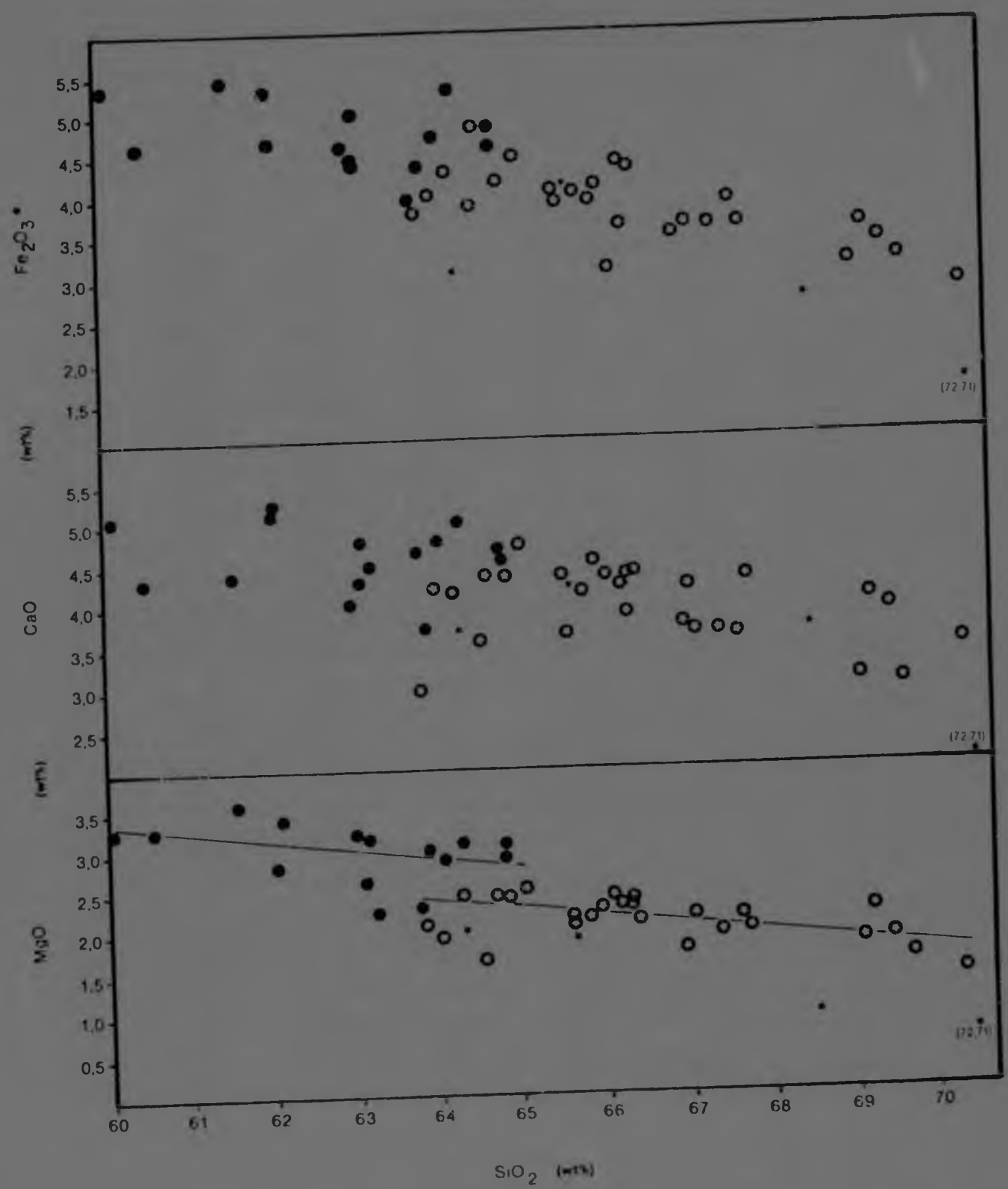

Figure 53 : *Selected Harker plots for samples from the Knap Valley tonalite pluton. Dots represent hornblende tonalites, encircled stars represent hornblende + biotite tonalites and asterisks represent the fine-grained tonalitic dykes. Data is from Table 21. The value (72,71) refers to the SiO_2 content of one of the tonalitic dykes which falls outside the range shown in the diagram. Approximate best-fit lines are drawn through the hornblende and hornblende + biotite tonalite trends in the MgO v SiO_2 plot, in order to emphasize the difference between the two phases.*

more silica than SKV 34 it nevertheless has a higher Fe_2O_3* + MgO content. As tonalite compositions generally experience a decrease in iron and magnesium with increasing silica, it is not unreasonable to suggest that sample SKV 33 has been affected by its close proximity to the dyke. Although variations in the trace element contents of the two samples occur, these can be seen to be insignificant in terms of inter-sample variations. These considerations indicate that it is unlikely that either mafic dykes or mylonitized shear zones have appreciably affected inter-sample chemical variations, particularly in view of the fact that the samples were usually collected away from the influence of such features and generally showed no signs of alteration whatsoever.

In the preceding section the two broad subdivisions of the Kaap Valley tonalite were described and differentiated in the field on the basis, firstly, of mafic content and secondly, on the presence of biotite. The major element chemistry of the body as a whole provides a third diagnostic criterion whereby the hornblende tonalites may be differentiated from the hornblende + biotite tonalites. Variations in the composition of the Kaap Valley pluton are best illustrated in the form of Harker diagrams in Figure 53. These plots are informative in that they again serve to distinguish between the two tonalitic sub-groups. Particularly well shown in the Fe_2O_3*, CaO, MgO and Al_2O_3 v SiO_2 diagrams is the fact that a distinct compositional hiatus is apparent between the hornblende and hornblende + biotite tonalites. This break defines the hornblende tonalites as generally having SiO_2 < 64,75%, MgO > 2,5% and Fe_2O_3* > 4,5% whereas the less mafic hornblende + biotite tonalites have silica in the range of 65 - 70% and distinctly lower iron and magnesium contents. The systematic variation in major element composition in the dominant rocks of the Kaap Valley pluton is considered to have important petrogenetic significance and this topic is discussed more fully in a later section.

Although volumetrically insignificant, it is interesting to compare the chemistry of the fine-grained tonalitic dykes and veins with that of the hornblende and hornblende + biotite tonalitic phases. The tonalitic dykes (i.e. samples LKV 9, LKV 13, LKV 15B and LKV 27) have compositions that are similar to the hornblende + biotite tonalites (i.e. with SiO_2 on the range 65 - 72%) but with significantly lower (Fe_2O_3* + MgO) and TiO_2 contents (Figure 53). These trends, together with features such as their similar mineralogical character and their

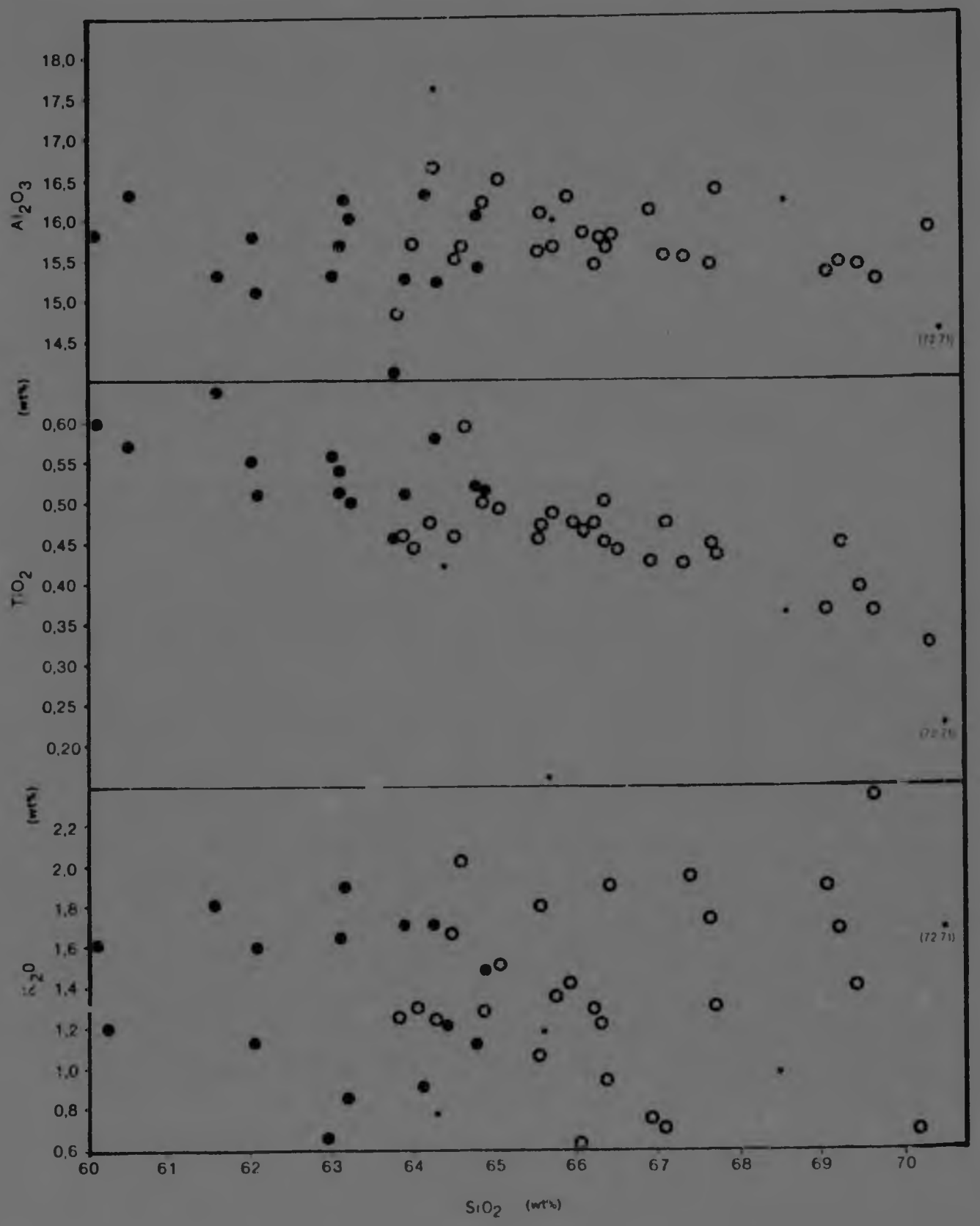

Figure 53 (continued) :

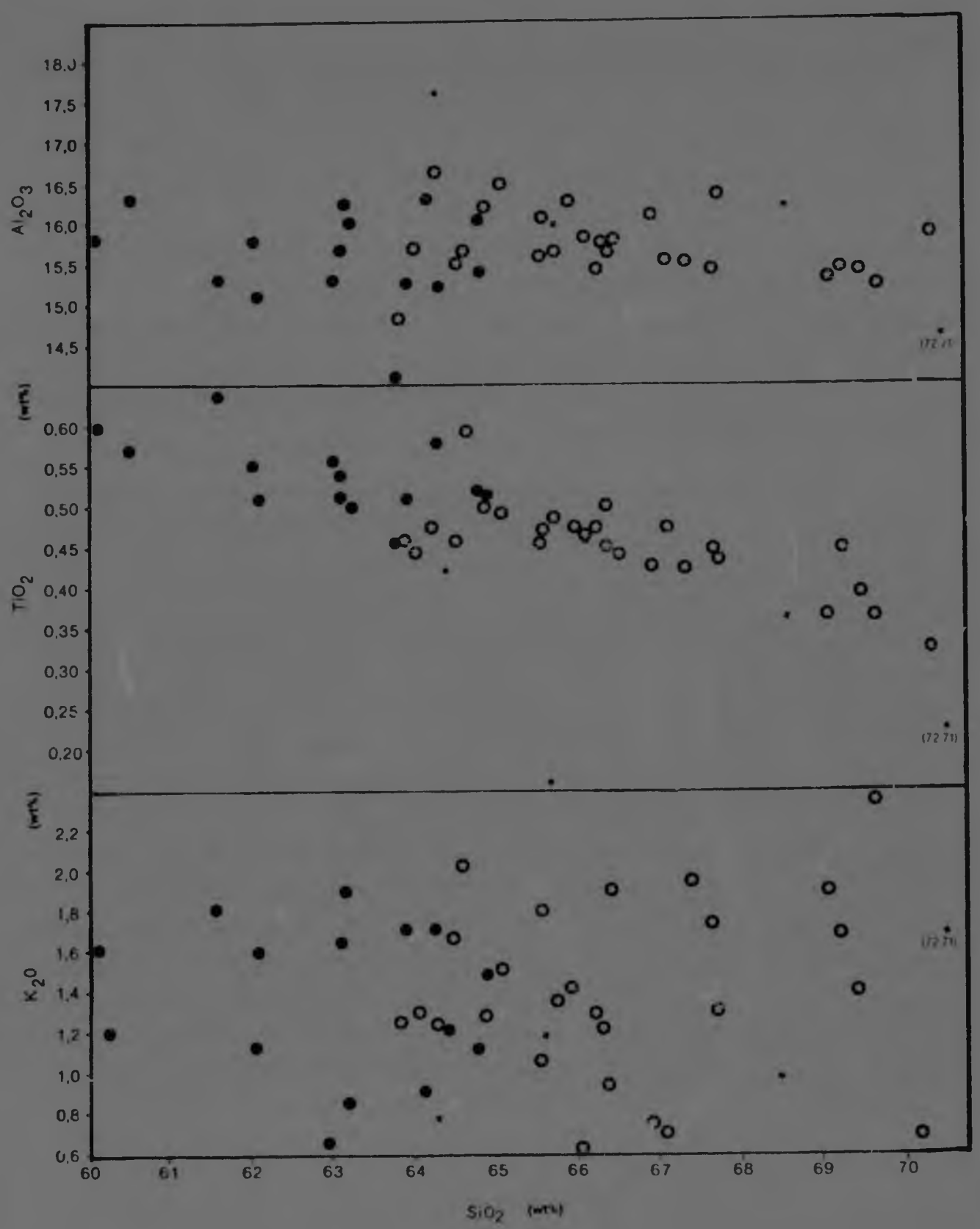

Figure 5.3 (continued) :

emplacement as dykes, suggest that they are probably cogenetic with the main phases of the Kaap Valley tonalite but represent a more felsic differentiated liquid intruded soon after the final emplacement of the pluton as a whole. However, the tonalite dykes are not preferentially enriched in incompatible phases such as K_2O and Rb and, as a result, this suggestion awaits verification with more detailed work.

The Goede Hoop trondhjemitic phase is characterized by high SiO_2 (70 . 73%), low mafics and a high Na_2O content (6 - 7%) in comparison to the typical Kaap Valley tonalites (Table 21). These facts, together with the distinctive nature of the rocks in the field, render it unlikely that they are genetically related in any way to the Kaap Valley pluton.

2.3. Trace element (Rb, Sr and Ba) chemistry

The concentrations of Rb, Sr and Ba were determined for all the samples that were analysed for major elements and these results are also listed in Table 21. The trace element characteristics of the Kaap Valley tonalite are illustrated in Rb v Sr and Rb v Ba diagrams in Figure 54. Unlike the major elements, these particular trace elements do not serve to distinguish between the hornblende tonalites and the hornblende + biotite tonalites and a complete overlap is evident. In addition, trends on both plots are somewhat obscure and a wide range of concentrations occur. In the Rb v Sr plot in particular, five samples are seen to be widely scattered and this can probably be attributed to element mobility resulting from alteration (sericitization and saussuritization) in certain of the samples analysed. The Rb, Sr and Ba contents of the finer-grained tonalitic dykes are also plotted on Figure 54, and are essentially indistinguishable from the tonalitic host rocks. No case can be made for an enrichment of incompatible elements (i.e. Rb and Ba) that might indicate a differentiated origin for these dykes.

In spite of the wide scatter of data points illustrated in Figure 54 it is nevertheless possible to detect a broad positive relationship between Rb and Ba and a contrasting inverse relationship between Rb and Sr. These relationships may be related to the petrogenesis of the suite and are discussed again in a later section. It is important to note, too, that Rb/Sr ratios remain relatively constant over the pluton as a whole, in spite of fairly significant variations in the Rb content (23 - 83 ppm). The

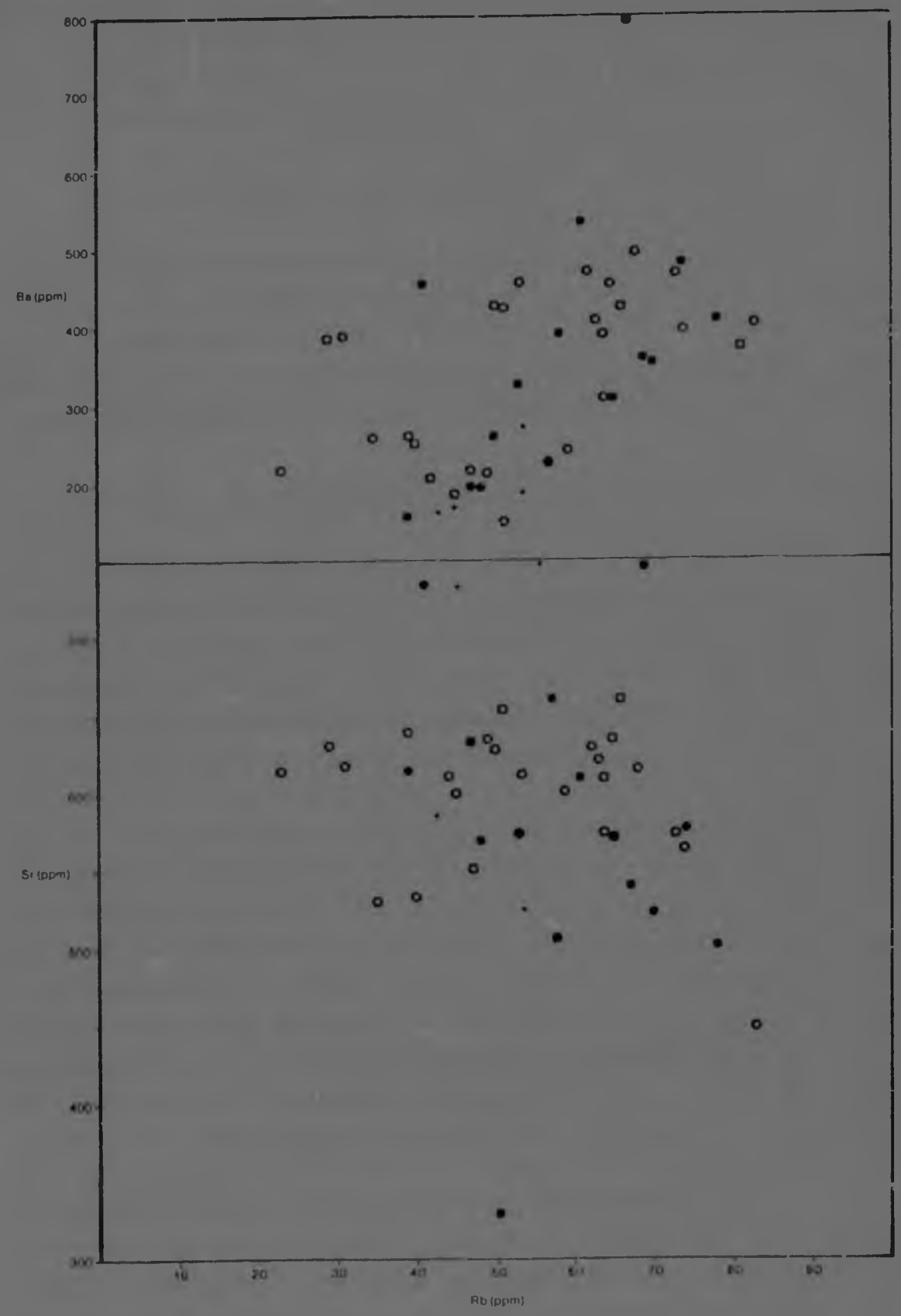

Figure 54 : *Plots of Rb v Sr and Rb v Ba for samples from the Kaap Valley tonalite. Data is from Table 21; symbols used for the various phases are the same as those in Figure 53.*

average Rb/Sr ratio for the dominant tonalitic phases is 0,09, which is very similar to the values characteristic of the more felsic biotite trondhjemite gneisses that occur to the southwest of the Barberton greenstone belt (see Chapter 6). The average Rb content of the Kaap Valley tonalite is actually 56 ppm (Table 36, Chapter 6) by comparison with figures of 45 ppm for the Nelshoogte, Stolzberg and Theespruit trondhjemite gneiss plutons (Glikson, 1976a) and 49 ppm for the same three plutons (Condie and Hunter, 1976). The fact that the Kaap Valley tonalite has similar (if not slightly higher) Rb contents to the more felsic trondhjemites is perhaps unusual in view of its markedly more mafic composition. This feature, which has, in fact, been noted on a previous occasion (Condie and Hunter, 1976), is discussed again in a later section.

7.4. Rare-earth element (REE) chemistry

A total of 24 samples from the mapped area were analysed for selected rare-earth elements using epithermal neutron activation techniques; this data, of which five samples are representative of the hornblende tonalites and thirteen of the hornblende + biotite tonalites, is presented in Table 22. The remainder of the analyses are representative of the minor phases in the Kaap Valley pluton.

Because it is impractical to plot all the individual REE traces on a chondrite normalized diagram, the evelopes of hornblende tonalites and hornblende + biotite tonalites are plotted in Figure 55A. Although the data envelopes plotted in this figure show a complete overlap, significant differences do occur between the two tonalite sub-types. In general, the hornblende + biotite phase is more enriched in the LREE and depleted in the HREE than are the hornblende tonalites. Consequently the Ce_N/Yb_N ratio is usually higher in the former than in the latter. This would appear to indicate that the Ce_N/Yb_N ratio in the Kaap Valley tonalite is a function of fractionation which is, itself, reflected in increasing SiO_2 content in the suite as a whole. This relationship is emphasized in a plot of Ce_N/Yb_N v SiO_2 (Figure 56) where a broad positive correlation between these two parameters exists. This diagram also indicates the lower average Ce_N/Yb_N ratio of the hornblende tonalite (i.e. 9,5) compared to that for the hornblende + biotite tonalites (i.e. 11,1).

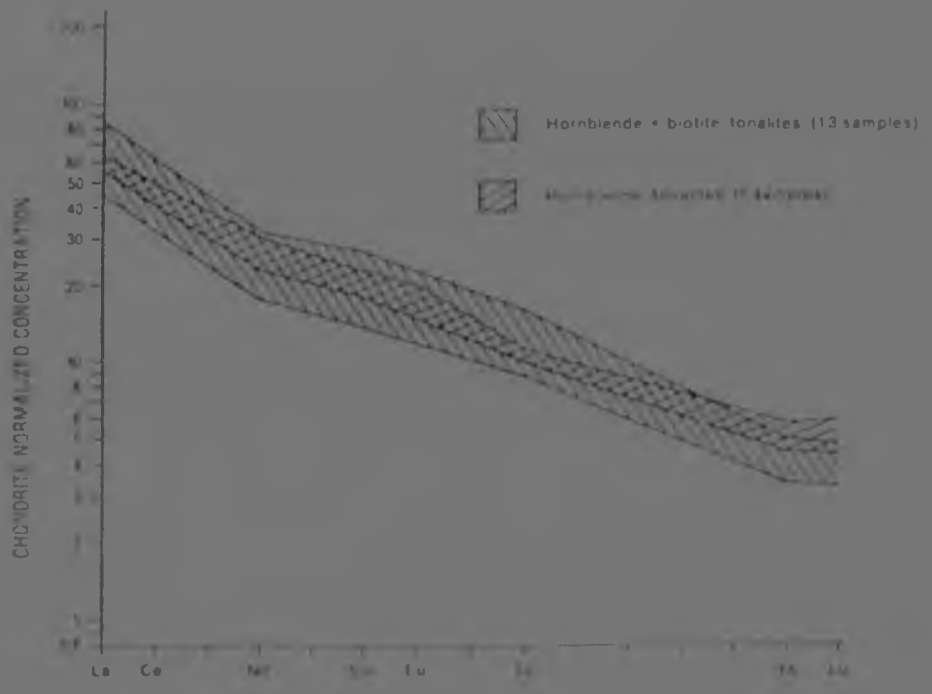

Figure 55A : Chondrite normalized rare-earth element plot of hornblende and hornblende + biotite tonalite samples from the Kaap valley pluton. Although the two fields overlap, the hornblende + biotite tonalites have, on average, greater concentrations of LREE than the hornblende tonalites (see Figure 57).

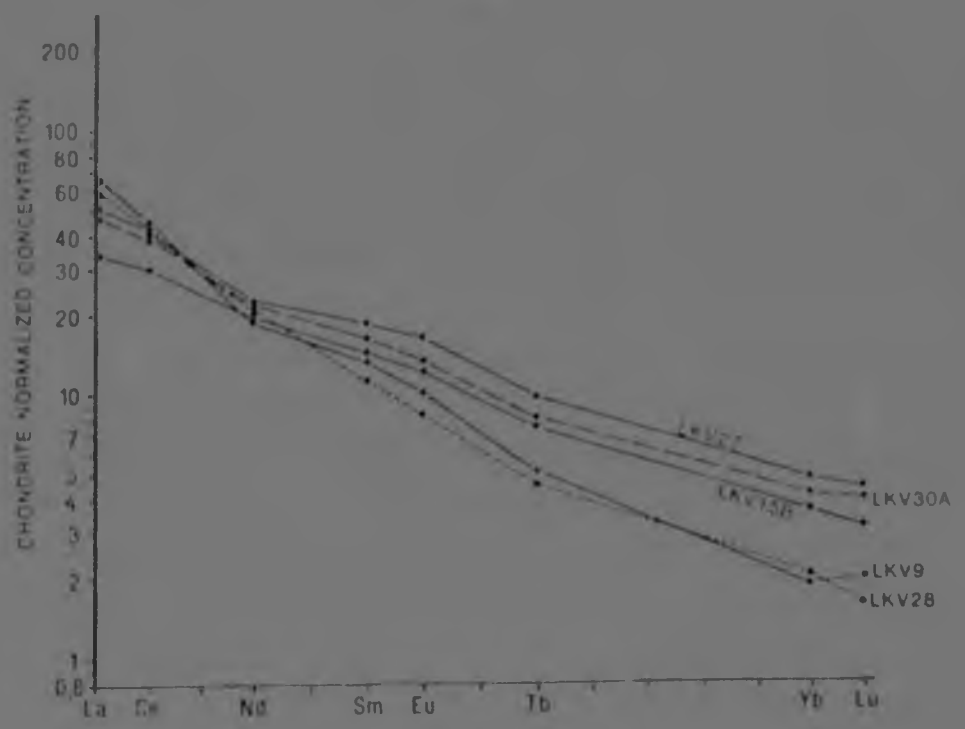

Figure 55B : Chondrite normalized rare-earth element plot of minor phases related to the Kaap Valley tonalite pluton. Samples LKV9, LKV15B and LKV27 are fine-grained tonalitic dykes; sample LKV30A is a sheared tonalite and sample LKV28 is from the Goede Hoop trondhjemite.

TABLE 22

RARE EARTH ELEMENT ANALYSES OF SELECTED SAMPLES FROM THE KAAP VALLEY TONALITE PLUTON AND RELATED PHASES

ppm		La	Ce	Nd	Sm	Eu	Tb	Yb	Lu
LKV 1	*	14,8	29,5	14,3	3,39	1,12	0,40	0,80	0,14
LKV 3	*	19,5	43,6	15,5	4,28	1,38	0,52	0,91	0,10
LKV 4	*	12,6	28,2	12,7	3,26	1,03	0,40	0,67	0,12
LKV 6	*	13,7	29,7	13,1	2,90	0,88	0,37	0,77	0,13
LKV12	*	18,4	43,1	15,6	3,83	1,22	0,55	1,06	0,17
LKV15(A)	*	11,9	22,7	9,0	2,41	0,79	0,26	0,45	0,06
LKV18	*	17.5	32,2	13,7	3,29	1,14	0,37	0,73	0,10
LKV20	*	15,4	31,4	10,8	2,84	0,88	0,32	0,79	0,10
LKV23	*	12,9	25,3	9,6	2,39	0,87	0,30	0,62	0,10
LKV25	*	14,0	32,6	14,7	3,34	1,07	0,43	0,99	0,15
LKV30	*	11,1	23,2	8,7	2,25	0,72	0,27	0,63	0,10
SKV 5	*	21,1	42,4	13,1	2,75	0,84	0,28	0,64	0,11
SKV 8	*	14,4	32,2	12,9	2,82	0,95	0,34	0,79	0,15
SKV12	*	13,6	30,3	11,6	3,21	0,98	0,38	0,85	0,13
SKV1[illegible]	*	14,9	33,7	13,9	3,24	1,09	0,41	0,99	0,16
SKV22	*	15,2	31,1	11,3	2,86	0,92	0,35	0,69	0,11
SKV28	•	14,0	23,7	8,8	2,41	0,83	0,30	0,73	0,10
SKV34	•	18,1	36,0	14,7	3,82	1,11	0,43	0,78	0,11
LKV 9	fg	15,8	28,7	9,1	2,07	0,59	0,19	0,32	0,05
LKV15(B)	fg	8,4	19,0	9,2	2,17	0,70	0,29	0,60	0,08
LKV21	fg	12,8	26,5	10,5	2,89	0,95	0,35	0,77	0,11
LKV30(A)	st	11,5	25,8	10,3	2,55	0,76	0,30	0,67	0,10
LKV28	GHT	14,7	28,3	9,4	1,75	0,49	0,17	0,33	0,04
LKV28(A)	GHT	10,4	18,9	6,1	1,49	0,51	0,17	0,37	0,06

Analyst: E.J. Robb

Concentrations obtained using neutron activation analysis techniques.

* - Hornblende-bearing tonalites

• - Hornblende + biotite-bearing tonalites

fg - Fine-grained tonalitic dykes

GHT - Goede Hoop trondhjemite phase

st - Sheared tonalite

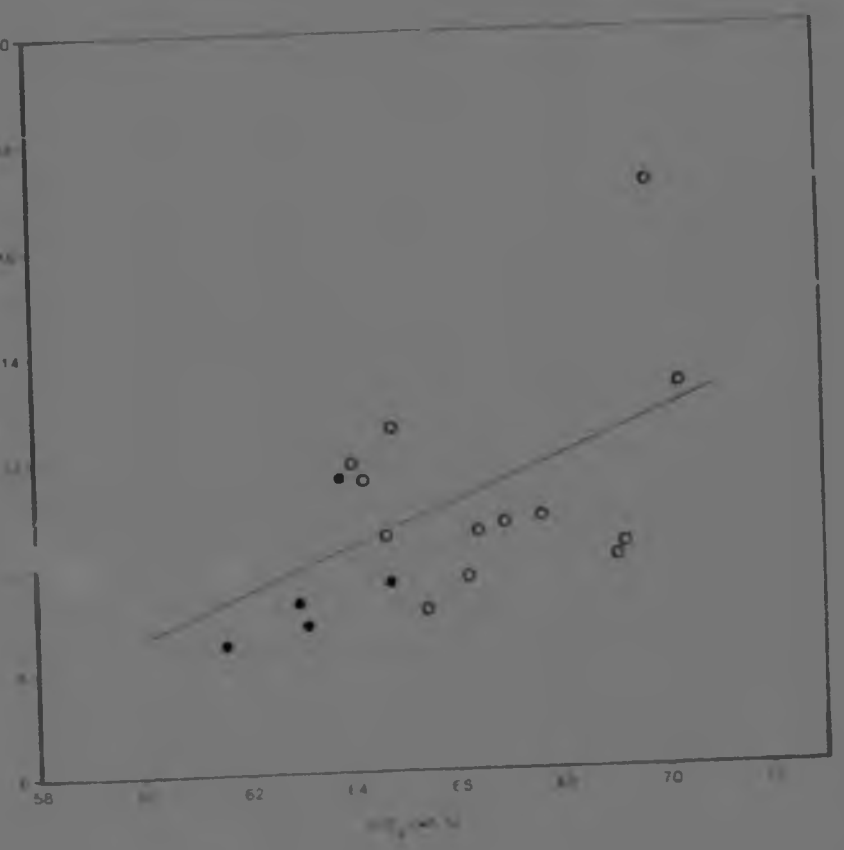

Figure 56 : Plots of (Ce_N/Yb_N) against SiO_2 for hornblende tonalites (dots) and hornblende + biotite tonalites (open circled stars) from the Kaap Valley Pluton. The best-fit line is a visual estimate.

It is instructive at this stage to compare the REE contents of the more typical, leucocratic biotite trondhjemites occurring to the southwest of the Barberton greenstone belt, with those of the Kaap Valley pluton. The available data shows that the total rare-earth element content (Σ REE) of the latter is greater, on average, than that of the trondhjemites and, in particular, LREE contents are higher by a factor of 10 - 20% (Figure 57). This particular feature has also been noted previously by Condie and Hunter (1976) who commented on the fact that the most mafic member of the tonalite-trondhjemite suite in the Barberton region was enriched in the LREE relative to more felsic equivalents. This observation presented these workers with difficulties in considering a partial melt origin for the Barberton tonalitic-trondhjemitic magmas, as the generation of the more mafic Kaap Valley tonalite would logically require a greater degree of partial melt from a basaltic parent than that envisaged for the more felsic trondhjemites. As the REE are preferentially partitioned into melt phases, this would imply that the more mafic magmas were correspondingly depleted in the rare-earth's relative to a magma that had formed by a smaller degree of melting. This reasoning led Condie and Hunter (1976) to a consideration of the mafic composition of the Kaap Valley tonalite in terms of 10 - 20% mixing (contamination) of a typical trondhjemitic magma with low-alkali tholeiites. Simple mixing considerations for the relevant rocks do not, however, necessarily uphold this viewpoint. In Figure 57, a representative REE trace of a Barberton-type basaltic komatiite (data from Herrmann et al., 1976 and Sun and Nesbitt, 1978) is compared with an average biotite trondhjemite and the average of the two main phases of the Kaap Valley tonalite. This diagram shows that it is not possible to derive the LREE-enriched patterns of the Kaap Valley tonalite phases by simply mixing any two proportions of typical leucocratic biotite trondhjemite and basaltic komatiite. This process could only be feasible in terms of the REE if the original Kaap Valley magma, prior to contamination, was itself enriched in the LREE and, thus, did not resemble the typical leucocratic trondhjemites in the area.

2.5 Mineral compositions in the Kaap Valley tonalite

A number of analyses of plagioclase, hornblende and biotite were carried out on samples from the Kaap Valley tonalite using the electron

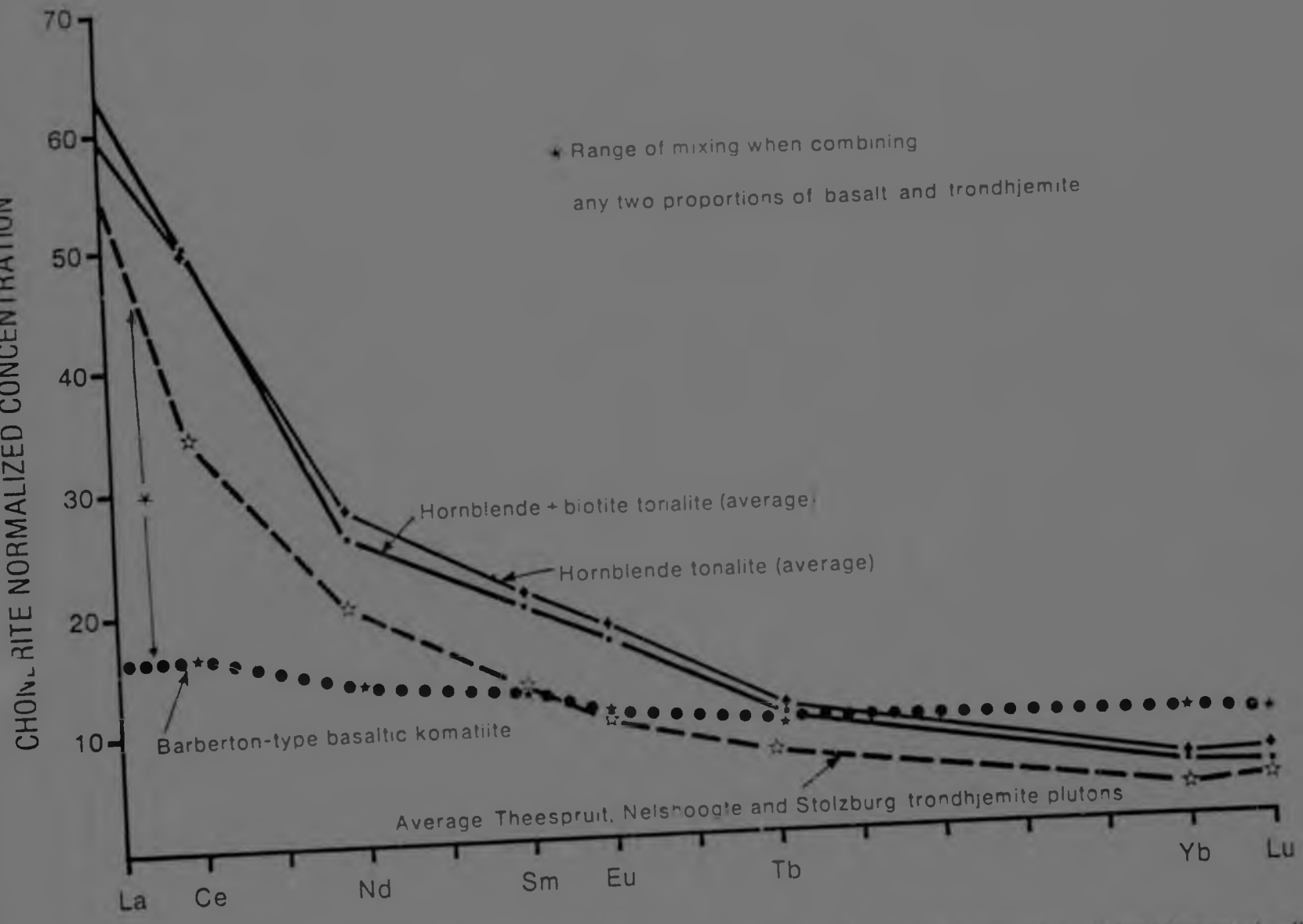

Figure 57 : *Averaged chondrite normalized rare-earth element plots for basaltic komatiite (dotted curve), Kaap Valley tonalite (linear curve) and trondhjemite gneiss (dashed curve) from the Barberton area. Average hornblende and hornblende + biotite tonalites are taken from the data in Table 22; Barberton-type basaltic komatiite is from data by Herrmann et al. (1978) and Sun and Nesbitt (1978); average Theespruit, Nelshoogte and Stolzburg trondhjemite plutons is from Condie and Hunter (1976). The diagram shows that it is not possible to derive the LREE enriched patterns of the Kaap Valley tonalite by simple mixing (or contamination) of typical leucocratic biotite trondhjemite with a basalt.*

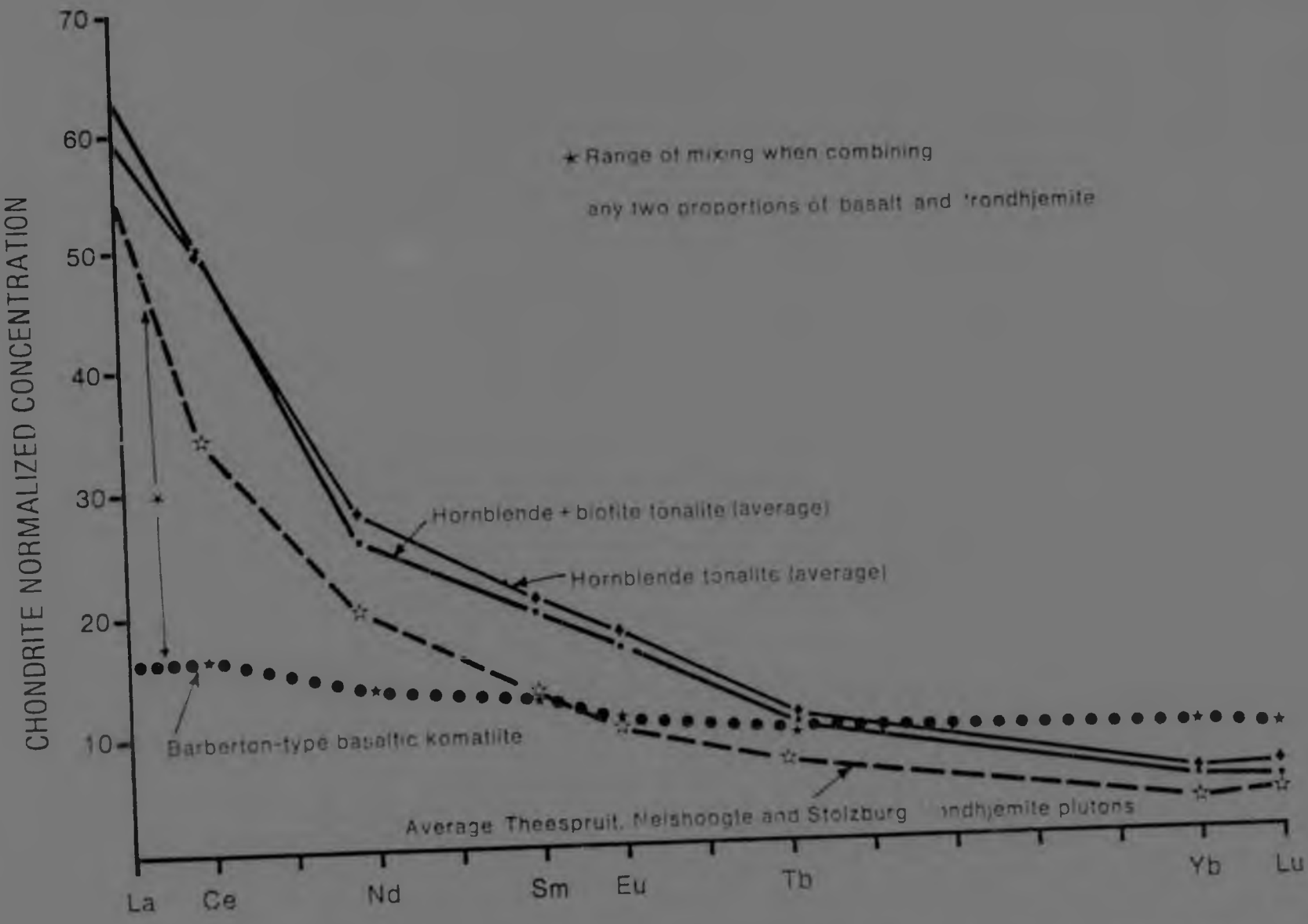

Figure 57 : *Averaged chondrite normalized rare-earth element plots for basaltic komatiite (dotted curve), Kaap Valley tonalite (linear curve) and trondhjemite gneiss (dashed curve) from the Barberton area. Average hornblende-and hornblende + biotite tonalites are taken from the data in Table 33; Barberton-type basaltic komatiite is from data by Herrmann et al. (1978) and Sun and Nesbitt (1976); average Theespruit, Nelshoogte and Stolzburg trondhjemite plutons is from Condie and Hunter (1976). The diagram shows that it is not possible to derive the LREE enriched patterns of the Kaap Valley tonalite by simple mixing (or contamination) of a typical leucocratic biotite trondhjemite with a basalt.*

micro-probe facility at the Geological Survey, Pretoria; these data are presented in Tables 23, 24 and 25. The purpose behind the mineral analyses of the Kaap Valley tonalite was to assess whether any of the components of the rock were xenocrystic and possibly derived either from the source region of the tonalite, or by stoping of overlying material during emplacement.

2.5.1. *Plagioclase*

The plagioclase compositions of ten samples from the Kaap Valley pluton are listed in Table 23. In most cases a number of analyses of the same grain were carried out to determine the range in composition existing between grain margins and cores; care was taken to avoid zones of intense sericitization during this process. The compositional ranges within single plagioclase grains are illustrated in Figure 58, where CaO v SiO_2 is plotted for samples specifically from the hornblende and hornblende + biotite tonalites. In both suites, single plagioclase grains vary in composition from approximately An_2 (margins) to An_{40} (cores) although there is a tendency for the margins of plagioclases from the hornblende + biotite tonalites to be less albitic than those from the hornblende tonalites. This may be related to the fact that plagioclases from the former are not as prominently zoned as those from the latter suite, but may also be due to the sericitization that has affected most of the analysed grains.

A diagnostic feature of plagioclase grains in granitoids that have been derived by the partial melting of mafic precursors, is that they may often contain relic xenocrystic cores of a composition that reflects the nature of their source (i.e. intermediate-to-high anorthite contents). White and Chappell (1977) have, for example, used this feature in recognizing granites that have been derived from an igneous source (i.e. their I-type granites). The most anorthitic plagioclase core analysed in the Kaap Valley tonalite (An_{40}) corresponds to the composition of andesine and it is unlikely that the latter represents a relic xenocryst as these would probably be more calcic (i.e. An_{80}, White and Chappell, 1977), particularly if a basaltic komatiite is considered to be the parent. The variation in plagioclase compositions can, therefore, be solely attributed to systematic changes in the composition of the liquid from which the plagioclases were crystallizing.

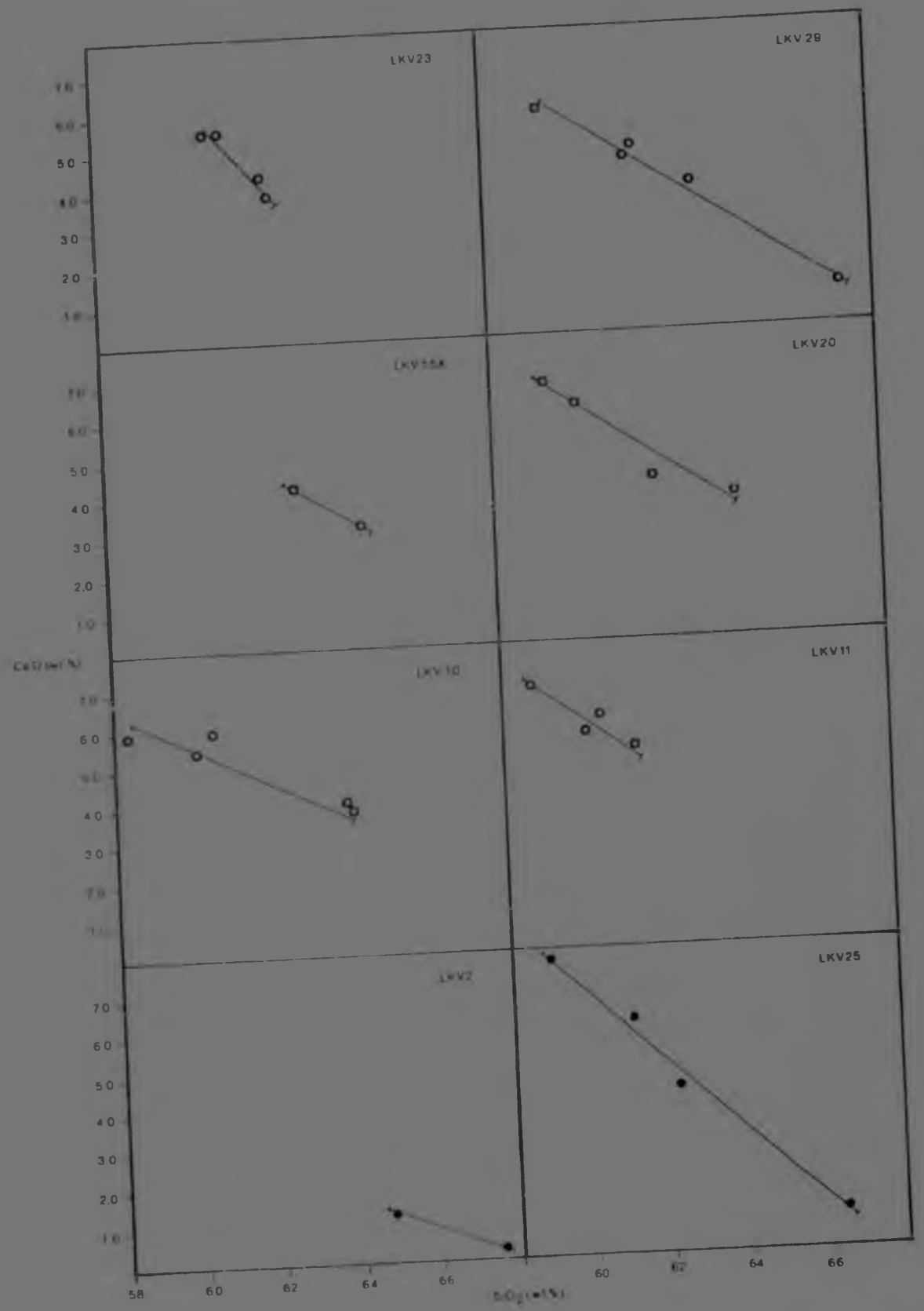

Figure 58 : *Plots of CaO against SiO2 showing the variation in plagioclase compositions between selected samples from the Kaap Valley tonalite pluton. Symbols used are the same as those in Figure 56. The data is from Table 23.*

TABLE 23

PLAGIOCLASE COMPOSITIONS IN SAMPLES FROM THE KAAP VALLEY TONALITE AND RELATED PHASES

			fq	*	*	*
	LKV 2	LKV 2	LKV 9	LKV10	LKV10	LKV10
SiO_2	67,58	64,56	60,71	63,87	60,55	63,93
Al_2O_3	19,42	21,45	23,42	23,18	24,50	22,97
Wt.% FeO +	0,09	0,27	0,19	0,08	0,21	0,18
CaO	0,26	1,18	5,53	4,13	5,92	3,99
Na_2O	11,55	11,52	8,28	9,20	7,89	9,44
K_2O	0,11	0,69	0,29	0,19	0,46	0,21
TOTALS	99,01	99,67	98,42	100,65	99,53	100,72
Structure*	32	32	32	32	32	32
Si	11,932	11,865	10,961	11,206	10,825	11,221
Al	4,042	4,646	4,984	4,794	5,162	4,753
Fe	0,014	0,041	0,028	0,012	0,030	0,026
Ca	0,049	0,232	1,069	0,777	1,134	0,750
Na	3,955	2,053	2,899	3,130	2,737	3,212
K	0,025	0,164	0,067	0,042	0,105	0,049
% An	1,3	5,8	27,4	20,5	29,4	19,8

Analyst: R.C. Wallace, Geological Survey, Pretoria.

FeO + - Total iron as FeO
Structure* - Calculated on the basis of 32 oxygens
% An - Calculated in terms of wt.% CaO

Ψ - Hornblende tonalites
* - Hornblende + biotite tonalites
fq - Fine-grained tonalitic dykes

TABLE 23 (Continued)

		*	*	*	*	*	*
		LKV10	LKV10	LKV11	LKV11	LKV11	LKV11
Wt.%	SiO_2	58,42	60,12	60,54	61,37	60,87	58,76
	Al_2O_3	25,64	24,52	24,02	24,15	24,49	25,44
	FeO +	0,28	0,26	0,16	0,26	0,26	0,19
	CaO	5,87	5,40	5,97	5,22	5,63	6,83
	Na_2O	7,76	8,31	8,09	8,60	8,33	7,25
	K_2O	0,41	0,34	0,26	0,36	0,32	0,48
	TOTALS	98,38	98,95	99,04	99,96	99,90	98,35
	Structure*	32	32	32	32	32	32
	Si	10,587	10,810	10,871	10,914	10,839	10,598
	Al	5,475	5,196	5,084	5,061	5,140	5,408
	Fe	0,043	0,039	0,025	0,038	0,039	0,028
	Ca	1,139	1,039	1,148	0,995	1,075	1,320
	Na	2,724	2,894	2,816	2,966	2,878	2,540
	K	0,049	0,078	0,059	0,082	0,073	0,109
	% An	29,1	26,8	29,6	25,9	27,9	33,8

TABLE 23 (Continued)

		*	*	fg	fg	fg	*
		LKV15A	LKV15A	LKV15B	LKV15B	LKV15B	LKV20
Wt.%	SiO_2	64,60	62,93	62,61	64,11	62,70	59,43
	Al_2O_3	21,04	22,57	23,61	22,15	23,06	25,67
	FeO	0,17	0,22	0,20	0,17	0,21	0,23
	CaO	3,18	4,23	4,72	3,25	4,59	6,75
	Na_2O	9,62	8,76	8,79	9,63	8,88	7,44
	K_2O	0,23	0,50	0,42	0,31	0,31	0,53
	TOTALS	98,84	99,21	100,35	99,62	99,75	100,05
	Structure*	32	32	32	32	32	32
	Si	11,446	11,224	11,064	11,356	11,126	10,603
	Al	4,519	4,745	4,916	4,623	4,835	5,397
	Fe	0,025	0,033	0,030	0,026	0,031	0,035
	Ca	0,604	0,809	0,894	0,616	0,875	1,291
	Na	3,304	3,028	3,011	3,308	3,029	2,575
	K	0,053	0,113	0,094	0,069	0,072	0,121
	% An	15,8	21,0	23,4	17,4	22,8	33,5

TABLE 23 (Continued)

	*	*	*	*	*	*
	LKV20	LKV20	LKV20	LKV23	LKV23	LKV23
SiO_2	64,18	60,17	62,17	61,32	62,28	60,96
Al_2O_3	22,46	24,65	22,58	24,08	23,34	24,51
FeO +	0,27	0,29	0,21	0,16	0,28	0,16
CaO	3,95	6,09	4,18	5,47	4,29	5,52
Na_2O	9,15	7,84	9,01	8,14	9,25	8,24
K_2O	0,43	0,28	0,25	0,63	0,26	0,53
TOTALS	100,44	99,32	98,40	99,80	99,70	99,92
Structure*	32	32	32	32	32	32
Si	11,296	10,781	11,181	10,931	11,085	10,859
Al	4,660	5,206	4,787	5,060	4,896	5,145
Fe	0,041	0,044	0,031	0,023	0,042	0,024
Ca	0,745	1,169	8,05	1,045	0,817	1,053
Na	3,124	2,724	3,142	2,814	3,191	2,846
K	0,097	0,065	0,055	0,144	0,058	0,121
% An	19,6	30,2	20,7	27,1	21,3	27,4

Wt.%

TABLE 23 (Continued)

	LKV23	LKV25	LKV25	LKV25	LKV25	LKV29
SiO_2	62,52	61,08	59,00	62,16	66,38	61,88
Al_2O_3	23,34	23,31	25,32	23,09	20,50	24,05
FeO	0,22	0,38	0,27	0,16	0,10	0,21
CaO	3,79	6,06	7,68	4,34	0,98	4,83
Na_2O	9,35	7,81	6,99	8,90	10,78	8,72
K_2O	0,56	0,56	0,30	0,24	0,31	0,18
TOTALS	99,78	100,20	99,56	98,85	99,05	99,87
Structure*	32	32	32	32	32	32
Si	11,115	10,859	10,588	11,121	11,741	10,980
Al	4,891	5,094	5,356	4,871	4,274	5,031
Fe	0,033	0,056	0,040	0,025	0,014	0,032
Ca	0,722	1,155	1,477	0,833	0,186	0,920
Na	3,224	2,691	2,431	3,090	3,698	3,000
K	0,127	0,127	0,070	0,056	0,070	0,041
% An	18,8	30,1	38,1	21,5	4,9	24,0

Wt.%

TABLE 23 (Continued)

	*	*	*	*
	LKV29	LKV29	LKV29	LKV29
SiO_2	67,06	59,53	63,36	61,75
Al_2O_3	19,60	25,20	23,63	23,83
FeO +	0,09	0,17	0,19	0,21
CaO	1.00	5,79	3,83	4,55
Na_2O	10,83	8,10	9,39	8,71
K_2O	0,12	0,52	0,24	0,33
TOTALS	98,70	99,31	100,64	99,38
Structure*	32	32	32	32
Si	11.882	10,686	11,132	11,013
Al	4,093	5,331	4,894	5,008
Fe	0,013	0,026	0,028	0,031
Ca	0,189	1,113	0,722	0,867
Na	3,720	2,821	3,194	3,012
K	0,028	0,118	0,053	0.076
% An	5,0	28,8	19,0	22,5

Wt.%

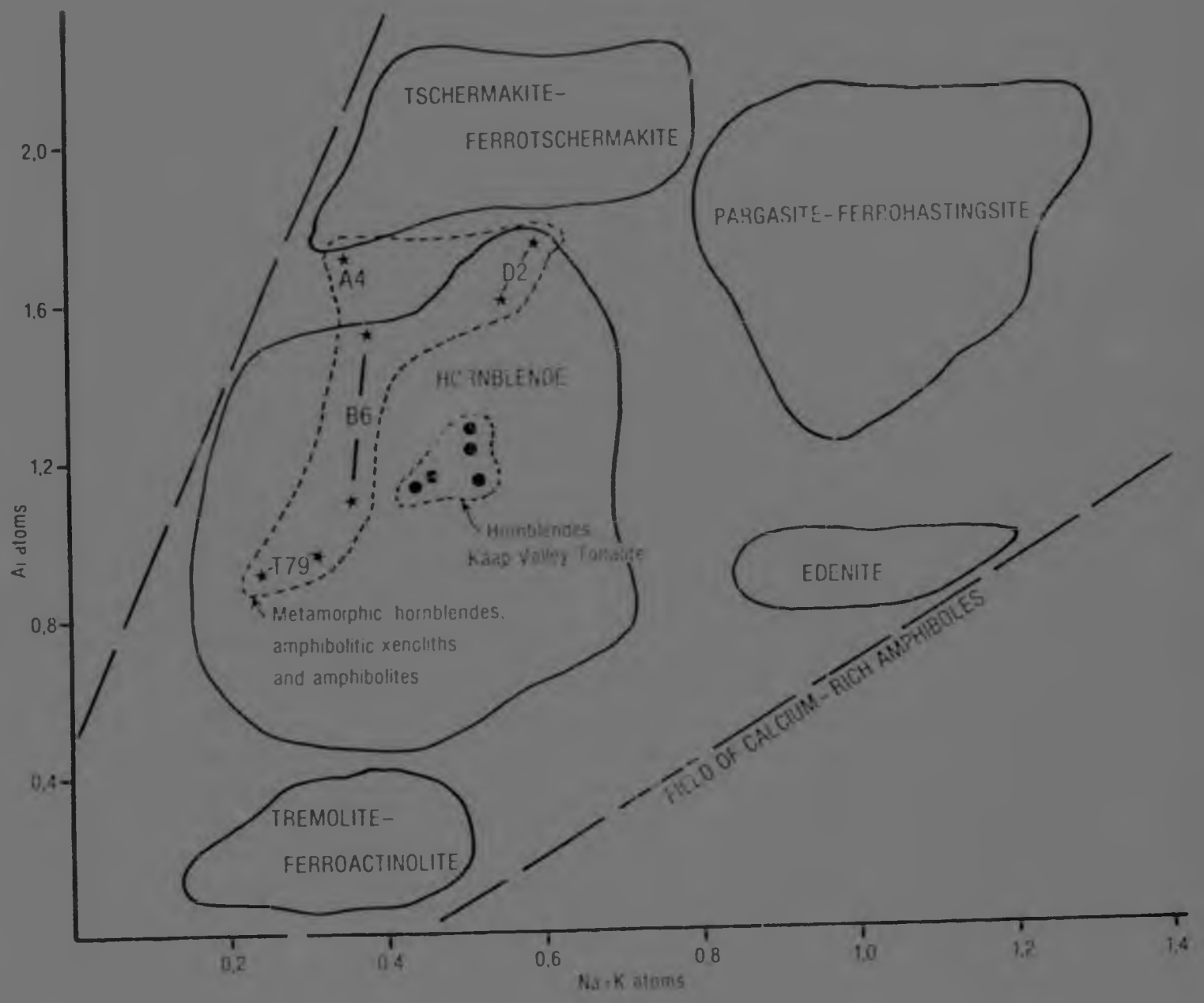

Figure 59 : Plot of Al against (Na + K) for hornblendes from the Kaap Valley tonalite pluton; data is from Table 24. In addition, metamorphic hornblendes from amphibolites sampled at a variety of localities in the Barberton Mountain Land are also plotted for comparison. The latter data and sample localities are presented in Table 26. Amphibolite compositional fields are from Deer et al. (1971).

The composition of plagioclases from the finer-grained tonalitic dykes are identical to those of the host rocks. These grains have compositions in the oligoclase range and exhibit similar variations in composition between margin and core (see samples LKV 9 and LKV 15B, Table 23) as observed for plagioclases in the host rock. Again, no criteria are present that might serve to differentiate the tonalitic dykes from the main phases of the Kaap Valley tonalite.

2.5.2. *Hornblende and Biotite*

The compositions of hornblende and biotite from a number of samples of the Kaap Valley tonalite are presented in Tables 24 and 25. It is of particular interest to examine the hornblende compositions in the light of suggestions made previously that this mineral may be xenocrystic in origin and that the more mafic nature of the Kaap Valley tonalite as a whole, could be due to assimilation of greenstone material. In a plot of Al v (Na + K) (Figure 59) the compositions of hornblende from the Kaap Valley tonalite are seen to fall in a tight cluster that is well within the field of hornblende compositions defined by Deer et al. (1971). The slight variations in hornblende compositions cannot be correlated in any way with the bulk composition of the rock from which the hornblendes were derived (i.e. to possible differences between hornblende and hornblende + biotite tonalites). On the same diagram the compositions of hornblende in the Kaap Valley tonalite can be compared with metamorphic hornblendes found in a variety of amphibolitic meta-basalts from different localities in the Barberton region. These compositions (Table 26) are seen to encompass a much broader field on the Al v (Na + K) plot and one which is quite distinct from the field of tonalitic hornblendes. On this basis it is reasonable to conclude that the amphibolite phase in the Kaap Valley pluton is not xenocrystic but has probably crystallized directly from the magma, resulting in a mineral of limited compositional variation. Hornblendes from the amphibolitic meta-basalts, on the other hand, have formed under conditions of variable pressure and temperature and have reacted to varying degrees with felsic magmas of differing compositions (particularly with respect to Na and K); these hornblendes can, therefore, be expected to exhibit the broader range of compositions observed.

TABLE 24

HORNBLENDE COMPOSITIONS IN SAMPLES FROM THE KAAP VALLEY TONALITE PLUTON AND RELATED PHASES

		†	*	*	fg	†
		LKV 2	LKV11	LKV15A	LKV15B	LKV25
Wt.%	SiO_2	47,33	47,61	48,22	46,77	46,82
	TiO_2	1,50	1,47	1,04	1,21	1,35
	Al_2O_3	7,02	6,43	6,34	7,05	6,44
	FeO +	15,25	15,43	14,06	16,72	16,08
	MnO	0,45	0,48	0,66	0.51	0,40
	MgO	13,35	13,40	13,16	12,63	12,99
	CaO	10,83	10,69	10,97	11,69	11,30
	Na_2O	1,40	1,47	1,18	1,36	1,23
	K_2O	0,59	0,49	0,55	0,61	0,56
	TOTALS	97,72	97,47	96,18	98,55	97,17
	Structure*	23	23	23	23	23
	Si	6,980	7,042	7,176	6,908	6,986
	Ti	0,167	0,164	0,116	0,135	0,151
	Al	1,221	1,121	1,111	1,229	1,132
	Fe	1,880	1,909	1,750	2,065	2,006
	Mn	0,056	0,060	0,083	0,064	0,050
	Mg	2,934	2,954	2,519	2,782	2,888
	Ca	1,711	1,694	1,749	1,851	1,807
	Na	0,401	0,427	0,342	0,391	0,355
	K	0,111	0,093	0,105	0,116	0,106

Analyst: R.C Wallace, Geological Survey, Pretoria.

* - Number of oxygens

FeO + - Total iron as FeO

† - Hornblende tonalites

* - Hornblende + biotite tonalites

fg - Fine-grained tonalitic dykes

TABLE 25

BIOTITE COMPOSITIONS IN SAMPLES FROM THE KAAP VALLEY TONALITE PLUTON AND RELATED PHASES

	fg	fg	*	*	fg
	LKV 9	LKV 9	LKV11	LKV15A	LKV15B
SiO_2	35,95	36,04	37,10	37,50	36,43
TiO_2	4,13	4,15	3,77	3,52	3,74
Al_2O_3	13,80	14,67	15,3€	14,90	14,98
FeO +	18,79	19,64	19,24	17,21	18,87
MnO	0,57	0,52	0,15	0,25	0,34
Wt.% MgO	11,28	10,10	11,75	11,93	11,13
CaO	0,07	0,07	0,06	0,08	0,07
Na_2O	0,11	0,09	0,09	0,10	0,10
K_2O	9,96	10,41	9,64	10,06	10,23
TOTALS	94,66	95,69	97,16	95,55	95,89
Structure*	22	22	22	22	22
Si	5,556	5,535	5,537	5,652	5,543
Ti	0,480	0,479	0,423	0,399	0,427
Al	2,514	2,656	2,701	2,646	2,686
Fe	2,429	2,522	2,401	2,168	2,401
Mn	0,075	0,068	0,020	0,032	0,044
Mg	2,598	2,313	2,614	2,680	2,524
Ca	0,013	0,012	0,010	0,013	0,011
Na	0,034	0,026	0,027	0,030	0,030
K	1,963	2,040	1,836	1,936	1,986

Analyst: R.C. Wallace, Geological Survey, Pretoria.

Structure * - Number of oxygens

FeO + - Total iron as FeO

* - Hornblende + biotite tonalites

fg - Fine-grained tonalitic dykes

TABLE 26

HORNBLENDE AND CLINOPYROXENE ANALYSES FROM AMPHIBOLITIC META-BASALTS SAMPLED AT A VARIETY OF LOCALITIES IN THE BARBERTON MOUNTAIN LAND

	*	*	+	*	*	+	*	*	*
	B6	B6	B6	D2	D2	D2	T79	T79	A4
SiO_2	46,13	47,78	50,99	47,10	46,09	52,95	48,77	49,22	47,59
TiO_2	0,67	0,44	0,17	0,64	0,59	0,17	0,26	0,86	0,48
Al_2O_3	8,69	6,16	1,17	9,39	10,08	1,08	5,20	5,40	10,21
FeO*	16,58	16,32	9,37	12,59	12,70	7,37	15,78	15,32	13,77
MnO	0,30	0,55	0,41	0,23	0,25	0,18	0,39	0,24	0,21
Wt.% MgO	12,37	12,67	13,43	13,92	13,97	14,45	13,88	12,83	11,71
CaO	11,19	12,15	23,11	11,62	10,77	22,75	11,95	11,46	11,88
Na_2O	0,86	0,97	0,43	1,33	1,41	0,60	0,58	0,66	1,07
K_2O	0,70	0,46	-	0,94	1,05	-	0,42	0,67	0,24
TOTALS	97,49	97,50	99,08	97,76	96,91	99,55	97,23	96,66	97,16
STRUCTURE	23	23	6	23	23	6	23	23	23
Si	6,847	7,099	1,940	6,855	6,772	1,975	7,226	7,304	6,951
Ti	0,075	0,049	0,005	0,070	0,065	0,005	0,029	0,096	0,053
Al	1,520	1,079	0,053	1,611	1,746	0,048	0,908	0,945	1,758
Fe	2,059	2,027	0,298	1,532	1,560	0,230	1,955	1,901	1,681
Mn	0,038	0,069	0,013	0,028	0,031	0,006	0.049	0,030	0,026
Mg	2,737	2,805	0,762	3,020	3,059	0,803	3,064	2,839	2,549
Ca	1,780	1,934	0,942	1,811	1,696	0,909	1,897	1,822	1,859
Na	0,250	0,274	0,032	0,374	0,402	0,043	0,167	0,191	0,302
K	0,133	0,088	-	0,175	0,196	-	0,080	0,126	0,045

Analyst: R.C. Wallace, Geological Survey, Pretoria.

* - Hornblende - structure calculated on the basis of 23 oxygens

\+ - Clinopyroxene - structure calculated on the basis of 6 oxygens

FeO* - Total iron as FeO

Samples:
- B 6 - Amphibolitic meta-basalt from the Theeboom outcrop
- D 2 - Amphibolitic meta-basalt from the Mara outcrop
- T79 - Amphibolite from the Jamestown Schist Belt (sample locality see Anhaeusser, 1972)
- A 4 - Amphibolitic meta-basalt from the Boekenhoutrand outcrop

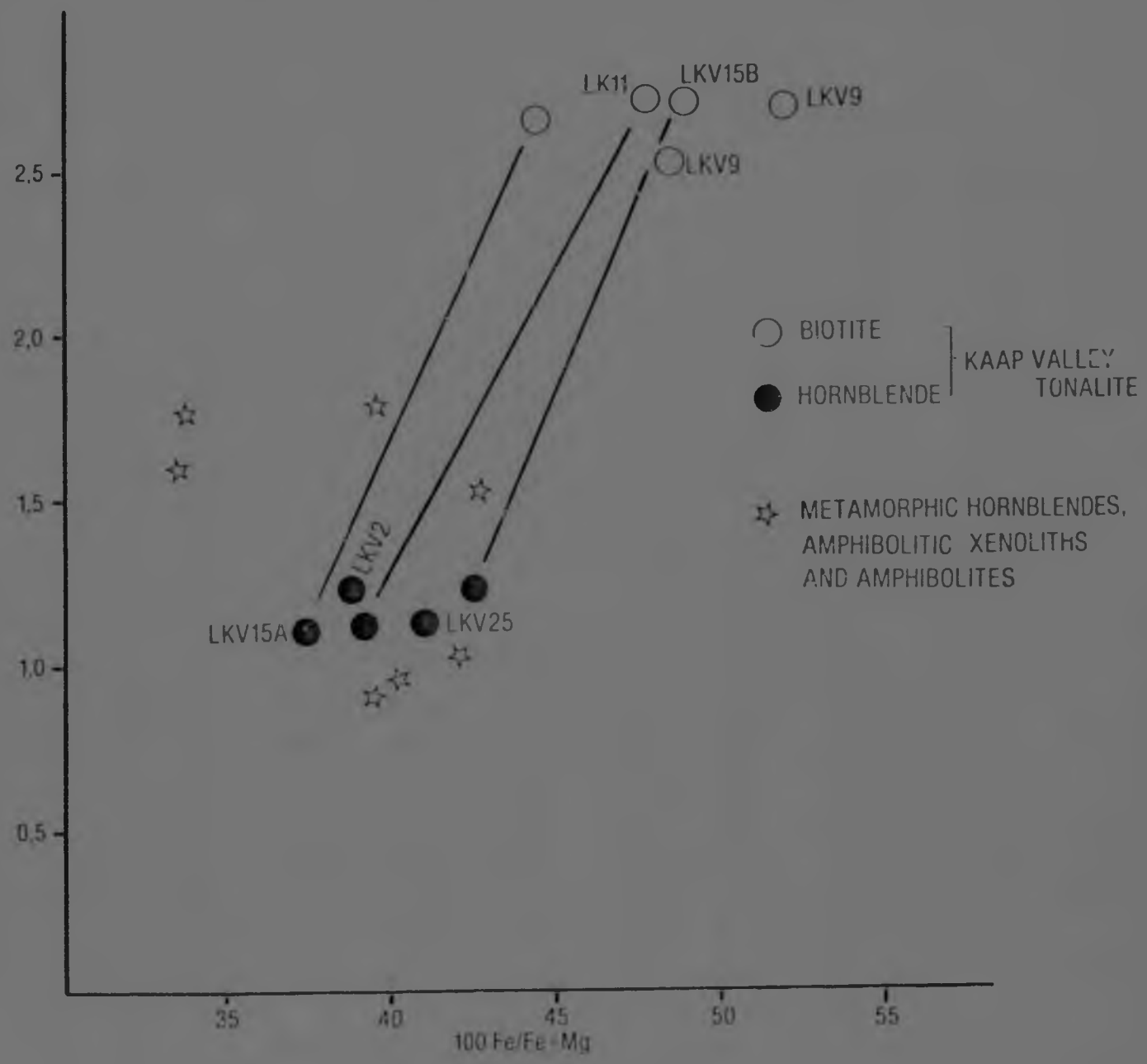

Figure 60 : Plot of Al against the ratio 100.Fe/Fe + Mg for hornblendes and biotites from the Kaap Valley tonalite pluton. Hornblendes from amphibolites in Table 26 are also plotted. The remainder of the data is from Tables 24 and 25. Tie-lines join coexisting hornblende and biotite from the same sample.

The differences in composition between the Kaap Valley tonalite hornblendes and those of metamorphosed mafic xenoliths are again emphasized in a plot of Al v 100.Fe/Fe + Mg in Figure 60. In this diagram the compositions of biotites from the Kaap Valley tonalite are also plotted and, like the amphiboles with which they coexist, are restricted to a relatively narrow range that is manifest mainly in a variation of the Fe/Fe + Mg ratio. It is interesting to note that similar systematic changes in the Fe/Fe + Mg ratio occur in coexisting biotite and hornblende from the same sample, and this is evident from the sub-parallel tie-lines in Figure 60. Although not readily correlatable with changes in the bulk composition of these samples, these systematic variations are most probably related to subtle changes occurring during the crystallization of coexisting biotite and hornblende and suggests that the two phases were probably in equilibrium. This observation also militates against the view that hornblende in the Kaap Valley tonalite was derived by assimilation rather than by direct crystallization from a liquid phase.

3. ORIGIN AND MODE OF FORMATION OF THE KAAP VALLEY TONALITE

In the preceding sections the geological and chemical characteristics of the Kaap Valley tonalite have been outlined. In the petrogenetic considerations that follow, an attempt is made to explain those features of the body which serve to distinguish it from the more typical biotite trondhjemite gneisses that occur in the region to the southwest of the Barberton greenstone belt (*). The diagnostic features of the Kaap Valley tonalite pluton which require explanation in terms of any petrogenetic considerations are :-

(i) the ubiquitous presence of hornblende and the significantly more mafic nature of the body as a whole;

(ii) the evidence discussed previously (i.e. petrographic observations, light rare-earth element content and hornblende compositions) which suggests that the high ferromagnesian content of the body is not due to widespread contamination of a typical trondhjemitic magma by incorporation of surrounding greenstone material;

(*) Footnote : The petrogenesis of these bodies, of which 12 distinct units have been defined, is described in Chapter 6 of this thesis.

(iii) the systematic major element variations and an apparent chemical hiatus between hornblende and hornblende + biotite tonalites; and

(iv) no evidence for a depleted incompatible element content (i.e. LREE and Rb) in comparison to the leucocratic trondhjemite gneisses, as might be expected from a suite which, logically, would appear to have been generated by a greater degree of partial melting than the latter.

The following sections give consideration, firstly, to certain aspects of the suggested melt origin of the Kaap Valley tonalite and, secondly, to crystal fractionation in this body during its subsequent cooling history.

3.1. The melt origin of the Kaap Valley tonalite

There is a marked consensus in recent literature as to the origin of Archaean tonalitic and trondhjemitic magmas and a summary of current thoughts related to this topic is presented in Chapter 6 of this thesis. Certain workers in this field envisage, for example, 10 - 20% partial melting of an eclogitic or quartz-eclogitic parent of tholeiitic composition (Arth and Hanson, 1975; Condie and Hunter, 1976) whereas others argue for a higher proportion of near-liquidus melting of a komatiitic basalt parent (Glikson, 1979a). In the present study the view is adopted that most tonalite and trondhjemite magmas in the Barberton area have formed as a result of partial melting of amphibolites with basaltic komatiite compositions. This topic is dealt with in detail in Chapter 6 where petrologic mixing considerations indicate that the Kaap Valley tonalite can be formed by approximately 35% melting of a Barberton-type basaltic komatiite. Trace element contents are also shown to be compatible with this viewpoint.

The general consensus over a mafic igneous parentage for tonalitic and trondhjemitic magmas means that the interpretation and significance of the major element variations over the Kaap Valley pluton as a whole (as illustrated in the Harker diagrams in Figure 53) can be assessed from two possible points of view. The first, and more commonly held view, is that a trend of increasing silica in a suite of rocks represents the fractionation of a mineral assemblage from a liquid undergoing a similar

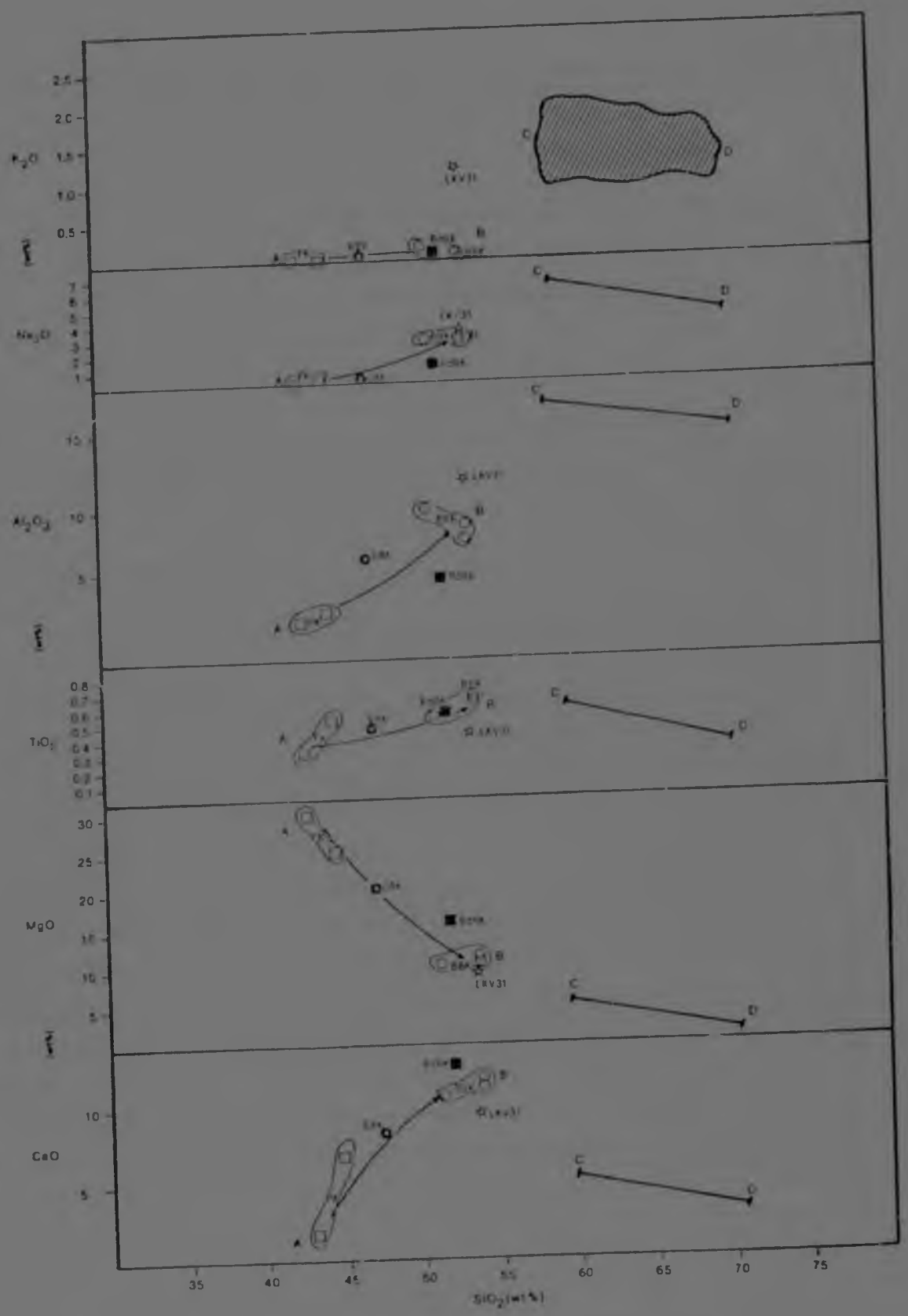

Figure 61 : *Harker-type diagram plotting SiO_2 against CaO, MgO, TiO_2, Al_2O_3, Na_2O and K_2O for average peridotite and basaltic komatiite compositions (data from Viljoen and Viljoen, 1969c). For comparison with the komatiitic trend (A-B), the approximate Kaap Valley trend (i.e. C-D, gauged roughly from the Harker plots in Figure 53) is also plotted. PK - peridotitic komatiites; GBK - Geluk-type basaltic komatiite; BdBK - Badplaas-type basaltic komatiite; BBK - Barberton-type basaltic komatiites. LKV31 is a small amphibolitic remnant from the Kaap Valley pluton (see Table 21).*

change in composition. A second viewpoint is that a linear trend of this nature represents a mixing line between a siliceous partial melt and a depleted residue or restite (White and Chappell, 1977). Depending on the viewpoint adopted, therefore, Harker-type trends such as those in Figure 53, might reflect either, partial melt processes (the latter implying that the composition of the parental material is to be found in a position on the trend intermediate between that of siliceous melt products and depleted residues) or, processes of fractionation (in which case the parental composition is controlled by that of the combined crystal extract). If the Kaap Valley trends in Figure 53 represent portions of melt-restite mixing curves, then the compositions of parent and residue (not plotted in this diagram) presumably lie in the back-projection of this curve, if it is assumed that the precursor had a basaltic composition. In Figure 61 the relationship between peridotitic and basaltic komatiites on the one hand (trend A - B) and the Kaap Valley trend on the other (C - D), are shown together, in the form of Harker diagrams. It is quite clear here, particularly in the case of CaO. Al_2O_3, Na_2O and K_2O that the Kaap Valley trend itself does not represent a portion of a melt-restite mixing curve, as the compositions of likely parental basalts (e.g. BBK, Figure 61) are neither colinear with, nor plot in the back-projection of, the tonalitic trend. The variation in major element composition in the Kaap Valley tonalite may, therefore, be more profitably interpreted as a fractionation trend and this topic is discussed in a later section.

It is interesting, at this stage, to contemplate the gap in compositional space represented by the interval B - C in Figure 61 and to speculate on its significance. The trend (A - B) defined by peridotitic and basaltic komatiites encompasses a range of between 43 - 53% SiO_2, suggesting that the processes which inter-relate these rocks (see section 4.2., Chapter 3 for discussion of this topic) do not appear to generate intermediate magmas with silica contents between approximately 53 - 60% (note that the calc-alkali volcanics that dominate the upper greenstone successions are probably genetically unrelated to the komatiitic series). If, however, BBK (in Figure 61) was regarded as the parent from which the Kaap Valley magma were partially melted, then the components of a melt-restite mixing curve would lie on a trend in the vicinity of the gap B - C. The orientation of this trend for each of the individual Harker plots, would be determined by the slope of an imaginery line joining B - C in each case. The fact

that, in Archaean terranes, rock suites with compositional trends reflecting such melt-restite mixing curves are rarely, if ever, sampled or reported, probably indicates that the residues of basalt melting are no longer preserved. As Glikson (1979a) has pointed out, near- or above-liquidus tonalitic melts do not usually contain restite material, the latter probably having sunk back into the crust. Sign ficantly, however, the composition of a small amphibolitic xenolith (sample LKV31, Table 21) possibly representing cognate material, plots approximately in the interval B - C in Figure 61. This partly assimilated amphibolitic remnant may, therefore, represent a component in a melt-restite mixing curve, in which case it could be interpreted as a cognate xenolith rather than a raft simply broken off the adjacent greenstone assemblage.

3.2. The partial melt origin of the Kaap Valley tonalite in terms of its incompatible element content

As mentioned previously, the Kaap Valley tonalite contains greater concentrations of the LREE and possibly Rb, than do the more felsic biotite trondhjemite gneisses in the Barberton region. Furthermore, in terms of its more mafic bulk composition it would appear feasible to derive the tonalite by a slightly greater degree of partial melting than that required to form the trondhjemites. This particular aspect is discussed in terms of major elements in Chapter 6, where petrologic mixing considerations indicate that the Kaap Valley tonalite can be derived by approximately 35% melting in comparison to a figure of < 30% indicated for the more leucocratic trondhjemites. Whereas this figure explains the increased matic content of the tonalite, it is incompatible with the increased (or at least similar) LREE and Rb contents of the latter. This point is emphasized in Table 27 where consideration is given to the enrichment of REEin a batch melt from a basaltic komatiite. It is clear, here, that enrichment factors are expected to be markedly *lower* in a melt derived from an increased degree of partial melting and comparisons between the 20% and 30% columns in Table 27 show that the LREE should, in fact, be less enriched in the latter by a factor of approximately one fifth. These melt fractions are also compared with the envelope of Kaap Valley samples in Figure 62, where it is clear that neither 20% nor 30% batch melting of a basaltic komatiite will yield liquids with the LREE enrichment of the Kaap Valley tonalite. It appears likely, therefore, that the higher abundances of Rb and the LREE noted, both in this study as well as in that of Condie and Hunter (1976), may be a

TABLE 27

RARE-EARTH ELEMENT ENRICHMENT FACTORS IN TONALITIC MELTS DERIVED BY 20% and 30% PARTIAL MELTING OF A BASALTIC KOMATIITE

	AVE. REE CONTENT - BASALTIC KOMATIITE (*)	K_D - BASALTIC KOMATIITE (+)	K_D - TONALITIC MELT (γ)
La	3,95	0,14	0,29
Ce	10,25	0,27	0,39
Nd	6,50	2,20	0,72
Sm	1,89	3,20	0,91
Lu	0,61	2,70	2,11
Tr	0,39	3,30	0,90
Yb	1,49	3,90	1,07
Lu	0,22	3,60	0,98

(*) Average after Sun and Nesbitt (1978) and Herrmann et al. (1976).

(+) Comprising:- 80% hornblende, 10% plagioclase, 10% quartz.

(γ) Comprising: 66% plagioclase, 21% hornblende, 13% quartz.

(Partition coefficients listed in Appendix 2)

USING THE BATCH MELT EQUATIONS OF SHAW (1970), THE REE COMPOSITIONS OF 20% and 30% PARTIAL MELTS ARE AS FOLLOWS :-

	20%	Enrichment Factor	30%	Enrichment Factor
La	14,0	3,5	11,2	2,8
Ce	26,1	2,5	22,6	2,2
Nd	2,9	0,45	2,8	0,43
Sm	0,59	0,31	0,57	0,30
Eu	0,25	0,41	0,26	0,43
Tb	0,12	0,31	0,12	0,31
Yb	0,38	0,25	0,38	0,25
Lu	0,06	0,27	0,06	0,27
Ce_N/Yb_N	17,8		15,4	

function of processes that concentrated these trace elements more efficiently than those quantitatively expressed in terms of the conventional equations for partial melting or fractional crystallization.

The concept of zone refining (Pfann, 1952), as applicable to metallurgical sciences, was initially developed for the purification and refining of metals and alloys. The process involves the movement of a small melt zone slowly along a bar or rod of the metal to be cleansed. As the melt zone moves, all metal impurities (i.e. constituents which are not accommodated within the metal lattice) are effectively partitioned into the liquid phase and retained therein during the zone's traverse. In practice a high degree of refining is accomplished by repeated traverses of the zone melt along the bar.

In the earth sciences, the concept of zone refining has had a limited petrological application with respect to a process referred to specifically as "zone melting". The process of zone melting has been considered relevant in the production of mafic magmas where near-total melting at mantle depths has taken place (Harris, 1957; Schilling and Winchester, 1967). The upward movement of a melt zone within a column of rock is carried out by the progressive melting of roof material in the magma chamber (presumably facilitated by the upward movement of volatile phases) and the simultaneous crystallization of a similar amount of material at the bottom of the chamber. As Harris (1957) has pointed out, two considerations are important from a geological point of view. Zone melting differs, firstly from conventional magmatic differentiation, in that incompatible elements are not derived from the magma itself but are continually scavenged by the melting of new roof material and, secondly from assimilation, in that bulk additions to the magma are negligible. The process is considered, rather, as a prolonged reaction of a magma with surrounding rocks and the subsequent retention in the liquid, of incompatible trace elements that are not readily accepted into the lattices of common rock-forming minerals. It is also important to note that once the melt zone intersects the solidus, crystal fractionation takes place along conventional lines and therefore the process affects only the final composition of the magma prior to solidification. Zone melting was successfully applied to the generation of alkali-rich basalts that are anomalously enriched in large-ion lithophile elements such as K, Rb and Cs (Harris, 1957).

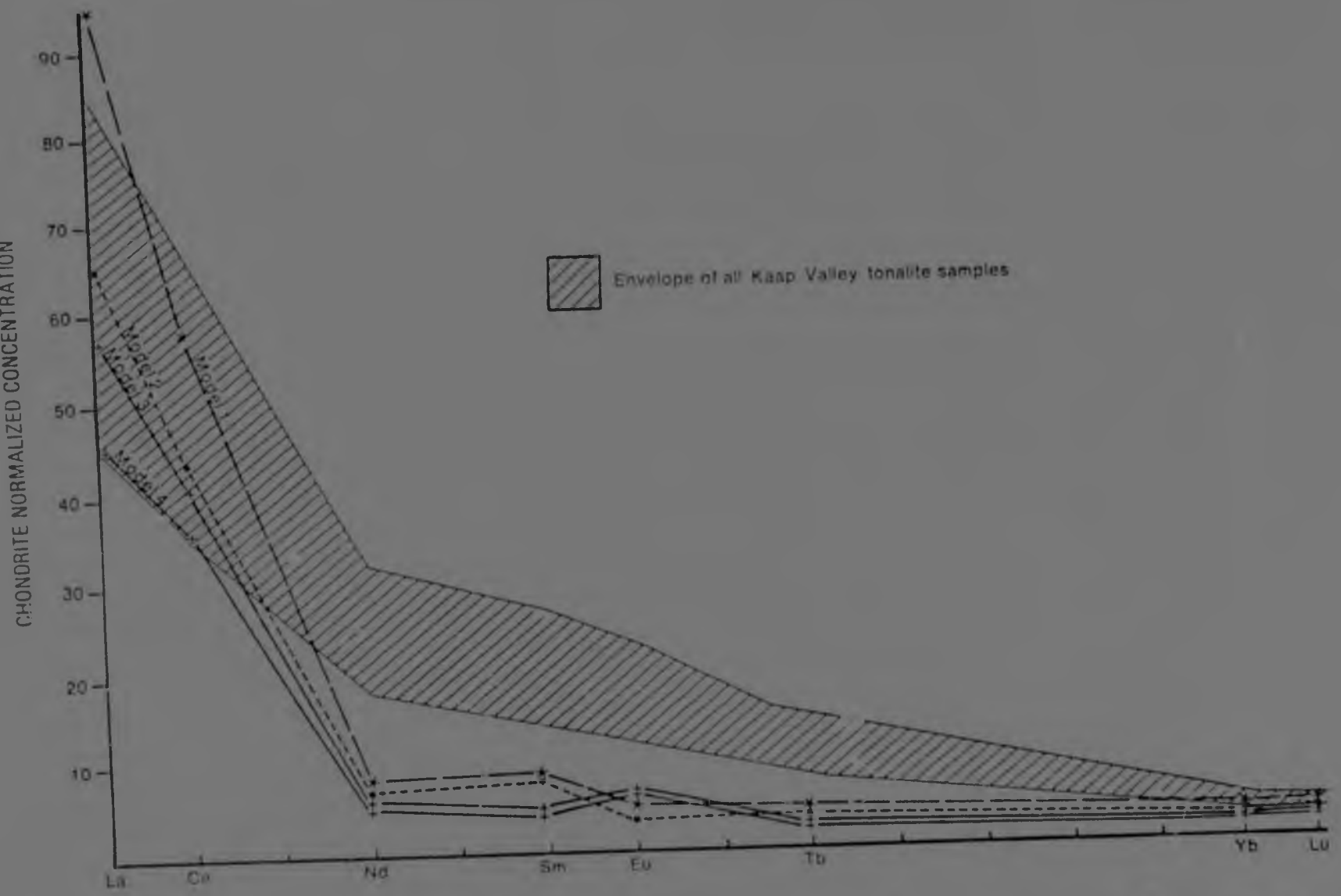

Figure 62 : Chondrite normalized rare-earth element model plot for the generation of a Kaap Valley-type tonalitic melt from a basaltic komatiite parent. Model 1 represents the concentrations of REE in a zone melt fraction (as calculated in Table 28); Model 2 represents the concentrations of REE after 80% equilibriu crystallization of the Model 1 liquid (see Table 31). Models 3 and 4 illustrate the relatively LREE-depleted character of 20% and 30% (respectively) batch melts from a basaltic komatiite parent (see Table 27).

In terms of the Kaap Valley tonalite, therefore, it may be possible to attribute, both the high mafic content of the rock, as well as the apparent enrichment in LREE (and possibly Rb), to a melting process that is analogous to zone melting. In terms of the REE, a model can be derived predicting the expected concentrations of these elements in a zone melt passing through a column of basaltic komatiite and the details of this procedure are presented in Table 28. A chondrite normalized plot of this model is provided in Figure 62 where it is compared with the envelope of samples from the Kaap Valley tonalite and also with the 20% and 30% batch melt solutions derived in Table 27. It is clear that a significant enrichment of the LREE (and a depletion of the HREE) occurs in the komatiite-derived zone melt and that the degree of this enrichment is more compatible with the Kaap Valley tonalite than the concentrations envisaged in terms of the 20% and 30% batch melt models. It should be emphasized that the same bulk partition coefficients and parental compositions were used in both the zone melt and partial (batch) melt considerations outlined in Tables 27 and 28 and in Figure 62.

It is pertinent at this stage to consider what the physical conditions are under which zone melting begins to approximate the conventional partial melt process. In Appendix 4, mathematical considerations show that where the zone length factor (i.e. height of rock column/ height of melt zone) is large, incompatible element concentration during zone melting is equivalent to that taking place during a very small degree of batch melting. Thus, whereas very small degrees of partial melting are required in order to generate nigh concentrations of incompatible trace elements (a feature which is geologically unrealistic particularly in terms of the large volumes of tonalitic or trondhjemitic magma discussed here), similar concentrations can be attained by zone melting processes, where volume constraints (*) are less likely to represent a restriction in terms of their viability (see Appendix 4). It is suggested, therefore, that the enriched incompatible element concentrations in the Kaap Valley tonalite, whilst nevertheless consistent with a melt origin from a basaltic komatiite precursor, appear to have formed by prolonged equilibration of the melt phase with its source material; such a process can be viewed as being analogous to zone melting as incompatible elements are more effectively concentrated into the liquid.

(*) Footnote : Note that there are no limitations to the breadth (or horizontal dimensions) of a melt zone.

TABLE 28

RARE-EARTH ELEMENT CONCENTRATIONS IN THE KAAP VALLEY TONALITE IN TERMS OF ZONE MELTING

The distribution of incompatible elements between melt zone and parental material is given by the following equation :

$$\frac{Cl}{Co} = \frac{1}{K_D} - \left(\frac{1}{K_D} - 1\right)e^{-K_D.\ell} \quad \ldots\ldots\ldots 1.$$ (after Pfann, 1952)

Where Co = original concentration of trace element in parent

Cl = concentration of trace element in melt zone

K_D = bulk partition coefficient of the parent rock

ℓ = zone length factor or height of rock column/height of melt zone.

Zone length factor (ℓ) :

If the melt zone is taken as 10 km thick (i.e. the radius of the Kaap Valley pluton) and it considered to have moved through 20 km of the crust before solidifying, then

$$\ell = 20/10 = 2$$

Using the above equation (1), the concentrations of REE in a zone melt that is derived from a basaltic komatiite parent are (*) :

	(ppm)
La	23,6
Ce	36,4
Nd	3,49
Sm	1,28
Eu	0,23
Tb	0,14
Yb	0,38
Lu	0,06
Ce_N/Yb_N	24,8

(* Parental compositions and bulk partition coefficients are identical to those used in the batch melt model discussed in Table 27).

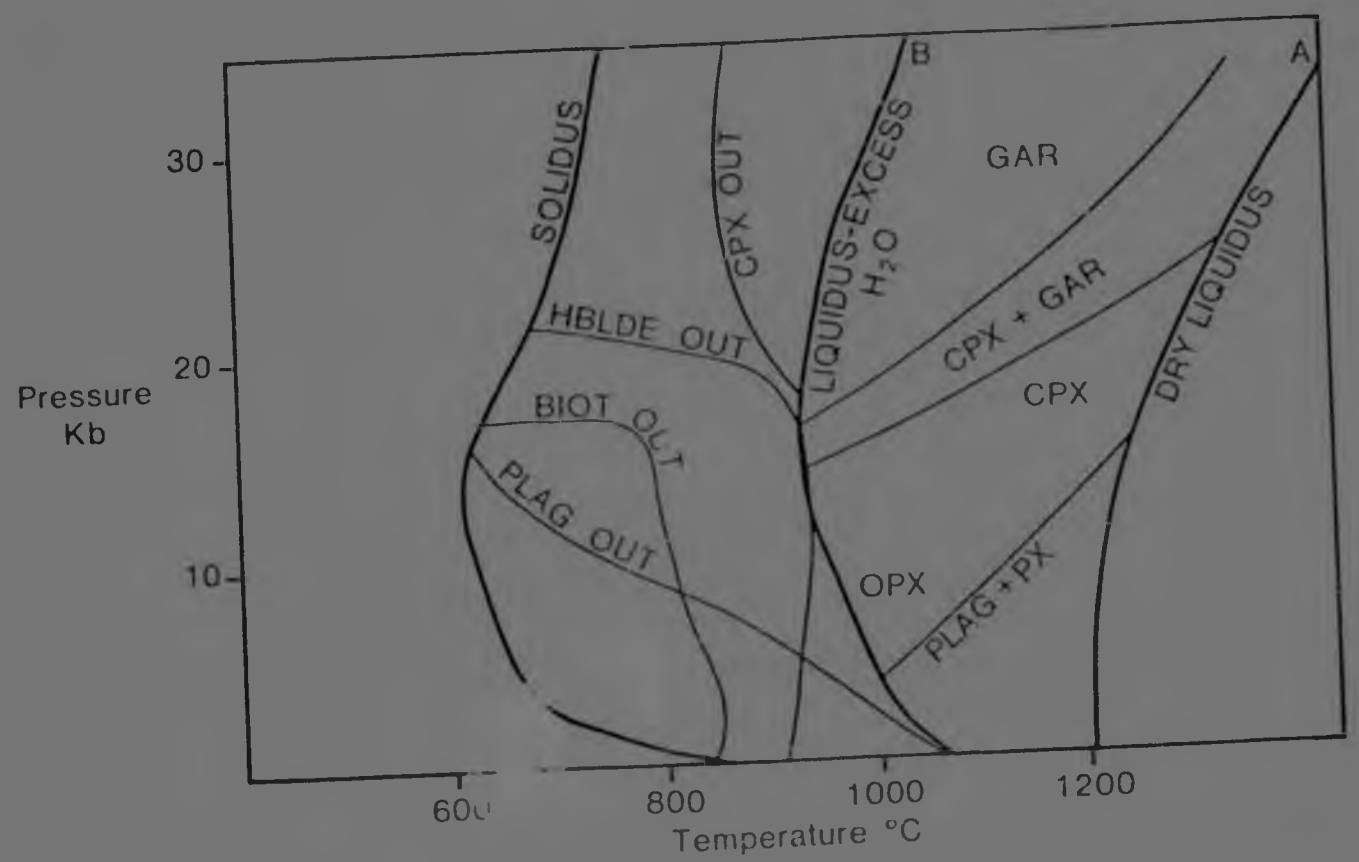

Figure 63 : A. *Phase relationships for tonalite showing the liquidus curves (A and B) for both dry and excess-H_2O conditions (after Stern et al., 1975).*

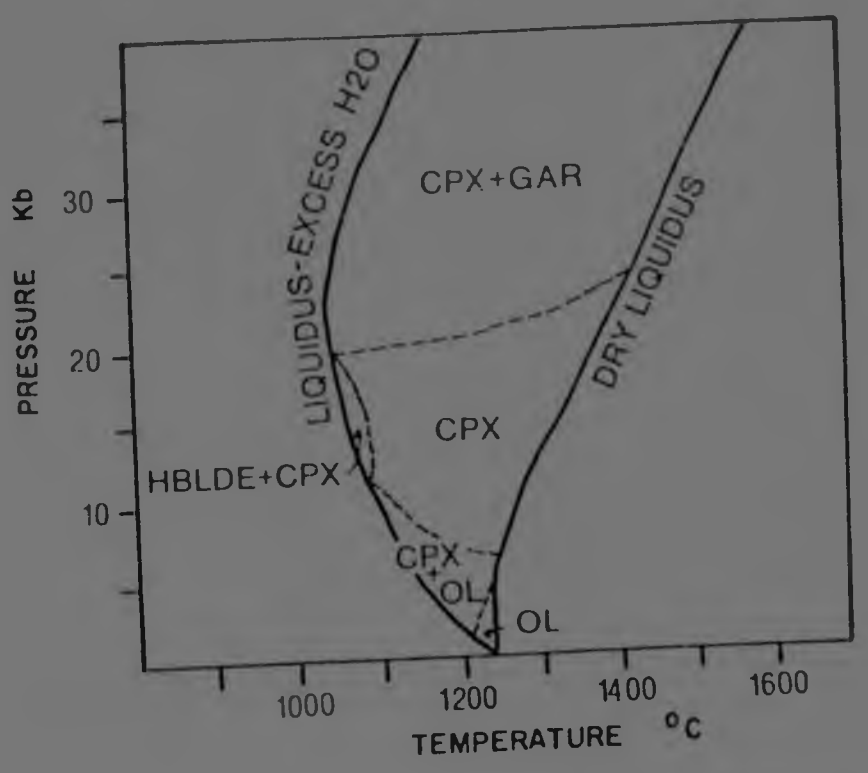

B. *Liquidus phase relations for olivine tholeiite showing the effect of H_2O on the temperature of the liquidus surface (after Stern et al., 1975).*

3.2.1. *Bulk composition of magmas generated by zone melting*

Most of the previous considerations regarding zone melting have revolved around the trace element (more specifically the REE and, to a lesser extent, Rb) content of the Kaap Valley tonalite. The process can only, however, be considered viable if it is found to be compatible with the bulk (major-element) composition of magmas so derived and in keeping with their phase relationships (see Figure 63). The process of zone melting would appear to be incompatible with the generation of granites (*sensu lato*) as the former requires that near-total melting of a zone occurs during the upward migration of the liquid, whereas the production of felsic magmas from a mafic parentage logically assumes only minimum temperature *partial* melts. Moreover, zone melting requires the propagation of a melt zone upwards through a column of rock and this may not be possible if the magma moves progressively into environments characterized by temperatures below its liquidus. The following discussion speculates on how these two problems may be overcome in terms of a zone-melt origin for the Kaap Valley tonalite.

As shown in Figure 63B, the liquidus temperatures for olivine tholeiites decrease progressively with the availability in the system of excess water-vapour. For the purposes of this discussion it is assumed that a similar situation would apply with respect to a basaltic komatiite. If partial melting of a basaltic or eclogitic parent occurs at temperatures of, for example, between 1100 - 1200^{o}C (i.e. below the dry liquidus in Figure 63B) it is probable that the melt phase will be relatively enriched in water-vapour. Assuming that the volatiles will move upwards in the newly-formed magma chamber, they will be responsible for decreasing the liquidus temperature of roof material. This shift in the liquidus will probably result in the generation of a greater proportion of melt such that conditions become analagous to those envisaged during zone-melting, where total or near-total fusion occurs. Furthermore, as the volatile phases move upwards, so the basal portions of the melt zone will become H_2O-depleted, causing the concomitant crystallization of melt phases in that region. Thus, a mechanism for the propagation of a zone melt by ".....solution of roof material and crystallization of a similar amount at the bottom....." (Harris, 1957) appears viable in terms of the above considerations.

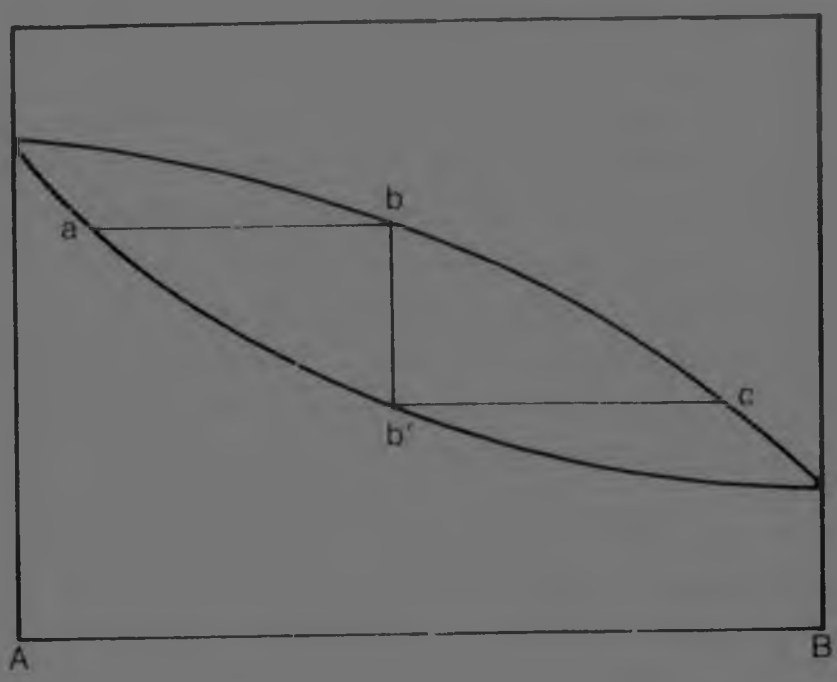

Figure 64 : Simplified binary solid-solution series between two end-member components A and B. The system is similar, for example, to that for the plagioclase felspars.

Additional considerations, however, concern the possibility of changes in the bulk composition of the melt zone as it moves up the rock column. According to Harris (1957), such changes can be envisaged in terms of a simple, binary solid-solution reaction series and this is demonstrated in Figure 64. If the original melt zone had a composition at b in the above diagram, then a mineral or minerals crystallizing at the bottom of the melt zone will have had a composition at a, the latter being more enriched in the end-member component A. As a result of this fractionation, successive melt zones will change composition along the liquidus from b to c, and will thus become enriched in the end-member component B. A corresponding change in the composition of the deposited solid phases will take place from a to b'. The final deposited solid at the base of the uppermost melt zone will have a composition at b' but the melt zone will retain the characteristics of a composition that is lower in the so-called reaction series. Such a composition, naturally, is more akin to a partial melt than it is to a melt that has resulted from near-total fusion of a mafic parent. In this light, therefore, it may be feasible to derive a tonalitic (or andesitic) magma by zone melting of a more basic parent.

It is not possible, however, to realistically quantify these considerations and the process of zone melting (*sensu stricto*) as applicable to the Kaap Valley tonalite, must remain speculative. Nevertheless, it is suggested that zone refining theory may be more widely applicable in geological processes than hitherto realized, especially where rocks are anomalously enriched in incompatible trace elements. Particularly relevant in the process is the means whereby a melt is allowed to continuously equilibrate with previously 'unrefined' material, a feature which is not taken into account in conventional partial melt considerations.

3.3. Crystal fractionation in the Kaap Valley tonalite

The previous discussion has been concerned only with certain of the processes related to the generation of a tonalitic magma similar in character to that envisaged as the igneous precursor to the Kaap Valley pluton. The following discussion considers the mode of formation of the rock itself during the subsequent crystallization of this magma; such considerations are thought to be particularly important in view of mounting

evidence suggesting that granitic (*sensu lato*) compositions may not wholly reflect the liquids from which they were derived. Numerous studies have recently indicated that granitic magmas undergo fractional crystallization, either by progressive inward nucleation (Parslow, 1971; Wolhuter, 1973; McCarthy and Robb, 1978; Groves and McCarthy, 1978; Bateman and Nockleberg, 1978; Bateman and Chappell, 1979; Brown et al., 1979) or by subtle, gravitationally induced, crystal settling (Emeleus, 1963; Taylor, 1975; Couturie, 1977; P.C. Bateman, personal communication, 1979). Either of these processes will result in heterogeneity in granitic plutons and may be applicable to the mineralogical variations observed in the Kaap Valley tonalite.

3.3.1. *Major element variations*

A subtle chemical hiatus (best illustrated in Harker plots of SiO_2 v Al_2O_3 v MgO and SiO_2 v Fe_2O_3*, in Figure 53) serves to distinguish between hornblende tonalites and hornblende + biotite tonalites in the Kaap Valley pluton. Specifically, the Harker trend of the hornblende + biotite tonalites is higher in alumina and lower in magnesium, calcium and iron than that for the hornblende tonalites and it is clear that, for certain elements, the two trends are displaced relative to each other. It is considered that this feature may be the result of the decreasing hornblende/biotite ratio that is commensurate with the incoming of biotite at a somewhat advanced stage in the crystallization history of the body. Thus, crystallization of the major mineral phases in the Kaap Valley tonalite is envisaged as being a step-wise process, with an assemblage comprising plagioclase + hornblende + quartz initiating the solidification of the magma. This assemblage is modified as biotite becomes a liquidus phase and the hornblende/biotite ratio decreases with progressive crystal fractionation. A decreasing hornblende/biotite ratio is a feature that has been noted before in fractionating granitic assemblages (Piwinski, 1968; McCarthy and Fripp, 1980) and is usually attributed to the residual enrichment of potash in differentiated liquid phases. As shown later (Figure 72), the Kaap Valley pluton is preferentially enriched in K_2O in its central portions, which is that area dominantly underlain by the hornblende + biotite tonalites.

The effect of this step-wise crystallization sequence, which is also largely compatible with the petrographic descriptions outlined above, can

TABLE 29

MAJOR ELEMENT VARIATIONS DURING THE CRYSTALLIZATION OF THE KAAP VALLEY TONALITE

A. MINERAL COMPOSITIONS

		PLAGIOCLASE (*)	HORNBLENDE (*)	BIOTITE (*)	K-FELSPAR (+)	QUARTZ
Wt.%	SiO_2	61,7	47,6	36,1	63,9	99,50
	TiO_2	-	1,5	4,2	-	-
	Al_2O_3	23,8	6,4	14,7	19,6	-
	Fe_2O_3	0,2	15,4	19,6	-	-
	MnO	-	0,5	0,5	-	-
	MgO	-	13,4	10,1	0,3	-
	CaO	4,5	10,7	0,1	0,01	-
	Na_2O	8,7	1,5	0,1	2,18	-
	K_2O	0,3	0,5	10,4	12,82	-

(* - Representative analyses from Tables 23, 24 and 25.
+ - after Robb (1977))

B. MODES IN EACH OF EIGHT CONSECUTIVE CRYSTALLIZATION STEPS

	1	2	3	4	5	6	7	8
Plagioclase	66	65	64	63	60,5	59	56	52
Quartz	11	14	17	19	21,5	23	25,5	28
Hornblende	21	19	17	13	11,5	10	8,5	7
Biotite	-	-	-	2	3	4	5	6
K-Felspar	2	2	2	3	3,5	4	5	7

C. WHOLE ROCK COMPOSITIONS OF EACH MODE

		1	2	3	4	5	6	7	8
Wt.%	SiO_2	62,8	64,3	65,7	66,5	67,4	68,0	68,7	69.8
	TiO_2	0,32	0,29	0,26	0,28	0,30	0,32	0,34	0,35
	Al_2O_3	17,4	17,1	16,7	16,7	16,3	16,0	15,5	15,2
	Fe_2O_3	3,4	3,1	2,8	2,5	2,5	2,4	2,4	2,4
	MgO	2,81	2,55	2,28	1,94	1,84	1,74	1,65	1,55
	CaO	5,2	4,9	4,7	4,2	3,9	3,7	3,4	3,1
	K_2O	0,57	0,54	0,52	0,85	1,0	1,15	1,36	1,70

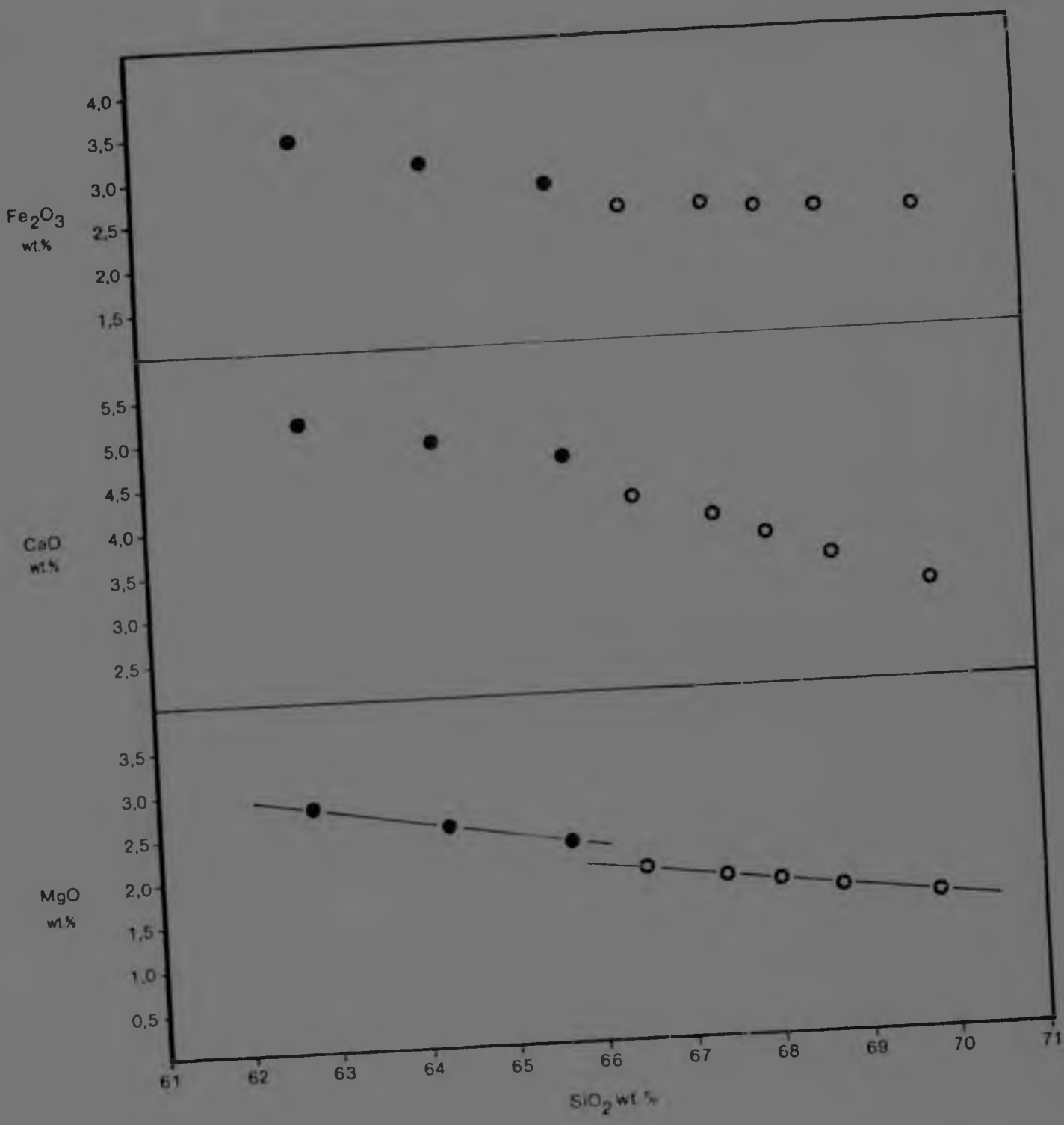

Figure 65 : Model fractionation trends for the hornblende (dots) and hornblende + biotite (encircled stars) tonalites in the Kaap Valley pluton. The trends are calculated by considering eight distinct fractionation increments; a crystal extract comprising plagioclase + quartz + hornblende is considered in the first three increments, whilst the assemblage plagioclase + quartz + hornblende + biotite is considered for the latter five increments (see Table 29). The trends may be compared with the Harker diagrams in Figure 53.

be quantitatively assessed as the compositions of the principal mineral phases of the tonalite are known (Table 29). In Figure 65, the expected changes in composition of a rock crystallizing these phases is calculated by considering eight consecutive crystallization modes; the first three consist of plagioclase + hornblende + quartz + K-felspar (and involve a systematic decrease in plagioclase and hornblende and increase in quartz content with increasing fractionation) whilst the remaining five comprise the same assemblage, but with the addition of biotite. The latter five crystallization increments envisage a continuing decrease in hornblende and plagioclase and an increase in biotite, K-felspar and quartz content as fractionation proceeds. The resulting whole rock composition of each of the eight modes is calculated by multiplying the weight fraction of each mineral phase by its average composition and adding the combinations representative of each mode. The average mineral compositions used, the mineral characteristics of each of the eight modes and the resultant whole rock compositions are presented in Table 29.

The results from this table are plotted in Figure 65 where it is seen (by comparison with Figure 53) that the fractionation trend, as well as the chemical hiatus between the two tonalitic sub-groups can, in most instances, be reasonably well simulated in terms of the above considerations. In the case of Fe_2O_3, MgO, Al_2O_3 and CaO the tonalites crystallizing biotite contain fewer mafic materials (i.e. hornblende + biotite) and this undoubtedly accounts for the "steps" observed in the empirical data (this has been emphasized in the plots of MgO v SiO_2 in Figures 53 and 65). However, the contrasting slopes of the trends of the two tonalite sub-groups are related to the fact that an additional mineral (i.e. biotite) is crystallizing in the latter group. In the case of most elements the differences in model slopes are similar to those observed in the empirical trends, but discrepancies do exist. The most noticeable of these are found in the model curves for SiO_2 v TiO_2 and SiO_2 v K_2O (Figure 65). In the case of both TiO_2 and K_2O, the crystallization of biotite in the model trends causes an increase in concentration with continued fractionation. In the case of TiO_2, the model bears no resemblance to the empirical trend (Figure 53) and this may be the result of the presence of rutile and sphene particularly during the later stages of crystallization, a factor not considered in the model calculation. The empirical data for K_2O (Figure 53) is highly scattered and exhibits no

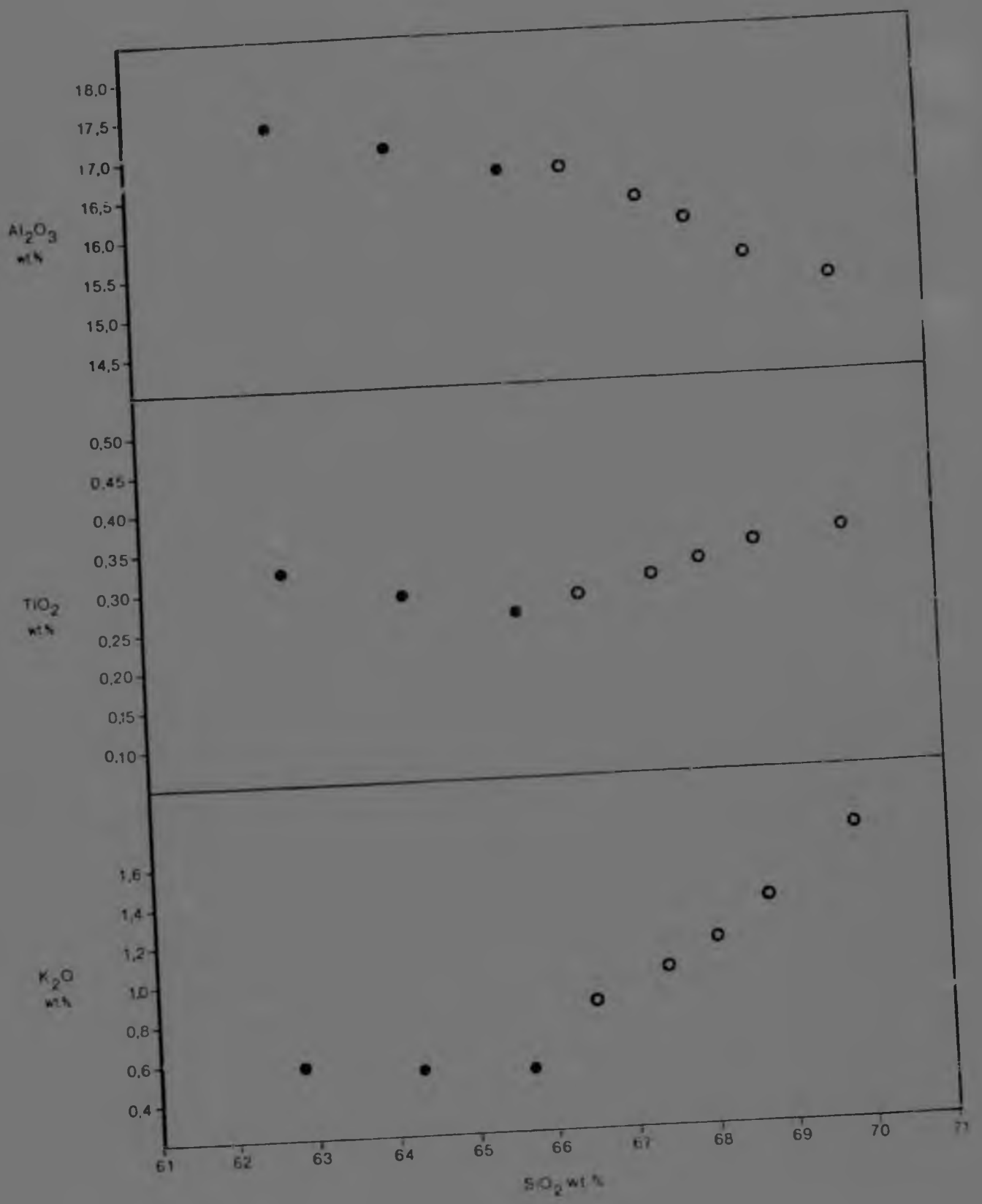

Figure 65 (continued) :

systematic relationship with respect to SiO_2. This may be due to inconsistencies in the amount of K-felspar present in the rock, a factor which, as suggested by McCarthy and Robb (1978), may be due to the presence of "intercumulus" mineral phases in the crystallizing granite.

Hence, the above considerations augment the suggestions made previously that the major eleme variations in the Kaap Valley pluton do not reflect melt-restite m s such as those occasionally suggested for Harker-trends of this nature (White and Chappell, 1977). Rather it is envisaged that the compositional variations point to solidification processes, where step-wise crystallization of the relevant mineral phases has taken place. This idea is developed further in the sections that follows.

3.3 2. *Trace element (Rb, Sr and Ba) variations*

The crystallization sequence envisaged above may also be viewed in terms of the partitioning of trace elements (Rb, Sr and Ba) between melt and fractionating mineral phases. Thus, the crystallization, initially of an assemblage consisting of plagioclase + hornblende + quartz, and subsequently, of plagioclase + hornblende + quartz + biotite can be portrayed in terms of a quantitative trace element model. Such a model would have to simulate the broad increase in Rb and Ba and the decrease in Sr observed in the empirical trends of the Kaap Valley tonalite (Figure 54).

In the trace element model discussed below, solidification is considered to occur by equilibrium crystallization. However, this is not meant to imply that the entire pluton will be characterized by a uniform trace element content which is similar to that in the original magma. Equilibrium crystallization equations are used in preference to those of fractional crystallization as the observed range in trace element content is not as wide as might be expected for the latter process (see, for example, McCarthy and Robb, 1978). In a large pluton such as the Kaap Valley body, it is considered likely that certain portions (probably on the margins) will freeze before others. In addition, it is unlikely that equilibrium (*sensu stricto*) will be maintained throughout the

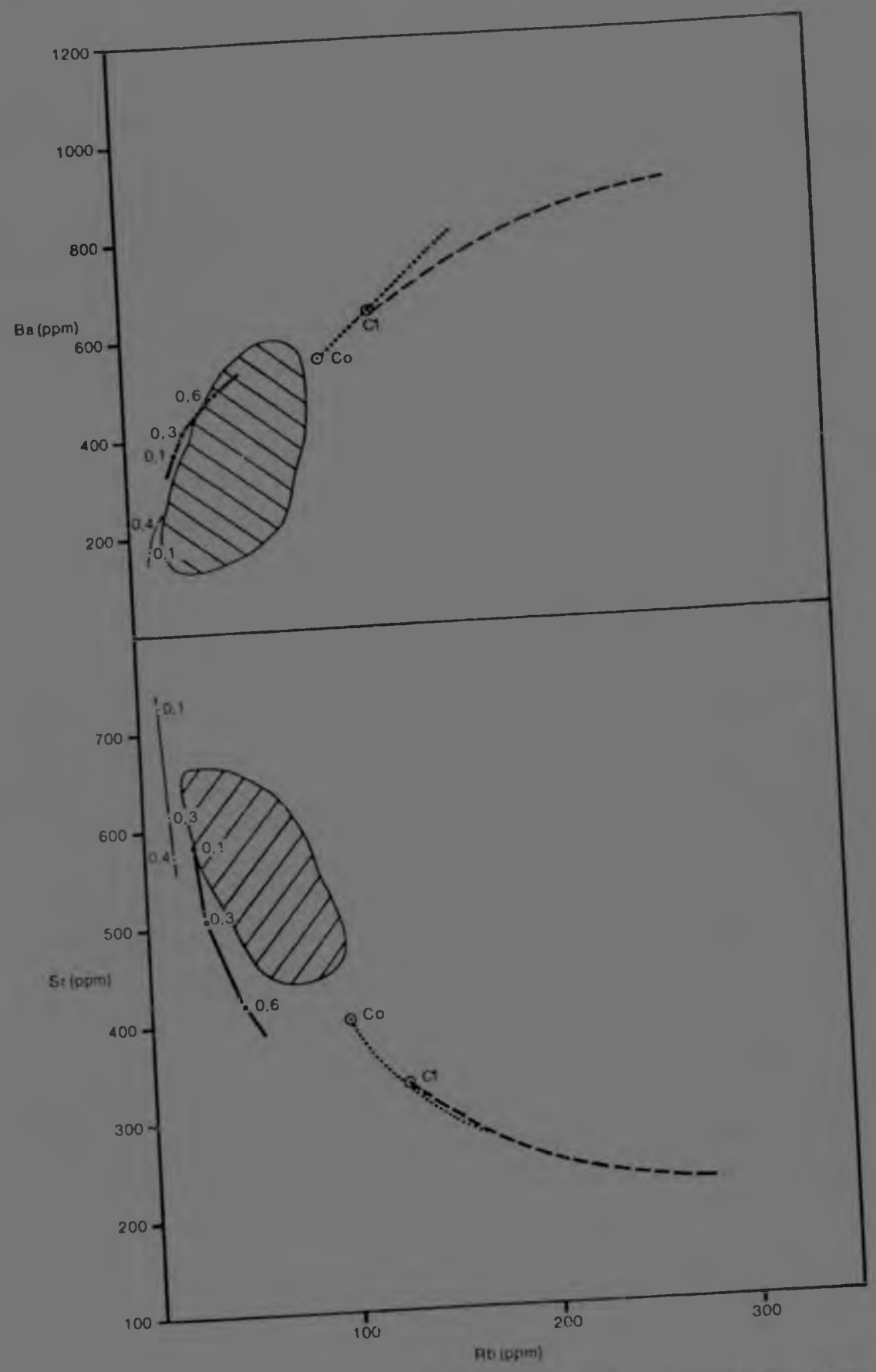

Figure 66 : *Model plots of Rb v Sr and Rb v Ba for crystal fractionation in the Kaap Valley tonalite (see Table 50). Solid trend lines represent the trace element contents of hornblende tonalite (derived from a magma at Co) and hornblende + biotite tonalite crystallizates, the latter being derived from a differentiated magma (at C1) formed after 30% equilibrium crystallization of the former. Dashed trend lines are the residual liquid compositions. The numbers 0,1; 0,3; 0,4 etc. represent the degree of crystallization; the hatched fields are envelopes representing data for the Kaap Valley tonalite, from Figure 54.*

solidification process so that subdued magma differentiation will in fact occur, possibly along the lines of the "incremental equilibrium crystallization" mode suggested by McCarthy and Hasty (1976). The trace element models that follow are viewed in terms of these considerations which are probably more realistic than those which entail the mere application of the relevant formulae.

As seen in Figure 66 the range in trace element composition of the Kaap Valley tonalite coincides approximately with model trends representing solids that have crystallized (essentially in equilibrium) from a liquid of composition Co (see Table 30). Two trends are considered; the first represents the crystallization of the hornblende tonalites from a magma with initial composition Co, whilst the second trend represents the crystallization of hornblende + biotite tonalites from the differentiated liquid (C1) that had formed after approximately 30% crystallization of the hornblende tonalites. Because of the bulk incompatibility of Rb and Ba these two elements will become enriched in the liquid, in contrast to strontium ($K_D > 1$) which will become depleted. Thus, an increase in Rb and Ba and a decrease in Sr takes place as crystal fractionation progresses and this is broadly reflected in the empirical data as well as indicated in the model trends (Figure 66). It is noticeable, however, that whilst the model satisfactorily accounts for the ranges in Sr and Ba concentration in the Kaap Valley tonalite, the Rb concentrations are lower (by a factor of approximately 2) than those observed in the empirical trends for the body, *in spite* of the fact that the original magma composition was considered to contain 100 ppm Rb. A Rb concentration of 100 ppm in a magma considered to have been derived by the partial melting of a basic source is excessive, and a consideration of batch melting from a basaltic komatiite source will demonstrate this (*). As a result it would appear that the Kaap Valley tonalite contains more Rb than can be accounted for by conventional means, a factor that is in accordance with the suggestions made previously that the original magma may have been derived by processes akin to zone melting.

It is important to stress that the distribution of Rb, Sr and Ba in the Kaap Valley tonalite is not particularly systematic and does not rigidly conform to the crystallization scheme outlined above. This is

---

(*) Footnote : A consideration of 30% batch melting (after Shaw, 1970) of a basaltic komatiite containing 5 - 10 ppm Rb will result in no more than 3 - 4x enrichment of Rb in the resultant tonalitic melt.

TABLE 30

THE DISTRIBUTION OF Rb, Sr AND Ba DURING THE CRYSTALLIZATION OF THE KAAP VALLEY TONALITE

A. HORNBLENDE TONALITES

MODE 1	K_D	ORIGINAL COMPOSITION OF MAGMA (Co)
Plagioclase - 66%	Rb - 0,10	Rb - 100 ppm
Hornblende - 21%	Sr - 2,00	Sr - 400 ppm
Quartz - 11%	Ba - 0,33	Ba - 550 ppm
K-felspar - 2%		

B. HORNBLENDE + BIOTITE TONALITES

MODE 2	K_D	COMPOSITION OF MAGMA (C1) AFTER APPROXIMATELY 30% CRYSTALLIZATION OF MODE 1
Plagioclase - 60%	Rb - 0,18	Rb - 130 ppm
Hornblende - 12%	Sr - 1,85	Sr - 340 ppm
Quartz - 22%	Ba - 0,55	Ba - 640 ppm
Biotite - 3%		
K-felspar - 3%		

NOTE : (i) Original composition of magma is assumed

(ii) Trace element distribution is calculated for equilibrium crystallization

(iii) Partition coefficients listed in Appendix 2

evident in Figure 54 where considerable scatter is observed in the empirical data and the two tonalitic sub-types exhibit a large measure of overlap. This is undoubtedly due to the fact that these trace elements have not remained immobile during secondary processes and, in this particular case, therefore, are not entirely suitable for petrogenetic modelling. However, the empirical data trends in Figure 54 do exhibit a broad positive relationship between Rb and Ba, and a negative relationship between Rb and Sr, suggesting that the primary trace element distribution may have been a function, at least in part, of the crystallization scheme envisaged above. In the case of the Kaap Valley tonalite, this aspect of the data must be viewed semi-quantitatively and in the light of the more systematic behaviour of the major and rare-earth elements.

3.3.3. *Rare-earth element (REE) variations*

The REE data for a number of samples of the Kaap Valley tonalite exhibit a significant variation that is illustrated in diagrammatic form in Figures 55A and 57. As indicated previously, the LREE enrichment of the Kaap Valley tonalite is, on average, slightly greater than that apparently characteristic of the more felsic trondhjemite plutons in the region (Figure 57) and this is attributed to a process that is possibly analogous to zone melting. It is also apparent in Figure 57 that the more felsic hornblende + biotite tonalites are, on average, more LREE enriched (and HREE depleted) than the hornblende tonalites, although the envelopes of data for the two phases overlap (Figure 55A).

The variations in the chondrite-normalized REE pattern for the Kaap Valley tonalite can probably best be explained in terms of crystal fractionation where solidification occurs along the lines suggested in the previous section. Variations in the degree of LREE enrichment and the Ce_N/Yb_N ratio are envisaged being a function of progressive crystallization over the pluton as a whole. In Figure 56, where the Ce_N/Yb_N ratio is plotted against SiO_2, it is clear that the more mafic hornblende tonalites are characterized by lower Ce_N/Yb_N ratios than the hornblende + biotite tonalites. Hence, as indicated below, the REE appear to be consistent with the scheme of progressive, step-wise solidification, whereby the crystallization of a plagioclase + quartz + hornblende assemblage preceded

the appearance of biotite on the liquidus, the latter forming only after a significant interval of magma differentiation.

In view of the considerations regarding crystal fractionation in the Kaap Valley tonalite, it is of interest to quantitatively assess the likely distribution of REE on solidification, in terms of a similar process to that envisaged for Rb, Sr and Ba. Again it is emphasized that the final distribution of trace elements in a rock body is independent of the processes by which the magma originally formed (i.e. zone melting in this case) but is determined by its cooling history and the differentiation processes that accompany crystallization. In Table 31 the concentrations of the REE in a hornblende tonalite assemblage are calculated for the cases where 50% and 80% crystallization have occurred. The table shows that progressive crystallization results in variations in the REE content and also in the Ce_N/Yb_N ratio, the latter increasing as solidification progresses. The question arises as to whether the observed REE (or trace element) variations can realistically be equated to model rocks which, theoretically, have only partially crystallized. This may, in fact, be the case if, as noted before, equilibrium is not perfectly attained and/or the final stages of crystallization are speeded up. In the latter case, for example, degassing might result in an increase in the liquidus temperatures so that subsequent nucleation of crystals becomes more rapid and equilibrium is no longer maintained. Rocks which have effectively only "partially crystallized" can also be viewed in terms of an assemblage comprising of intercumulus liquid (McCarthy and Hasty, 1976). If early formed mineral phases are allowed to crystallize together with an intercumulus liquid and the resultant rock does not re-equilibrate with remaining magma, then it may reflect a trace element distribution similar to a model assemblage which has, theoretically, only partially solidified. Hence, it is feasible for the hornblende tonalites to have different REE patterns to those of the hornblende + biotite tonalites, with the latter forming later in the crystallization history of the body as a whole.

In Figure 62 the chondrite normalized REE trace (calculated in Table 31) of a tonalitic solid that formed after 80% crystallization from the magma derived in Table 28, is plotted. Clearly the LREE enrichment in this model curve is compatible with that observed in the Kaap Valley tonalite. Together with the previous considerations involving major and

TABLE 31

THE DISTRIBUTION OF RARE-EARTH ELEMENTS DURING THE PROGRESSIVE CRYSTALLIZATION OF THE KAAP VALLEY TONALITE

	50%	ENRICHMENT FACTOR	80%	ENRICHMENT FACTOR
La	10,6	0,45	15,8	0,67
Ce	20,4	0,56	27,7	0,76
Nd	2,9	0,84	3,2	0,93
Sm	1,22	0,95	1,26	0,98
Eu	0,31	1,35	0,27	1,17
Tb	0,13	0,93	0,14	1,00
Yb	0,42	1,10	0,38	1,00
Lu	0,06	1,00	0,06	1,00
Ce_N/Yb_N	12,2		18,7	

NOTE :

(i) REE distribution is calculated for equilibrium crystallization.

(ii) 50% and 80% columns represent the concentration of REE in the solid phase after 50% and 80% crystallization respectively.

(iii) Original composition of the liquid is considered to be that calculated in terms of the zone melting model in Table 28.

(iv) Tonalitic bulk partition coefficients are from Table 27.

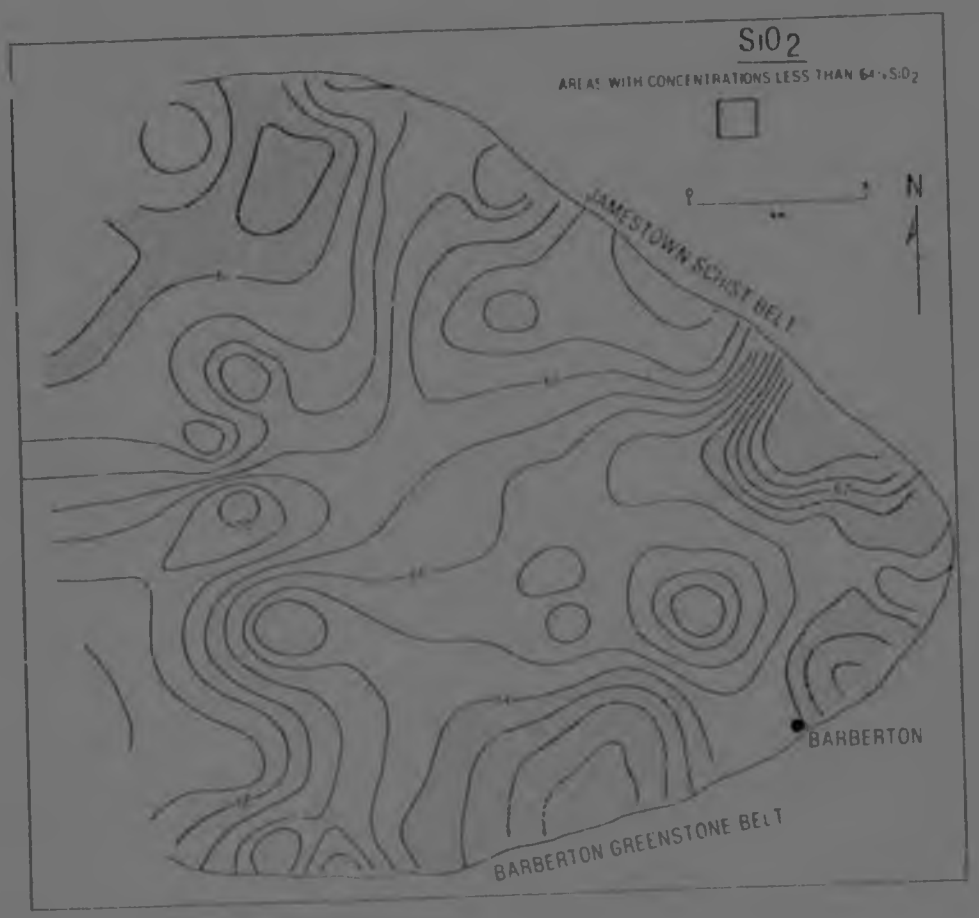

Figure 67

Figuren 67-77 : Contour maps of SiO_2, TiO_2, CaO MgO, Fe_2O_3, K_2O, Rb, Sr, Ba, Na_2O and Al_2O_3 respectively, for the Kaap Valley pluton. The maps were computer-drawn from the analyses at 41 individual sample localities representing hornblende a[illegible]rnblende ± biotite tonalites (Table 31). T[illegible]mple localities are shown, together with the g[illegible]ical details, in Figure 53. Stippled areas, [illegible] each case, represent areas of either high or lo[illegible]ncentrations, as indicated on the individual maps. Contour intervals, either in wt.% or ppm are variable, and indicated by the values posted on the actual contour diagram.

trace elements, these facts collectivelv imply that the compositional variations over the Kaap Valley pluton were caused by crystal fractionation. As mentioned previously, granitic magmas in general may solidify either by progressive inward nucleation of crystals or, by gravitationally induced settling and that examples of both mechanisms are known to exist. In terms of the above discussion, either process may have influenced the compositional and mineralogical variations evident in the Kaap Valley body. If a knowledge of the spatial distribution of major and trace elements over the pluton is known, then it may be possible to further test the crystallization mode suggested above; these aspects are considered in detail in the following section.

4. THE SPATIAL DISTRIBUTION OF ELEMENTS IN THE KAAP VALLEY PLUTON

4.1. Contoured distribution of major and trace element variations and possible relationships to crystal fractionation.

The distribution of major and trace elements analysed from 41 samples of hornblende and hornblende + biotite tonalites (Table 21) is plotted on contour maps in Figures 67 - 77. These maps (which are all computer drawn and not, therefore, biased by a subjective approach) indicate that the elemental distribution is closely related to the distinction between the two tonalitic sub-types, as defined in Figure 52. The contour diagram for SiO_2 (Figure 67) shows that low values of SiO_2 (i.e. < 64%, shown as a stippled area) occur in an arcuate belt centred around Barberton in the southeastern portion of the pluton, as well as in a small elongate zone diagonally opposite, in the northwestern quadrant of the body. These areas of low SiO_2 content are clearly related to the distribution of the more mafic hornblende tonalites demarcated in the geological map (Figure 52). The contour diagrams for TiO_2, CaO, MgO and Fe_2O_3 (Figures 68 - 71) all exhibit remarkably similar, but inverse, characteristics with respect to the pattern for SiO_2. These maps all show high values (again shown as a stippled area) in the southeastern portion of the body as well as in the smaller elongate zone in the northwestern quadrant. The geometry of these more mafic zones is of particular interest and it is clearly seen on all four of these maps that the contours in the southeastern belt are characterized by two distinct lobes (one on either side of Barberton) that are partially pierced by an

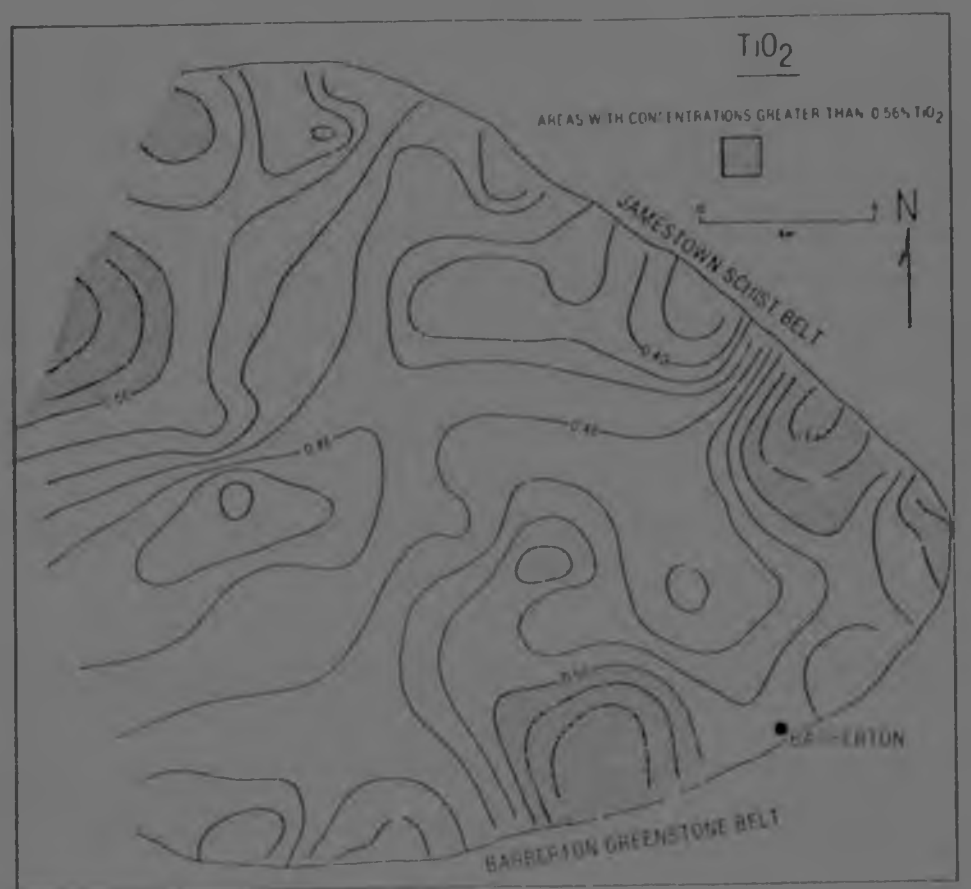

Figure 68

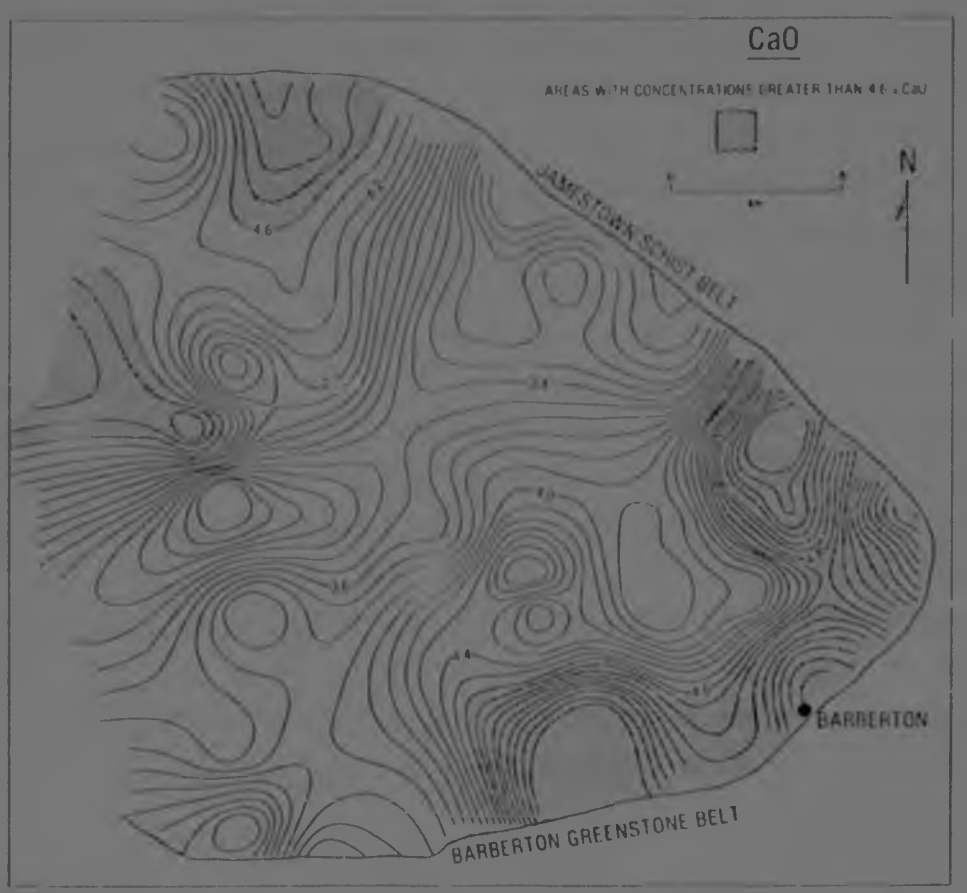

Figure 69

embayment of contour values. These two lobes are matched, either by two similar lobes, or by two discrete zones of higher values, diagonally opposite in the northwestern quadrant of the pluton. It is obvious that high values of TiO_2, MgO, CaO and Fe_2O_3 do *not* characterize the entire margins of the Kaap Valley tonalite, as might have been expected had its more mafic phases been the result of the assimilation of significant portions of the surrounding greenstone belt during its emplacement. Rather, the more mafic phases occur in geographically discrete zones within the confines of which, hornblende tonalites predominate (compare Figure 52 with Figures 67 - 71).

The contour maps for K_2O and Rb, Sr and Ba (Figures 72 - 75) are somewhat different from those described above. In the case of K_2O, the pattern is less systematic than those shown in Figures 67 - 71, although low K_2O values are still approximately located in the southeast and northwest quadrants of the pluton. Here, however, the distribution of potassium is dependent not only on the occurrence of K-felspar but also on the presence of biotite, and its distribution, therefore, is likely to be less predictable. The distributions of Rb, Sr and Ba are similar in that the margins of the body are depleted in these elements relative to the central portions. This feature is probably related to the partitioning of Rb, Sr and Ba into K-felspar and biotite, both of which tend to occur more frequently towards the centre of the pluton. (Note that Sr and Ba are partitioned into K-felspar and Rb and Ba are partitioned into biotite, see compilation of partition coefficients in Appendix 2).

Two of the diagrams, namely those of Na_2O and Al_2O_3 (Figures 76 and 77) have a contour pattern that is not readily relatable to the distribution of the tonalitic sub-types in the pluton. Low values of Al_2O_3 tend to be concentrated in certain marginal areas of the pluton, whereas low soda values also appear sporadically distributed. The albite content of the plagioclases does not seem to relate to these patterns as earlier evidence pointed to the fact that this mineral exhibited a similar range in composition for both hornblende and hornblende + biotite tonalites. The Harker trends discussed previously did illustrate a small systematic decrease in alumina with increasing silica and this was accounted for in the model considerations of crystal fractionation by decreasing the amount of plagioclase present as crystallization progressed. Although this is reflected in a pronounced central soda low in Figure 76, it does not appear

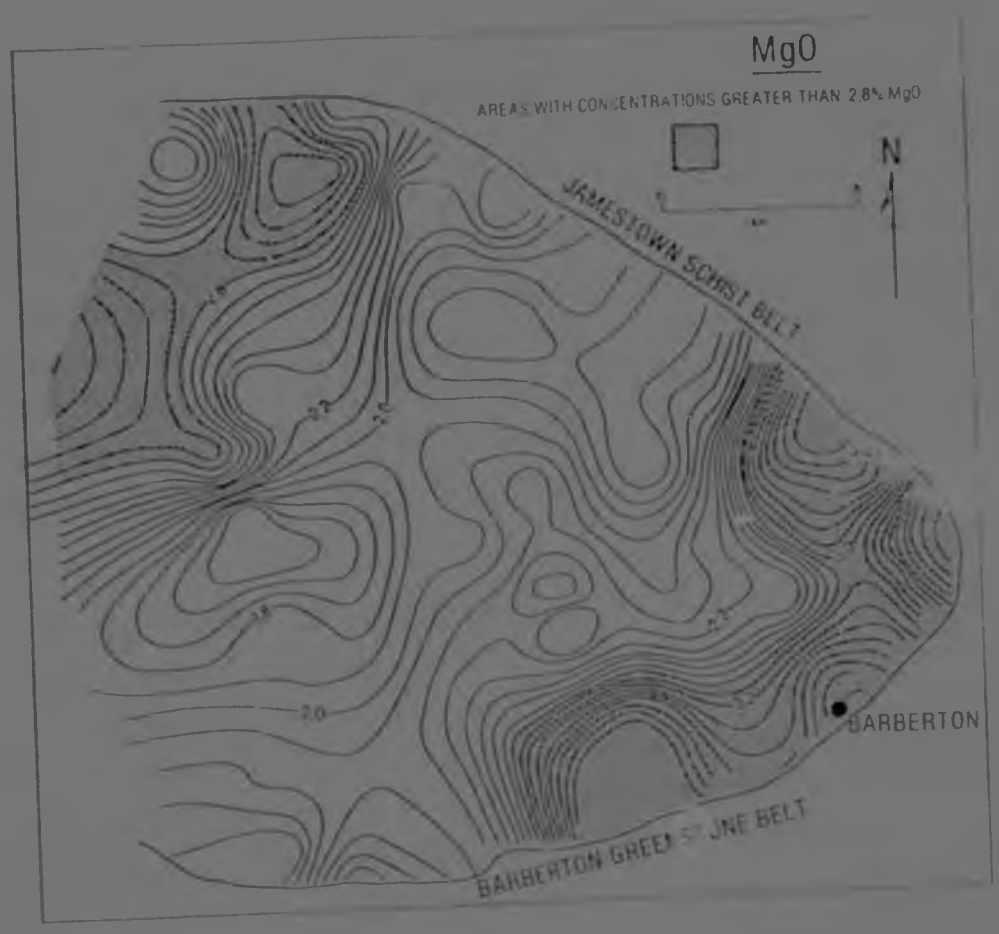

Figure 70

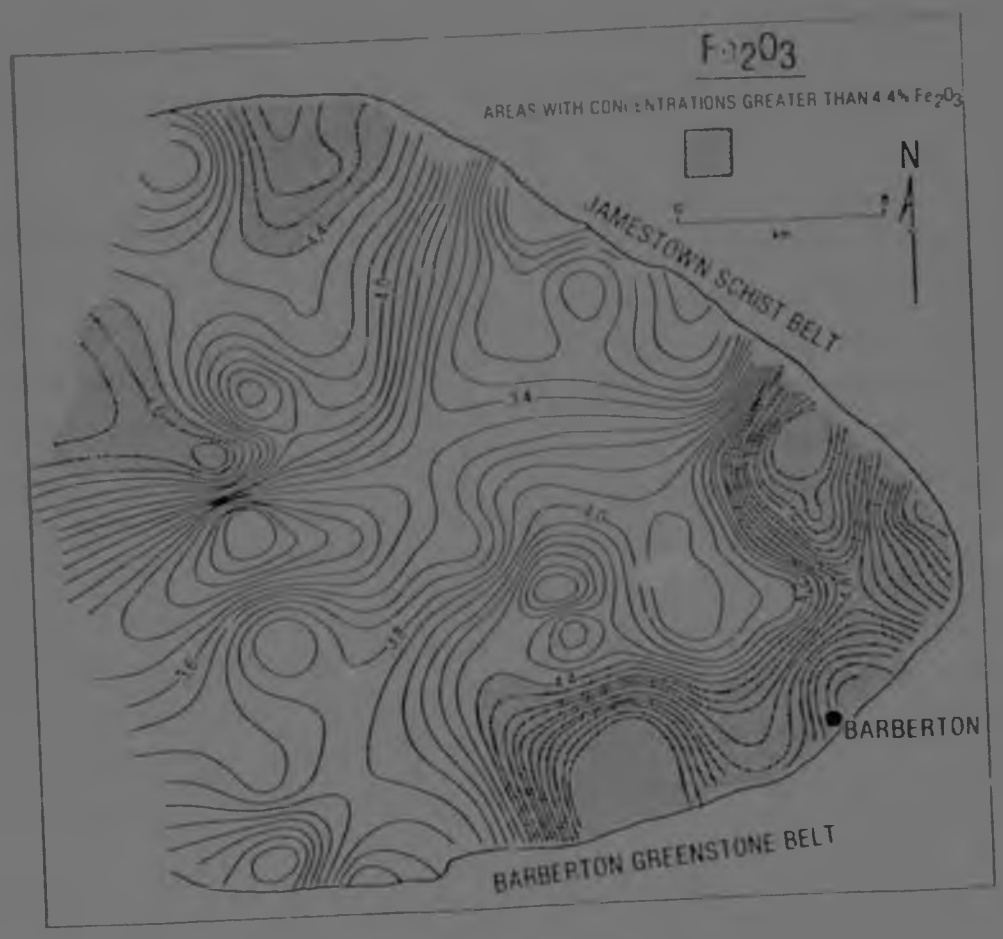

Figure 71

in the alumina contours. A possible reason for this is that the central portions of the contour diagrams are not represented by as many samples as the margins, because of poorer exposure, and do not, therefore, reflect the more subtle compositional variations in the true manner.

The chemical variation in the Kaap Valley pluton, as illustrated in the contour maps described above, could possibly be explained in two ways; firstly, as the result of crystal fractionation or, secondly, by the assimilation of wall-rock (greenstone) material. The latter process, however, is largely inapplicable because of the arguments presented previously (see the sections on petrography and mineral compositions), and also because extensive trains of xenolithic material in various stages of digestion are not found in the marginal portions of the pluton. A number of small greenstone xenoliths do nevertheless occur (Figure 52) but these can be regarded as sporadic roof-pendants. Moreover, the presence of smallish amphibolitic remnants found throughout the pluton are viewed as possibly representing entrained cognate xenoliths or restite material. The contour diagrams clearly indicate that the distribution of those major elements that are likely to be diagnostic of pervasive contamination by wall-rock material (i.e. CaO, MgO, Fe_2O_3 and TiO_2, in particular) are not uniformly enriched along the edges of the body, as might be expected had this process been uniformly applicable. As a result, crystal fractionation by inward nucleation of crystals, by crystal settling and accumulation, or by components of both processes would appear to provide the best means of explaining the observed variations.

In simple terms the inward nucleation of crystal growth, as a result of a temperature gradient between wall-rock and the interior of the magma chamber, will presumably take place at an equal rate in all directions. Thus, if the shape of the Kaap Valley tonalite is at all representative of its original magma chamber (i.e. it crystallized more or less *in situ*), chemical variations should appear as an approximately concentric pattern on a contour diagram. Only the trace elements Rb, Sr and Ba show any indication of a concentric distribution and, as mentioned, this is probably due to the concentration of biotite and K-felspar towards the centre of the pluton. The definitive major elements (i.e. SiO_2, TiO_2, CaO, MgO and Fe_2O_3) all exhibit either a concentration or depletion at diagonally opposite extremes of the body, a pattern that is not consistent

Figure 72

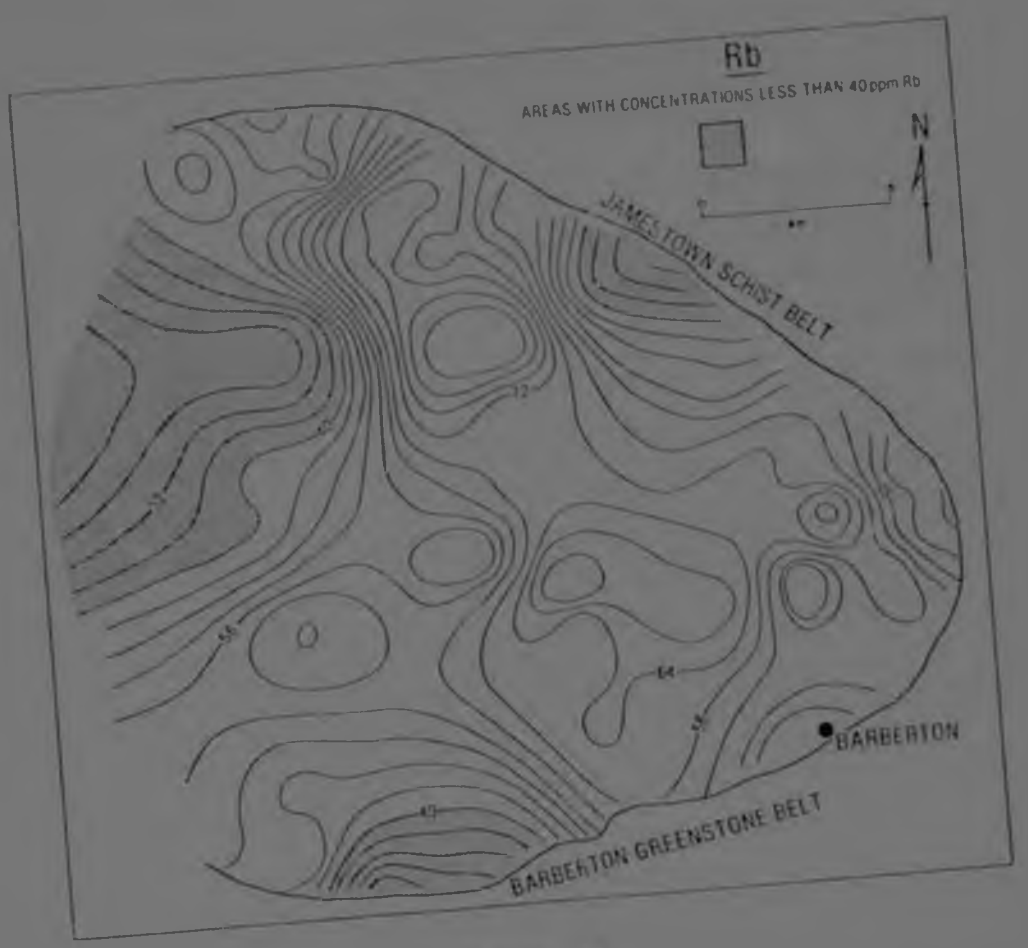

Figure 73

with a simple progressive inward nucleation of crystal growth. If, however, the original shape of the pluton had been structurally modified during, for example, diapiric (gravitationally induced) readjustments of the early Archaean crust, a more complex distribution pattern would be observed. This consideration is particularly relevant if the original chemical variations in the Kaap Valley tonalite were sub-horizontally stratified, as the result of crystal settling rather than inward nucleation. If this were the case then areas of upwarp would tend to expose the lower stratifications (i.e. presumably the earlier formed, more mafic fractionates) whereas synformal warps would preserve the upper portions of the magma chamber. A classic example of where the effects of crystal settling in a granitic pluton have been modified by structural upwarping, has been described from the Puscac pluton in Peru, by Taylor (1975). It is instructive, therefore, to consider the regional structural trends over the Kaap Valley pluton in the hope that they will shed light on the mechanisms of crystal fractionation in the body.

4.2. Regional structural considerations over the Kaap Valley pluton

A number of broad structural lineaments in the Barberton Mountain Land are obviously related to both the position and presence of the Kaap Valley pluton and these are outlined in Figure 78. For example, broad synclinorial areas are represented by the Jamestown schist belt and also the Nelshoogte schist belt, as defined in the regional mapping of Anhaeusser (1969; 1972). These down-warped areas are represented by C-C' and D-D' respectively, in Figure 78, where it is significant to note that both these synclinoria occur as northwesterly trending greenstone protuberances. It follows from these observations that, intermediate to these two down-warped areas, the Kaap Valley pluton itself, must represent a broad, northwesterly trending upwarp that would be parallel to B-B' in Figure 78. Orthogonal to these trends, Anhaeusser (1969) has identified a broad upwarped lineament (parallel to A-A', Figure 78) on the basis of the interpretation of the gravity field in the area. Anhaeusser's (1969) overall structural interpretation of the Barberton region, therefore, viewed the Kaap Valley pluton on a culmination of two intersecting upwarps roughly parallel to A-A' and B-B'.

These broad structural lineaments may, however, be refined if the suggestion made previously (namely that areas of upwarp will expose the

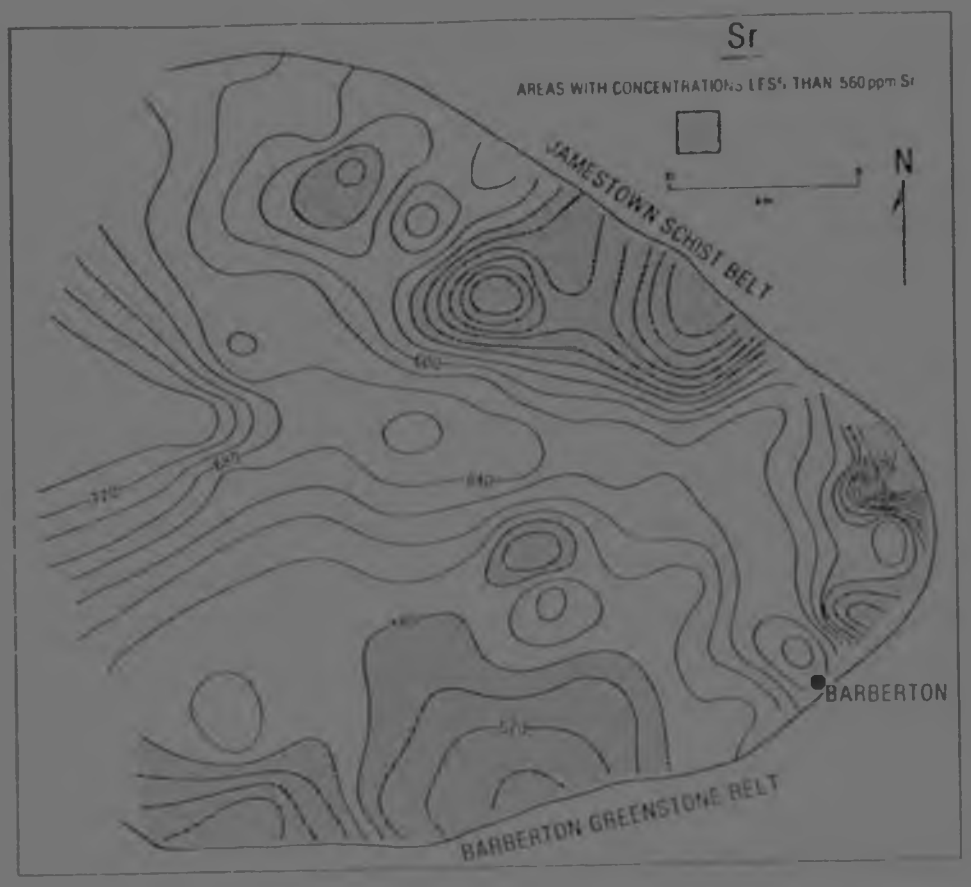

Figure 74

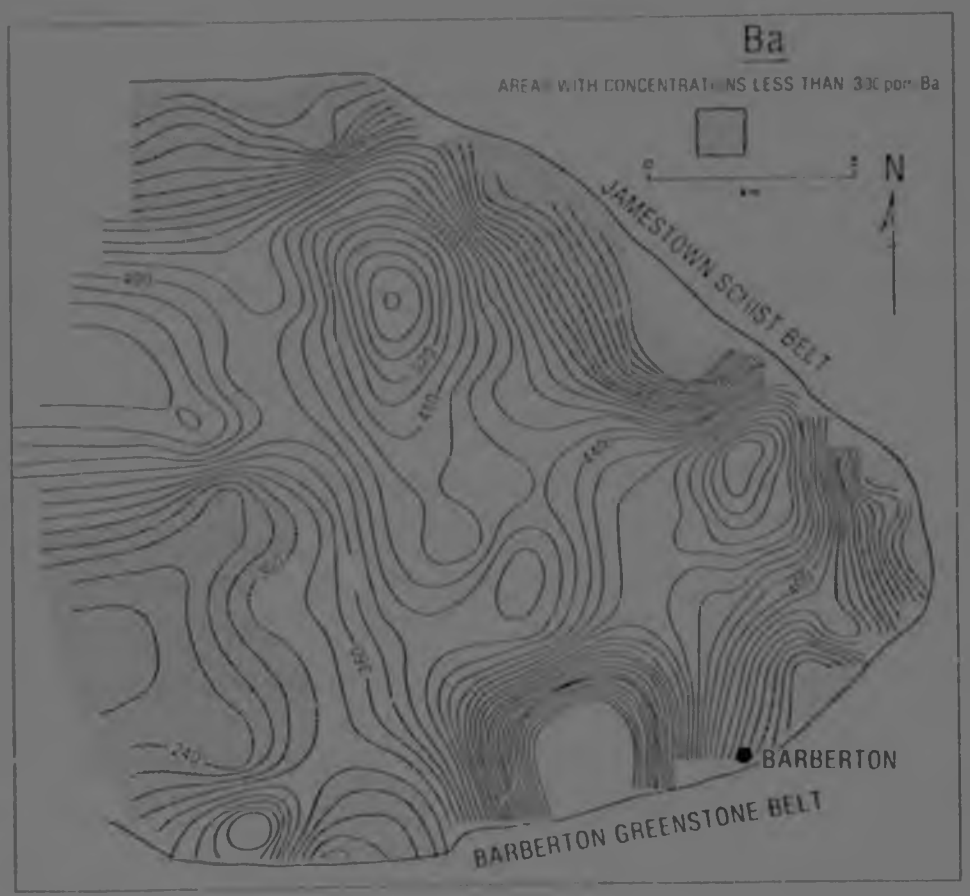

Figure 75

lowermost layers of a pluton that has been subjected to sub-horizontal crystal settling) is considered applicable to the Kaap Valley pluton. If the arcuate region of hornblende tonalites underlying the southeastern quadrant of the pluton (defined in Figure 52 and also Figures 67 - 71) is considered representative of what was originally the lower portion of the magma chamber, then the lineament E-E' can be included in Figure 78 as a broad upwarped region. Following the lines of this reasoning, the trend F-F' may be viewed as a concomitant down-warp, which would explain the preservation of the more felsic (hornblende + biotite) tonalites in its vicinity. Similarly, the overall upwarped trend parallel to B-B' envisaged earlier, can be resolved into two trends on the basis of the discrete lobes described in the shape of contours for SiO_2, TiO_2, CaO, MgO and Fe_2O_3 (Figures 67 - 71). The presence of two upwarped trends in this area (i.e. parallel to B-B', Figure 78) would result in four intersection points with respect to the upwarps A-A' and E-E', resulting in the occurrence of four areas of positive culmination. It is considered more than fortuitous that the areas of positive culmination broadly coincide with areas mapped as being underlain by more mafic hornblende tonalites (Figure 52), as well as with the contoured lobes described from the maps showing the chemical variation of definitive major elements (Figures 67 - 71). A down-warped trend (B-B', Figure 78) intermediate to the two upwarps, will result in an area of negative culmination in the centre of the pluton which serves to preserve the more felsic (hornblende + biotite) tonalites possibly representative of what was originally the upper portion of the magma chamber. Finally, it is suggested that the frequency with which the northwesterly trending upwarps and downwarps occur, implies that two further structural lineaments (G-G' and H-H', Figure 78) can be situated in the diagram. It is interesting to note that detailed mapping of the tonalite-greenstone contact between Barberton and the Nelshoogte schist belt (D-D' Figure 78) resulted in an independent suggestion of the existence of these structures (Wuth, 1980). It must, nevertheless, be pointed out that these interpretations are based largely on data which does not include detailed structural analysis; as such they can only be viewed in terms of the petrogenetic considerations regarding the body and not as a strict tectonic appraisal of the pluton.

In conclusion, however, it is not unreasonable to suggest that the Kaap Valley pluton has been structurally reactivated subsequent to solidifi-

Figure 76

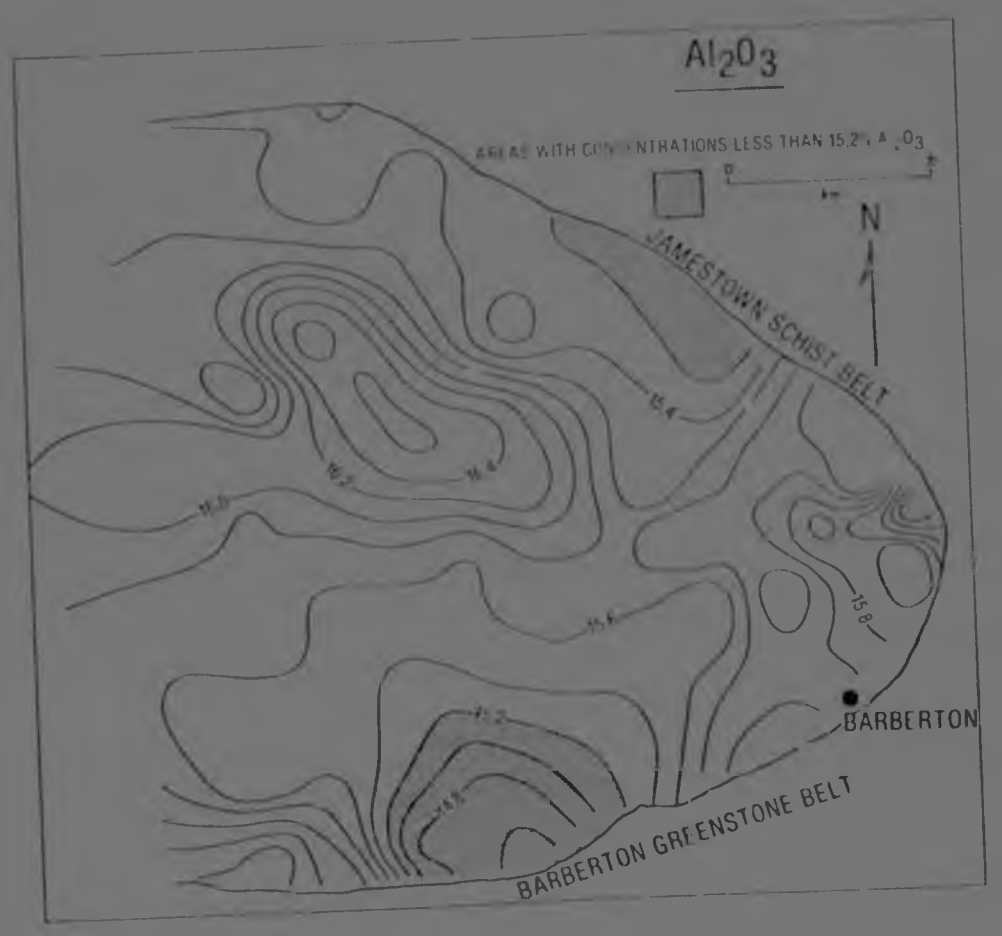

Figure 77

cation and possibly emplaced into its present position as a result of gravitationally induced readjustments in the early Archaean crust. As mentioned previously, this process is now widely recognized in the shield areas of Canada (Drury, 1977; Fyson et al., 1978; Gorman et al., 1978; Schwerdtner et al., 1978; Schwerdtner and Lumbers, 1980) and is also consistent with previous suggestions which regarded the Kaap Valley pluton as dominantly responsible for the deformation along the northern flank of the Barberton greenstone belt (Anhaeusser, 1972). The above discussion implies, however, that the suggested diapiric emplacement of the body was a complex process that may well have been episodic, taking place over a considerable period of geologic time. For example, the preferred orientation of Proterozoic dykes that intrude the Kaap Valley tonalite coincides with the northwesterly trending set of upwarps and downwarps. It is also possible, however, that the interference pattern envisaged over the body may, in some way, be related to the emplacement of younger granitic masses such as the Nelspruit batholith to the north. As mentioned above, the lack of detailed structural information places a constraint on these considerations which, ideally, require a more detailed approach which may not be entirely possible in view of the paucity of outcrop. The available evidence does, however, suggest that the distribution of major elements in the Kaap Valley tonalite is a reflection of an orthogonal pattern of up-warps and down-warps. If these structural lineaments are correct, this implies that crystal fractionation in the original tonalitic magma chamber was horizontally (rather than concentrically) induced. Although it cannot be ascertained whether this process was influenced by gravity and, hence, crystal settling *per se*, it would appear that the earlier-formed, more mafic, portions of the tonalite occupied the lowermost portions of the magma chamber and that successive fractionates became more felsic in an upward direction.

5. CONCLUSIONS

The work presented in this chapter outlines a number of new ideas with regard to the origin and mode of formation of the Kaap Valley tonalite pluton, the latter being the largest of the tonalite-trondhjemite plutons in the Barberton Mountain Land. Although certain of the conclusions that have arisen out of this study may apply to other bodies in the area, the Kaap Valley pluton has a number of distinguishing characteristics which

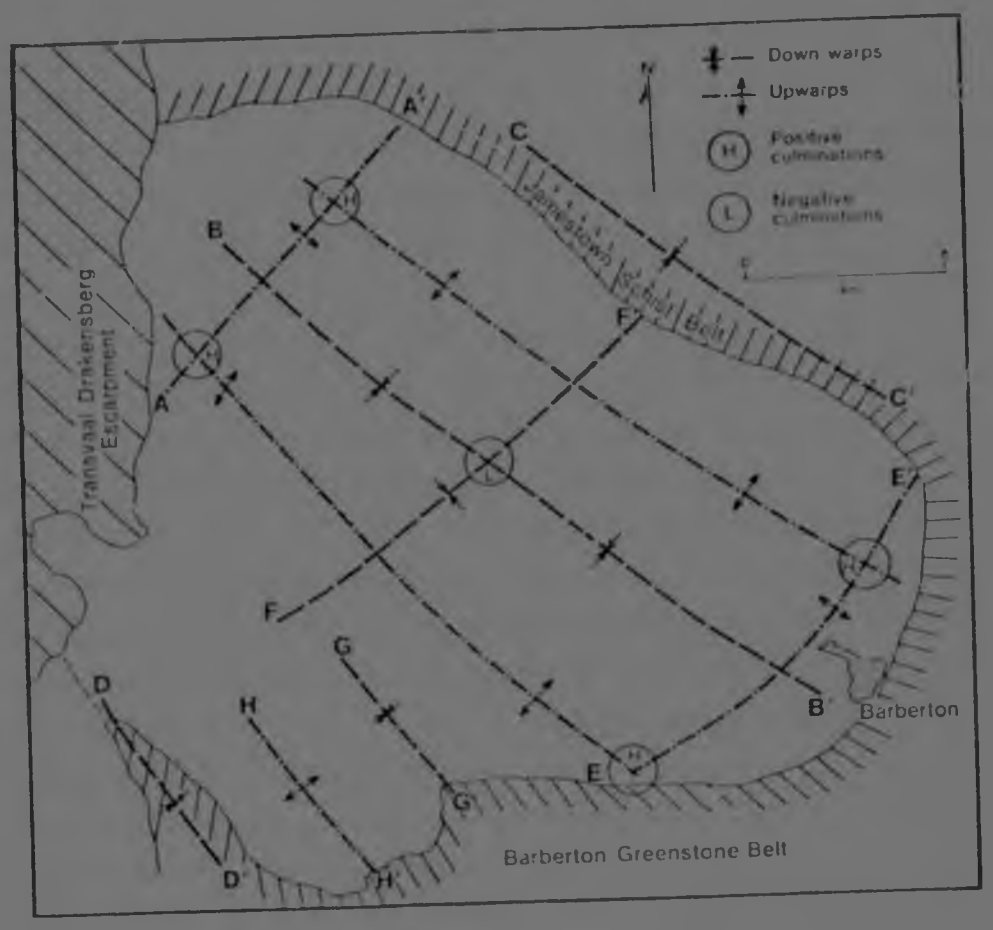

Figure 78 : Schematic diagram of the Kaap Valley pluton showing suggested structural lineaments over the body. Trends C-C'and D-D' (the Jamestown and Nelshoogte schist belts respectively) represent greenstone synclinoria, after Anhaeusser (1969, 1972). The trend A-A'represents an upwarped gravity high taken from the same source. The three major trends parallel to B-B'as well as E-E'and F-F'are inferred from the contour maps in Figures 67-71. The trends G-G'and H-H'were independently derived on the basis of structural mapping of the granite-greenstone contact area by Anhaeusser (1969) and Kuth (1980).

have required specific explanation. The main conclusions to be derived from this study are summarized below :-

(i) The Kaap Valley pluton is the most mafic of the tonalite-trondhjemite bodies in the vicinity of the Barberton greenstone belt. Its dominant mafic mineral is hornblende, in contrast to more leucocratic tonalites or trondhjemites which are invariably characterized by biotite. Although remarkedly homogeneous in texture, the body can be subdivided into hornblende and hornblende + biotite tonalites, with the latter being less mafic. In addition, finer-grained tonalitic dykes occur throughout most of the pluton but these are volumetrically insignificant.

(ii) Whereas previous workers had considered that the more mafic nature of the Kaap Valley tonalite was due to pervasive assimilation or contamination of a trondhjemitic magma by the greenstone material through which it intruded, the present study could not verify this contention and considers that both hornblende and biotite crystallized directly out of a magma that was *originally* more mafic in composition. The small, often assimilated, amphibolitic remnants that do occur in the pluton could represent cognate, or restite material; occasional, randomly located greenstone xenoliths are viewed as roof-pendants.

(iii) Although the mafic nature of the Kaap Valley tonalite suggests an origin involving a higher degree of partial melt of a basaltic precursor than that required, for example, to form a typical trondhjemitic protolith, the incompatible trace element contents of the body as a whole, do not support this idea. Rb and LREE contents of the Kaap Valley tonalite are, on average, similar, or slightly higher, than those that characterize the more leucocratic trondhjemite gneisses in the area (Table 36 and Figure 57). As a result this tonalitic magma is considered to have formed by a melt process whereby existing magma continually equilibrated with new, previously undepleted, parental material. This process can be regarded as being analogous to zone melting and provides a means whereby incompatible trace constituents are more efficiently distributed into melt phases than in conventional

partial (or batch) melt considerations. Such a process, which requires near-total fusion of the melt zone, would also seem to be compatible with the originally more mafic composition envisaged for the Kaap Valley tonalite.

(iv) Crystal fractionation in the Kaap Valley tonalite is reflected in terms of its mineralogy and also major, trace and rare-earth element variations. The two tonalitic sub-types (i.e. hornblende and hornblende + biotite tonalites) are considered to have formed as the result of the initial crystallization of a plagioclase + quartz + hornblende assemblage which was subsequently modified to include biotite. The latter mineral probably started crystallizing only after differentiation had sufficiently enriched the liquid in potash. Trace and rare-earth element variations are considered to reflect the mode of crystallization in the tonalite body. Solidification is regarded as having occurred by processes more akin to equilibrium rather than fractional crystallization as the observed range in trace element contents is not as wide as might be expected from the latter. However, in a body the size of the Kaap Valley pluton, it is unlikely that perfect equilibrium between magma and crystallizing phases will be attained throughout. In addition it is probable that certain portions of the pluton (possibly peripheral) will crystallize before others and will not, therefore, equilibrate with the remaining magma. Thus, a form of subdued magma differentiation undoubtedly occurs, although definitive trends appear to be obscured by various processes which possibly include crystallization in the presence of an intercumulus melt phase and the mobilization of trace elements during secondary alteration.

(v) The distribution of elements over the Kaap Valley pluton is considered to reflect both crystal fractionation processes and regional structural lineaments that accompanied the emplacement of the body. An orthogonal set of structures has been identified on the basis of regional mapping in the area and, to a lesser extent, gravity interpretation. On the supposition that upwarped lineaments have exposed rocks that are representative of what was originally the lowermost portions of the magma chamber, the

distribution of the definitive major elements in the pluton suggest that crystal fractionation was horizontally induced. Hence, hornblende tonalites crystallized in the lowermost portion of the chamber and rock compositions became more felsic in an upward direction. The preservation of the more felsic hornblende + biotite tonalites is enhanced in the centre of the pluton where the intersection of two down-warps occurs. The pattern of orthogonal structural lineaments in the Kaap Valley pluton is probably related to the diapiric (solid-state) emplacement of the body into its present position as the result of gravitational instabilities in the early Archaean crust. Confirmation of this view requires a considerable amount of additional structural data which is not readily available in view of the poor outcrops in the Kaap Valley area.

CHAPTER 5

GEOLOGICAL AND GEOCHEMICAL CHARACTERISTICS

OF THE DOORNHOEK PLUTON

GEOLOGICAL AND GEOCHEMICAL CHARACTERISTICS OF THE DOORNHOEK PLUTON

1. INTRODUCTION

During the course of the mapping programme related to the Geodynamics Project in the Barberton region, a number of individual granitic (*sensu lato*) plutons were mapped. In the dominantly tonalitic-trondhjemitic gneiss terrane southwest of the Barberton greenstone belt (Figures 2 and 82) most of the plutons or "cells" that have now been defined (see Chapter 6) were mapped as part of the regional 1:10000 mapping programme (Anhaeusser, unpub. data). However, other bodies such as the Kaap Valley tonalite and the Theespruit pluton were examined in greater detail, particularly from the point of view of extensive geochemical sampling and analysis (Chapter 4 and Anhaeusser, unpub. data respectively). The Doornhoek pluton, which is discussed below, is another of the bodies that have been examined in greater detail from the point of view of both geological and chemical characteristics.

The Doornhoek pluton is the smallest of the twelve tonalite-trondhjemite bodies that are collectively discussed later in Chapter 6. It is approximately 1 kilometre in length and 0.4 kilometres in width, at its widest point (Figure 79). Furthermore, it is the only pluton in the Barberton Mountain Land which is wholly located within the greenstone belt and is completely surrounded by mafic and felsic schists belonging to the Theespruit Formation of the Tjakastad Subgroup (Viljoen and Viljoen, 1969c). The body was mapped on a scale of approximately 1:8000 using aerial photographs; the resulting geological map is presented in Figure 79.

2. GEOLOGICAL CHARACTERISTICS

The Doornhoek pluton consists almost entirely of coarse-grained trondhjemite which is relatively well-exposed and occurs mainly as low "whaleback" platforms and boulders. Texturally the body is remarkably homogeneous with the exception of two small areas towards the centre and southeastern portion of the pluton, where a distinctly finer-grained

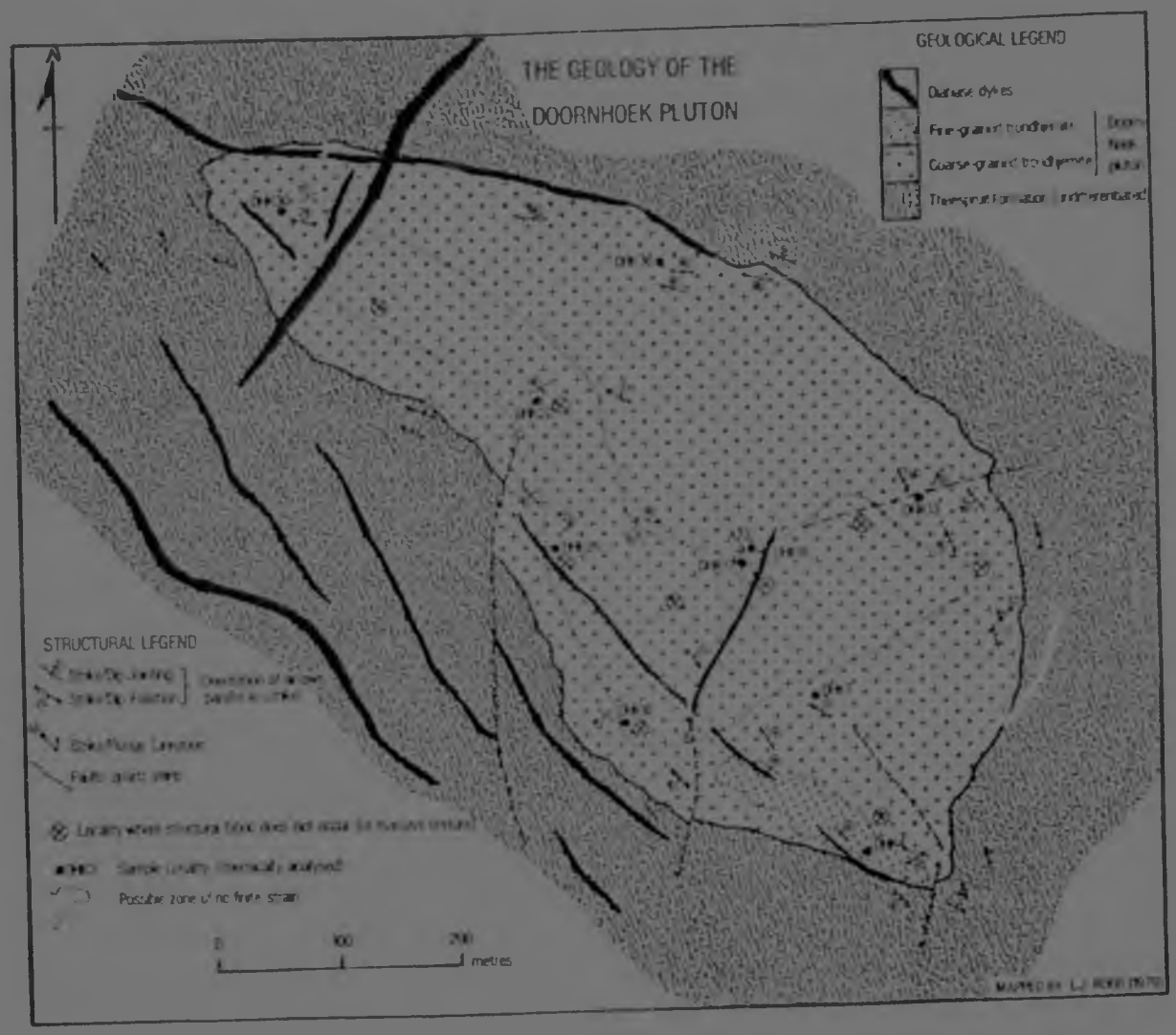

Figure 79 : *Geological map of the Doornhoek trondhjemite pluton.*

trondhjemitic phase occurs (Figure 79). In the southeastern part of the pluton the fine-grained trondhjemite outcrops in a linear zone that is topographically slightly higher than the surrounding trondhjemites. A small zone of fine-grained trondhjemite also occurs in the vicinity of samples DHK 16 and DHK 17 where a distinct contact between the latter and the coarser phase is present. It is clear here that the finer-grained phase intrudes the more dominant coarser trondhjemite and, in both places, therefore, occurs as dykes within the latter.

The Doornhoek trondhjemite consists predominantly of plagioclase and quartz together with lesser amounts of biotite and K-felspar. Plagioclase laths form large grains (5 - 10 mm in diameter) which are always extensively sericitized in thin-section. Twinning is poorly developed but sericitization defines a clearly zoned structure in most of the plagioclase grains. Quartz grains are commonly fragmented, exhibit intensely undulose extinction, and are characterized by sutured grain boundaries. Biotite is the only ferromagnesian mineral present and usually appears as large euhedral flakes, 5 - 10 mm in diameter. Some biotite is partially altered to chlorite and accessory amounts of rutile occur in the vicinity of these grains. Variable amounts of microcline occur in the rock and may occupy up to 10% of the volume according to the thin-sections examined. The K-felspar invariably occupies an interstitial position with respect to plagioclase and quartz and may have crystallized from an "intercumulus" liquid. Reaction between plagioclase and microcline is often reflected in a marginal zone of reversed polysynthetic twinning in the former. The finer-grained trondhjemite phases consist of an identical mineral assemblage except that muscovite and biotite commonly co-exist. The rock is considerably finer-grained with plagioclase and biotite being approximately one-tenth the size of the coarse-grained equivalents.

As mentioned previously the Doornhoek pluton is completely surrounded by greenstones that are correlated with the Theespruit Formation. Immediately flanking the pluton is an assemblage comprising chlorite and talc-chlorite schists with minor serpentinites and felsic (quartz-sericite) schists. The strike of these rocks is generally conformable with the granite-greenstone contact and dips, where measured, are almost invariably sub-vertical (Figure 79). The actual contact between trondhjemite and greenstone is directly exposed in only a few places and, where seen, it is sheared and there

is no evidence of igneous intrusion of one into the other. It would appear, rather, that the Doornhoek pluton was diapirically emplaced in a solid state, having originally formed part of a less dense trondhjemitic body that originally underlay the greenstone successions. This implies that the body was either, originally a basement to the greenstones or, was magmatically intrusive to a certain structural level and subsequently diapirically emplaced to its present position.

A number of structural measurements were taken over the pluton during the course of mapping. One characteristic feature that emerged was the fact that, in marked contrast to the Theespruit pluton, which occurs only a few hundred metres to the west, the Doornhoek body has a very poorly-developed structural fabric (i.e. foliation or lineation). Even at the trondhjemite-greenstone contact, mineral foliations are weakly developed and towards the centre of the pluton, no fabric is detectable whatsoever (Figure 79). The perimeter of the pluton generally has a foliation with sub-vertical dips, although in certain places, particularly in the southern portion, the recognition of a fabric was equivocal making an assessment of strike or dip very difficult. The centre of the pluton is characterized by a broad belt where neither foliation nor lineation is developed and this is outlined as a possible zone of no finite strain in Figure 79. Where a weak foliation is developed in the central portions of the pluton this is often inclined at a shallower angle than that present at the margins.

The structural features described above are considered to be compatible with those characteristic of certain portions of diapiric structures. Dixon (1975) has shown experimentally that gravitationally induced diapiric structures are characterized by a zone of no finite strain in the region of the interface between underlying less-dense material and its overburden. Schwerdtner et al. (1978) have shown that in the Canadian shield, natural examples exist where the zone of no finite strain is preserved and that the latter is often located within the less dense medium (i.e. displaced downwards because of frictional effects at the actual interface). In this light, it is suggested, therefore, that the preservation of areas of low strain in a region which has otherwise been highly deformed (Viljoen and Viljoen, 1969c; Williams and Furnell, 1979), is particularly instructive in pointing to the deformation style in the area. The Doornhoek pluton can be viewed, in terms of its present erosion level, as representing an exposure close to the trondhjemite-greenstone interface, where the intersection

of vertical extension in the buoyant mass, with horizontal stretching in the denser overburden, results in an area of neutral strain. In contrast, other tonalitic or trondhjemitic plutons may have been eroded to a deeper level where more pronounced sub-vertical foliations reflect zones of, often intense, sub-vertical tensile strain. These ideas appear to have considerable merit in the Barberton region (see Chapter 4) and provide an acceptable mechanism whereby the overall deformation of the greenstone belt may have taken place. As in the Canadian shield areas, however, these processes require quantification and a more detailed structural study of the Doornhoek, and other, plutons remains to be undertaken. If it is to be accepted that the Doornhoek body was diapirically emplaced into its present position then it is not possible to determine, unequivocally, the actual age relationships between trondhjemite and greenstone. As suggested previously, the pluton may originally have been intrusive but structurally reactivated to its present position or, it could represent a greenstone basement which was also structurally emplaced after the deposition of a dense greenstone overburden.

3. GEOCHEMICAL CHARACTERISTICS

A total of ten samples from the Doornhoek pluton were analysed for major and trace (Rb, Sr and Ba) elements whilst two of these samples were also analysed for selected rare-earth elements; this data is presented in Table 32.

The major element compositions of samples from the Doornhoek pluton are characterized by uniformly high silica contents that vary between ≈70 - 75% SiO_2. As such, this compositional range is complementary to the chemical characteristics of the Kaap Valley tonalite which has uniformly lower silica contents between approximately 60 - 70% SiO_2 (see Figure 83, Chapter 6 for comparisons). In contrast, most other trondhjemitic bodies exhibit a range in silica content that is intermediate between the Kaap Valley and Doornhoek trends and which overlap the tonalite-trondhjemite range. In terms of the tonalite-trondhjemite definition of Barker (1979), which appears in the next chapter, the Doornhoek pluton is wholly trondhjemitic by comparison with the Kaap Valley pluton where most of the analysed samples are tonalites.

TABLE 32

CHEMICAL ANALYSES OF SAMPLES FROM THE DOORNHOEK TRONDHJEMITE PLUTON

	1	2	3	4	5	6	7	8	9	10
	DHK 4	DHK 7	DHK13	DHK16	DHK17	DHK18	DHK22	DHK26	DHK30	DHK36
SiO_2	71,29	74,65	71,15	73,83	72,31	71,68	70,62	70,51	74,51	72,93
TiO_2	0,19	0,11	0,27	0,14	0,21	0,23	0,23	0,28	0,09	0,23
Al_2O_3	14,28	14,39	15,77	14,40	14,83	16,01	16,22	14,95	15,04	14,62
Fe_2O_3*	1,98	1,56	2,82	1,66	2,17	2,45	2,54	2,96	1,29	2,48
MnO	0,02	0,02	0.01	0,05	0,03	0,07	0,01	0,01	0,01	0,03
MgO	0,65	0,22	0,87	0,34	0,53	0,75	0,72	0,81	0,29	0,71
CaO	2,22	1,49	3,06	1,79	2,41	2,60	2,92	3,00	1,46	2,48
Na_2O	4,28	4,16	4,13	4,39	4,02	4,33	4,51	3,98	4,21	4,53
K_2O	2,52	3,00	1,75	2,47	2,33	1,96	1,87	1,20	3,09	2,03
P_2O_5	0,06	0,03	0,08	0,04	0,06	0,07	0,07	0,08	0,03	0,07
L.O.I.	0,72	0,54	0,82	0,69	0,45	0,78	0,64	0,38	0,39	0,53
TOTALS	98,21	100,17	100,73	99,80	99,35	100,93	100,35	98,16	100,41	100,64
Rb	106	85	43	51	121	38	39	31	117	49
Sr	188	97	211	129	240	163	162	210	109	161
Ba	418	291	207	245	287	194	185	180	218	238
La	-	-	14,2	-	-	-	-	-	8,9	-
Ce	-	-	24,4	-	-	-	-	-	17,3	-
Nd	-	-	8,8	-	-	-	-	-	6,8	-
Sm	-	-	2,5	-	-	-	-	-	1,9	-
Eu	-	-	0,80	-	-	-	-	-	0,44	-
Tb	-	-	0,63	-	-	-	-	-	0,65	-
Yb	-	-	0,16	-	-	-	-	-	1,63	-
Lu	-	-	0,02	-	-	-	-	-	0,18	-
K_2O/Na_2O	0,59	0,72	0,42	0,56	0,58	0,45	0,41	0,30	0,73	0,45
K/Rb	197	292	337	402	160	488	397	322	219	343
Rb/Sr	0,56	0,88	0,20	0,39	0,50	0,23	0,24	0,15	1,07	0,30

(Analyst: L.J. Robb

Fe_2O_3* - Total iron as Fe_2O_3)

Sample localities shown in Figure 79

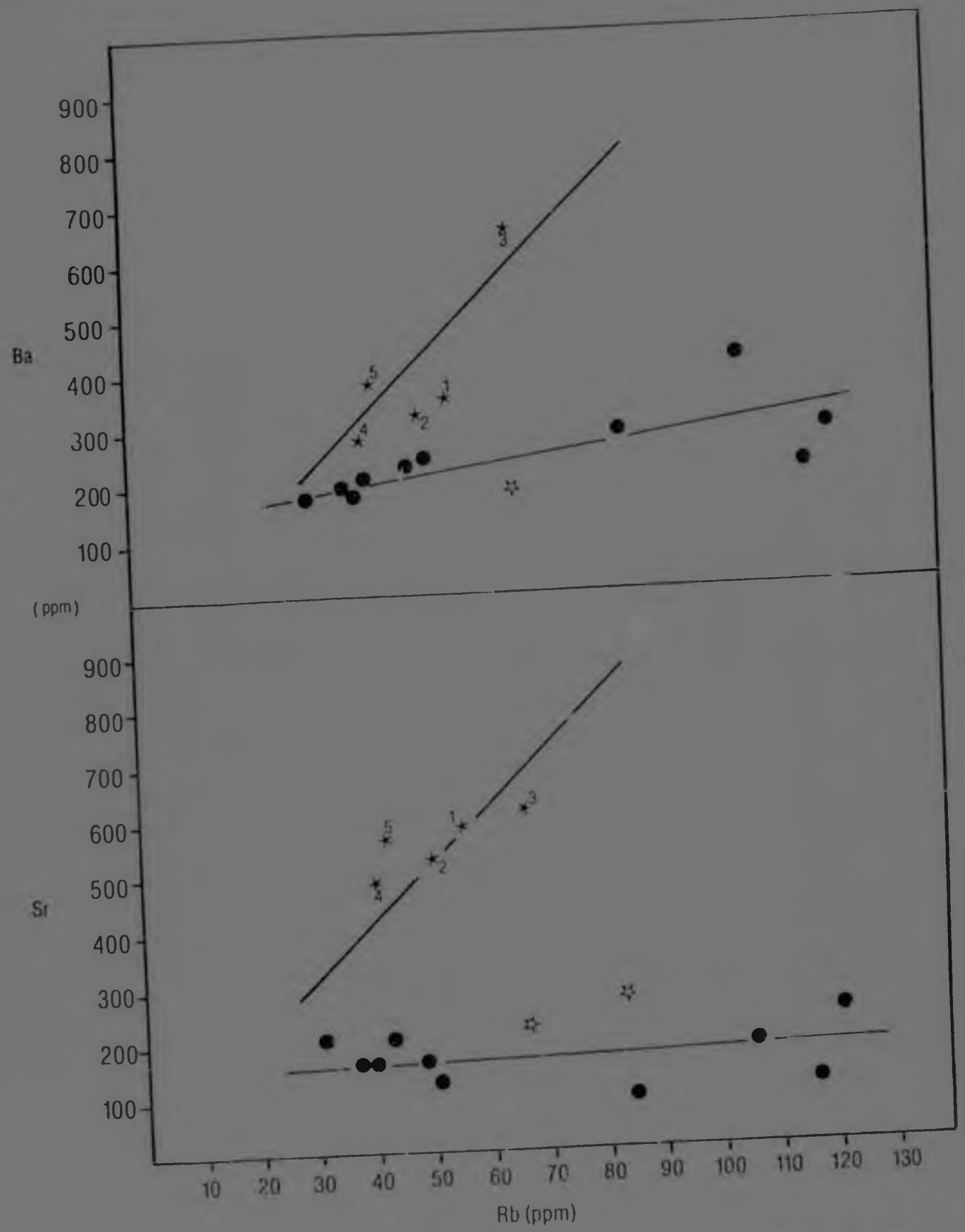

Figure 80 : *Plots of Rb v Sr and Rb v Ba for samples from the Doornhoek pluton (shown in black dots, data from Table 33). Also plotted as stars on the diagram are average Rb, Sr and Ba values (from Table 36) for the Kaap Valley tonalite (1), the Theespruit pluton (2), the Stolzburg pluton (3), the Nelshoogte pluton (4) and the Roothoogte cell (5). The lines drawn through these points represent Rb/Sr = 0,1 and Rb/Ba = 0,1 in each of the diagrams. The line through the Doornhoek data is an approximate best fit. The open stars are average values for the Ancient Gneiss Complex in Swaziland, also taken from the data in Table 36. (Note that Ba data is not available for one of these points).*

The Doornhoek pluton is characterized by a relatively limited range in composition with Al_2O_3 varying between 14,3 - 16,2%, Fe_2O_3* + MgO varying between 1,6 - 3,8% and CaO between 1,5 - 3,1% (Table 32). Certain of the analysed samples also have K_2O contents that are marginally higher than those normally characteristic of the trondhjemite gneisses in the region and K_2O varies between 1,20 - 3,09%. The average K_2O/Na_2O ratio, however, is 0,52, this being compatible with Barker's (1979) trondhjemite definition. The major element variations over the Doornhoek pluton are illustrated in terms of a Harker diagram in Figure 83, where the compositional trend is compared with major element variations in other trondhjemitic bodies from the area southwest of the Barberton greenstone belt. It is clear from this diagram that the Doornhoek pluton (trend line number 10, Figure 83) does not have the low ferromagnesian contents expected of a rock suite that is more siliceous, on average, than the remainder of the trondhjemitic kindred in the area. As illustrated in Figure 84 the trondhjemitic rocks of the Barberton area also appear to exhibit an antipathetic relationship between (Fe_2O_3* + MgO) and Na_2O ; the Doornhoek pluton is characterized by low Na_2O values and a relatively high ferromagnesian content and, hence, major element variations are not entirely silica-dependent. A discussion regarding the melt origin of the Doornhoek pluton in relation to its major element characteristics is provided in Chapter 6, where comparisons are made between a number of tonalite-trondhjemite bodies in the region.

Variations in the Rb, Sr and Ba content of the Doornhoek pluton are illustrated in Rb v Sr and Rb v Ba diagrams in Figure 80. The Doornhoek body is seen to be characterized by significant variations in rubidium (i.e. 30 - 120 ppm) whereas Sr and Ba exhibit much smaller percentage variations of between ~100 - 200 ppm for Sr and ≈200 - 300 ppm for Ba. These characteristics are unusual in comparison to other tonalitic and trondhjemitic plutons in the area and this is emphasized in Figure 80 where, in addition to the Doornhoek data, average Rb, Sr and Ba values from five major tonalite-trondhjemite plutons in the area are also plotted. Typical tonalites and trondhjemites in the region are seen to have Rb/Sr and Rb/Ba ratios approximately equal to 0,1 whereas the Doornhoek pluton has averages of 0,41 and 0,27 respectively. The high Rb/Sr ratio is particularly a function of the very low Sr content of the body, the latter being 2 - 3 times more depleted in this element than other trondhjemites plutons with broadly similar compositions. The low Sr content of the Doornhoek pluton is again

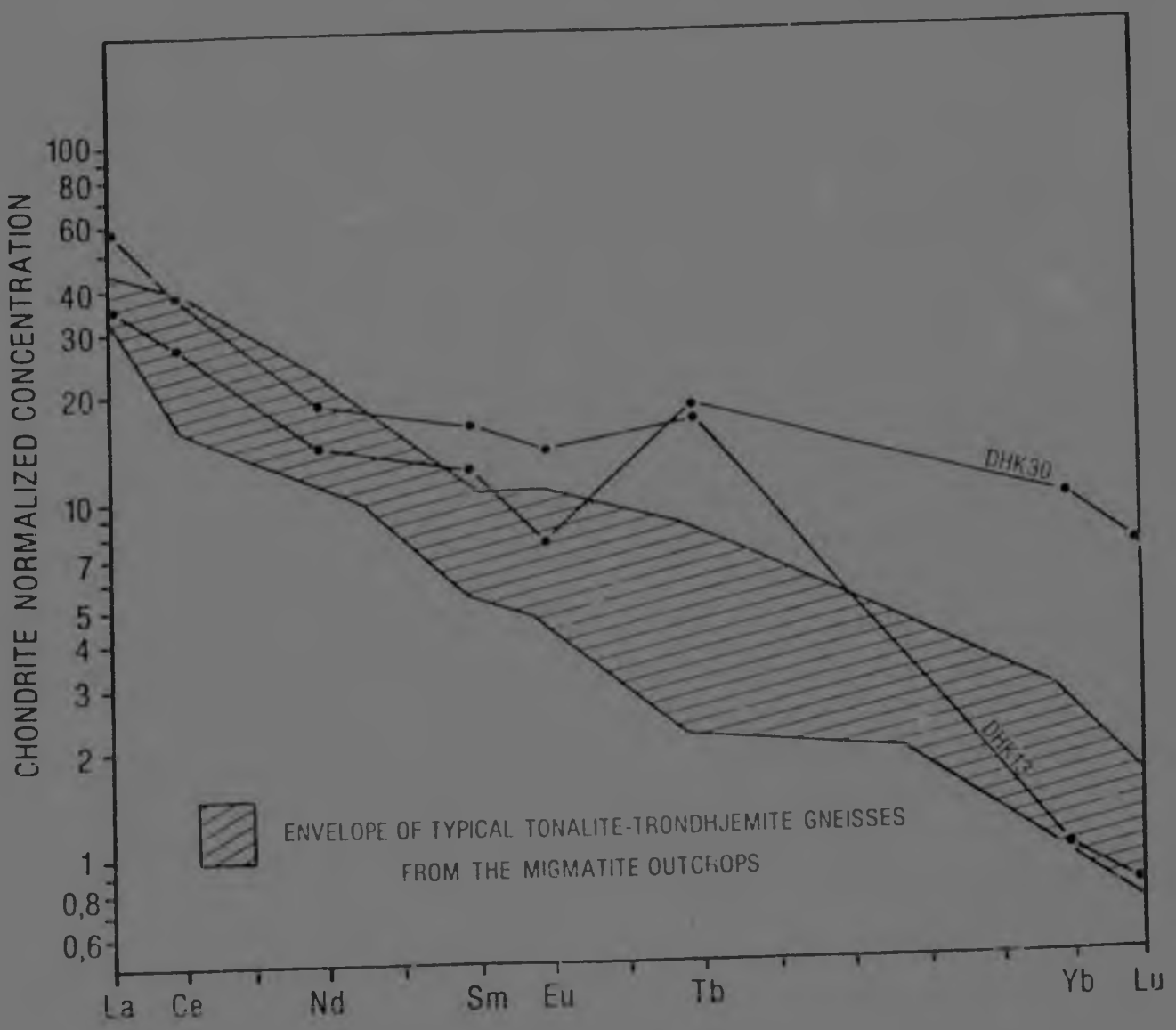

Figure 81 : Chondrite normalized rare-earth element plot of samples from the Doornhoek pluton (Table 32). Also shown for comparison, is the envelope of samples (from Figure 20) of migmatite-related tonalite and trondhjemite gneisses described in Chapters 2 and 3.

emphasized in a plot of SiO_2 v Sr (Figure 85) where the data from Table 32 is compared with over one hundred analyses of tonalites and trondhjemites from the Barberton region as a whole. This diagram shows that the Doornhoek pluton has a lower Sr content (and a higher Rb/Sr ratio, see Table 36) than any of the other tonalitic or trondhjemitic bodies in the Barberton Mountain Land. Although concentrations such as this are unusual in the immediate Barberton region, low Sr values and high Rb/Sr ratios have been reported for trondhjemitic gneisses of the Bimodal Suite in the Ancient Gneiss Complex (AGC) of Swaziland (Hunter et al., 1978). As seen in Figure 80, these gneisses have average Rb, Sr and Ba values that are compatible with those of the Doornhoek pluton. Thus, the claim that the geochemical characteristics of certain units of the AGC in Swaziland cannot be duplicated in the terrane southwest of the Barberton greenstone belt (Hunter et al., 1978) is unfounded and the present data adds strength to the arguments of Robb and Anhaeusser (1979) who suggested that the two areas are broadly similar in nature. A more detailed account of the petrogenesis of the Doornhoek trondhjemite in the light of its unusual Rb and Sr contents is given in Chapter 6, where suggestions are put forward as to the possible reasons why tonalites and trondhjemites with similar major element characteristics and bulk compositions may have differing trace and rare-earth element contents.

Chrondrite-normalized rare-earth element traces of two samples from the Doornhoek pluton are plotted in Figure 81. The limited amount of data suggests that REE traces are as variable as the Rb/Sr ratios of the body, and Ce_N/Yb_N is seen to vary between 2,7 and 39,4. It is clear from Table 32, that the sample with a low Ce_N/Yb_N ratio (i.e. DHK 30) and, hence, the flat REE pattern, is characterized by a high Rb/Sr ratio, whereas sample DHK 13, with a high Ce_N/Yb_N ratio has a much lower Rb/Sr ratio. Generally, therefore, it would appear that the REE characteristics of the Doornhoek pluton are not altogetner typical of other tonalitic and trondhjemitic rocks from the Barberton Mountain Land and this is emphasized in Figure 81 where data from the former is compared with the envelope of gneisses analysed from the migmatite outcrops described previously.

It is interesting to note that trondhjemitic gneisses from the AGC in Swaziland that have high Rb/Sr ratios, may also be characterized by flat REE patterns with low Ce_N/Yb_N ratios (Figure 91, Chapter 6). This further strengthens the statement made above, that portions of the AGC do

have chemical equivalents in the Barberton area and that the two terranes are not entirely exclusive. The high Rb/Sr and low Ce_N/Yb_N ratios of these units does imply, however, that different petrogenetic considerations apply to these units. In rocks that owe their origin to partial melting, depleted Sr and enriched HREE contents in the liquid phase suggest that residual phases consisted of a different mineral assemblage to the case where tonalites and trondhjemites with high Sr contents and a depleted HREE pattern were forming. Considerations such as these are discussed in detail in Chapter 6, where it is proposed that differences in crustal level, as well as isochemical mineral phase changes, may have been responsible for the discrepancies observed in trace element contents.

4. CONCLUSIONS

A number of the geological and geochemical features pertaining to the Doornhoek pluton serve to distinguish it from other tonalite and trondhjemite bodies in the area. The pluton is the smallest discrete trondhjemite pluton in the Barberton Mountain Land and is totally surrounded by greenstone lithologies of the Theespruit Formation. As such, its shape is rigidly outlined, by comparison with other plutons that are only partly circumscribed by greenstone material.

The structural level at which the Doornhoek pluton is presently exposed reveals the presence of a low strain environment (i.e. reflected in a very poorly developed foliation/lineation) in an area that is otherwise characterized by intense deformation. It is inferred that this lack of mineral fabric represents a zone of neutral strain which formed in the upper portions of a gravitationally induced diapiric structure. It follows that the Doornhoek pluton was emplaced into rocks of the Theespruit Formation in a solid (or near-solid) state and is not, therefore, a magmatic intrusive feature. A similar style of tectonism probably applied to other tonalitic and trondhjemitic plutons but these may have been eroded to a level below that of the plane of neutral strain and, hence, the latter preserve well-developed sub-vertical foliations or lineations.

The Doornhoek pluton is characterized by a trondhjemitic bulk composition similar to that of other trondhjemites in the area. Certain analysed samples, however, have K_2O and Rb contents that are slightly higher than average. A distinctive feature of the body is the low Sr content

of all the analysed samples (and, as a result, the high average Rb/Sr ratios) and the low Ce_N/Yb_N ratio of the high Rb samples. These features differ from the typical tonalite-trondhjemite gneisses in the region, where Sr values are significantly higher, Rb/Sr ratios are approximately 0,1 and HREE are relatively depleted. The trace and rare-earth element characteristics of the Doornhoek pluton are similar to those of certain trondhjemite gneisses from the Ancient Gneiss Complex in Swaziland. The discrepancies in trace element contents of tonalite and trondhjemite gneisses with otherwise similar bulk compositions, is possibly attributable to the crustal depth at which the magma protoliths were formed. It is envisaged that under conditions of varying pressure and temperature, the mineral components of melt residues will undergo isochemical phase changes, resulting in different distributions of the trace elements. Considerations such as these are presented in detail in Chapter 6, where the chemical characteristics of the Doornhoek pluton are compared with other bodies from both the Barberton and Swaziland regions.

PART 3

THE TONALITE AND TRONDHJEMITE GNEISS TERRANE SOUTHWEST OF THE BARBERTON GREENSTONE BELT

CHAPTER 6

GEOCHEMICAL AND PETROGENETIC CHARACTERISTICS OF TONALITE AND TRONDHJEMITE PLUTONS IN THE AREA SOUTHWEST OF THE BARBERTON GREENSTONE BELT

CHEMICAL AND PETROGENETIC CHARACTERISTICS OF TONALITE AND TRONDHJEMITE PLUTONS IN THE AREA SOUTHWEST OF THE BARBERTON GREENSTONE BELT

1. INTRODUCTION

Most published maps of the Barberton Mountain Land which differentiate between granite types in the area show that the terrane immediately to the west and southwest of the Barberton greenstone belt is underlain by tonalitic or trondhjemitic gneisses. This region, and the rocks within it, have received only cursory attention in the past (Viljoen and Viljoen, 1969f, g) and only recently has the area been mapped in detail (Anhaeusser and Robb, 1980a; Anhaeusser, 1980). Published geochemical and petrogenetic studies of the tonalite-trondhjemite gneisses that dominate in the area are limited to two accounts (viz. Glikson, 1976a; Condie and Hunter, 1976), both of which refer to these rocks only in the context of the evolution of the granitic terrane in the Barberton-Swaziland region as a whole.

The recent mapping to the southwest of the Barberton greenstone belt has shown that the area is underlain by numerous greenstone remnants and complex multi-component migmatitic rocks usually spatially related to the greenstone remnants. The area is dominated, however, by homogeneous tonalite and trondhjemite gneisses (Anhaeusser and Robb, 1980a and Figures 2 and 82). Within this area a number of discrete tonalite-trondhjemite plutons are readily defined by their, generally, elliptical shapes which are outlined by enveloping greenstone material. As such, many of the plutons in this area have long been named (e.g. the Kaap Valley, Nelshoogte, Stolzburg and Theespruit plutons, see Figure 82) and, as a result, have formed part of previous investigations in the Barberton Mountain Land. However, the new additional data now available, which includes approximately one hundred and twenty-five chemical analyses, has led to the recognition of a number of previously undefined, but nevertheless geographically discrete, tonalite-trondhjemite bodies whose shapes are not necessarily elliptical and whose outlines are not defined by greenstone material. These bodies have now also been named and, in order to distinguish them from the previously defined

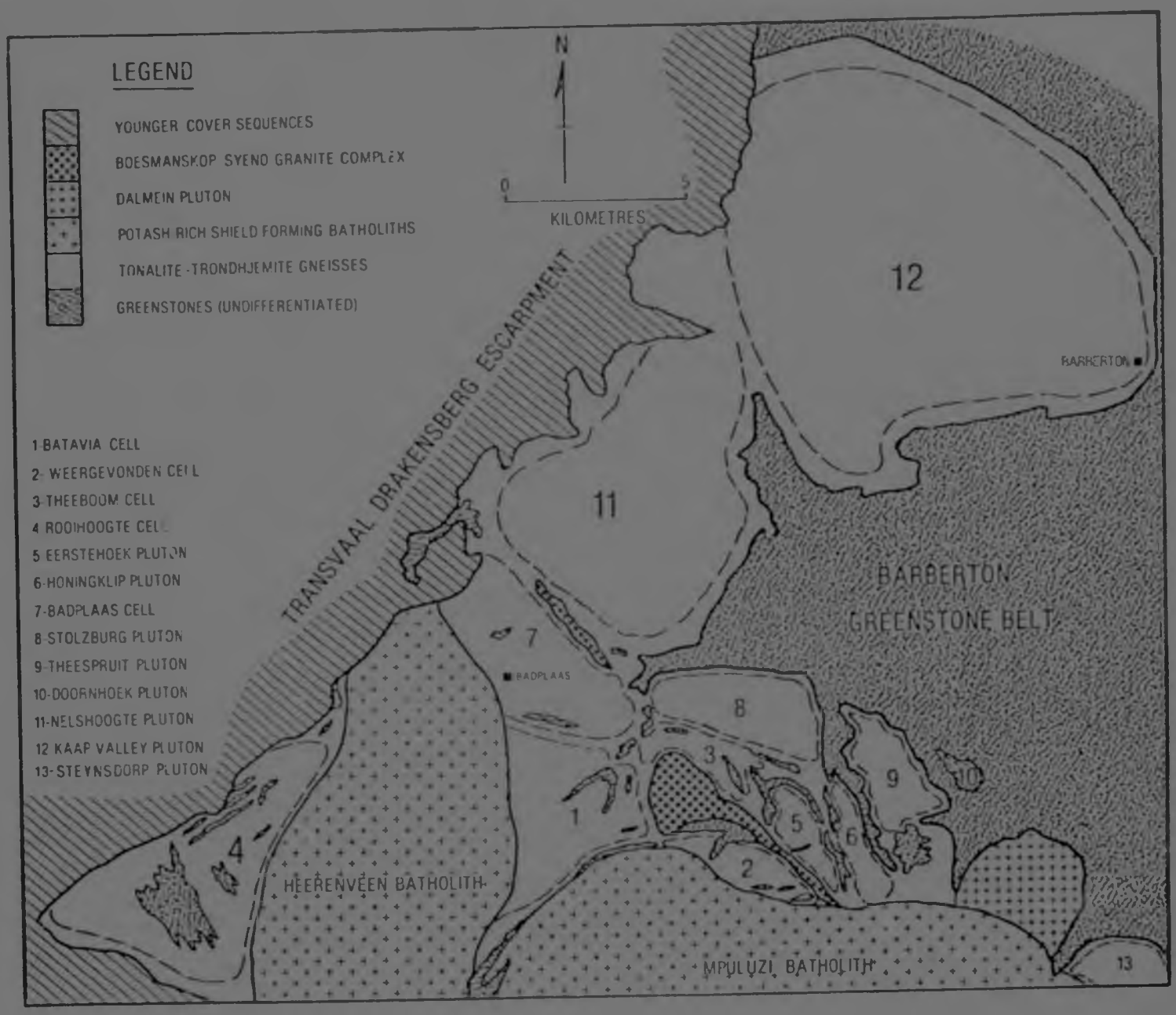

Figure 82 : Simplified geological map showing the suggested geological outlines (dashed lines) of tonalite-trondhjemite plutons and cells in the area southwest of the Barberton greenstone belt. Twelve of the plutons (i.e. numbers 1-12) are described in the text in terms of presently available chemical analyses. The thirteenth body (i.e. the Steynsdorp pluton) is included on the map but not discussed in the text, as representative chemical data is not yet available.

bodies, are referred to specifically as "cells". The distinction between a pluton and a cell is important as the outlines of the latter are not easily recognized in the field and the differentiation between one cell and another is done on the basis of their compositional (chemical) characteristics (Figure 82).

On the map in Figure 82, it is seen that a total of five cells have been defined on the basis of the above criteria. These cells, as mentioned, are geographically discrete areas, each with a similar and systematic chemical characteristic. The implication attached to the definition of these cells is that they represent individual, genetic units in the same way that each of the plutons are recognized on the basis of their own particular features (see, for example, Chapters 4 and 5). It is quite likely, however, that continued work will be responsible for the definition of new units, perhaps *within* the existing ones. For example, Anhaeusser (1980) has defined two separate plutons (namely the Nederland and Weergevonden plutons) within the Weergevonden cell; in the present study, however, the cell nomenclature is preferred in this case as the chemical characteristics of these two plutons are so similar that they are likely to represent a single cogenetic unit.

The object of this chapter is to compare and contrast the chemical and petrogenetic characteristics of the twelve tonalite-trondhjemite plutons and cells that occur in the area to the southwest of the Barberton greenstone belt and shown in Figure 82; a summary of the source and number of chemically analysed samples presently available for each of the defined plutons and cells is also presented in Table 33. In addition, reference will also be made to chemical similarities existing between the study area and the Ancient Gneiss Complex in Swaziland.

1.1 Definition of tonalite-trondhjemite

For the purpose of this thesis the conceptual definition of tonalite and trondhjemite is taken to be that suggested by Barker (1979), i.e. that a trondhjemite be defined as a leucotonalite. More specifically, andesine-bearing leucotonalite should be termed calcic trondhjemite with the term "trondhjemite" being restricted to albite and oligoclase-bearing leucotonalite. In terms of this definition, therefore, a trondhjemite is described as the

TABLE 33

THE DEFINITION OF, AND SOURCES OF DATA FOR, THE TONALITE-TRONDHJEMITE GNEISS PLUTONS AND 'CELLS' IN THE REGION SOUTHWEST OF THE BARBERTON GREENSTONE BELT

NAME	NO. OF SAMPLES/ ANALYSES	SOURCE
1. BATAVIA CELL	6	Anhaeusser (unpub. data) (*).
	3	This thesis, Table 37.
2. WEERGEVONDEN CELL	6	Anhaeusser (unpub. data).
3. THEEBOOM CELL	7	Anhaeusser (unpub. data).
	2	This thesis, Columns 1-2, Table 2.
4. ROOIHOOGTE CELL	8	Anhaeusser (unpub. data).
5. EERSTEHOEK PLUTON	2	Anhaeusser (unpub. data).
6. HONINGKLIP PLUTON	2	Anhaeusser (unpub. data).
7. BADPLAAS CELL	4	Anhaeusser (unpub. data).
8. STOLZBURG PLUTON	1	Anhaeusser (unpub. data).
	2	This thesis, Columns 1-2, Table 1.
	2	Viljoen and Viljoen (1969g) and Condie and Hunter (1976).
9. THEESPRUIT PLUTON	31	Anhaeusser (unpub. data).
	3	Viljoen and Viljoen (1969g) Condie and Hunter (1976) and Glikson (1976a).
10. DOORNHOEK PLUTON	10	This thesis, Table 32.
11. NELSHOOGTE PLUTON	1	Anhaeusser (unpub. data).
	2	Viljoen and Viljoen (1969g) and Condie and Hunter (1976).
12. KAAP VALLEY PLUTON	41	This thesis, Table 21
TOTAL	133	

(*) The unpublished data referred to in this Table will be presented in the official Geodynamics Project publication on the Barberton study strip

silicic, end-member variant of the tonalitic kindred. Barker (1979) has provided the following quantitative major-element definition of a *trondhjemite*:-

$68\% < SiO_2 < 75\%$
$Al_2O_3 > 15\%$ at $70\% SiO_2$
$Fe_2O_3^* + MgO < 3,4\%$
$1,5\% < CaO < 3,0\%$
$4\% < Na_2O < 5,5\%$
K_2O always $< 2,5\%$

Two features in the above definitions are worthy of note; firstly, the restrictions implied in terms of the K_2O/Na_2O ratio (i.e. usually < 0,6) coincides with the broader definition of tonalite given by Harpum (1963) and secondly, the above range of chemical compositions ensures that trondhjemites are almost always corundum normative. In terms of the above definition, the most practical distinction between tonalites and trondhjemite occurs in terms of SiO_2, such that the former have $SiO_2 < 68\%$ and vice versa for the latter.

In the following section it will become apparent that individual plutons or cells generally exhibit a range in composition such that certain samples are clearly tonalitic whereas others are trondhjemitic. In general, however, most of the samples are trondhjemitic in character (see Figure 85) with the marked exception of the Kaap Valley pluton which is dominantly tonalitic. As a result, most of the plutons or cells (with the one exception), are referred to as trondhjemites.

1.2 The petrogenesis of Archaean tonalites and trondhjemites - current thoughts

As tonalites and trondhjemites generally constitute a significant component of Archaean terranes and because this suite of rocks usually represents the oldest granitic (*sensu lato*) event in such an environment, they have been the object of numerous studies in various parts of the world. Many of the recent published works on Archaean tonalites and trondhjemites are characterized by an almost singular consensus in the fact that these rocks have been derived by partial melting of precursors with basaltic compositions (Hanson and Goldich, 1972; Arth and Hanson, 1972, 1975; Arth and

Barker, 1976; Glikson, 1976a; Condie and Hunter, 1976; O'nions and Pankhurst, 1978; Collerson and Bridgwater, 1979; Tarney et al., 1979; Payne and Strong, 1979). This widely recognized genetic relationship between tonalite and basalt is based on a number of parameters which include rock associations, isotopic studies (in particular primitive initial $^{87}Sr/^{86}Sr$ ratios), laboratory melting experiments (Helz, 1976) and trace and rare-earth element modelling.

In spite of this consensus, it is, nevertheless, possible to generate tonalitic-trondhjemitic magmas in a number of different ways. It is instructive, therefore, to examine these various mechanisms from the point of view of understanding how the special conditions applicable in the Archaean caused these particular tonalites to have the characteristics that they in fact show. Tonalitic-trondhjemitic liquids can be generated in the following ways :-

(i) partial melting of dehydrated basalt at mantle depths leaving an eclogitic (i.e. garnet + clinopyroxene) residue (e.g. Arth and Hanson, 1975);

(ii) partial melting of amphibolite at crustal depths leaving behind a hornblende-bearing residue (e.g. Arth and Barker, 1976);

(iii) fractionation of plagioclase + hornblende from a wet basalt to produce a range in compositions including gabbro-diorite-tonalite-trondhjemite (e.g. Arth et al., 1978),

(iv) severe fractional crystallization of basalt (i.e. plagioclase + clinopyroxene + orthopyroxene + olivine) to produce a volumetrically insignificant mesostasis fraction of plagiogranitic composition (e.g. Coleman and Peterman, 1975); and

(v) special cases where melting of sialic crust, already depleted in incompatible elements, appears to have taken place (e.g. Bridgwater and Fyfe, 1974).

In a typical Archaean setting many of these mechanisms can be discounted; for example, fractionation of hornblende + plagioclase tends to

form a range of rock compositions that are likely to exhibit cumulate characteristics, whereas more severe fractional crystallization will not produce the large volumes of tonalitic-trondhjemitic rock presently observed in typical Archaean terranes. Depleted sialic crustal precursors have not been widely documented in Archaean terranes and the fifth mechanism is not, therefore, likely to be the general case. The partial melting of eclogite is a viable mechanism in creating the Archaean tonalites-trondhjemites but suffers from the fact that eclogites, particularly in the form of remnant cognate xenoliths, are not found in typical granite-greenstone terranes. Hence, at least within typical Archaean environments, partial melting of amphibolite is the most probable mechanism of producing significant quantities of tonalitic-trondhjemitic magma.

The petrogenesis of Archaean tonalites-trondhjemites along the lines suggested above, has been particularly well-constrained by the specific rock associations commonly encountered in these terranes. It has been noted that granite-greenstone areas are characterized by a bimodal tonalite-basalt assemblage (Barker and Peterman, 1974; Barker and Arth, 1976) and that rocks of intermediate composition such as andesite and gabbro are noticeably lacking. Barker and Arth (1976) have suggested that this association is further evidence for the partial melting of amphibolite (i.e. metamorphosed basalts) to form tonalitic melts. These workers also envisage that at low load pressures and P_{H_2O}, and for small degrees of partial melt, a certain amount of plagioclase will be retained in melt residues, this resulting in the generation of low-Al_2O_3 tonalitic melts. With more advanced partial melting and an increase in P_{H_2O}, plagioclase will be totally consumed and the more typical high-Al_2O_3 tonalitic melts will result. However, a limit on the amount of partial melting that can take place will be imposed as the residual basalts become progressively dehydrated. Thus, as tonalitic and trondhjemitic liquids are continually removed from the source region, the amphibolitic residue becomes unstable with a subsequent transformation of hornblende to pyroxene. Such an assemblage is likely to be situated below its solidus such that further melting is prohibited and the approximately 40% anatexis envisaged for the formation of andesites (Barker and Arth, 1976) is never attained. These arguments support an origin of formation for tonalitic magmas by partial melting of hydrated basalts, whilst also providing an explanation for the bimodal association mentioned above.

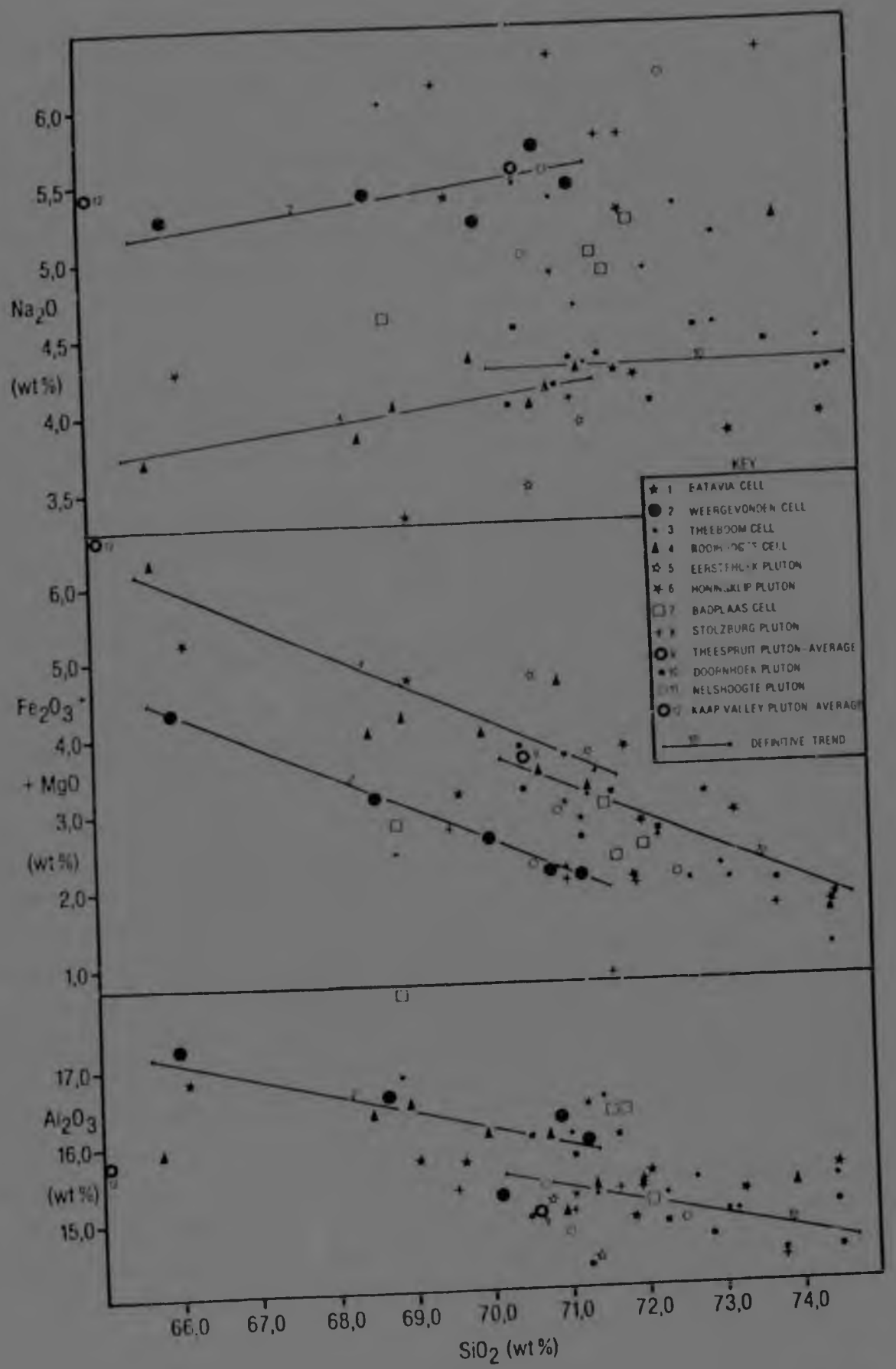

Figure 83 : Selected Harker diagrams showing the more definitive chemical characteristics of the tonalite and trondhjemite plutons and cells from the study area. Data sources are outlined in Table 33.

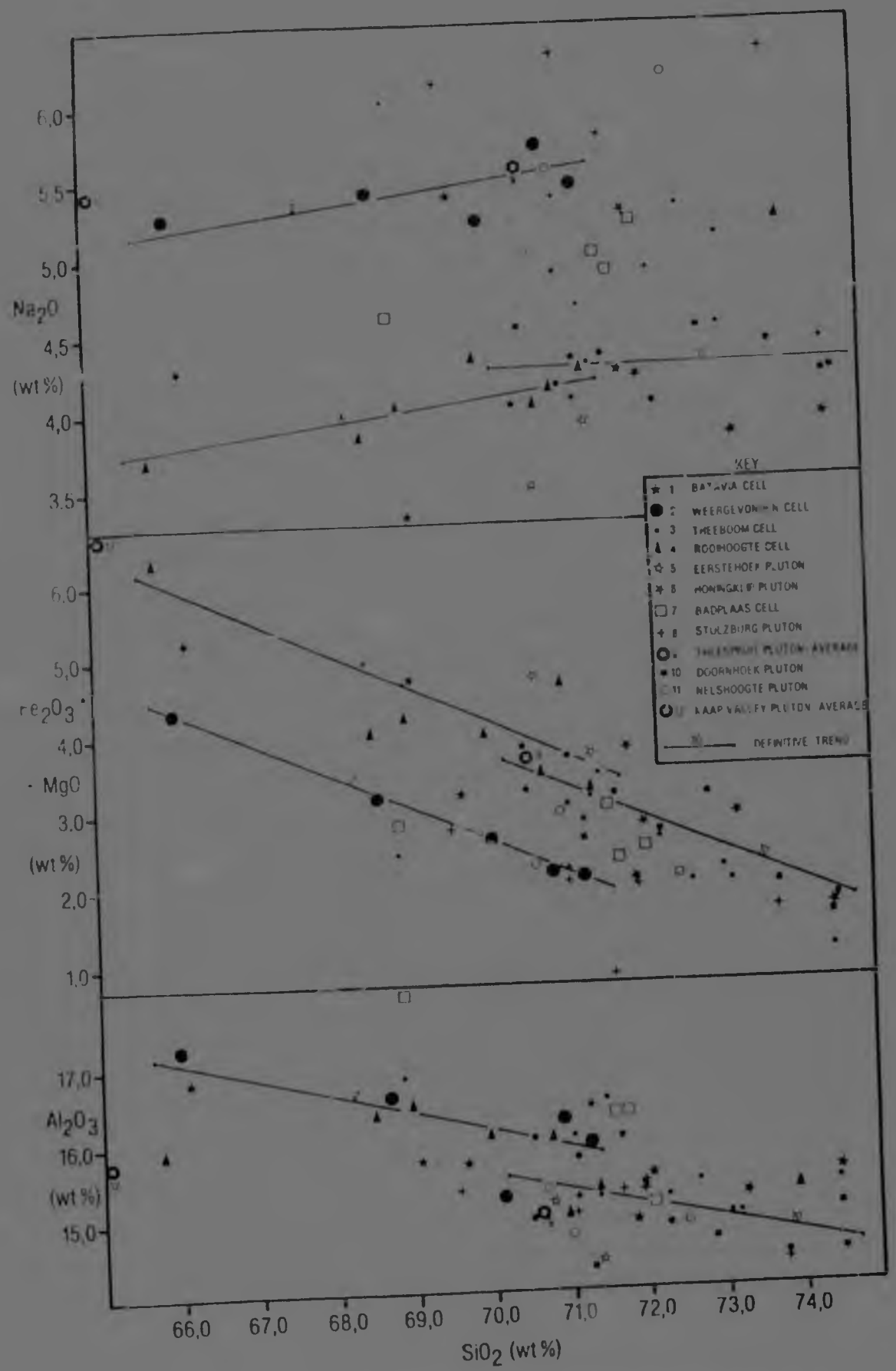

Figure 8.1: Selected Harker diagrams showing the more definitive chemical characteristics of the tonalite and trondhjemite plutons and cells from the study area. Data sources are outlined in Table 33.

The following sections are concerned with an examination of the characteristics of the twelve tonalite-trondhjemite plutons or cells that have now been defined in the area southwest of the Barberton greenstone belt, in the light of the current thoughts on tonalite-trondhjemite genesis. It will be shown that, although the ideas summarized above are generally applicable to the study area, the availability of a large quantity of data, such as that presented below, produces a refinement to some of these existing thoughts.

2. MAJOR ELEMENT CHEMISTRY

As mentioned above and described in Table 33, this section examines the characteristics of 133 major and trace element analyses from the tonalite-trondhjemite gneisses in the study area. Seven of these analyses have been published and the references are cited in Table 33; fifty-eight analyses are presented in this thesis, whereas the remainder are taken from the unpublished data of C.R. Anhaeusser. The latter samples, together with new data from other granitic bodies in the Barberton Mountain Land, will be presented in the South African Geodynamics Project volume on the Barberton study area.

The major element characteristics of most of the twelve tonalite-trondhjemite plutons or cells are plotted on selected Harker diagrams in Figure 83. Because there is a strong sampling bias towards the Kaap Valley and Theespruit plutons (i.e. 72 samples come from these two bodies) and also for the sake of clarity, these two plutons are represented by single average values in Figure 83; complete details of major-element variations over the Kaap Valley pluton are presented in Figure 53, Chapter 4. Two of the plots in Figure 83, namely SiO_2 v Al_2O_3 and SiO_2 v (Fe_2O_3* + MgO) exhibit typical Harker trends with generally decreasing alumina and mafics with increasing silica. The third plot of SiO_2 v Na_2O shows no distinct overall pattern whatsoever, except with respect to the characteristics of the individual plutons or cells.

2.1 The tonalite-trondhjemite bodies in terms of Harker trends

2.1.1. SiO_2 v Al_2O_3

This diagram (Figure 83) shows that alumina contents are generally

silica dependent; in the light of Barker's (1979) definition which suggests that high-alumina trondhjemites have Al_2O_3 > 15% at 70% SiO_2, it is clear that all the trondhjemites under consideration, as well as the Kaap Valley tonalite (see Figure 53) can be classified as high-alumina types. A petrogenetic implication of this observation is that the magma precursors of the tonalite-trondhjemite gneisses were derived from a parent-melt system that contained insignificant quantities of plagioclase in the residue. A close scrutiny of the overall trend indicates that certain of the tonalite-trondhjemite bodies have a different composition as a whole, to other bodies. The Weergevonden (2) and Rooihoogte (4) cells have slightly higher alumina contents (for any value of silica) than the Doornhoek (10) and Theespruit (9) plutons, whereas most of the other bodies have indefinitive, or intermediate, trends.

2.1.2 SiO_2 v $Fe_2O_3^* + MgO$

Although this diagram also illustrates the overall dependence of the ferromagnesian content of the tonalite-trondhjemite gneisses, to their silica content, the trends that appear in this diagram are particularly instructive in distinguishing between plutons or cells with slightly different mafic contents. Certain bodies such as the Weergevonden cell (2) and Stolzburg pluton (8) have a markedly lower ferromagnesian content over the total range of their silica contents, than other plutons (such as the Kaap Valley (12) and the Rooihoogte cell (4)) which may exhibit similar ranges in SiO_2. The Doornhoek pluton (10) also has a relatively high $Fe_2O_3^* + MgO$ content in view of the fact that it is characterized by uniformly high silica values (i.e. 70,5% < SiO_2 < 75,0%, see Figure 85). Most of the other plutons or cells have indefinitive or intermediate trends.

2.1.3 SiO_2 v Na_2O

Most of the tonalite-trondhjemite bodies do not define a systematic silica-dependent trend on this diagram. However, certain bodies appear to be characterized by a distinctive Na_2O content, which appears, in certain cases, to bear a positive correlation with SiO_2. The Weergevonden cell (2), Stolzburg pluton (8) and, to a lesser extent, the Nelshoogte pluton (11) are all characterized by soda contents in excess of 5,25%. In contrast the Rooihoogte

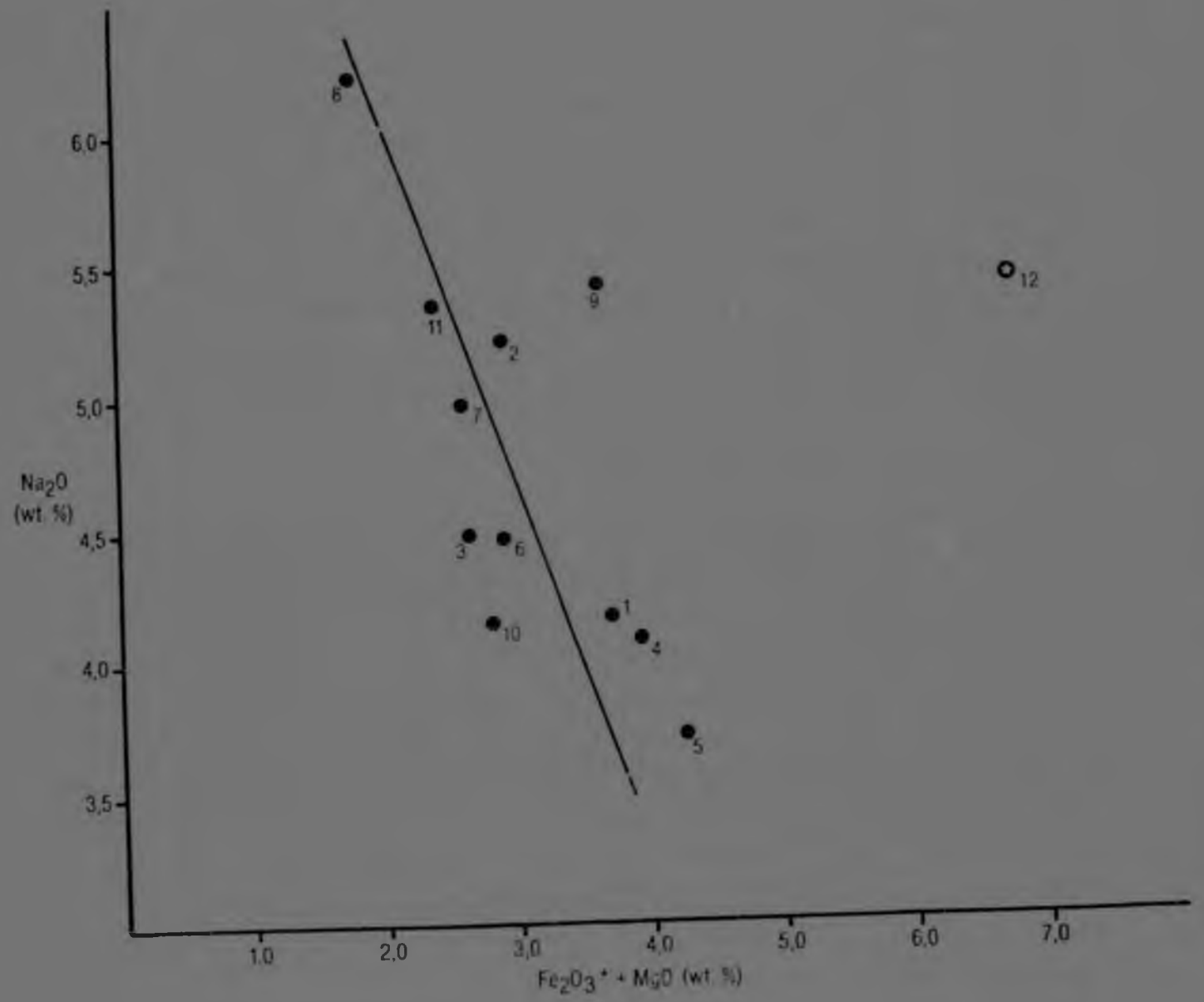

Figure 84 : Plot of the average values of ($Fe_2O_3^* + MgO$) and Na_2O for each of the tonalite-trondhjemite bodies in the study area. The data sources are provided in Table 33, which also provides the key to the numbers that identify each of the plotted points. Four discernible groupings can be identified from this diagram; (i) the anomalously high ferromagnesian Kaap Valley tonalite (12), (ii) a high ferromagnesian, low soda group (1, 4 and 5), (iii) a low ferromagnesian, high soda group (2, 7, 8, 9 and 11), and (iv) an intermediate group comprising units 3, 6 and 10.

cell (4), the Doornhoek pluton (10), the Eerstehoek pluton (5) and the Batavia cell (1) all have values of Na_2O = 4%. The Kaap Valley and Theespruit plutons are also characterized by relatively high average values of Na_2O, whereas the other plutons or cells have indefinitive or intermediate trends.

It is apparent when taking all three of the Harker diagrams into account, that certain of the tonalite-trondhjemite plutons or cells are characterized, *in toto*, by significant and systematically different chemical compositions, in spite of the fact that they all qualify for a tonalitic or trondhjemitic nomenclature. This distinction is not particularly noticeable in terms of silica where all the bodies exhibit a similar range from ≅ 66% to ≅ 74% SiO_2 (with the exceptions of the Kaap Valley pluton with uniformly low silica and the Doornhoek pluton with uniformly high silica). Neither is the distinction particularly prevalent in terms of alumina, titanium or calcium, again with the exception of the Kaap Valley tonalite, which is markedly higher in TiO_2 and CaO than the trondhjemitic bodies. However, the Harker diagrams in Figure 83 point to the fact that Na_2O and Fe_2O_3* + MgO, which exhibit a broad inverse relationship, appear to differentiate most effectively between the various trondhjemitic bodies in the study area. In Figure 84 the average values of Na_2O and Fe_2O_3* + MgO are plotted for each of the twelve plutons or cells in the study area. The dominantly trondhjemitic bodies form a fairly distinct trend, such that rocks with high ferromagnesian contents have low Na_2O values and vice versa. In complete contrast, the Kaap Valley tonalite plots distinctly away from this trend with an anomalously high ferromagnesian content.

The distribution of the average data points in Figure 84 suggests that, rather than comparing and contrasting each pluton or cell as an individual entity, reasonably definitive groupings of tonalite-trondhjemite sub-types may be considered. Four such groupings are suggested on the basis of this diagram and these include the anomalously mafic Kaap Valley tonalite (12), a high ferromagnesian-low soda category (1, 4 and 5), a low ferromagnesian-high soda group (2, 7, 8, 9 and 11) and an intermediate group comprising units 3, 6 and 10. This grouping is discussed in the following section with a view to understanding the reasons behind [illegible]mpositional differences.

2.2 Tonalite-trondhjemite magma types and petrologic mixing considerations

Compositional differences in spatially unrelated tonalitic or trondhjemitic magmas may be the result of either, differences in the degree of partial melting undergone during the derivation of that magma or, differences in the nature of the crystal fractionation processes that may have been experienced by the body on cooling. In Chapter 4, the processes of crystal fractionation in the Kaap Valley tonalite were given considerable attention particularly from the view-point of the hornblende and hornblende + biotite tonalitic phases. In the present considerations, however, although individual plutons or cells exhibit an *in situ* compositional variation that may be related to crystal fractionation, it is apparent, both in Figure 83 and 84, that when comparing one pluton with another, significant *overall* differences exist between them. For the purposes of the following discussion, it is assumed that systematic variations from one pluton to another, reflect differences in the original composition of the melt from which each of these bodies was derived. As a result, the four groupings outlined above can possibly be regarded in terms of different degrees of partial melting of the same, or similar basaltic precursors, a tenet that can be assessed by using conventional petrologic mixing considerations.

With this objective in mind it is important to stress that excellent constraints on basalt-melt systems, within the stability field of hornblende, have been established by the experimental studies of Helz (1976) and it is instructive to summarize some of the pertinent conclusions of this work :-

(i) for small degrees of partial melting, melt compositions are generally insensitive to the original basalt composition, although the Na/Ca ratio may be dependent on that of the parent, whilst the breakdown of hornblende during higher degrees of partial melting may also cause more significant variations;

(ii) the incongruent melting behaviour of hornblende is such that successive melt compositions differ disproportionately from each other (see later) and will also be different in composition from the minerals contributing to the melt; and

(iii) in spite of the previous consideration, as temperatures increase (i.e. the degree of partial melting increases) melt compositions will be characterized by a generally systematic decrease in SiO_2, an increase in Al_2O_3 (until a maximum is reached near the upper stability limit of hornblende, i.e. between 950-1 000°C at P_{H_2O} = 5 Kb), a non-uniform increase in FeO and MgO (depending on the extent to which hornblende has broken down), an increase in CaO and a decrease in K_2O whilst Na_2O remains relatively constant or increases slightly.

With respect to Archaean tonalites-trondhjemites, these results indicate that it does not really matter what the exact composition of the basaltic parent is, as melt compositions will be broadly similar for small degrees of partial melt (i.e. < 30). Furthermore, in the light of Helz's (1976) experimental data, certain predictable changes in melt compositions do occur as the temperature of melting increases. It is possible, therefore, to gauge the effect that small variations in the degree of partial melting will have on a body of magma. Using this approach, the four distinct tonalite-trondhjemite groupings, each of which has been allocated a representative magma composition in Table 34, can be evaluated in terms of derivation from a basaltic parent and whether fluctuations in partial melting will account for the observed differences in tonalite-trondhjemite compositions. This is done by using the petrologic mixing programme devised by Wright and Doherty (1970), in which each of the four magma types are combined with a hornblende-bearing residue in proportions which will provide a minimum combined least squares error with respect to a fixed basaltic komatiite parent. In this process the parent is considered to be a Barberton-type basaltic komatiite (the most voluminous basalt species in the lower Onverwacht Group) and the residue is considered to be composed entirely of hornblende of a residual nature (*),

---

(*) Footnote: The composition of the residual hornblende used in the calculation of Table 34 is similar to those analysed by Helz (1973) who documented the changes in residual hornblende compositions with progressive partial melting of tholeiites. However, komatiitic hornblende compositions (see Table 26) have lower Al_2O_3 contents than Helz's residual hornblendes and this factor is introduced into the composition of the model residual hornblendes used above.

the composition of which, together with that of the basaltic precursor, is provided in Table 34. The results of the petrologic mixing assessments are summarized in Table 35. Here it is shown that the variations in tonalite-trondhjemite magma type can be reasonably well explained in terms of *small* differences in the degree of partial melting. The calculated composition of the basaltic parent from a combination of the most convenient proportions of each of the magma types with a hornblende-bearing residue is, in each case, very close to the actual composition. Sum squares of errors are approximately 5 in each of the calculations; this figure is somewhat high and is probably due to the fact that the composition of the hornblende in the residue (from Helz, 1973) may not be truly realistic. The actual results suggest that melting varied only from ≈ 35% in the formation of the Kaap Valley tonalite to ≈ 25% for the Weergevonden. Stolzburg and related plutons. Although these differences in degree of melting are small, Helz (1976) has shown that compositions do not change dramatically over a wide range of melt temperatures (200-300°C) but that significant changes, particularly in CaO, FeO and MgO start occurring only as *hornblende* melts, particularly near its upper stability limit. Thus, the significantly more ferromagnesian nature of the Kaap Valley tonalite is consistent with a more advanced degree of partial melting (perhaps akin to zone melting; see Chapter 4) where, at a critical temperature, the breakdown of hornblende is such that a sharp rise in the FeO + MgO content of the melt occurs (see Figure 2B in Helz, 1976). In contrast, the more leucocratic trondhjemitic compositions may have formed at temperatures below this critical value so that the melts were significantly less enriched in ferromagnesian components.

Again with respect to Helz's (1976) experimental data, it appears that the compositional variations in melt increments, as observed in the tonalites-trondhjemites, is not as systematic as that indicated in the laboratory. Although increased partial melting is concomitant with broadly decreasing SiO_2 and increasing Fe_2O_3* + MgO, as indicated in the experimental studies, the rocks considered to have formed from the smallest degree of melting in the above considerations are not depleted in alumina and contain more Na_2O than their more mafic counterparts. These apparent discrepancies may be accounted for by the complex nature of the incongruent melting of hornblende, a phenomenon which can be explained in the following way:-

TABLE 34

SUGGESTED TONALITIC-TRONDHJEMITIC MAGMA TYPES;
PARENTAL AND RESIDUAL COMPOSITIONS FOR
PETROLOGIC MIXING CONSIDERATIONS

		1	2	3	4	5	6
Wt.%	SiO_2	65,50	70,30	71,80	70,70	52,70	44,0
	TiO_2	0,47	0,37	0,22	0,40	0,90	2,5
	Al_2O_3	15,70	15,90	15,50	16,10	9,80	8,0
	Fe_2O_3*	4,30	2,80	2,20	1,80	10,90	13,0
	MnO	0,07	0,06	0,02	0,04	0,22	0,2
	MgO	2,40	1,30	0,80	0,70	10,10	15,0
	CaO	4,20	3,30	2,50	2,40	10,00	11,5
	Na_2O	5,40	3,80	4,30	5,30	2,65	1,5
	K_2O	1,40	1,40	2,00	1,80	0,40	0,5
	TOTALS	99,44	99,23	99,34	99,24	97,67	96,2

(Fe_2O_3* - Total iron as Fe_2O_3
P_2O_5 omitted from petrologic mixing assessment)

Columns 1 - Representative analysis of the Kaap Valley pluton (from Table 21).

2 - Representative analysis of the Batavia cell (1), the Rooihoogte cell (4) and Eerstehoek pluton (5).

3 - Representative analysis of the Doornhoek pluton (10), Theeboom cell (3) and Honingklip pluton (6).

4 - Representative analysis of the Weergevonden cell (2), Stoltzburg pluton (8), Badplaas cell (7), Theespruit pluton (9) and Nelshoogte pluton (11).

5 - Average Barberton-type (i.e. low MgO) basaltic komatiite (Viljoen and Viljoen, 1969c).

6 - Inferred composition of hornblende residue (estimated on the basis of data from Helz, 1973).

TABLE 35

PETROLOGIC MIXING CONSIDERATIONS - PROPORTIONS OF TONALITIC-TRONDHJEMITIC MAGMA TYPES THAT WILL COMBINE WIT- A HORNBLENDE-BEARING RESIDUE TO FORM A BARBERTON-TYPE BASALTIC KOMATIITE

	SiO_2	TiO_2	Al_2O_3	Fe_2O_3*	MnO	MgO	CaO	Na_2O	K_2O	Proportions
1.	53,96	0,92	10,03	11,16	0,23	12,34	10,24	2,71	0,41	
2.	52,55	1,87	10,85	10,37	0,16	11,09	9,31	2,88	0,92	Magma Type 1 - 33,4% Residue - 66,6%
3.	53,32	1,93	10,64	10,29	0,16	11,29	9,35	2,24	0,79	Magma Type 2 - 29,5% Residue - 70,5%
4.	53,35	1,92	10,41	10,27	0,15	11,35	9,25	2,33	0,95	Magma Type 3 - 28,0% Residue - 72,0%
5.	52,99	1,97	10,56	10,19	0,16	11,38	9,24	2,63	0,89	Magma Type 4 - 27,8% Residue - 72,2%

(Fe_2O_3* - Total iron as Fe_2O_3)

Rows : 1 - Average Barberton-type basaltic komatiite (from Table 34) normalized to 100%

2 - 5 - Compositions of the parental basalt calculated by combining the relevant proportions (see right-hand side of Table) of the various tonalite-trondhjemite magma types (i.e. 1-4 in Table 34) with a hornblende-bearing residue. These compositions are also normalized to 100%. Comparison of Row 1 with Rows 2-5 is a measure of the fit of the various magma-residue mixtures to the actual parental composition.

TABLE 35

PETROLOGIC MIXING CONSIDERATIONS - PROPORTIONS OF TONALITIC-TRONDHJEMITIC MAGMA TYPES THAT WILL COMBINE WITH A HORNBLENDE-BEARING RESIDUE TO FORM A BARBERTON-TYPE BASALTIC KOMATIITE

	SiO_2	TiO_2	Al_2O_3	Fe_2O_3*	MnO	MgO	CaO	Na_2O	K_2O	Proportions
1.	53,96	0,92	10,03	11,16	0,23	10,34	10,24	2,71	0,41	
2.	52,55	1,87	10,85	10,37	0,16	11,09	9,31	2,88	0,92	Magma Type 1 - 33,4% Residue - 66,6%
3.	53,32	1,93	10,64	10,29	0,16	11,28	9,35	2,24	0,79	Magma Type 2 - 29,5% Residue - 70,5%
4.	53,35	1,92	10,41	10,27	0,15	11,35	9,25	2,35	0,95	Magma Type 3 - 28,0% Residue - 72,0%
5.	52,99	1,97	10,56	10,19	0,16	11,36	9,24	2,63	0,89	Magma Type 4 - 27,8% Residue - 72,2%

(Fe_2O_3* - Total iron as Fe_2O_3)

Rows : 1 - Average Barberton-type basaltic komatiite (from Table 34) normalized to 100%

2 - 5 - Compositions of the parental basalt calculated by combining the relevant proportions (see right-hand side of Table) of the various tonalite-trondhjemite magma types (i.e. 1-4 in Table 34) with a hornblende-bearing residue. These compositions are also normalized to 100%. Comparison of Row 1 with Rows 2-5 is a measure of the fit of the various magma-residue mixtures to the actual parental composition.

In a situation where perfect fractional crystallization occurs, the system can be described as follows :-

Parent = Differentiated residue + Fractionating Mineral 1 + Fractionating Mineral 2 + ... etc.

In such a case the solution of such a mass-balance equation is rigidly constrained by the composition of phenocryst assemblages. In a partial melt situation, however, the situation is slightly different :-

Parent = Partial Melt + Residual Mineral 1 + Residual Mineral 2 + ... etc.

In this case, if any of the residual minerals are compositionally invariant (e.g. quartz) or exhibit simple binary solid solution (e.g. plagioclase and olivine) then melt compositions can also be reasonably well-constrained in terms of predictable end-member compositions. If, however, the residual mineral phases are characterized by complex solid solutions (such as hornblende and augite) then, as shown by Helz (1976), the change in composition of partial melt increments in any specified temperature interval may be very different from the change in composition of minerals contributing to the melt. For example, Helz (1976) has shown that during the melting of an olivine tholeiite in the temperature range 725-825°C, hornblende will absorb Na and Al from the melted plagioclase phase leaving Ca and Si enriched in the melt increment forming *in that temperature interval*. At a higher temperature interval, however, continued breakdown of hornblende will redress the soda and alumina content of subsequent melt compositions. In another example, during the melting of an alkali basalt, Ca and Al are partitioned into hornblende between 725-825°C whilst the melt is enriched in Na and Si. Again, at a higher temperature (after a greater amount of melt had formed) Ca and Al became preferentially partitioned into the melt relative to the continually changing hornblende (residual) composition. Thus, resorption of minerals involved in a partially melted system will cause complex changes in the composition of successive melt increments which may, as a result, be largely unpredictable.

It is extremely difficult, therefore, in the absence of voluminous quantities of the relevant experimentally-derived phase relations, to quantify the more subtle compositional variations that occur in what are

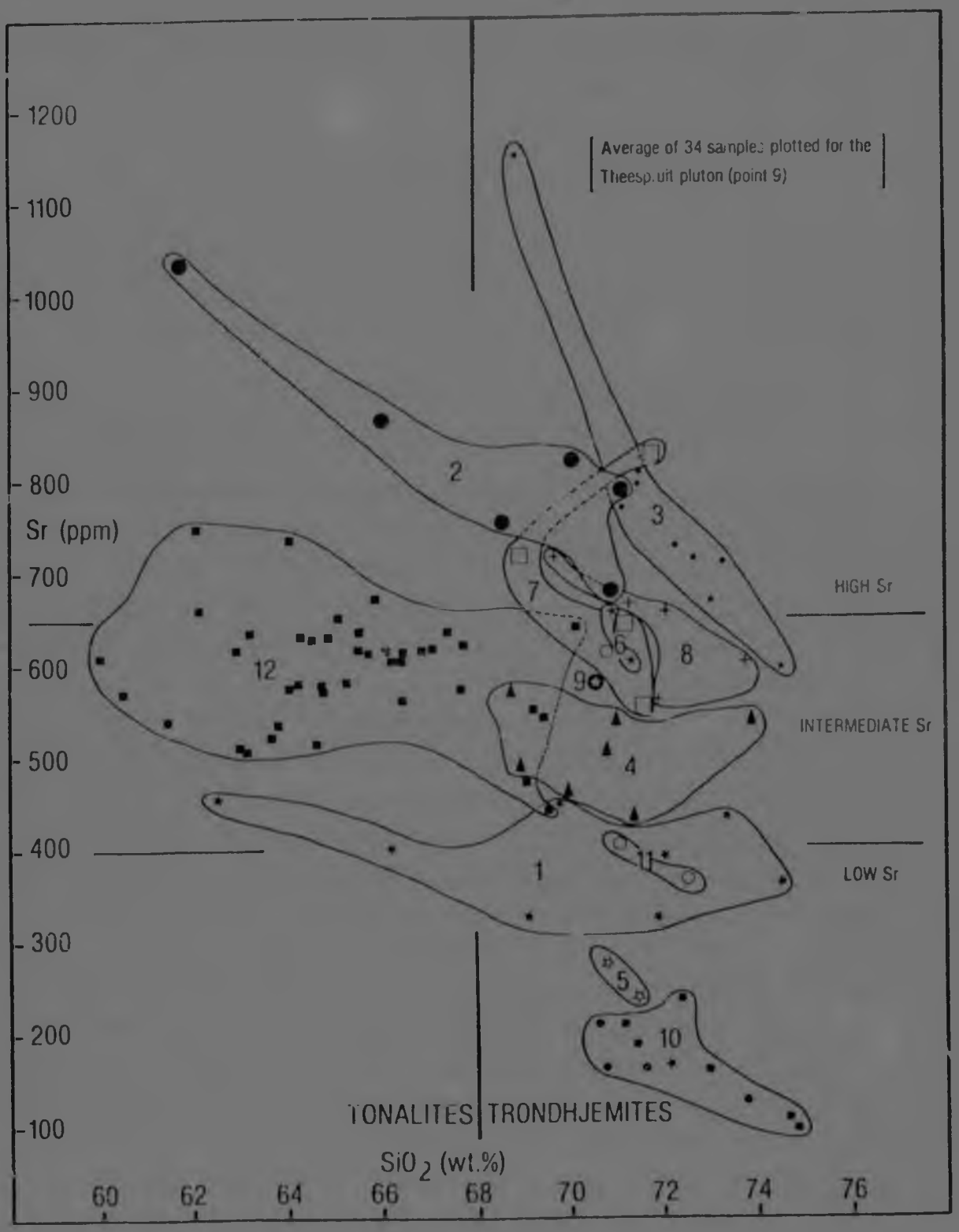

Figure 85 : Plot of SiO_2 against Sr for the twelve tonalite-trondhjemite plutons and cells defined in the area southwest of the Barberton greenstone belt (Figure 82). Data sources are listed in Table 33, which also provides the key to the numbers representative of each of the fields in the diagram. Low-, intermediate- and high-Sr categories are arbitrarily defined. Symbols are the same as those used i Figure 83.

considered to be the original magma compositions of tonalite-trondhjemite bodie in the study area. It is highly feasible that small temperature differences during anatexis, complex solid solution of the probable residual phases (i.e. hornblende) and the likelihood of small, but variable, amounts of plagioclase in the residue, all contribute to these fluctuations A final factor which undoubtedly adds one other variable to these considerations, is the precipitation of near-liquidus phases and consequent differentiation of the melt *during* the emplacement of the tonalitic-trondhjemitic magma.

2.3 Tonalite-trondhjemite characterization

The preceding sections have pointed to, and discussed some of the ramifications of, subtle variations in the major element chemistry of the various tonalite-trondhjemite bodies in the study area. This section examines the chemical variables that best serve to maximize the differences between these bodies, and hence distinguish them one from another.

The clearest distinction between the twelve tonalite-trondhjemite plutons or cells described above is made on a plot which involves their Sr contents. In Figure 85, a plot of SiO_2 v Sr serves to distinguish between tonalites and trondhjemites on the basis of their SiO_2 contents and also illustrates the fact that each of the twelve bodies is characterized by a reasonably definitive Sr "fingerprint". Although individual bodies may exhibit a variation in SiO_2, which spans the full range of the tonalite-trondhjemite spectrum (i.e. 62% < SiO_2 < 74), the Sr fingerprint of each body appears to be reasonably definitive and is SiO_2 independent. In Figure 85 most of the bodies have a discrete compositional field in terms of both SiO_2 and Sr, with the latter ranging from ≈ 150 ppm in the Doornhoek pluton to an average of 750-850 ppm in the Weergevonden and Theeboom cells. Naturally, as there is a considerable amount of data, overlaps do occur, particularly in the range 600-750 ppm Sr and, because of this, the 34 data points available for the Theespruit pluton (see Table 33) are plotted as a single average. Because of the data overlap, the SiO_2 v Sr diagram is best regarded as distinguishing between plutons of low Sr (i.e. the Doornhoek pluton, Eerstehoek pluton, Batavia cell and possibly the Nelshoogte pluton), intermediate Sr (i.e. the Rooihoogte cell, Kaap Valley pluton, Honingklip pluton, Theespruit pluton,

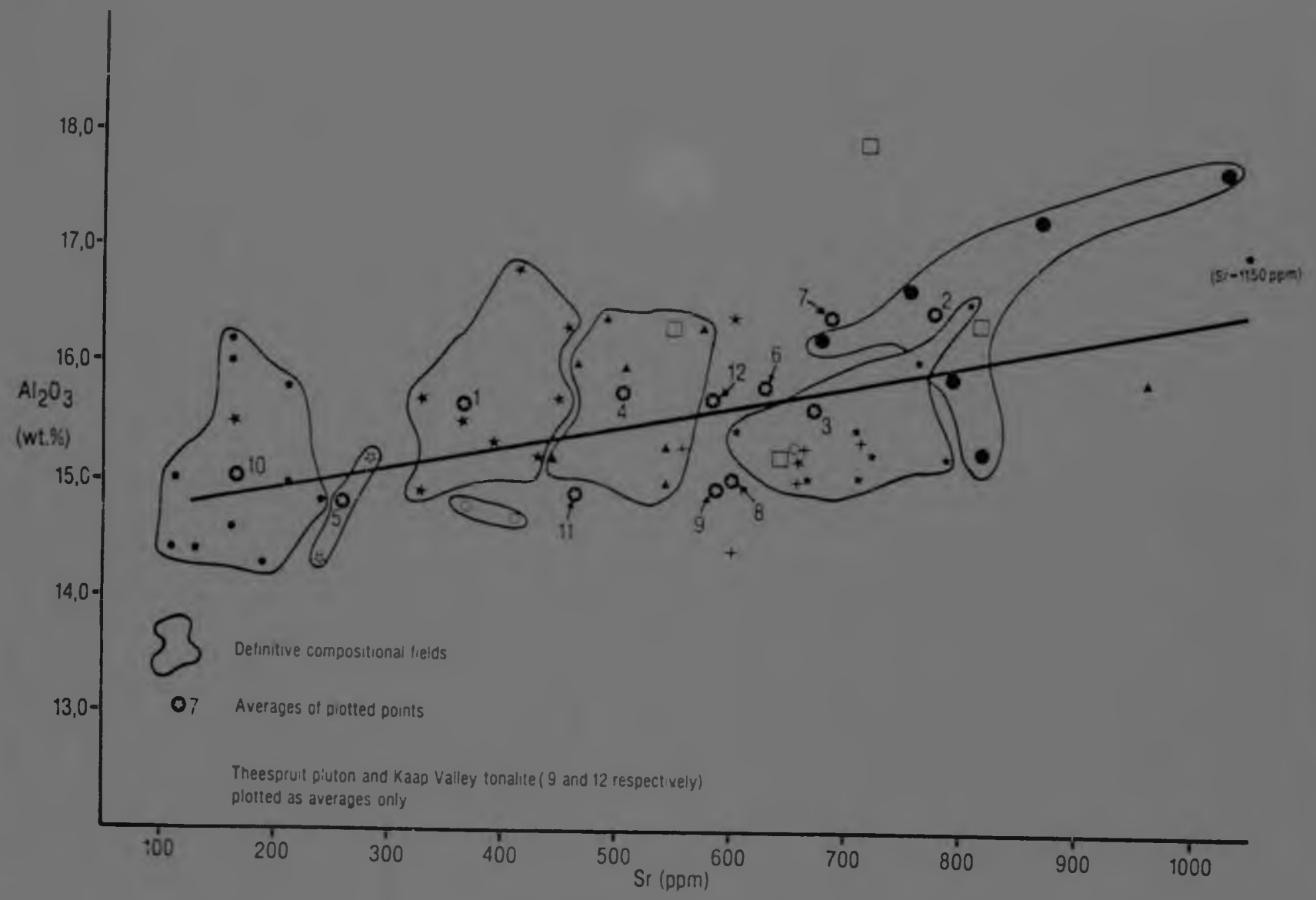

Figure 86 : Plot of Al_2O_3 against Sr for the tonalite-trondhjemite plutons and cells southwest of the Barberton greenstone belt. Data sources are listed in Table 32 which also provides the key to the numbers representing each of the fields in the diagram. Only the definitive compositional fields have been outlined. The best-fit line is visually estimated. Symbols used are the same as those in Figure 83.

Badplaas cell and Stolzburg pluton) and high Sr (i.e. the Weergevonden and Theeboom cells). These four inter-related parameters (i.e. SiO_2, low-, intermediate- and high-Sr) are offered as those best serving to characterize and distinguish between the tonalite-trondhjemite bodies of the Barberton Mountain Land.

The approximately four-fold variation of Sr in the various plutons and cells of the Barberton region is an interesting observation and one that must certainly have a bearing on the petrogenesis of these rocks. In view of this, a detailed consideration of trace element characteristics of the tonalite-trondhjemite bodies is presented in the following section. It is also instructive, however, to consider the possible dependence of Sr on the major element characteristics of these rocks. As Sr is strongly partitioned into plagioclase and the tonalites-trondhjemites are dominantly plagioclase bearing, it is possible that a distinctive relationship between Al_2O_3 and Sr exists in these bodies. Alumina is particularly relevant as Barker and Arth (1976) have shown that the difference between trondhjemites with high- and low-Al_2O_3 contents may be due to the presence, or lack, of residual plagioclase during the anatectic formation of these rocks. In Figure 86, a plot of Sr v Al_2O_3 shows that a slight positive correlation between these two variables exists. Although, as mentioned previously, all the tonalites-trondhjemites can be categorized as high-Al_2O_3 types (i.e. Al_2O_3 > 15% at 70% SiO_2) and none can, therefore, be said to have formed in the presence of significant amounts of residual plagioclase, this trend implies that, to a limited extent, Sr is proportional to the plagioclase component in these rocks. The question arises, however, as to whether the large variations of Sr can be attributed to cumulus enrichment by a fractionating, plagioclase-dominated assemblage. Although fractionation was described in the Kaap Valley tonalite it is nevertheless evident that most tonalite-trondhjemite bodies have similar amounts of plagioclase so that crystallization of this mineral is unlikely to be solely responsible for the observed Sr variations. Furthermore, cumulus plagioclase would result in rocks with pronounced positive Eu anomalies, a factor definitely not characteristic of tonalites and trondhjemites in the study area (see Figures 20, 55 and 91). The observed range in Sr, therefore, remains something of an unusual phenomenon in rocks with otherwise broadly similar chemical characteristics and is considered again in the following sections.

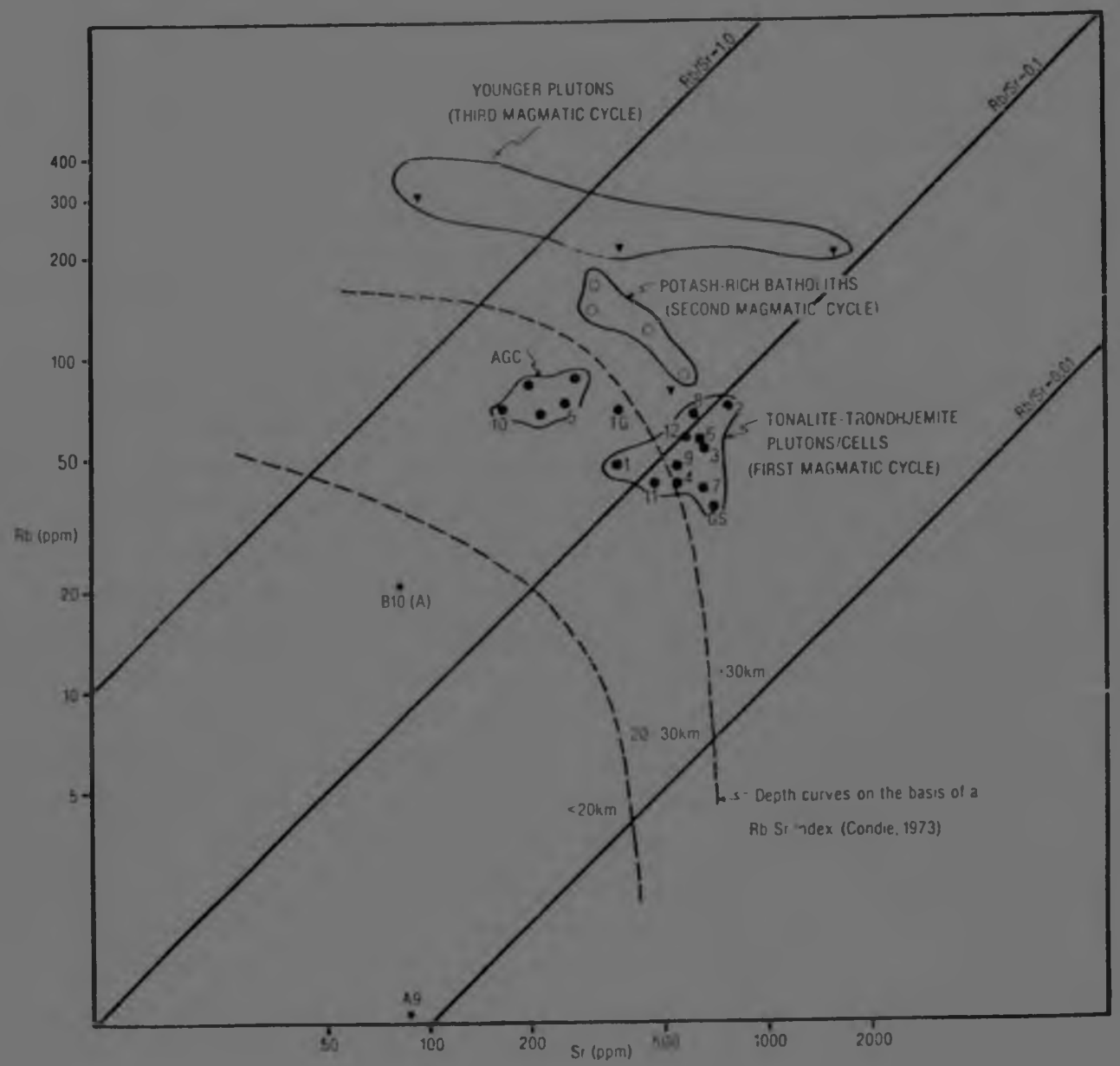

Figure 87 : Plot of Rb against Sr showing the average values for tonalite and trondhjemite plutons or cells from the region southwest of the Barberton greenstone belt. The data is taken from Table 36 which also provides the key for the numbers allocated to each of the plotted points. Dots represent units categorized into the first magmatic cycle (see Chapter 7); units 1-12 are from the Barberton Mountain Land; TG (the Tsawela gneiss), GS (the Granodiorite Suite) and AGC (three points; the Ancient Gneiss Complex) all represent various units from Swaziland. Points from the potash-rich shield-forming batholiths (open circles) and the various post-tectonic younger plutons (inverted triangles) are also from Table 36. Samples of migmatite-related plagiogranites (B10(A) and A9, from Tables 1 and 2) are also plotted for the sake of comparison. The depth curves (after Condie, 1973) are considered to reflect the depths from which the various components shown on this type of diagram, may have been generated.

3. TRACE ELEMENT CHEMISTRY

A considerable amount of data has accumulated in the recent literature regarding the trace element contents of typical Archaean "grey gneisses" particularly with regard to their use as petrogenetic indicators. Most instructive in this sense are Rb, Sr, Ba and the rare-earth elements which appear, in most cases, to have remained relatively immobile so that systematic variations can be interpreted as being indicative of the origin of these rocks. The following section examines the trace element characteristics of the twelve tonalite-trondhjemite bodies being studied and compares them to similar rock-types from other areas.

3.1 Rubidium, strontium and barium

Particularly diagnostic in terms of previous granite-related petrogenetic studies has been the Rb/Sr ratio which, in conjunction with Rb-Sr isotope studies may point to the nature of the source of a particular rock as well as defining the evolution of its isotopic growth vector (see later).

In Figure 87, a Rb v Sr plot illustrates the average rubidium and strontium values of each of the twelve tonalite-trondhjemite bodies, together with average data from a number of other granites (*sensu lato*) in the region. These data, and their source, are provided in Table 36. It is apparent, from this diagram that, in spite of the significant variation in Sr contents mentioned in the previous section, the Rb/Sr ratios of the majority of the tonalite-trondhjemite bodies are remarkedly similar, being generally in the range $\cong$ 0,08 - 0,13. In contrast, to the general tendency, however, the Doornhoek and Eerstehoek plutons (points 10 and 5, Figure 87) have significantly higher Rb/Sr ratios (i.e. 0,3-0,4) that are similar to three values obtained for siliceous gneisses from the Ancient Gneiss Complex (AGC) in Swaziland (see Table 36). In addition, as might be expected, younger granitic rocks in the Barberton and Swaziland regions (i.e. the second and third magmatic cycles in Figure 1) are characterized by higher average Rb contents and plot in fields that are discrete from those either of the AGC or the tonalites-trondhjemites.

Because partial melting processes generally tend to increase the Rb/Sr ratio in the derived products, the distribution of values in Figure 87,

TABLE 36

AVERAGE Rb, Sr AND Ba CONTENTS OF SELECTED GRANITES *(SENSU LATO)* FROM THE BARBERTON REGION AND SWAZILAND

Rock	ppm				Sources
	Rb	Sr	Ba	Rb/Sr	
1. Batavia cell	47	368	209	0,13	Average of 3 analyses, Table 37 and 6 analyses, Anhaeusser (unpub. data).
2. Weergevonden cell	69	779	664	0,09	Average of 6 analyses, Anhaeusser (unpub. data).
3. Theeboom cell	53	675	408	0,08	Average of 7 analyses, Anhaeusser (unpub. data) and 2 analyses, Table 2.
4. Rooihoogte cell	43	563	378	0,08	Average of 8 analyses, Anhaeusser (unpub. data).
5. Eerstehoek cell	72	257	230	0,28	Average of 2 analyses, Anhaeusser (unpub. data).
6. Honingklip pluton	55	630	317	0,09	Average of 2 analyses, Anhaeusser (unpub. data).
7. Badplaas cell	39	683	411	0,06	Average of 4 analyses, Anhaeusser (unpub. data).
8. Stolzberg pluton	67	604	646	0,11	Average of 1 analysis, Anhaeusser (unpub. data) and 2 analyses, Table 1.
9. Theespruit pluton	51	527	317	0,10	Average of 3 analyses, Condie and Hunter (1976); 1 analysis, Glikson (1976a) and 1 analysis, Viljoen and Viljoen (1969g).
	46	589	330	0,08	Average of 31 samples, Anhaeusser (unpub. data)
10. Doornhoek pluton	68	167	246	0,41	Average of 10 analyses, Table 32
11. Nelshoogte pluton	41	491	279	0,08	Average of 2 analyses, Condie and Hunter (1976); 2 analyses Glikson (1976a) and 1 analysis, Viljoen and Viljoen (1969g).
12. Kaap Valley pluton	56	586	343	0,09	Average of 41 samples, Table 21.
	59	552	450	0,11	Average of 5 samples, Condie and Hunter (1976).
13. Bimodal Suite	67	226	183	0,30	Average of 6 analyses, Condie and Hunter (1976) and 5 analyses of siliceous gneisses, Hunter et al. (1978).
	84	276	-	0,30	Average of 10 samples, Barton et al. (1980).
14. Banded gneisses (AGC-Mankayane)	82	197	-	0,42	Average of 3 analyses, Davies (1971).
15. Tsawela gneiss	69	361	330	0,19	Average of 2 samples, Hunter et al. (1978).
16. Granodiorite Suite	35	723	-	0,05	Average of 5 analyses, Hunter et al. (1978).
17. Hebron granodiorite	135	305	673	0,44	Average of 4 analyses, Robb (1977).
18. Nelspruit porphyritic granite	118	453	764	0,26	Average of 18 analyses, Robb (1977).
19. Mpuluzi batholith (Lochiel granite)	162	316	711	0,51	Average of 6 analyses, Condie and Hunter (1976); 3 analyses, Glikson (1976a) and 1 analysis Viljoen and Viljoen (1969g).
20. Cunning Moor tonalite	62	522	427	0,12	Average of 9 analyses, Robb (1977).
21. Dalmein pluton	86	583	672	0,15	Average of 10 analyses, Robb (unpub. data).
22. Mliba pluton	77	534	767	0,14	Average of 3 dated samples, Davies (1971).
23. Boesmanskop syenite	198	1591	1750	0,12	Average of 8 samples, Anhaeusser, Robb and Barton (1979).
24. Sicunusa pluton	305	94	454	3,24	Average of 3 dated samples, Davies (1971) and 3 analyses, Condie and Hunter (1976).
25. Mpageni pluton	210	372	1506	0,56	Average of 9 samples, Van Nierop (unpub. data) and 2 samples, Condie and Hunter (1976).

appears to have some petrogenetic significance. The tonalites-trondhjemites must have been derived from material with Rb/Sr < 0,1 (i.e. such as basalt) and, as Condie and Hunter (1976) have pointed out, are not likely to have been anatectic by-products of components of the AGC. The AGC itself, at least on the basis of the Rb v Sr plot, would appear to have been derived from different material from that of tonalite-trondhjemite parentage although it is shown below that this need not necessarily be the case. It is, instructive therefore, to model the distribution of Rb, Sr and also Ba, in order to assess the reasons behind the differences in Rb/Sr in the Doornhoek/Eerstehoek plutons and AGC on the one hand, and the remainder of the tonalite-trondhjemite bodies, on the other.

Siliceous gneisses of the AGC are characterized by tonalite-trondhjemite compositions (Hunter et al., 1978), by very low initial $^{87}Sr/^{86}Sr$ ratios (Barton et al., 1980) and could, as a result, owe their origin to a process such as the partial melting of primitive, mafic precursors. As mentioned previously, such a process is generally associated with the formation of Archaean tonalites and trondhjemites, implying that the suites in both the Barberton Mountain Land and the AGC can be modelled in terms of similar source rocks and melt increments. Thus, the following trace element model considerations regard the formation of the tonalite-trondhjemite suite (including components of the AGC) solely in terms of a basaltic parent, but explores the effects of isochemical phase changes in melt residues on the generation of melts with differing trace element contents.

The following parameters are considered :-

Trondhjemitic modal proportions:-	Quartz	- 35%	K_D	Rb	- 0,38
	Plagioclase	- 50%		Sr	- 1,61
	Biotite	- 10%		Ba	- 1,12
	K-felspar	- 5%			

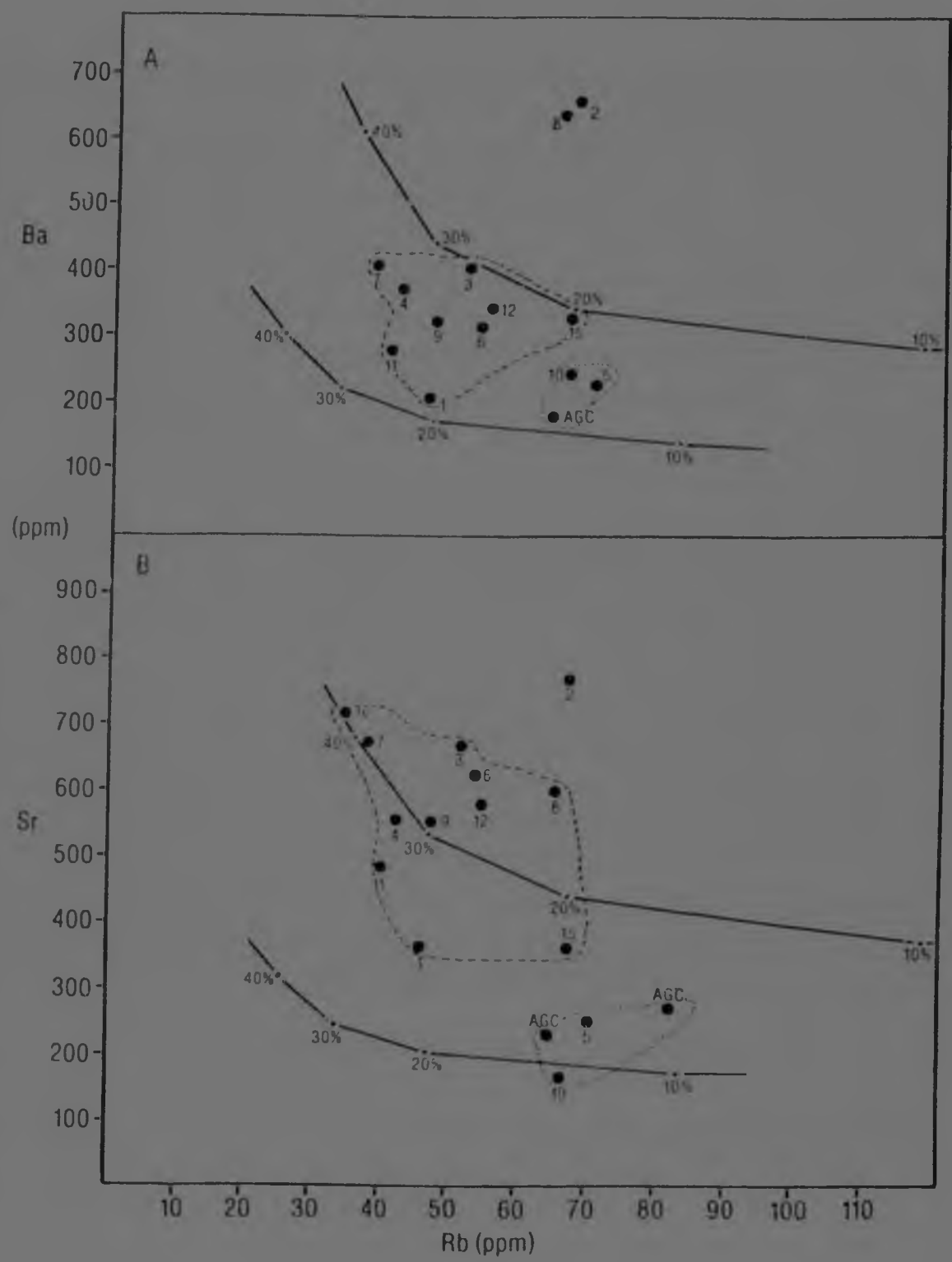

Figure 88 : *Model plots of Rb v Ba (A) and Rb v Sr (B) for averaged data from the twelve tonalite-trondhjemite plutons or cells as well as units from the AGC in Swaziland (see Table 36 for key to numbers). In each diagram the upper model curve is derived from 10-40% melting of Parent 1 whereas the lower curve from similar melt increments from Parent 2 (see text). Components of the high Rb/Sr types are encircled with a dotted line, the low Rb/Sr types with a dashed line. Units 2 and 8 (see Table 36) have Sr and Ba contents that are apparently too high to be accounted for by partially melting Parent 1.*

Basaltic komatiite modal proportions:-		K_D (*)	
	Hornblende - 80%		Rb - 0,02
	Plagioclase - 10%		Sr - 0,45
	Quartz - 10%		Ba - 0,08

The above bulk partition coefficients (K_D) can be used to model the origin of tonalite-trondhjemite magmas from both the AGC and Barberton areas. However, because the AGC and Doornhoek/Eerstehoek plutons have much lower Sr contents (and, as a result, higher Rb/Sr ratios) than the remainder of the tonalite-trondhjemite bodies, it is necessary to consider the possibility that the basaltic komatiite parent for each of the two types may have had somewhat differing trace element contents. Parent 1, below is typically representative of the trace element content of a Barberton-type basaltic komatiite that may, conceivably, have been slightly altered or contaminated prior to melting (after the data of Herrmann et al., 1976 and Glikson, 1979b). Parent 2 is a possibly more pristine basalt that contains less Rb, Sr and Ba than Parent 1:-

Parent 1	Rb - 10 ppm	Parent 2	Rb - 7 ppm
	Sr - 150 ppm		Sr - 70 ppm
	Ba - 20 ppm		Ba - 10 ppm

Using the batch melt equations of Shaw (1970) curves representing consecutive increments of partial melt from the two above parental compositions can be calculated. These are plotted in Figure 88a and b, together with the relevant averaged data from Table 36. In both the Rb v Ba

---

(*) Footnote: The bulk partition coefficients for a dominantly amphibolitic residue are subject to some uncertainty with respect to Rb, Sr and Ba. The partition coefficients used in this calculation are those of Condie and Hunter (1976), with the exception of the value for Sr. The K_D value for the latter can be derived either by assuming a small proportion of plagioclase in the residue (which will not markedly affect the values for Rb and Ba) or by using the partition coefficient for Sr as summarized by Arth (1976). The Arth (1976) values for Sr into hornblende (i.e. in basaltic rocks) are considerably higher than those used by Condie and Hunter (1976), as shown in Appendix 2; in this instance it appears that the relevant empirical concentrations of Rb and Ba favour the lower values, whereas Sr requires the higher partition coefficient.

TABLE 37

CHEMICAL ANALYSES OF SAMPLES FROM THE BATAVIA CELL

		1	2	3
		BT10(A)	BT19	BT32
Wt.%	SiO_2	71,99	69,71	72,11
	TiO_2	0,18	0,27	0,21
	Al_2O_3	15,33	15,71	15,47
	Fe_2O_3*	1,68	2,49	2,24
	MnO	0,01	0,01	0,01
	MgO	0,35	0,70	0,57
	CaO	1,77	2,85	2,48
	Na_2O	5,26	5,36	4,20
	K_2O	2,12	1,06	2,22
	P_2O_5	0,05	0,06	0,07
	L.O.I.	0,57	0,51	0,53
	TOTALS	99,31	98,73	100,11
ppm	Rb	40	30	61
	Sr	390	450	163
	Ba	195	67	236
	La	12,4	-	-
	Ce	19,9	-	-
	Nd	8,6	-	-
	Sm	2,03	-	-
	Eu	0,58	-	-
	Tb	0,41	-	-
	Yb	0,79	-	-
	Lu	0,08	-	-

(Analyst : L.J. Robb

Fe_2O_3* - Total iron as Fe_2O_3)

and Rb v Sr model diagrams, it is seen that the trace element content of the majority of the tonalite-trondhjemite bodies can be reasonably well accounted for by ≈ 20-30% partial melting of a "Parent 1" type basaltic komatiite. The degree of partial melting to form the required trace element concentrations is in accord with the petrologic mixing considerations discussed above. Likewise, the low Sr (i.e. high Rb/Sr) suite can apparently be accommodated for by melting of the "Parent 2" type basalt. The model curves in Figure 88a and b suggest a lower degree of partial melting for the latter but this is merely a function of the Rb content of this arbitrarily chosen parent. It should also be stressed that the fit of model to empirical trends in this diagram requires a broad outlook to the data and can only be viewed in a semi-quantitative perspective.

It is evident from Figure 88, however, that the four-fold variation in Sr content of the tonalites and trondhjemites (Figure 85) cannot simply be accounted for by differences in the degree of partial melting, particularly as the model trends indicate that the compatible elements (i.e. Sr and Ba with $K_D > 1$ in the melt phase) remain relatively constant during the early stages of anatexis. The question also arises as to whether it is realistic to explain the lower Sr content and higher Rb/Sr ratio of the second suite of rocks, by merely considering the parent of the latter to have been relatively depleted in certain of the large-ion lithophile (LIL) elements. With regards, at least to the AGC in Swaziland, suggestions have been made that minor granulite facies remnants are preserved in this area (Hunter, 1974) whilst, on the basis of structural arguments, Jackson (1979) has argued that the Dwalile Metamorphic Suite (the greenstone component of the AGC) is preserved at a much lower crustal level than its time equivalents in the Onverwacht Group. Hunter et al. (1978) have also stated that the AGC includes the most highly metamorphosed portions of the Archaean basement in the eastern Transvaal. These considerations suggest that certain of the tonalite-trondhjemite kindred in the region may have been derived from a higher-grade, possibly granulite facies, environment where depletions of LIL elements (such as U, Th, Rb and Cs) are known to occur. By comparison, the remainder of the tonalite-trondhjemite bodies may have originated in an amphibolite facies environment where such depletions are not present. The following discussion considers whether it is feasible for these general observations to account for the

origin of the high Rb/Sr tonalites and trondhjemites in terms of granulite facies parental material that is characteristically depleted in Sr.

A considerable amount of data is available on the geochemical characteristics of granulite facies terranes (Heier, 1964, 1973; Lambert and Heier, 1967, 1968; Tarney, 1976). This work has shown that granulitic rocks occupying the lower portions of the crust have lower Rb/Sr and initial $^{87}Sr/^{86}Sr$ ratios but higher K/Rb ratios than broadly similar rocks located in the upper portions of the crust (i.e. < 10-15 km depth). It is argued that Rb becomes depleted with respect to Sr in these high P-T environments because of widespread melting of K-felspar and hydrous, near-solidus mineral phases such as the micas. As Rb is concentrated preferentially into these phases it is conceivable that depletion of most of the incompatible LIL elements will take place under these conditions, where the presence of a fluid (hydrous) phase will facilitate partial melt processes. The means for fractionating ^{87}Sr with respect to ^{86}Sr is also explainable in these terms as the strontium daughter isotope will most likely occupy lattice sites formerly occupied by its rubidium parent and, hence, be mobilized together with it. However, the case for Sr, which is not a typically LIL element, is different and the geochemical data on granulitic rocks does not uphold as realistic the suggestion that the low Sr, high Rb/Sr suite can be simply derived from an apparently depleted parent which may have had granulitic affinities. In fact Tarney (1976) has stated specifically that "..... Ba, Sr and Zr ..... are notably enriched in granulites" whilst Heier (1964) has mentioned that, "No case can be made for a corresponding decrease in Sr with metamorphism and it should be expected that Rb/Sr ratios decrease in rocks undergoing metamorphism". Consequently the suggested derivation of the AGC and Doornhoek/Eerstehoek plutons by partial melting of a Sr-depleted mafic precursor would not appear to be compatible with the geochemical characteristics of the granulite facies environment from which this material was considered to have been derived. An alternative explanation, therefore, is required, but one which is, nevertheless, constrained by the fact that both suites are probably derived by equivalent degrees of partial melting from a basaltic parent of broadly similar major element composition..

One further point is that the low Sr and high Rb/Sr characteristics of the AGC and Doornhoek/Eerstehoek plutons are not unique to Archaean

"grey gneiss" (tonalite-trondhjemite) terranes. The 3,6 b.y. old Uivak gneisses in Labrador are generally characterized by Rb/Sr ratios > 0,1 (Bridgwater and Collerson, 1976) whilst their age equivalents in west Greenland, the Amitsoq gneisses, are also characterized by a range of Rb/Sr between ≡ 0,1 and ≡ 0,6 (Lambert and Holland, 1976). An explanation of high Rb/Sr ratios in the Barberton region may also, therefore, be relevant to certain Archaean tonalite and trondhjemite gneisses in other parts of the world.

It is felt that the solution to the problem arising out of these discrepancies may lie in a consideration of differences in the depth of melting of these various rocks. Such differences may result in a change in the nature of residual phases that are generated by the partial melting process. As the bulk distribution coefficient of the residue is the most important factor affecting the concentration of a given element in the melt relative to its parent, these considerations may prove more fruitful than those depending on assessments of the bulk parental composition. In this light it is instructive, therefore, to consider the phase transitions experienced by basalts undergoing an increase in pressure and temperature. At pressures in excess of 16 kb a rock with a primary gabbroic mineralogy will undergo an isochemical phase transition along the lines of the following equation :-

1. $\underset{\text{enstatite-ferrosilite}}{4(Mg,Fe)SiO_3} + \underset{\text{anorthite}}{CaAl_2Si_2O_8} \rightleftharpoons \underset{\text{almandine-pyrope}}{(Mg,Fe)_3Al_2Si_3O_{12}} + \underset{\text{diopside}}{Ca(Mg,Fe)Si_2O_6} + \underset{\text{quartz}}{SiO_2}$

(after Green and Ringwood, 1967)

The assemblage on the right-hand side of the above equation is that characteristic of high pressure granulites (i.e. eclogites) and describes the nature of the phase changes involved in the progressive metamorphism of a primary gabbroic assemblage. If, however, the parental basalts have been retrogressed to a dominantly amphibolitic mineralogy, as is commonly the case in Archaean terranes, then a different situation applies. Helz (1973) and Wyllie et al. (1976) have shown that for both basaltic and tonalitic/andesitic compositions at temperatures greater than ≡ 1 000°C, hornblende is not stable even in the presence of excess H_2O. The breakdown of hornblende under relatively high pressures may, therefore, take place according to the following reaction :-

2. $\underset{\text{hornblende}}{4(Na_{0,5}Ca_2Mg_4Al_{2,5}Si_{7,5}O_{22}(OH)_2)} \rightarrow \underset{\text{garnet}}{4CaMg_2Al_2Si_3O_{12}} + \underset{\text{diopside}}{4CaMgSi_2O_6}$ (+ minor jadeite olivine and H_2O)

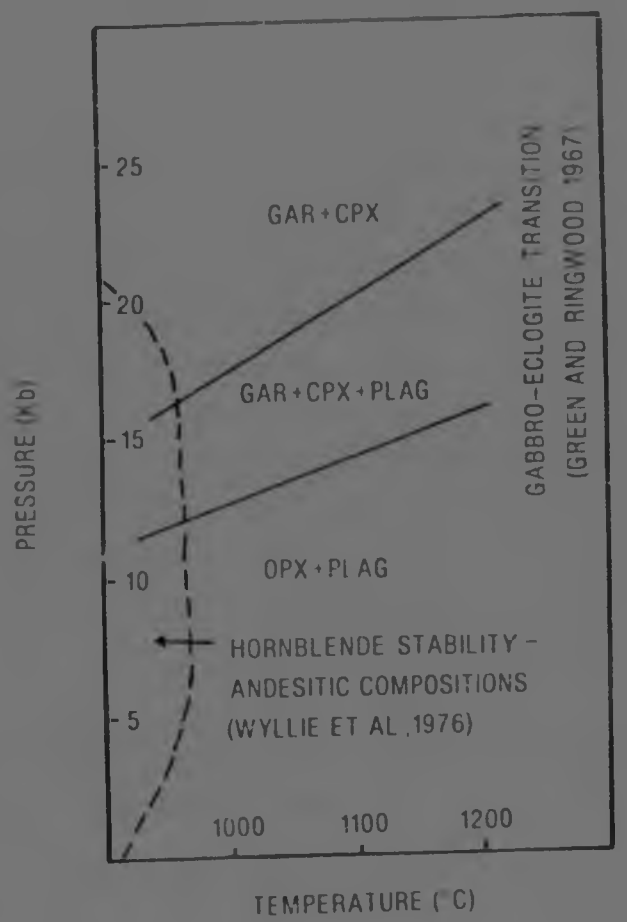

Figure 89 : Diagram showing the approximate pressures and temperatures involved in the gabbro-eclogite transition as well as the upper limit of the hornblende stability field for andesitic compositions.

This reaction, which is also derived from the experimental study by Green and Ringwood (1967) indicates that eclogite would probably be the stable mineral assemblage in dry basaltic rock at the base of a 35 km thick crust under conditions of a normal geothermal gradient. The pressure and temperature conditions involved in the gabbro-eclogite transition and in the breakdown of hornblende are shown in Figure 89. It is evident from this diagram that a basalt consisting dominantly of hornblende, together with minor plagioclase and quartz, will start undergoing a phase transition in an intermediate-to-high pressure granulite facies environment (i.e. at pressures > 12 kb and temperatures > 900°C). The nature of this transition is probably quite complex as between 10-15 kb the reactions provided above will probably not go to completion. As a result, the first appearance of garnet and the last disappearance of plagioclase takes place over a range of ≅ 5 kb, depending on the temperatures involved (Figure 89). Garnet ⇄ plagioclase equilibrium is also likely to be affected by the breakdown of both hornblende and plagioclase together, to form the garnet molecule.

With the above considerations in mind, the possible effects of high P-T mineral assemblages as residual phases during the partial melting of a basaltic parent to form tonalitic-trondhjemitic magmas may be considered. In order that this situation can be modelled with respect to the distribution of Rb, Sr and Ba, it is first necessary to consider what proportions these phases would occur in, after the isochemical transformation of amphibolitic meta-basalt to an eclogitic mineralogy. Previous considerations regarding the petrogenesis of tonalites-trondhjemites used an amphibolite with a Barberton-type basaltic komatiite composition as the likely parental material. It is necessary, therefore, to consider what proportions of diopside, jadeite and garnet (i.e. the main constituents on the right-hand side of equation 2 above) are likely to form from a basaltic composition of this nature, whose main characteristics are a low TiO_2 content, a relatively high MgO content and a high CaO/Al_2O_3 ratio. This can be achieved using the petrologic mixing programme of Wright and Doherty (1970) and the results of this procedure are provided in Table 38. This data shows that the proportions of clinopyroxene: garnet that are likely to form from a Barberton-type basaltic komatiite (Row 1, Table 38) are approximately in the ratio 6:1, whereas in the case of the Badplaas-type basaltic komatiite, where alumina contents are considerably lower (Row 2, Table 38), the proportion of clinopyroxene:garnet is higher, being

TABLE 38

PROPORTIONS OF TYPICAL ECLOGITIC MINERAL PHASES LIKELY TO FORM FROM BASALTIC KOMATIITE COMPOSITIONS

	SiO_2	TiO_2	Al_2O_3	Fe_2O_3*	MnO	MgO	CaO	Na_2O	K_2O	PROPORTIONS (1)		PROPORTIONS (2)	
1.	52,70	0,90	9,80	10,90	0,22	10,10	10,00	1,65	0,40				
2.	52,22	0,56	5,42	9,90	0,22	15,25	12,83	1,20	0,10				
3. (CPX)	52,00	0,20	2,00	9,00	0,40	14,00	21,00	0,50	0,10	56,4%	85,2%	79,0%	93,1%
4. (JADEITE)	60,00	0,10	25,00	0,50	0,00	0,20	0,10	13,00	0,20	28,8%		14,1%	
5. (GARNET)	40,50	1,50	22,70	16,60	0,50	12,40	15,80	0,30	0,10	14,8%		6,9%	

Fe_2O_3* - Total iron content of rock or mineral presented as Fe_2O_3

Row : 1. Representative Barberton-type basaltic komatiite } on the basis of data from
2. Representative Badplaas-type basaltic komatiite } Viljoen and Viljoen (1969c).

3 - 5. Representative analyses of typical eclogitic mineral phases; clinopyroxene (cpx) is taken from microprobe analyses of amphibolitic meta-basalts from the study area (Table 26, Chapter 4); jadeite is from Deer, Howie and Zussman (1971); and garnet is from a coexisting garnet-clinopyroxene pair in equilibrium with a tholeiitic melt at 1100°C and 20 kb (Raheim and Green, 1974).

PROPORTIONS (1) - are the proportions of Rows 3 - 5 that best combine to form the analysis in Row 1.

PROPORTIONS (2) - are the proportions of Rows 3 - 5 that best combine to form the analysis in Row 2.

(NOTE: Sum squares of errors in the above calculations are high because of the arbitary nature of the three eclogitic phases chosen, in the absence of clinopyroxene and garnet analyses in equilibrium with a komatiitic melt, realistic compositions are not available).

approximately in the ratio 13:1. These ratios are particularly significant in a partial melt situation, especially when the relevant reactions have not gone to completion, as they imply that if the relevant minerals are consumed at an equal rate during partial melting, then little or no garnet will remain in the residue. For example, if the parental basaltic granulite originally contained only 15% garnet, then, after approximately 30% melting of equal proportions of quartz + garnet + pyroxene (i.e. in a quartz-eclogite), as little as 5% garnet may remain in the residue. Bulk partition coefficients will, therefore, be calculated virtually in terms of clinopyroxene alone, and this may substantially alter the trace element characteristics of the melt, particularly with regard to the heavy rare-earth elements (see later).

It is interesting to note that the existence of upper mantle rocks with considerably more clinopyroxene than garnet have been suggested previously and that partial melting of such material has been used to explain the high CaO/Al_2O_3 ratios in Archaean komatiites (Cawthorn and Strong, 1974). These authors suggested that a, once, chemically-layered upper mantle exhibited an inverse relationship between clinopyroxene and garnet content, with clinopyroxene more abundant at shallower depths. The variable CaO/Al_2O_3 ratios in komatiites was, therefore, envisaged as being the result of partial melting at variable, yet shallow, mantle depths, with secular decreases in geothermal gradient causing the notable absence of komatiites in younger periods of earth history.

The following section considers the effect on the Rb, Sr and Ba content of tonalitic-trondhjemitic melts generated in the presence of a dominantly clinopyroxene (+ garnet) residue, rather than an amphibolitic residue, as was considered earlier. In the preceeding discussion low values for the partition coefficient of Rb and Ba into hornblende were used, these being similar to the values selected in the petrogenetic models of Condie and Hunter (1976). In the compilation of partition coefficients provided in the appendix, it is evident that the partition coefficients for Rb and Ba into clinopyroxene are similarly low and, hence, it is to be expected that Rb and Ba concentrations in partial melts will remain relatively unaffected by their generation in the presence of either amphibolitic or pyroxenitic residues. The case for Sr, however, is different and concentrations of this element in partial melts may differ depending on whether prevailing pressure and temperature conditions

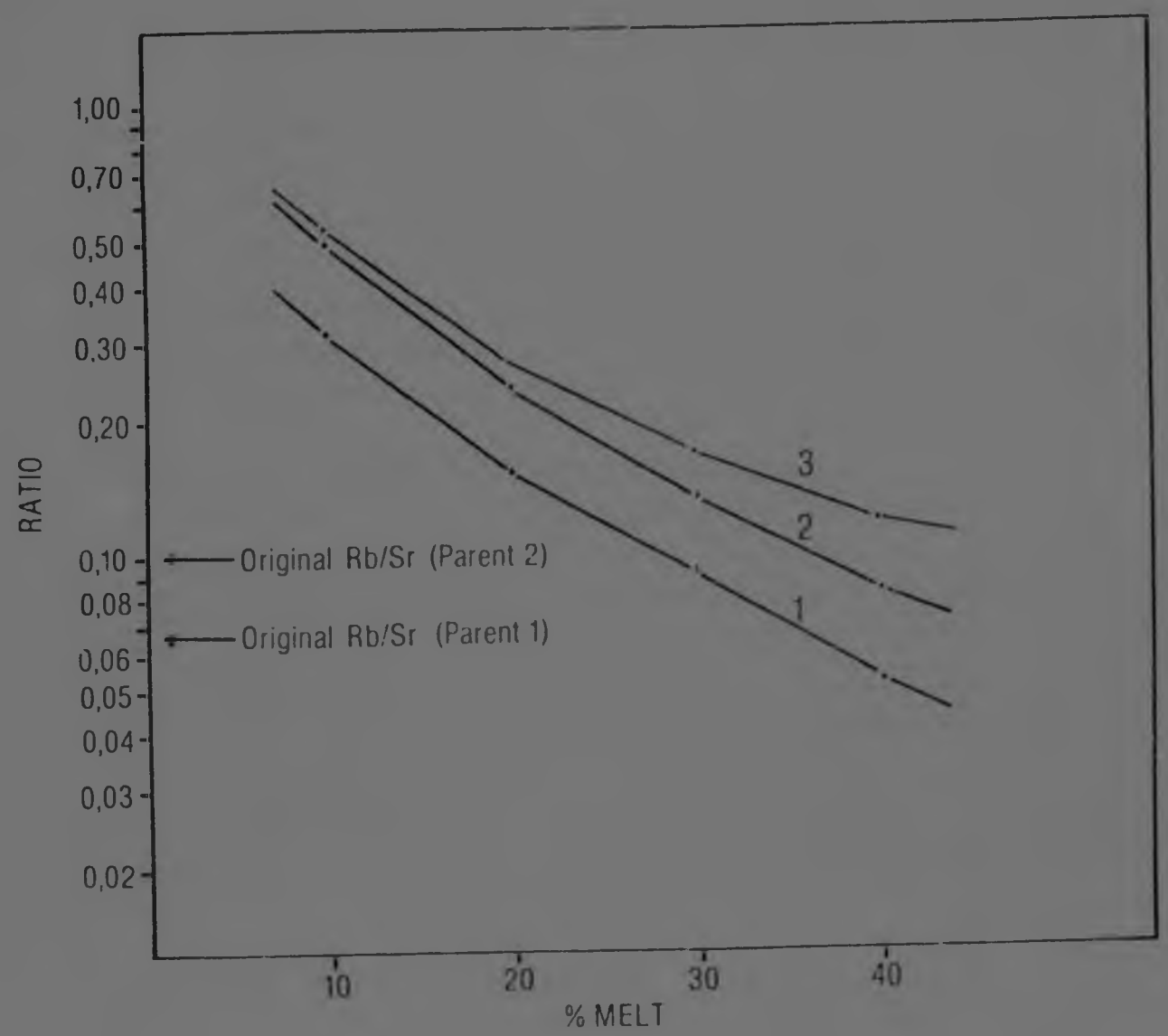

Figure 90 : Model diagram showing the change in Rb/Sr ratio with successive partial melt increments calculated using the batch melt equations of Shaw (1970). Curves 1 and 2 represent the Rb/Sr ratios for Parent 1 and Parent 2 respectively as calculated for the model in Figure 89. Curve 3 represents the Rb/Sr ratios for Parent 1, but recalculated in terms of a dominantly clinopyroxenitic residue where $D_{Sr}^{cpx} > D_{Sr}^{hblde}$

suggest equilibration with a pyroxenitic or amphibolitic residue. In the previous model where a dominantly amphibolitic residue was being considered, the bulk partition coefficient of Sr was calculated at 0,45. It was argued that this value could either be derived by using the commonly quoted partition coefficient (Arth, 1976) or by using the values quoted by Condie and Hunter (1976) and assuming a small proportion (< 10%) of plagioclase in the residue. As such, the value is high (particularly if there is no plagioclase considered in the residue) suggesting that the values of Sr in the tonalitic-trondhjemitic melt for the amphibolitic model may even be *higher* than those shown in Figure 88. Significant variations in the partition coefficient of Sr into clinopyroxene are also known to occur and Philpotts and Schnetzler (1970) have reported values ranging between 0,10 and 0,43. Sun et al. (1974) have demonstrated that the distribution of Sr into clinopyroxene is strongly temperature dependent such that partition coefficients increase with decreasing temperature. These data shows that :

$$D_{Sr}^{cpx} \text{ at } \simeq 1\,160°C = 0{,}165$$

$$D_{Sr}^{cpx} \text{ at } \simeq 1\,130°C = 0{,}301$$

By extrapolation of Figure 36 in Sun et al. (1974) to lower temperatures,

$$D_{Sr}^{cpx} \text{ at } \simeq 1\,100°C = 0{,}670$$

It is to be expected, therefore, that, in the temperature range envisaged for the onset of granulite-facies metamorphism, the partition coefficients for Sr into clinopyroxene will attain their maximum possible values, possibly in the range 0,7 or greater. This value is, in fact, similar to the partition coefficient for Sr into clinopyroxene used by Condie and Hunter (1976). In this light it is quite likely, therefore, that under the conditions relevant to the argument, an assemblage consisting dominantly of clinopyroxene will have a higher bulk partition coefficient with respect to Sr than one consisting dominantly of an amphibole. As a result, melt compositions generated in the presence of a clinopyroxenitic residue will have lower Sr contents than those that equilibrated with hornblende. In Figure 90 the Rb/Sr ratios of 10-40% partial melts derived (from a basaltic composition) in the presence of a pyroxenitic residue are compared with the previously derived Rb/Sr ratios

where an amphibolitic residue was considered. The diagram was calculated using a bulk partition coefficient for Sr in the parent of 0,7 as compared to the value of 0,45 used previously; the concentrations of Rb in the melt were considered unchanged for the pyroxenitic model. This diagram shows that, in the light of the above considerations, 20-30% partial melting of a granulitic basalt assemblage will yield Rb/Sr ratios in the range 0,2 to 0,32. By comparison, the same degree of partial melting of an amphibolitic basalt assemblage will yield Rb/Sr ratios in the range 0,09 to 0,15. These values correspond with Rb/Sr in the AGC and Doornhoek/Eerstehoek plutons in the former case and with Rb/Sr in the remainder of the tonalitic-trondhjemitic bodies in the latter case (see Table 36). The consideration of a clinopyroxenitic as opposed to hornblende-bearing residue during the generation of a tonalitic-trondhjemitic partial melt, may also account, at least to some extent, for the observed variations in Sr content illustrated in Figure 85. The model diagram in Figure 90 also shows that melting of the inferred Rb, Sr and Ba depleted parent (i.e. Parent 2) in the previous discussion will not produce Rb/Sr ratios in the range 0,3 to 0,4 for 20-30% partial melts, as is required for the high Rb/Sr tonalite-trondhjemite suites.

The above discussion provides a possible means for explaining the variable Rb/Sr ratios in tonalitic-trondhjemitic rocks in the Barberton and Swaziland regions. Considerations along these lines obviate the need to genetically distinguish the major component of the Ancient Gneiss Complex from similar rocks in the Barberton region, and supports the contention of Robb and Anhaeusser (1979) that the two areas can be more profitably regarded as being similar, rather than divergent in origin. The argument presented above is, however, largely dependent on the relative values of partition coefficients of Sr into clinopyroxene and hornblende. Precise data on these values is not available because of the dependence of these partition coefficients on temperature *and* the bulk composition of the parental rock (Sun et al., 1974). In order to be at all viable, these considerations would, therefore, require support from other sources and the following sections examine the rare-earth element contents of the tonalitic-trondhjemitic rocks in question, as well as considering the likely effects on the bulk composition of melts so derived.

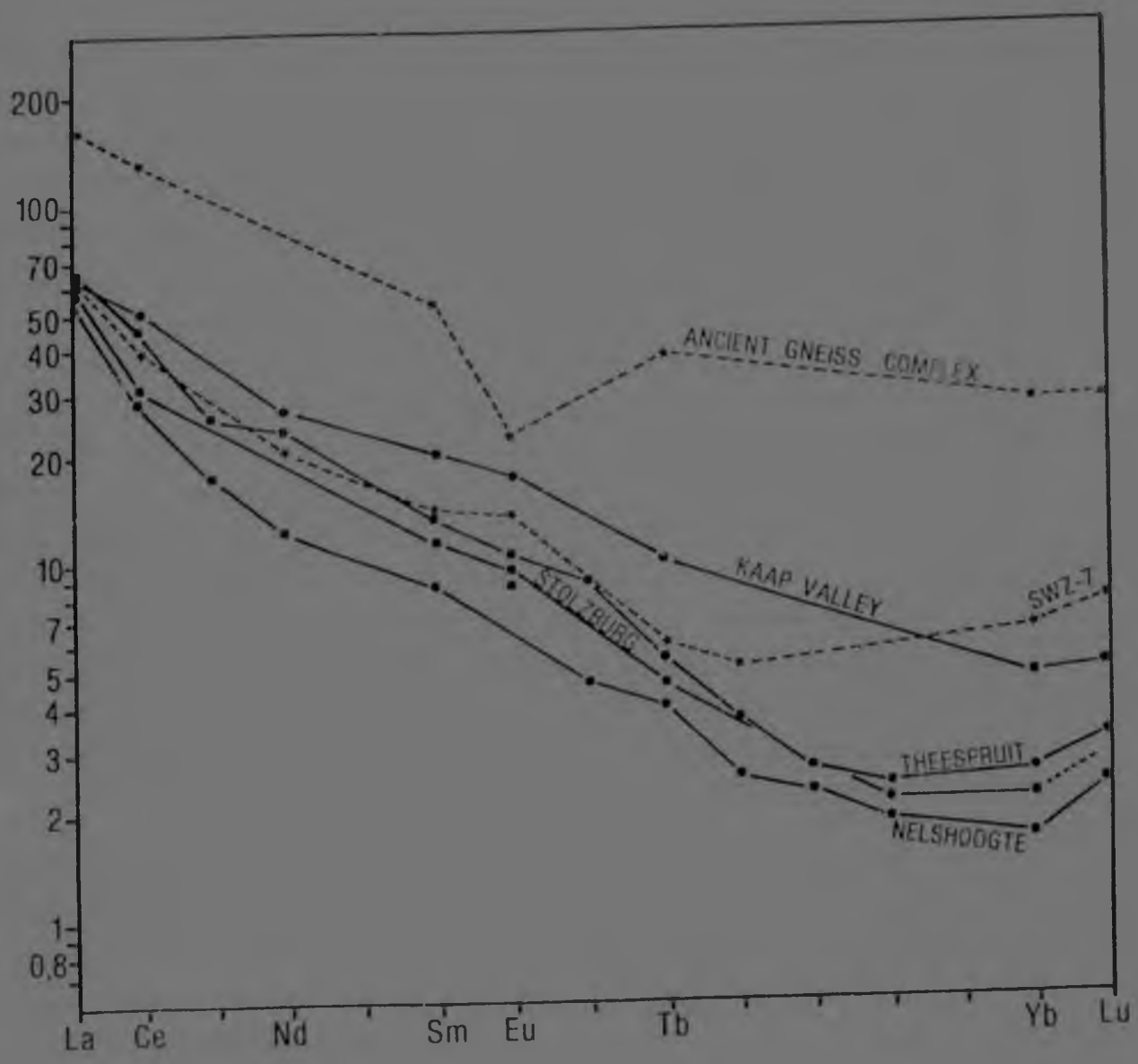

Figure 91 : Chondrite normalized rare-earth element plots of the four largest tonalite-trondhjemite plutons in the Barberton Mountain Land (from the data presented in Table 39). Also plotted (in dashed lines) are data representative of siliceous gneisses from the Ancient Gneiss Complex in Swaziland. Sample SWZ-7 is one such gneiss that has the LREE characteristics of the tonalite-trondhjemite plutons but is HREE enriched with respect to the latter. The AGC data and its source, is also presented in Table 39.

3.2. Rare-earth elements (REE)

Unlike the situation for Rb, Sr and Ba, rare-earth element analyses are not available over all twelve of the tonalite-trondhjemite bodies being studied. A number of tonalite and trondhjemite gneisses were analysed for REE in the study on migmatites (see Chapter 2) but these are not always characteristic or representative of the plutons or cells with which they are associated. Discarding this set of data, representative (average) REE analyses are, nevertheless, available for the four largest tonalite-trondhjemite plutons in the area southwest of the Barberton greenstone belt, namely the Theespruit, Stolzburg, Nelshoogte and Kaap Valley plutons. These data, together with two analyses representative of gneisses from the AGC in Swaziland, are presented in Table 39, as well as in chondrite-normalized form in Figure 91.

The REE plot in Figure 91 shows that the tonalite-trondhjemite plutons in the Barberton region all exhibit similar chondrite-normalized traces and are characterized by moderate LREE enrichment, significant HREE depletion (only slightly enriched relative to chondrites), Ce_N/Yb_N ratios of approximately 20 and no significant Eu anomaly. By contrast the plots representative of the AGC are more enriched in the LREE, have greater ΣREE contents(with relatively undepleted HREE concentrations) and Ce_N/Yb_N ratios of approximately 5, on average. Similarly contrasting patterns have been described from the Amitsoq gneisses in West Greenland where two distinct fields, with similar characteristics to those mentioned above, occur (O'nions and Pankhurst, 1978). Two questions require consideration with respect to the differences observed in the present study; firstly, is the normal rare-earth element pattern for the tonalite-trondhjemite bodies compatible with an origin by partial melting of amphibolitic meta-basalt as suggested by Barker and Arth (1976) and Arth and Barker (1976) and, secondly, is the different REE pattern for the AGC a function of tonalitic-trondhjemitic melts equilibrating with clinopyroxene rather than hornblende, as discussed above.

The first question can be tested by using the standard petrogenetic modelling techniques used above. The following set of parameters applies in this particular case :-

TABLE 39

REPRESENTATIVE RARE-EARTH ELEMENT ANALYSES FROM THE TONALITE-TRONDHJEMITE BODIES IN THE BARBERTON REGION AND FROM SILICEOUS GNEISSES IN THE ANCIENT GNEISS COMPLEX, SWAZILAND

		1	2	3	4	5	6
ppm	La	17,1	14,2	16,0	15,2	41,0	15,4
	Ce	28,9	18,3	20,0	31,7	84,0	25,4
	Pr	2,5	1,7	-	-	-	-
	Nd	11,1	5,9	-	12,4	-	9,8
	Sm	2,07	1,33	1,80	3,07	8,20	2,10
	Eu	0,61	0,50	0,56	0,99	1,30	0,79
	Gd	1,78	0,93	-	-	-	-
	Tb	0,20	0,15	0,16	0,37	1,40	0,22
	Dy	0,92	0,63	-	-	-	1,30
	Ho	0,15	0,13	-	-	-	-
	Er	0,39	0,31	-	-	-	-
	Yb	0,42	0,27	0,36	0,77	4,50	1,06
	Lu	0,08	0,06	-	0,12	0,70	0,19

Columns : 1 - Average of 5 analyses from the Theespruit pluton, after Condie and Hunter (1976), Glikson (1976a) and Hunter et al. (1978).

2 - Average of 4 analyses from the Nelshoogte pluton, after Condie and Hunter (1976) and Glikson (1976a).

3 - Average of 2 analyses from the Stolzburg pluton, after Condie and Hunter (1976).

4 - Average of 18 analyses from the Kaap Valley pluton, from Table 22.

5 - Average of 6 analyses from the Ancient Gneiss Complex, after Condie and Hunter (1976).

6 - Siliceous gneiss (SWZ-7), from the bimodal suite of the Ancient Gneiss Complex, with LREE enrichment typical of tonalite-trondhjemite gneisses from categories 1 - 4 above, after Hunter et al. (1978).

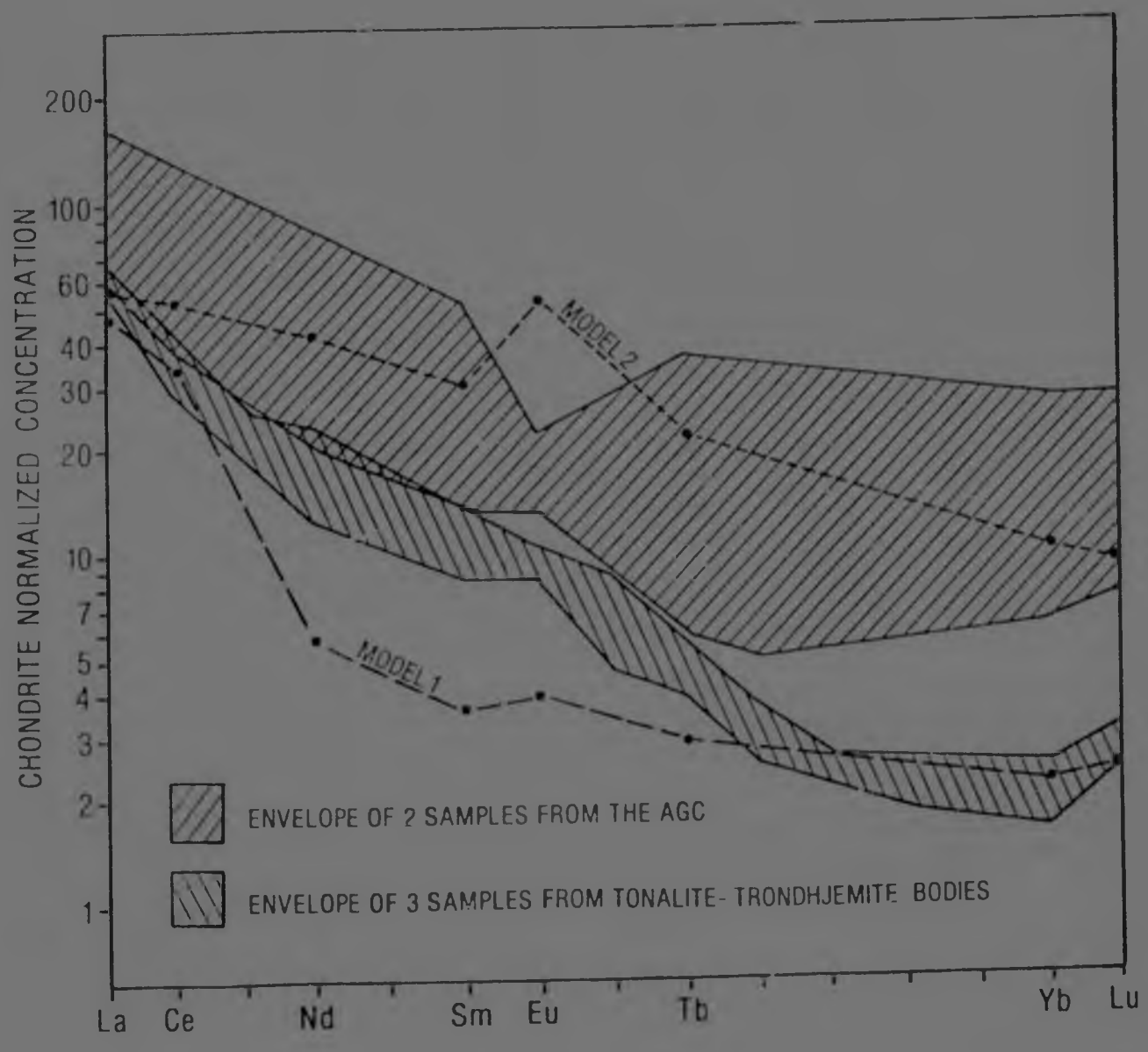

Figure 92 : Chondrite normalized rare-earth element model plots for tonalite-trondhjemite plutons from the Barberton Mountain Land and for siliceous gneisses of the AGC in Swaziland. Model 1 is the REE pattern for a 25% partial melt of an amphibolite with a Barberton-type basaltic komatiite composition; Model 2 is the pattern for the same degree of partial melt from a similar parent, but envisages a dominantly clinopyroxenitic residue. Data envelopes are taken from Figure 91.

Trondhjemitic modal proportions - same as those used in the case of Rb, Sr and Ba modelling.

	La	Ce	Nd	Sm	Eu	Tb	Yb	Lu
K_D	0,18	0,20	0,15	0,10	1,09	0,05	0,07	0,05

Basaltic komatiite modal proportions - same as those used in the case of Rb, Sr and Ba modelling

	La	Ce	Nd	Sm	Eu	Tb	Yb	Lu
K_D(*)	0,14	0,27	2,20	3,20	2,70	3,30	3,90	3,60

The parental REE content is that of a typical Barberton-type basaltic komatiite and concentrations are derived from the data in Chapter 2 and from Herrmann et al. (1976):

	La	Ce	Nd	Sm	Eu	Tb	Yb	Lu
ppm	4,0	10,3	6,5	1,89	0,61	0,39	1,49	0,22

Using the batch melt equation of Shaw (1970), the REE concentrations of a 25% melt from the above parental basalt are calculated as :-

	La	Ce	Nd	Sm	Eu	Tb	Yb	Lu
ppm	11,0	21,8	2,7	0,55	0,23	0,11	0,36	0,06

When plotted on the chondrite normalized plot in Figure 92 (i.e. Model 1), it is clear that the partial melting of an amphibolitic meta-basalt can result in a tonalitic or trondhjemitic magma with REE characteristics

---

(*) Footnote: The partition coefficients used in this calculation are not compiled by Arth and Hanson (1976) but are those of Arth and Barker (1976) which refer specifically to the distribution of REE's between a dacitic groundmass and phenocrystic hornblende. These values are much higher than the more commonly quoted ones and are necessary in order to adequately deplete the tonalitic-trondhjemitic melts in the HREE. A small amount of residual plagioclase will have little effect on the bulk partition coefficient of the REE's, except with respect to Eu.

similar to those actually observed. The replication of the relatively high Ce_N/Yb_N ratio (≈ 20) that characterizes these rocks is, however, dependent on partition coefficients between the REE's and a dominantly hornblende residue that are similar to those given by Arth and Barker (1976).

One can now consider the effects on the REE concentrations in melts that are derived from similar basalt compositions as above, but where slightly higher pressure and temperature conditions result in changes in the nature of residual mineralogy. As discussed previously, the onset of granulite facies metamorphism is responsible for the isochemical breakdown of hornblende to a dominantly clinopyroxene-garnet assemblage. Depending on the amount of alumina in the parental rock (which is likely to be low if komatiites are considered as the parent) then the amount of garnet in the residue (i.e. the proportion of garnet not consumed during melting) will probably be low if pyroxene and garnet are equally consumed during anatexis. As indicated in Table 38, a relatively small degree of partial melting (i.e. < 30%) of a Barberton-type basaltic komatiite will probably result in only a small amount (< 5%) of garnet remaining in the residue, whereas a similar degree of melting of a Badplaas-type basaltic komatiite will probably result in no residual garnet. Bulk partition coefficients, may, therefore, be calculated in terms of the following modal proportions:-

Clinopyroxene (including jadeite) - 95%
Garnet - 5%

	La	Ce	Nd	Sm	Eu	Tb	Yb	Lu
K_D	0,09	0,09	0,11	0,18	0,19	0,25	0,71	0,74

The above bulk partition coefficients are considerably different to those calculated in terms of a dominantly amphibolitic parent. The values for the heavy REE's are less than unity, in spite of the presence of the small amounts of garnet being considered, and if the latter mineral were not present, these values would be even smaller. Using the batch melt equations of Shaw (1970), again for a 25% melt situation, the following concentrations of the REE result from the partial melting of an identical parent to the one considered previously :-

	La	Ce	Nd	Sm	Eu	Tb	Yb	Lu
ppm	13,4	34,2	20,1	4,7	3,0	0,8	1,6	0,22

When plotted on the chondrite normalized diagram in Figure 92, it is evident that these melt concentrations (i.e. Model 2) have significantly different characteristics to those derived from the amphibolitic parent. The greater degree of LREE enrichment and the significantly lower Ce_N/Yb_N ratio are both consistent with the REE pattern of the AGC. It is interesting to note that the REE patterns of the Doornhoek pluton (which has similarly high Rb/Sr ratios to the AGC) are variable, with one analysis (i.e. DHK 30 with Rb/Sr = 1,07) having a pattern similar to the AGC (i.e. Ce_N/Yb_N = 3) and the other (i.e. DHK 13 with Rb/Sr = 0,20) having the higher Ce_N/Yb_N characteristics of the tonalite-trondhjemite bodies (Figure 81).

In summary, the considerations of trace and rare-earth element contents in tonalitic and trondhjemitic gneisses from the Barberton Mountain Land and Swaziland have indicated the presence of two distinct groups; the first has low Rb/Sr ratios (≤ 0,1) and a rare-earth element trace characterized by HREE depletion and a Ce_N/Yb_N ratio of approximately 20. In contrast, the second has higher Rb/Sr ratios (≥ 0,3-0,4) and ΣREE content but a lower Ce_N/Yb_N ratio. In terms of a partial melt model, and assuming a basaltic precursor, these trace element variations can be adequately explained in terms of equilibration of the tonalitic-trondhjemitic magma with respect to a dominantly hornblende-bearing residue in the first group and a dominantly clinopyroxenitic residue in the second. However, the limited amount of experimental work that has been carried out on the melting of dominantly clinopyroxenitic assemblages suggests that melts so-derived are *not* likely to have tonalitic or trondhjemitic bulk compositions. The following section considers this difficulty in terms of the major element compositions of the relevant phases.

3.3 Clinopyroxene residues in the partial melting of basaltic komatiite-major element considerations

In a previous section it was shown that it is feasible to generate significant quantities of tonalitic-trondhjemitic magma by the partial melting of a basaltic komatiite (Table 35); the residue from this

process was envisaged being a relatively silica-poor hornblende assemblage, the bulk composition of which was sufficiently depleted in SiO_2 to account for the acidic nature of the derived melt fractions. If, however, this residue was composed dominantly of clinopyroxene, rather than hornblende, its bulk composition could not be as silica-depleted, as residual clinopyroxenes have higher SiO_2 contents than equivalent hornblendes (Helz, 1973). In addition, partial melting of dominantly clinopyroxenitic assemblages has been shown to yield melts (albeit with a fairly large degree of melting) with the composition of mare (lunar) basalts (Huebner et al., 1973) and not tonalites or trondhjemites.

The nature of this problem is demonstrated in Table 40 where petrologic mixing considerations, similar to those presented in Table 35, are repeated, but in terms of a Kaap Valley-type partial melt in equilibrium with a dominantly clinopyroxenitic, rather than amphibolitic, residue. The least squares solution in this particular case, suggests that a 46% melt fraction would be derived, leaving behind a 54% clinopyroxene-bearing residual fraction. Besides the fact that this melt proportion is probably untenable, the mass balance solution (Column 4, Table 40) clearly indicates that the residue would be insufficiently depleted in SiO_2 and CaO to be able to realistically produce the required tonalitic melt. Thus, whereas the trace elements are compatible with the suggestions of a dominantly clinopyroxenitic residue for certain of the tonalite-trondhjemite bodies, considerations of bulk composition present significant problems to this notion.

Resolving this contradiction may lie in two possible avenues; the first is that clinopyroxene does not, in fact, form a dominant residual phase and that the high Rb/Sr and low Ce_N/Yb_N gneisses are not, therefore, genetically related to their low Rb/Sr, high Ce_N/Yb_N counterparts. The second involves a compromise situation whereby clinopyroxene exists in the residue together with another, more silica-depleted, phase such as hornblende or garnet. The first alternative is not compatible with geological or isotopic considerations which indicate that both groups of gneisses occur in very similar geological environments and appear to be derived from similar sources. Furthermore, the only significant difference between the two groups is emphasized by the AGC, which appears to be associated with a slightly higher grade metamorphic environment, a factor which is, in fact, *compatible* with the idea of having

TABLE 40

PARTIAL MELTING CONSIDERATIONS FOR THE KAAP VALLEY TONALITE IN TERMS OF A CLINOPYROXENE RESIDUE

Wt.%	1	2	3	4
SiO_2	49,00	65,50	53,96	56,64
TiO_2	1,00	0,47	0,92	0,75
Al_2O_3	3,50	15,70	10,03	9,16
Fe_2O_3*	10,00	4,30	11,16	7,35
MnO	0,50	0,07	0,23	0,30
MgO	16,00	2,40	10,34	9,68
CaO	20,00	4,20	10,24	12,65
Na_2O	0,30	5,40	2,71	2,67
K_2O	0,00	1,70	0,41	0,79

(Fe_2O_3* - Total iron as Fe_2O_3
P_2O_5 omitted from petrologic mixing assessment)

Columns :

1. Representative clinopyroxene composition (in equilibrium with a tholeiitic melt at approximately 1000°C and P_{H_2O} = 5 kb) after Helz (1973).
2. Representative analysis of the Kaap Valley tonalite from the data in Table 34.
3. Barberton-type basaltic komatiite (normalized to 100%) from the data in Table 34.
4. Least squares petrologic mixing solution for the combination of a clinopyroxenitic residue (Column 1) with a tonalitic melt (Row 2) to form a basaltic komatiite precursor (Column 3). Proportions of Column 1 and Column 2 that best combine to form Column 3 are 54:46.

a clinopyroxenitic, rather than hornblende-bearing, residue for the latter. The second alternative finds merit with respect to the hornblende option, evidence for which occurs in certain of the amphibolitic remnants found in the migmatite outcrops examined in Chapter 2. At the Theeboom outcrop, for example, the amphibolites were described as comprising approximately equal proportions of hornblende and clinopyroxene (see Table 26; where sample B6 has been analysed for both hornblende and clinopyroxene). Clearly, therefore, these two minerals may co-exist in a rock of bulk basaltic komatiite composition (see Table 2) and, as a result, both phases may well occur together in the residue derived from the partial melting of a precursor of this nature. Under conditions of progressive metamorphism it is likely that the relative proportions of clinopyroxene to hornblende in a meta-basalt will increase gradually as pressure and temperature increases and the upper stability field of hornblende (which also decreases as a function of increasing oxygen fugacity; Helz, 1973), gradually recedes. At any one time in the transition from amphibolite to granulite facies metamorphism, therefore, it is likely that clinopyroxene and hornblende will coexist (Figure 63B) and that the relative proportions will depend on the physio-chemical characteristics of the environment, as shown experimentally by Green and Ringwood (1968) and Lambert and Wyllie (1972). When such an assemblage undergoes partial melting, therefore, the residues will also consist of clinopyroxene and hornblende (i.e. of depleted composition); a sufficient amount of the former may exist in order to sufficiently deplete the melt in Sr and enrich it in the HREE, whilst the presence of silica-depleted hornblende enables the melt phases to become adequately felsic in order to comply with the tonalitic or trondhjemitic bulk composition.

In summary, therefore, it is suggested that differences in the trace element contents of the two groups of gneisses may be attributed to a *dominance* of residual clinopyroxene on the one hand, as opposed to a *dominance* of residual hornblende on the other. In reality this feature is likely to be reflected in a variable clinopyroxene/hornblende ratio which is determined by differing P-T conditions in the source environemnt. The formation of tonalitic-trondhjemitic melts in terms of these processes will, therefore, be constrained by the inability of rocks of increasing clinopyroxene/hornblende ratios either to melt at all, or to form partial melts with the required (highly siliceous) compositions.

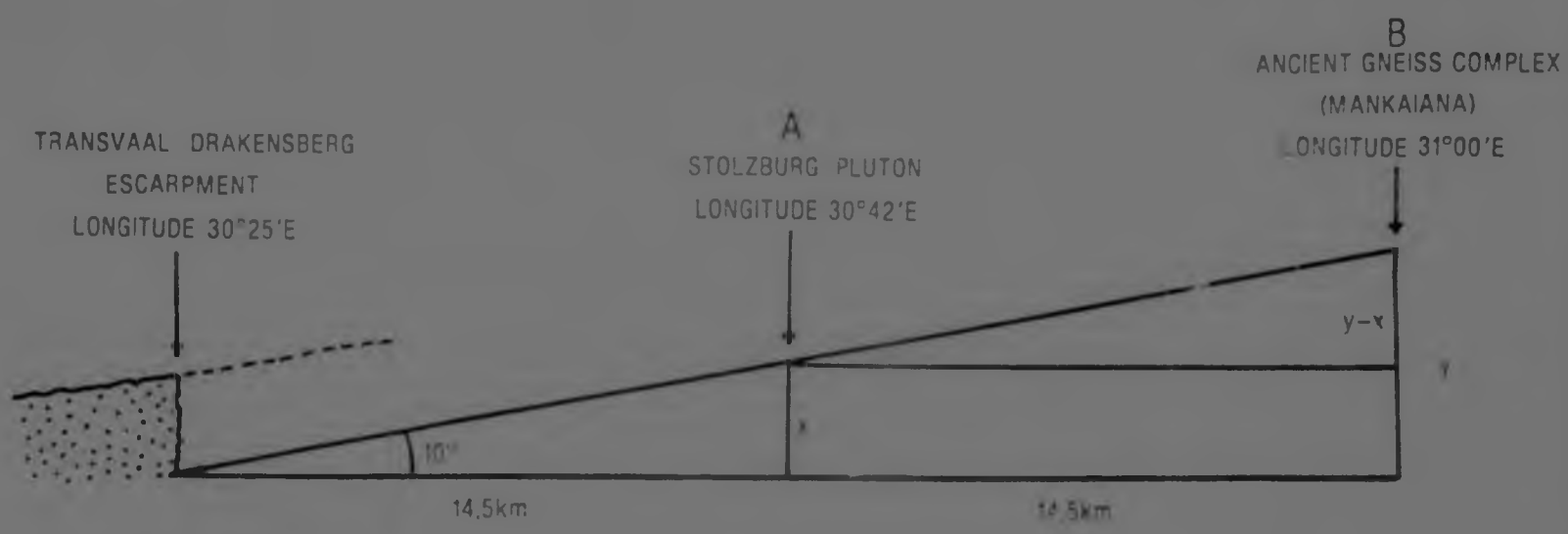

Figure 9? : *Schematic cross-sectional diagram illustrating a possible scheme for differences in crustal depth as exposed by the present erosion levels in the area southwest of the Barberton greenstone belt and Swaziland. A difference in crustal depth between point A and point B would emerge if the Archaean basement were tilted 10° to the west.*

4. CONSIDERATIONS OF CRUSTAL DEPTH IN THE ARCHAEAN TERRANE AROUND BARBERTON AND IN SWAZILAND

The above discussion on the chemical differences occurring in tonalite-trondhjemitic magmas that equilibrated with residues dominated either by amphibole or pyroxene, is presumably related to differences in the metamorphic grade of one source region as compared to the other. Little, if any, detailed metamorphi work has been undertaken in either the Barberton Mountain Land or Swaziland. In the Barberton region, however, metamorphic grades are commonly "telescoped" and are concomitant with the greenschist and amphibolite facies (Anhaeusser, 1969). No traces of granulitic assemblages have ever been detected in this area. In Swaziland, only limited observations have been made egarding the metamorphic grade of the Ancient Gneiss Complex and its supra-crustal component, the Dwalile metamorphic suite. Hunter (1971) stated that the AGC was subjected to a regional metamorphism in the higher grades of the cordierite-amphibolite facies but also referred to granulites of diopside-plagioclase-quartz assemblage. In view of the fact that amphibolites are as ubiquitous in the AGC as they are in the Barberton region, nothing definitive can be stated with regard to the metamorphic grade in either area. Detailed structural analysis in both areas is also somewhat limited but recent work carried out in Swaziland has suggested that the Dwalile metamorphic suite may have once occupied a deeper crustal level than its lithological and temporal equivalents (i.e. the Onverwacht Group) in the Barberton region (Jackson, 1979).

One possible approach to the question of different metamorphic grades in Barberton and Swaziland, however, is that related to the tilt of the Archaean basement caused by extensive and voluminous Proterozoic sedimentation. Basin tectonics and isostatic readjustments are undoubtedly responsible for a vertical component of movement in the earth's crust, the latter probably having a bearing on crustal depths with respect to present-day erosion levels. The schematic diagram in Figure 93 represents the geometrical situation that possibly exists in the eastern Transvaal with respect to basement tilt as affected by the Transvaal basin. Button (1973) has shown that (i) regional isopachs of sub-units of the Transvaal Supergroup extend considerably to the east of the basin limit defined at present by the

Transvaal Drakensberg Escarpment and (ii) the regional dip of the Transvaal basin in the eastern Transvaal is of the order of 10° to the west. It is feasible, therefore, that the Archaean basement may also be tilted regionally to the west and that, for any single horizontal datum (e.g. sea level), deeper levels of the crust are closer to the present day surface as a function of increasing eastward longitude. In Figure 93, point A corresponds to the longitude of the Stolzburg pluton (i.e. ≈ 30'42' E), whereas point B is the longitude of the Ancient Gneiss Complex in the south of Swaziland (i.e. ≈ 31°00' E). Assuming a uniform regional dip of 10° W it is seen that, with respect to a single horizontal datum represented by a plane of set altitude above sea-level, rocks exposed at Mankaiana are likely to represent a level approximately 2,6 km deeper in the crust than rocks in the region of the Stolzburg pluton. Assuming a geothermal gradient ≈ 3,0 b.y. ago, of 30-60° C/km (Collerson and Fryer, 1978) this difference could mean that rocks of the presently exposed AGC equilibrated in an environment that was 75-150 °C hotter than that envisaged for the rocks presently exposed over the Stolzburg pluton. As seen in Figure 89, such a temperature difference could be responsible for bridging the gap between the field of hornblende stability and that of incipient granulite facies metamorphism. Hence, if the tonalites and trondhjemites in the two areas have not moved great distances in the crust, then the diagram in Figure 93 may point to the fact that the source areas for the two suites were at different grades of metamorphism. Although grossly oversimplistic, a consideration such as this is based on an unquestionable regional observation and, therefore, adds credence to the petrogenetic arguments discussed in the preceding sections. A further implication of this is that below the tonalite-trondhjemite bodies to the southwest of the Barberton greenstone belt, one may well find the type of rock assemblages seen in the AGC around Mankaiana.

5. Rb-Sr ISOTOPIC CHARACTERISTICS OF THE TONALITE-TRONDHJEMITE SUITE IN THE BARBERTON REGION

A considerable amount of geochronological work has been carried out in the Barberton region and Swaziland by de Gasparis (1967), Oosthuyzen (1970), Davies (1971), and Davies and Allsopp (1976). In recent years this data has been considerably expanded, particularly with respect to the Rb-Sr

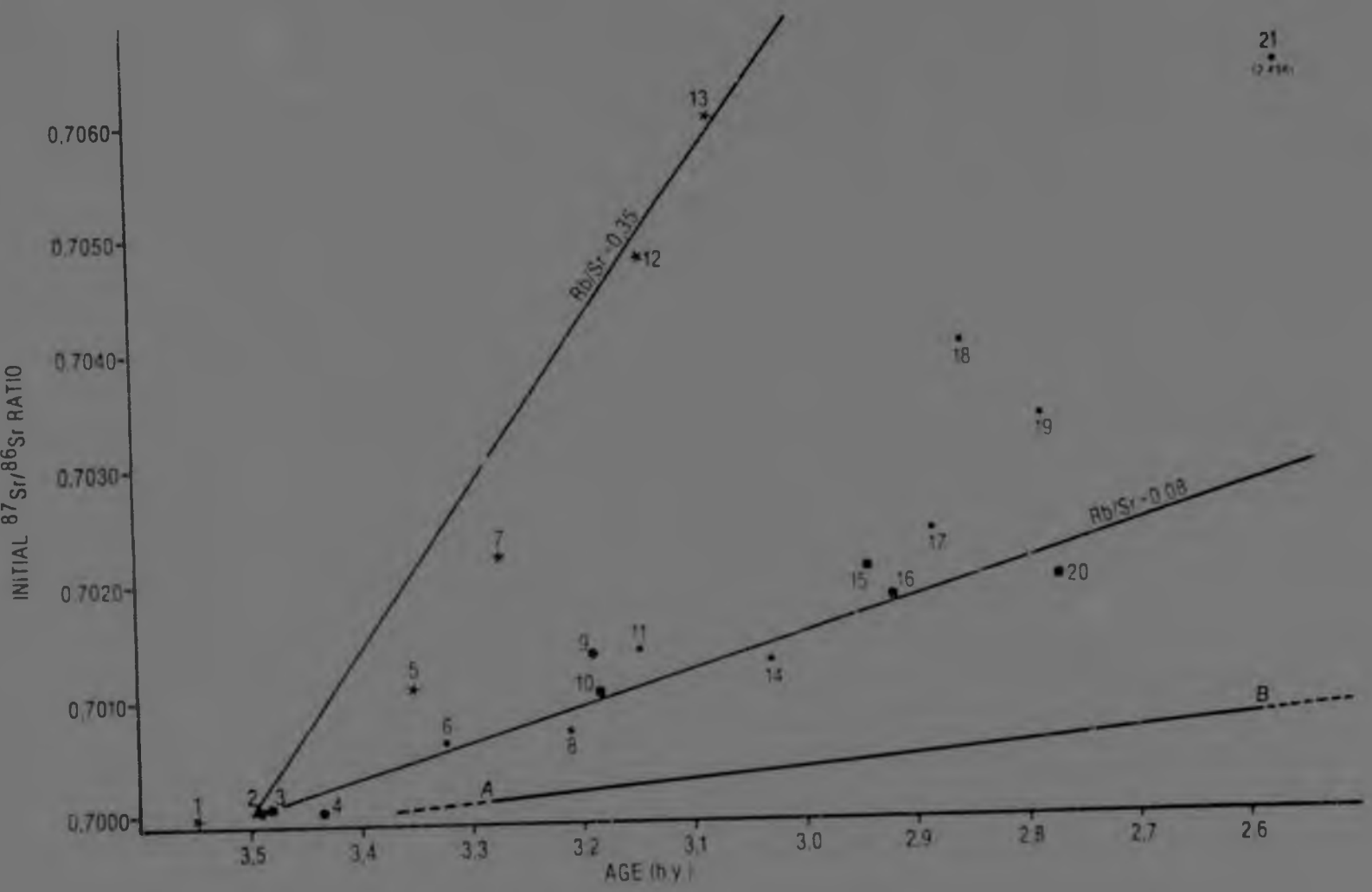

Figure 94 : Plot of initial $^{87}Sr/^{86}Sr$ ratio (R_o) against age for tonalitic and trondhjemitic gneisses from the Barberton Mountain Land and Swaziland. The sources of data are presented in Table 41 which also provides the key to the numbers of each of the plotted points. Dots represent tonalite-trondhjemite gneiss plutons or cells from the area southwest of the Barberton greenstone belt; stars, siliceous gneisses from the AGC and Granodiorite Suite in Swaziland; and asterisks, younger granitic (sensu lato) *phases. A-B represents a portion of the upper mantle growth curve (i.e. controlled by Rb/Sr = 0,02) after Moorbath (1977); the other two curves represent $^{87}Sr/^{86}Sr$ growth vectors controlled by Rb/Sr ratios of 0,08 and 0,35 respectively.*

systematics of the region, and well over 30 units in the granitic terrane alone have now been dated (Barton, 1980; Barton et al., 1981 and E. Barton, personal communication). Prior to this recent work, a number of the tonalite-trondhjemite units in the Ancient Gneiss Complex of Swaziland had been considered in terms of their Sr-isotope evolution. In a plot of initial $^{87}Sr/^{86}Sr$ ratio (R_0) against age, Davies and Allsopp (1976) identified a colinearity between various points representative of siliceous gneisses from different parts of Swaziland. This trend, which was also sub-parallel to $^{87}Sr/^{86}Sr$ growth vectors for each of the points, was interpreted as indicating that the rocks in question were genetically related in such a way that the younger units were derived by reworking (or localized partial melting) of the older ones and that the Rb/Sr ratio of these melts remained relatively constant throughout this evolutionary trend. This particular viewpoint conflicted with ideas that Moorbath (1975) had put forward stating that none of the dated gneissic units from the Archaean terranes of west Greenland and Zimbabwe had been derived from pre-existing sial, but rather from a primitive basaltic source. The recent work by Barton (1980) has added a considerable amount of data to the plot of R_0 v age used by Davies and Allsopp (1976). The new data from tonalites and trondhjemites in the Barberton region shows that the latter do not plot on the AGC trend defined by Davies and Allsopp, but define a flatter trend that itself is sub-parallel to $^{87}Sr/^{86}Sr$ growth vectors of a different magnitude to those that define the AGC trend. The following sections examine the Sr-isotopic characteristics of the tonalite-trondhjemite bodies from southwest of the Barberton greenstone belt in terms of their origin and also in terms of their possible relationship with respect to certain younger granites in the region.

5.1 Isotopic characteristics in terms of an R_0 v Age diagram

The geochronological data presently available for the tonalite-trondhjemite gneiss plutons and cells to the southwest of the Barberton greenstone belt, together with other pertinent data, are summarized in Table 41. This data is also presented diagrammatically in a plot of R_0 v age in Figure 94 and is essentially the same as that shown in Barton (1980) except that it concentrates on units from the first magmatic cycle, together with

TABLE 41

Rb-Sr WHOLE ROCK AGES AND INITIAL $^{87}Sr/^{86}Sr$ RATIOS OF SELECTED GRANITES *(SENSU LATO)* FROM THE BARBERTON REGION AND SWAZILAND

	ROCK	AGE (b.y.)	INITIAL $^{87}Sr/^{86}Sr$	SOURCE
1.	[illegible]dal Suite (AGC)	3,555	0,6999	Barton et al. (1981)
2.	Kaap Valley pluton	3,491	0,700[illegible]	" " " "
3.	[illegible]lzburg pluton	3,481	0,7002	" " " "
4.	[illegible]spruit pluton	3,432	0,7000	" " " "
5.	Granodiorite [illegible]te	3,350	0,7011	" " " "
6.	Tsawela gneiss	3,323	0,7006	Davies (1971)
7.	Banded gneiss (AGC, Pigg's Peak)	3,270	0,7022	" "
8.	Hebron granodiorite	3,211	0,7007	Barton et al. (1981)
9.	Trondhjemite gneiss (Theeboom cell)	3,186	0,7014	" " " "
10.	Nelshoogte pluton	3,180	0,7010	" " " "
11.	Nelspruit porphyritic granite	3,149	0,7014	" " " "
12.	Banded gneiss (AGC, Mankaiana)	3,138	0,7048	Davies (1971)
13.	Banded gneiss (AGC, Pigg's Peak)	3,072	0,7060	" "
14.	Nyluzi batholith (porphyritic phase)	3,028	0,7013	Barton et al. (1981)
15.	Trondhjemite gneiss (Theeboom migmatite outcrop)	2,939	0,7021	" " " "
16.	Tonalite gneiss (Weergevonden cell)	2,916	0,7018	" " " "
17.	Mliba pluton	2,879	0,7024	Davies (1971)
18.	Boesmanskop syenite	2,848	0,7040	Barton et al. (1981)
19.	[illegible]ing Moor onalite	2,784	0,7034	" " " "
20.	Trondhjemite gneiss (Batavia cell)	2,764(*)	0,7020(*)	" " " "
21.	Mpageni pluton	2,496	0,7065	de Gasparis (1967)

(*) [illegible]e of two distinct isochrons from the same rock unit.

certain younger granitic phases that are possibly genetically related to the tonalites and trondhjemites of the latter. Barton's (1980) diagram also illustrates the orientation of $^{87}Sr/^{86}Sr$ growth vectors for each of the individual points on the diagram, as calculated in terms of an average Rb/Sr ratio for the dated unit.

In Figure 94 the orientations of two $^{87}Sr/^{86}Sr$ growth vectors are plotted with respect to the points representing tonalite and trondhjemite gneisses from both the Barberton area (i.e. 2, 3, 4, 9, 10, 15, 16 and 20) and the AGC in Swaziland (i.e. points 1, 5, 7, 12 and 13). The vectors on this diagram distinguish clearly between the gneisses of the AGC and those of the Barberton area; the AGC samples define a relatively steep trend (similar to the one originally defined by Davies and Allsopp, 1976) which coincides with the $^{87}Sr/^{86}Sr$ growth vector controlled by a Rb/Sr ratio of 0,35, whereas the Barberton samples define a much flatter trend that coincides with a $^{87}Sr/^{86}Sr$ growth vector controlled by Rb/Sr = 0,08 (*). Thus, the trends defined by the isotopic characteristics of the two groups of tonalite-trondhjemite gneisses, substantiate the observations discussed previously which pointed to the different average Rb/Sr ratios (and REE patterns) in the two suites.

It is interesting to note that the AGC trend in Figure 94 has previously been regarded as largely fortuitous because the original Davies and Allsop trend was parallel to a growth vector controlled by a Rb/Sr ratio of 0,53. Hunter et al. (1978) have pointed out that the AGC has "..... Rb/Sr ratios typically 0,2-0,3 ....." and that the latter were not, therefore, in accordance with the Davies and Allsopp growth vector. However, the Davies and Allsopp data is calculated and plotted with respect to a ^{87}Rb decay constant that is different to that used by Barton (1980), and which is reflected in Figure 94. The more recent decay constant yields ages that, when recalculated, are slightly younger than those originally obtained by Davies and Allsopp (1976). Subsequently, the five AGC points in Figure 94

(*) Footnote: The calculation of the $^{87}Sr/^{86}Sr$ growth vectors plotted in Figure 94 is described in Appendix 5.

can be more accurately viewed in terms of a growth vector that is controlled by a lower Rb/Sr ratio (i.e. 0,35 as opposed to 0,53) than the one considered previously. It is argued on this basis, that the AGC trend is not a fortuitous one and corroborates the view held by Davies and Allsopp (1976) that the various units dated in the AGC are genetically related in such a way that the younger units were derived by reworking the older ones. In this light, the distinctive $^{87}Sr/^{86}Sr$ growth vector of the AGC trend is controlled by a tonalitic-trondhjemitic protolith that was itself characterized by a Rb/Sr ratio of 0,2-0,3. The generation of this high Rb/Sr protolith may well, therefore, have occurred in equilibrium with a dominantly clinopyroxenitic residual phase, as suggested in the previous sections.

In contrast to the AGC trend, the Barberton tonalites and trondhjemites (as well as the Granodiorite Suite from Swaziland, which has a low average Rb/Sr ratio, see Table 36) plot close to a $^{87}Sr/^{86}Sr$ growth vector that is controlled by a Rb/Sr ratio of 0,08 (Figure 94). In terms of the above argument, this group of gneisses may be inter-related in the same way as that envisaged for the various components of the AGC by Davies and Allsopp (1976). In this instance, however, the protolith would have been characterized by a lower Rb/Sr ratio (≅ 0,1) probably generated by partial melting of a basaltic precursor, but leaving behind a hornblende-dominated residue.

It is also pertinent to note in Figure 94, that the eight points representing the tonalite-trondhjemite gneisses of the Barberton trend exhibit a wide range of ages from ≅ 3,45 b.y. to 2,75 b.y. over a comparatively restricted range of initial $^{87}Sr/^{86}Sr$ ratios (i.e. ≅ 0,7000-0,7020). Current thinking in terms of field relationships (Anhaeusser and Robb, 1980b), however, does not envisage tonalite-trondhjemite magmatism extending significantly past ≅ 3,2 b.y. in age, as this figure marks the initial development of the potash-rich, shield-forming batholiths. As such, the younger tonalite-trondhjemite gneiss ages (i.e. < 3,2 b.y.) probably do not reflect primary ages and may have been isotopically reset. Barton (1980) has interpreted these younger gneisses, which have slightly higher values of R_O, as possibly representing remobilized units that originally formed as partial melts of oceanic crust but which were subsequently activated and emplaced at higher crustal levels. This interpretation is consistent with evidence discussed in Chapters 4 and 5 which suggested that many of the tonalite-trondhjemite plutons in the study area were diapirically emplaced into their present structural positions.

The question arises as to which of the plutons are represented by re-set ages and which have dates which reflect their actual origin in the Archaean crust. Barton (1980) has indicated that the original ages of certain plutons in the study area may be obtained by back-projecting their $^{87}Sr/^{86}Sr$ growth vectors onto the mantle growth curve. This is only valid, however, if the rock in question was derived in a single stage directly from mantle-like material and is, therefore, inapplicable to granites that originated from precursors, either with higher than mantle-like Rb/Sr ratios (i.e. a Rb/Sr ratio greater than approximately 0,02), or that had evolved along $^{87}Sr/^{86}Sr$ growth vectors with different slopes to that of the mantle. Thus, in many cases, the back projection of a $^{87}Sr/^{86}Sr$ growth vector may not result in a true reflection of the crustal prehistory of a particular rock type. Closely related to this point is the demonstration by Collerson and Fryer (1978) that certain of the best described candidates for early sialic crust are characterized by $^{87}Sr/^{86}Sr$ growth vectors, the slopes of which impose severe doubts on a realistic intersection with the upper mantle growth curve. For example, Collerson and Fryer calculated that the > 3,7 b.y. old Amitsoq gneisses of West Greenland appear to have had a crustal residence time of 410 m.y. assuming that the source of these gneisses had a Rb/Sr ratio as high as 0,1. They point out that a realistically lower Rb/Sr ratio would result in an even longer crustal residence time probably greater than that allowed in terms of the constraints imposed by the known age of the Earth. These authors argue, therefore, that crustal residence times and prehistories cannot be gauged by isotopic ratios and that ..... "Isotopic systems in general probably only become closed at the termination of widespread mantle and lower crustal degassing". As a result, it is difficult to assess quantitatively whether a tonalite pluton is characterized by a primary or re-set age although it is likely that older ages will generally reflect the former and vice versa.

The above considerations relate to two important points regarding the isotopic data pertaining to Archaean terranes. The first is that the interpretation of gneisses with low initial $^{87}Sr/^{86}Sr$ ratios as having insignificant crustal prehistories is dependent on whether, and when, isotope systems were closed. The second is that if an extensive degassing event was terminated at different times in different sections of the Archaean crust, it is likely that the maximum realistic ages obtained in any one

such area may reflect, not the true ages of the rocks, but the concomitant closure of the isotope systems. Hence, the degassing event in the circa 3,7 b.y. old Amitsoq gneisses or Limpopo mobile belt may have terminated some 200 m.y. prior to that in the Barberton Mountain Land where no ages older than approximately 3,5 b.y. have yet been obtained.

In terms of the above discussion, it is the writer's view that the wide range in apparent ages (i.e. 3,45 b.y. - 2,75 b.y.) of tonalite-trondhjemite gneisses from the region southwest of the Barberton greenstone belt, is difficult to interpret unequivocally. It is maintained that the crustal prehistories of these rocks cannot be realistically assessed and that the original ages of certain of the younger gneisses may not necessarily be determined by the back projection of isotopic growth vectors. Barton's (1980) suggestion that the gneisses have been structurally remobilized is in accordance with the views adopted in Chapters 4 and 5 that envisage diapiric emplacement of the Kaap Valley and Doornhoek plutons into the overlying greenstone successions. If, therefore, the ages obtained for the younger gneisses are not primary, it is likely that they have been reset by structural events related to the gravitational instability prevailing in the early Archaean crust (see Chapter 7).

5.2 Isotopic characteristics in terms of R_o v Rb and R_o v Sr diagrams

The plot of R_o v age (Figure 94) discussed above was shown to have a restricted petrogenetic application although two groups of tonalite and trondhjemite gneisses were distinguished on the basis of their initial $^{87}Sr/^{86}Sr$ ratios. In this diagram two broad trends occur, with the flatter of the two comprising tonalite-trondhjemite gneisses as well as certain other, younger and more potassic granite types (i.e. points 8, 11, 14, 17 and 19). A possible cogenetic relationship between the gneisses and these younger, more potassic, granitoids is suggested by the fact that they are colinear; this feature implies that the development of $^{87}Sr/^{86}Sr$ in the younger, more potassic phases was possibly governed by parental material with a Rb/Sr ratio that is similar to that characteristic of the tonalite-trondhjemite gneisses. Assessment of these possible relationships can be more instructively viewed, however, in terms of diagrams which combine the

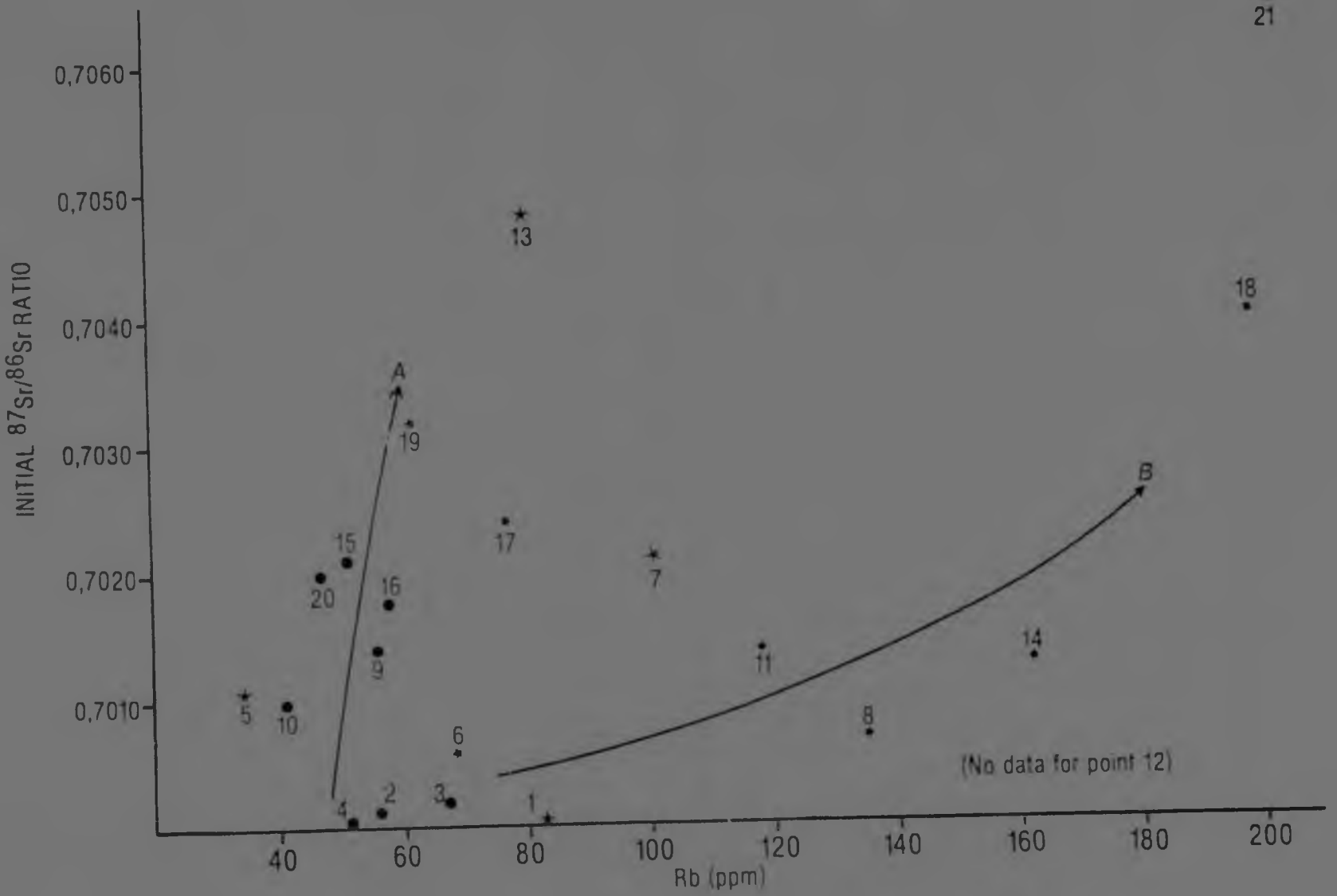

Figure 95 : Plot of initial $^{87}Sr/^{86}Sr$ ratio (R_o) against Rb for various granites (sensu lato) from the Barberton Mountain Land and Swaziland. The data is derived from Tables 30 and 41; the latter table provides the key to the numbers of each of the plotted points. Symbols are the same as those used in Figure 94. Trend A defines those rock types characterized by a limited range of Rb contents with increasing R_o, whereas trend B exhibits a wider range of Rb over the same range of R_o. No Rb and Sr data is available for point 12 (Table 41) and it is not, therefore, plotted on the diagram.

isotopic and chemical differences in each of the suites (i.e. R_O v Rb and R_O v Sr, Figures 95 and 96 respectively).

In Figures 95 and 96 the initial $^{87}Sr/^{86}Sr$ ratio is plotted against Rb and Sr respectively. In the case of the tonalite and trondhjemite gneisses from the area southwest of the Barberton greenstone belt (i.e. points 2, 3, 4, 9, 10, 15, 16 and 20), these two diagrams show differing patterns. In the R_O v Rb plot these samples exhibit a restricted range in Rb (≈ 40-60 ppm) for values of R_O ranging from 0,7000-0,7020 (Trend A, Figure 95). Clearly, this range in initial $^{87}Sr/^{86}Sr$ ratio is unlikely to be the result of variations in the degree of partial melting associated with the formation of these rocks, as this will almost certainly have produced a greater range in Rb contents (see Figure 88). In the plot of R_O v Sr, the same group of gneisses exhibit a broad, direct relationship between R_O and Sr with the latter ranging from approximately 500-800 ppm (Trend A-B, Figure 96). Because the initial $^{87}Sr/^{86}Sr$ ratios and the ages in this group of gneisses are inversely proportional (Figure 94), it is clear in Figure 96 that Sr appears to increase in concentration as individual units become progressively younger. This feature has been noted before (Anhaeusser and Robb, 1980a) but cannot be readily interpreted in a petrogenetic sense. Although systematic increases in the degree of partial melting will cause small increases in the Sr contents of these gneisses (Figure 88), this is not reflected in their Rb contents, nor is it likely that such processes will be time-dependent. The decay of ^{87}Rb to ^{87}Sr over a time span of ≈ 500 m.y. cannot possibly account for the observed increase in whole rock strontium and, likewise, the fractionation of ^{87}Sr with respect to ^{86}Sr during partial melting will not markedly affect this trend. It would appear, therefore, that the relationship between R_O and Sr in Figure 96 may, either be largely fortuitous, or related to the structural re-emplacement of certain of these bodies at higher crustal levels. Such a relationship, if real, most certainly requires additional data and more stringent evaluation than is presently available.

In the plot of R_O v Rb a clear distinction emerges between rock types of tonalitic-trondhjemitic composition and those of more potassic affinities (i.e. Trend B) with the latter being characterized by significantly higher Rb concentrations. In the R_O v Sr plot a similar distinction exists but here, the more potassic granites (*sensu lato*) are characterized by a trend

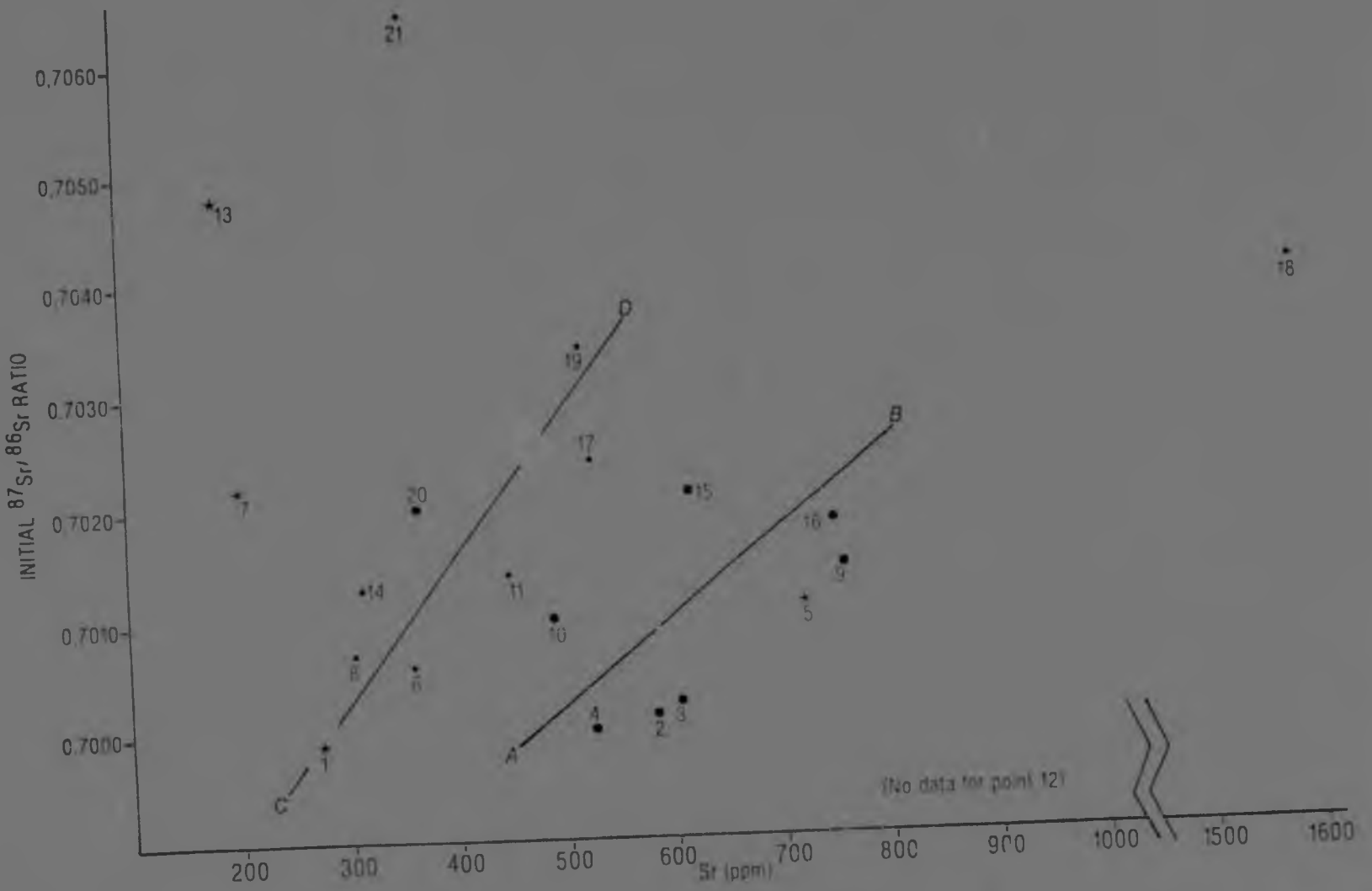

Figure 96 : *Plot of initial $^{87}Sr/^{86}Sr$ ratio (R_0) against Sr for various granites (sensu lato) from the Barberton Mountain Land and Swaziland. Data sources, sample numbering and symbols are identical to those in Figure 95. Trend A-B defines a high-Sr population that is dominated by the tonalite and trondhjemite gneisses from southwest of the Barberton greenstone belt; trend C-D defines a lower-Sr population that consists mainly of younger, potash-rich granite types.*

(i.e. C-D) of generally lower Sr contents than the tonalite-trondhjemite kindred. The notable exceptions in Figure 96, however, are certain components of the AGC which have Sr contents that are even lower than the C-D trend. These observations, together with the similar range of initial $^{87}Sr/^{86}Sr$ ratios found in both suites, suggest that the tonalite-trondhjemite gneisses in the Barberton area may form the precursors to the high-level, potash-rich batholiths found in the region. Such a relationship would assign a particularly significant role to these gneisses, not only in the initial development of sialic crust in the early Archaean, but also in the evolution of this terrane during subsequent periods.

5.3 A consideration of tonalites-trondhjemites as possible parental material for the generation of potash-rich batholiths

In the plot of R_0 v age (Figure 94) points 8, 11 and 14, representing components from the Nelspruit batholith to the north of the Barberton greenstone belt and from the Mpuluzi batholith to the south (see Figure 97), all lie on a colinear trend, the development of whose initial $^{87}Sr/^{86}Sr$ ratio is controlled by a low Rb/Sr ratio (i.e. approximately equal to 0,08). These three points all have low initial $^{87}Sr/^{86}Sr$ ratios in the range = 0,7010 - 0,7020 which suggests that they have been derived from material that itself had a low Rb/Sr ratio (i.e. a significantly higher Rb/Sr ratio would have resulted in a more rapid increase in the $^{87}Sr/^{86}Sr$ ratio per unit time). This evidence, together with the higher Rb and lower Sr mentioned above, all needs to be compatible with any considerations that regard the tonalite-trondhjemite gneisses in the region as the precursors to the potash-rich batholiths.

The older tonalitic-trondhjemitic gneisses in the Barberton Mountain Land, whose ages have probably not been reset by diapirism or structural re-emplacement, are characterized by low R_0 values (usually < 0,7010). Peterman (1979) has shown that tonalitic material of this nature can satisfactorily qualify as a source for granodioritic or adamellitic rocks that are, likewise, characterized by low (mantle-like) initial ratios. Peterman demonstrated, for example, that a 3,0 b.y. tonalite with R_0 = 0,7007 and a mean Rb/Sr = 0,075 could generate an anatectic by-product with

R_O = 0,7016 in the space of 300 m.y. These figures are entirely compatible with the data presented in Figure 94 where, in the case of material similar to the Theespruit pluton (R_O = 0,7000 and Rb/Sr = 0,1), partial melting could generate material such as the Nelspruit porphyritic granite (R_O = 0,7014) with a Rb-Sr whole rock age of some 300 m.y. younger (see Table 41). Hence, isotopic considerations in the Barberton area are not incompatible with the idea that the later sheet-like granodioritic/adamellitic batholiths could have been derived by anatexis of an earlier formed crust dominated by rocks of tonalitic-trondhjemitic composition.

The Rb and Sr relationships demonstrated in Figures 95 and 96 are also compatible with this notion. With regards Rb, the latter is an incompatible element (see Appendix 2) and will clearly be partitioned into melt phases rather than the residue. Strontium, however, is strongly partitioned into both plagioclase and alkali felspars and would not appear to be necessarily depleted in anatectic by-products. The following model considerations show that, under certain conditions this element could, however, be preferentially retained in residual phases :-

Possible modal melt proportions :	Quartz	- 30%	K_D for Sr - 2,1
	Plagioclase	- 35%	
	K-felspar	- 30%	
	Mafics	- 5%	
Possible residue after partially melting a tonalite :	Plagioclase	- 90%	K_D for Sr - 2,8
	Mafics	- 10%	

Using the batch melt equations of Shaw (1970) and considering a 50% melt of a tonalite with 600 ppm Sr :-

$$\text{Conc. (Sr) in melt} = 600/(2,8 + 0,5\ (1-2,1))$$
$$= \underline{267 \text{ ppm}}$$

It is apparent from the above calculation, that partial melting of a tonalite may be responsible for *depleting* the Sr content in resultant melts by a factor of two or more, if a residue comprising predominantly plagioclase remains. It is of interest to note that very similar considerations were given to the formation of the granodioritic phases in the Archaean Johannesburg-Pretoria granite dome, by McCarthy (1978). This granodiorite, which is

stratigraphically akin to certain portions of the Mpuluzi batholith south of the Barberton greenstone belt, is characterized by lower Sr and higher Rb contents than those in adjacent tonalite-trondhjemite gneisses. These trace element contents were accounted for by considering the granodiorite to have formed by 30% melting of a trondhjemite leaving a residue consisting dominantly of plagioclase together with minor hornblende and quartz (McCarthy, 1978). Likewise, Collerson and Fryer (1978), in referring generally to the genesis of younger potassic granites in typical Archaean terranes, stated that, " ..... these melts would display lower Sr contents and higher abundances of Rb, Th, U and Pb and higher Rb/Sr ratios than their tonalitic protoliths".

It is quite feasible, therefore, that the tonalite-trondhjemite gneisses in the Barberton region (and probably in other Archaean terranes too) have, in addition to forming the first vestiges of sialic crust in these areas, also provided the parental material for subsequently generated granitic magmas. Although quantified here, and also in the study of McCarthy (1978), this conclusion has long been evident as geological relationships, at least in the Barberton region, virtually preclude the possibility of deriving the potash-rich batholiths of the second magmatic cycle from anything *but* the tonalites and trondhjemites of the first cycle.

6. DISCUSSION AND CONCLUSIONS

In the preceding sections, consideration has been given to the major and trace element characteristics of tonalite and trondhjemite gneisses in the region southwest of the Barberton greenstone belt, with particular reference to the petrogenesis of these rocks. In so doing, comparisons of these characteristics with tonalite-trondhjemite gneisses of the Ancient Gneiss Complex in Swaziland, as well as with other later granitic (*sensu lato*) cycles in both regions, were undertaken. This comparative treatment of the available data has resulted in a better understanding of certain divergent petrogenetic factors that prevail in rocks of this kindred, as well as emphasizing features associated with the evolution of the Archaean granitic terrane in the broader region.

Unanimity exists in the literature regarding the origin of most Archaean tonalite-trondhjemite gneisses. Major element, trace element and isotopic characteristics of these rocks indicate that they are derived by

approximately 20-30% partial melting of material with a basaltic composition. The composition of melts derived by anatexis of basalts almost invariably coincides with that of tonalitic or trondhjemitic rocks (Helz. 1976); the range in compositions exhibited *within* a particular tonalitic-trondhjemitic body is probably the result of processes akin to fractional crystallization, as demonstrated in Chapter 4 and also in McCarthy (1978). However, the systematic differences in major element composition that exists *between* the various tonalite-trondhjemite plutons or cells in the area are considered to be the result of small differences in the degree of partial melting of similar source material. As it is not feasible that all of these units can have been derived by identical degrees of partial melting, it has been suggested that more felsic compositions (i.e. trondhjemites that are relatively depleted in Fe and Mg) represent smaller degrees of anatexis than tonalites (such as the Kaap Valley pluton) which have lower SiO_2 and higher ferromagnesian contents. These considerations do not account for observed variations in elements such as Na and Al and it is necessary to refer to the complex melting behaviour of hornblende to explain these discrepancies.

The oft-quoted reference to hornblende in terms of a partial melt origin of tonalites-trondhjemites is in accordance with the present study where it is suggested that the parental basalts were, for the most part, amphibolitic in nature. This consideration is based on geological observations which reveal that most of the (possibly cognate ?) xenoliths associated with tonalites and trondhjemites are dominantly hornblende-bearing. Model trace element considerations (i.e. Rb, Sr and Ba) also indicate that most, but not all, of the tonalite-trondhjemite magmas in the Barberton region can be accounted for by equilibration with a dominantly hornblende-bearing residue. The heavy rare-earth element depleted characteristics of these bodies can, likewise, be derived by the presence of hornblende (with high partition coefficients for the HREE) in residual phases. These features place constraints on the depths necessary to initiate the melting of tonalitic-trondhjemitic liquids from basaltic precursors, as the latter process is likely to be governed by pressures and temperatures compatible with the stability of hornblende. It is certainly not necessary to resort to mantle-like depths and eclogitic assemblages to derive Archaean tonalites and trondhjemites.

However, certain trondhjemite plutons in the Barberton region (in particular the Doornhoek pluton) as well as components of the Ancient Gneiss

Complex in Swaziland, have trace element characteristics that are not compatible with a derivation by partial melting of an amphibolitic meta-basalt. Rather than attempt to genetically differentiate these rocks from the more typical examples, as has been done in the past (Hunter et al., 1978), consideration has been given to the possibility that the latter have been derived from a lower level in the crust. Under conditions of higher pressure and temperature, basaltic komatiite compositions will be represented by an ecolgitic assemblage that is dominated by clinopyroxene rather than garnet, because of the low alumina contents in the suggested protoliths. A clinopyroxenitic, rather than amphibolitic, residue during the generation of tonalitic-trondhjemitic magmas will have the effect of not retaining the HREE as efficiently in the residue, resulting in lower Ce_N/Yb_N ratios and higher overall HREE contents. Trace element contents (in particular the Rb/Sr ratio) will be affected in a similar, but converse manner, with Sr being more effectively retained in a clinopyroxenitic residue and the resultant melts being characterized by a higher Rb/Sr ratio. Although the relevant partition coefficients for Sr are not as well documented as those for the REE, all the trace element data available are relatively consistent with the above ideas.

Despite the suggestion that the presence of residual clinopyroxene in the generation of tonalitic-trondhjemitic magmas satisfactorily accounts for differences in observed trace element patterns, it is not possible to derive highly siliceous partial melts from an assemblage comprising solely of this mineral. It is envisaged, therefore, that the transition from amphibolite to granulite facies metamorphism takes places over a prolonged range of P-T conditions and that hornblende and clinopyroxene are likely to coexist in relative proportions that are dependent on the prevailing upper limit of the stability field of hornblende. A constraint in the generation of tonalites-trondhjemites will, therefore, be imposed by the gradual dominance of anhydrous clinopyroxene over hornblende, such that anatexis will either be impaired (because of the higher liquidus temperatures of clinopyroxene) or, resultant melts will not have the required composition.

The implication of the discussion up until this stage in the preceding sections, is that although the data from the Barberton region is broadly compatible with previous ideas regarding the genesis of Archaean tonalites and trondhjemites, the existence of a large body of analytical data representing numerous discrete bodies, has shed a certain amount of new light on early magmatic processes in the

Archaean. The trondhjemitic kindred appear to exhibit systematic variations in composition that point to subtle variations in the degree of melting. Melt compositions, and in particular, trace and rare-earth element concentrations, reflect a complex equilibration with a hornblende-bearing residue. Other tonalites-trondhjemites with similar bulk compositions, but higher Rb/Sr ratios and flatter REE patterns, appear to have been derived from deeper in the crust where residues from melting had probably undergone isochemical phase changes. This feature would not affect the bulk melt composition but may significantly influence the partitioning of trace elements between liquid and residue. The melt origin of tonalites and trondhjemites must, therefore, be viewed as a complex process that is affected, not so much by compositional variations in the parental material, but by differences in the pressure, temperature and P_{H_2O} of specific source regions.

Rb/Sr isotope characteristics of the tonalite-trondhjemite bodies in the Barberton region are characterized by low initial $^{87}Sr/^{86}Sr$ ratios and ages that vary between 3,45 b.y. and 2,75 b.y. The younger ages are not interpreted as being primary and indicate that certain of these bodies have been remobilized (probably by gravitational instabilities) into their present positions. A weak correlation exists between the age and Sr content of certain tonalite-trondhjemite bodies. This does not appear to have a genetic significance but may be related to the fact that the younger bodies (with apparently higher Sr contents) have been remobilized, and, hence, have had a more involved crustal history.

Typical tonalite-trondhjemite gneisses are observed to have lower Rb but higher Sr contents than later, more potash-rich granite cycles in the region. This applies, in particular, to the large shield-forming batholiths in the Barberton region and Swaziland that have initial $^{87}Sr/^{86}Sr$ ratios that are only marginally higher than the pristine tonalites and trondhjemites. This indicates that the earlier formed gneisses probably represent the precursors for the generation of the later granodioritic-adamellitic phases in the area. It is envisaged that melting of the earlier gneisses was probably volatile-induced and may have been the result of a widespread "degassing" event from the lower crust, as outlined by Collerson and Fryer (1978). Although these batholithic bodies span enormous areas (a factor consistent with the above suggestion) they are considered to be sheet-

like and not extend to great depths. As a result, possible limitations that might arise out of the volume constraints of a tonalitic precursor do not hinder this suggestion, which is also compatible with observed geological relationships.

Tonalitic and trondhjemitic gneisses form a fundamental and significant component of the Barberton region and Swaziland, and, indeed, most other Archaean terranes the world over. They are almost invariably regarded as the oldest granitic phase in these terranes and, depending on both regional setting and the nature of prevailing ideas, are recognized as either pre-dating or post-dating the greenstone lithologies that usually accompany them. Irrespective of this, their characteristics are best explained by derivation from a mafic precursor and this tends to support the proponents of an early ensimatic crust in the Archaean. Subsequent to their formation and emplacement, tonalite-trondhjemite gneisses continued to play a role in the evolution of the earth's early crust. The fact that they probably constituted the parental material to later granitic events means that this suite of rocks has doubly contributed to the generation and stabilization of the sialic foundation upon which the present-day continents are based.

CHAPTER 7

DISCUSSION AND CONCLUSIONS

DISCUSSION AND CONCLUSIONS

The following chapter presents a summary of the conclusions as well as a discussion of pertinent points relating to the geological and geochemical evolution of tonalite-trondhjemite gneisses and migmatites in the Barberton Mountain Land. The data considered in the previous chapters represent the culmination of approximately three years of research carried out under the auspices of the Geodynamics Project in the Barberton region. The present study concentrated on a variety of aspects related to the tonalite and trondhjemite suite of rocks which collectively constitute the first, and oldest, magmatic cycle contributing to the evolutionary development of the Archaean granitic crust in this area. The discussion that follows considers, initially, the framework of magmatic cycles that has been erected for consideration in this region (Anhaeusser and Robb, 1980b) and refers particularly to the relevance of the first cycle in terms of the evolution of the granitic crust in the study area.

1. THE CONCEPT OF MAGMATIC CYCLES IN THE ARCHAEAN GRANITIC CRUST OF THE BARBERTON MOUNTAIN LAND

A schematic breakdown of the granitic rocks underlying the eastern Transvaal and Swaziland into three distinct subdivisions referred to as "magmatic cycles", is presented in Figure 97 (after Anhaeusser and Robb, 1980b). With respect to the terrane constituting the Geodynamics Project study strip (Figure 1) it is apparent that all three of the suggested magmatic cycles are represented in this area. The map in Figure 97 also shows the proposed reclassification of the granitic rocks of Swaziland in terms of the magmatic cycle scheme. This approach will undoubtedly be contentious in view of differences in interpretation of the Ancient Gneiss Complex (AGC), on the one hand and the migmatite and bimodal gneiss terrane immediately southwest of the Barberton greenstone belt, on the other (see Chapter 1). A discussion of possible differences in the two areas is presented in the section below, which considers the principal geological characteristics of the first magmatic cycle.

Figure 97 : *Simplified geological map of the eastern Transvaal and Swaziland showing the subdivision of granitic rocks in the region into three magmatic cycles (i.e. subdivisions 1, 2 and 3 in the map legend). The map is taken from Anhaeusser and Robb (1980b).*

1.1. First magmatic cycle

The migmatite and gneiss terrane southwest of the Barberton greenstone belt is characterized by Rb-Sr isochron ages ranging from 3 491 ± 166 m.y. to 2 764 ± 61 m.y. with a concomitant range in initial $^{87}Sr/^{86}Sr$ ratios of 0,7001 ± 0,0023 to 0,7020 ± 0,0009 (Barton et al., 1981). In Swaziland, the migmatitic and gneissic units of the Ancient Gneiss Complex range in age from 3 555 ± 111 m.y. to 3 138 ± 112 m.y. with initial $^{87}Sr/^{86}Sr$ ratios of between 0,6999 ± 0,0006 and 0,7048 ± 0,0022 (Barton et al., 1981). In relation to both these areas, therefore, the onset of felsic magmatism can be said to have taken place approximately 3,500 m.y. ago. Furthermore, the development of this early sialic material was largely coeval with the formation of oceanic crust now represented by the extrusive rocks of the Onverwacht Group, the latter having been dated at 3 510 ± 60 m.y. (Hamilton et al., 1979). The various components of the first magmatic cycle can be divided into two broad categories, each of which is described below.

1.1.1. Migmatites and bimodal gneisses

Migmatites and/or bimodal gneisses are best developed immediately southwest of the Barberton greenstone belt (Figure 2) and in the Ancient Gneiss Complex around Mankaiana in Swaziland (Hunter, 1970; Jackson, 1979). In both areas, the terrane is underlain dominantly by tonalite or trondhjemite gneisses intimately associated with subordinate amphibolites together with variable, but commonly significant, proportions of anatectic material. The migmatites are invariably associated with greenstone remnants correlated either with the Barberton greenstone belt (e.g. in the region southeast of Badplaas - Anhaeusser and Robb, 1980a, Anhaeusser, 1980) or with greenstone remnants forming part of the Dwalile metamorphic suite in the Mankaiana region (Jackson, 1979). The migmatites in both regions (Figure 97, see distribution of 1a) have been subjected to repeated deformation so that, commonly, the relationships between greenstone remnants and gneisses are obscure. Also characteristic of both areas are syn-tectonic mafic dykes which, in the Barberton area, probably represent an intrusive episode that was coeval with volcanism in the Geluk Subgroup (Robb, 1980) and, in the Ancient Gneiss Complex, are inferred to represent post-Dwalile intrusions (Jackson, 1979).

The interpretation of migmatites southwest of the Barberton greenstone belt is markedly different from that for migmatites or bimodal gneisses of the AGC, in spite of the apparent similarities referred to above. In the present study migmatization processes have been described as arteritic, forming in response to intruding tonalitic-trondhjemitic magmas, anatexis, palingenesis and assimilation (see Chapter 3). No unequivocal relationships point to primitive komatiitic basalts (i.e. largely correlatable with the older greenstone successions) post-dating the earliest recognized sial in the region. The dyke components in the migmatite exposures have a tholeiitic composition and cannot be shown to have fed the greenstone successions, suggesting that the sialic crust that they intrude did not form a basement to the latter.

In contrast to the above findings, the bimodal gneisses and migmatites in the Mankaiana area are considered by Hunter (1974, 1979) to pre-date the Barberton greenstone belt despite the fact that no direct evidence for this relationship exists and that the oldest age for these rocks (i.e. 3 555 ± 111 m.y., Barton et al., 1981) suggests that they were, at best coeval with the earliest developed ensimatic crust. The locally developed Dwalile metamorphic suite is considered to have been deposited above basement consisting of bimodal gneisses and migmatites even though repeated high strains have largely obscured relationships between the gneisses/migmatites and the supracrustals (Jackson, 1979). Jackson also suggested that the mafic dykes in the Mankaiana area might have fed an overlying greenstone supracrustal assemblage but no direct evidence for this is available.

Thus, although similarities between the rocks in the Mankaiana area and those of the present study exist (features which include lithological likenesses between the Onverwacht Group and the Dwalile metamorphic suite and the occurrence of banded and bimodal gneisses in both areas), attempts to correlate the areas in the past have proved contentious. However, as expressed in Robb and Anhaeusser (1979) and Anhaeusser and Robb (1980b), the present study tends to regard the two regions as largely similar although the petrogenetic considerations in Chapter 6 indicate that the dominant tonalite-trondhjemite gneisses that characterize both areas may have been derived from different levels in the crust. Further points of difference between the AGC and

the present study area are discussed below in relation to the other major component of the first magmatic cycle.

1 1.2. *Hornblende tonalites and leucocratic biotite trondhjemites*

Hornblende tonalite and biotite trondhjemite gneisses together constitute the dominant granitic (*sensu lato*) component in the first magmatic cycle (see distribution of 1b and 1c in Figure 97). These gneisses form homogeneous plutons or cells that are generally characterized by moderate to well-developed foliations which parallel the greenstone-gneiss contact. Archaean tonalite-trondhjemite gneisses are generally considered to have been derived by the partial melting of mafic precursors, the most likely candidates for which are the amphibolitic metabasalts that typically form the lower greenstone successions in the area (see Chapter 6). The tonalites and trondhjemites considered in this section are similar in composition to the leucocratic gneisses that are intimately associated with the migmatites described above.

The tonalite and trondhjemite bodies in the present study area have previously been described as elliptical or rounded, their shapes being outlined by the edges of the Barberton greenstone belt or by greenstone remnants. The absence of well-defined, elliptical tonalite/trondhjemite gneiss plutons, particularly in the Mankaiana area in Swaziland, has been used by Hunter (1973, 1979) and Hunter et al. (1978) as one reason suggesting that the Ancient Gneiss Complex should not be correlated with the tonalitic gneisses in the Barberton region. Recent work east of Badplaas (Figure 97) indicates, however, that the distribution of numerous greenstone enclaves in this granitic terrane largely invalidates the over-simplified impression that only rounded and well-defined plutons exist in the area (Anhaeusser and Robb, 1980b and Chapter 6). The few elliptical plutons that do occur are confined to the immediate edge of the Barberton greenstone belt, whereas some distance away, the shapes of tonalite/trondhjemite bodies are irregular and are not conspicously outlined by the scattered greenstone xenoliths. Nevertheless it is still possible to recognize discrete tonalite/trondhjemite bodies or "cells" on the basis of their trace element contents (particularly Sr). In the

Badplaas region, these "cells" have irregular shapes and may incorporate a number of small greenstone enclaves (Figure 82).

In the type area of the Ancient Gneiss Complex the distribution of numerous small, scattered remnants of the Dwalile supracrustals resembles that of the greenstone enclaves in the Badplaas region. No large, homogeneous tonalite/trondhjemite plutons occur in the Mankaiana region but remapping undertaken by the Swaziland Geological Survey (A.C. Wilson, personal communication, 1979) and Jackson (1979) indicates that a number of small elliptical bodies of hornblende-biotite tonalitic gneiss are present. These complement the large body of hornblende tonalite recorded by Hunter (1968) and subsequently included on other maps of the territory (Hunter, 1970, 1973, 1979).

These considerations, together with those in Robb and Anhaeusser (1979) suggest that the tonalite-trondhjemite plutons or cells constitute as much a component of the AGC in Swaziland as they do the equivalent gneiss/migmatite terrane southwest of the Barberton greenstone belt. These points, as well as those in the previous section, form the basis for the selection of units in the first magmatic cycle (Figure 97) and summarize the unifying features characteristic of this suite. A final point concerns the duration of the first magmatic cycle which, as mentioned previously, was apparently initiated some 3,5 b.y. ago. The data of Barton et al. (1981) show that certain tonalite-trondhjemite units may be as young as 2,9 - 2,7 b.y. old. The latter ages may not, however, reflect the original age of magma emplacement but rather a reset age indicating structural reactivation; as such, the duration of the first magmatic cycle is considered to be constrained by the inception of magmatism related to the second cycle.

1.2. Second magmatic cycle

The main components of the second magmatic cycle are made up of large, multi-component, potash-rich batholiths most of which exceed 1500 km^2 in extent (Figure 97, see distribution of 2a and 2b). Unlike the first magmatic cycle which is characterized by Na-rich tonalites and trondhjemites, the second cycle invariably involves more potash-rich rocks that are distinctive in terms of their mineralogy, texture, field appearance, age and style of emplacement. Unlike the plutons and cells

of the first cycle, which were probably diapirically emplaced by gravity inversion, the batholiths appear to have been intruded directly into their present positions by "passive" processes (Pitcher, 1979) involving stoping, cauldron subsidence and assimilation.

Two of the largest and better studied batholiths occur immediately to the north and to the south of the Barberton greenstone belt (Figure 97). The northernmost body consists dominantly of a coarse-grained, relatively homogeneous porphyritic adamellite or granite, known locally as the Nelspruit porphyritic granite (Robb, 1978) In addition an isotopically coeval phase known as the Hebron granodiorite occurs within the Nelspruit batholith,both as veins intruding the Nelspruit porphyritic granite and as a small, centrally situated, medium-grained, homogeneous pluton. The southernmost body, known as the Mpuluzi batholith, consists principally of coarse-grained, homogeneous porphyritic granite. The latter phase, has, however, also been invaded by dyke-like bodies of homogeneous, medium-grained, pink-to-grey adamellite which has been referred to previously as the Homogeneous Hood or Lochiel granite (Hunter, 1973, 1974; Viljoen and Viljoen, 1969 f,g).

Both batholiths described above are characterized by, often extensive, marginal, potash-rich migmatite and gneiss zones (see distribution of 2b in Figure 97). These areas represent zones of interaction between the homogeneous, passively-emplaced magmas of the main batholithic bodies and the crust that existed during the final stages in the evolution of the first magmatic cycle. The migmatitic zones themselves do not display sharp contacts with respect to the remainder of the body and the transition is usually evident in a decrease in porphyritic texture and the development of schlieren and assimilated relics of pre-exising rocks. The passive invasion of magma related to the K-rich batholiths has apparently allowed the preservation of pre-existing structures so that the batholith aureoles appear to have locally inherited the imprint of these earlier fabrics.

Various components of the Nelspruit batholith have been dated at between 3 211 ± 133 m.y. and 2 927 ± 137 m.y. with initial $^{87}Sr/^{86}Sr$ ratios ranging between 0,7007 ± 0,0011 and 0,7052 ± 0,0020 (de Gasparis, 1967; Barton et al. 1981). The data available for the Muluzi batholith indicate a range in Rb-Sr whole rock ages from 3 028 ± 14 m.y. to 2 936 ± 69 m.y. with initial $^{87}Sr/^{86}Sr$ ratios varying

between 0,7013 ± 0.0002 and 0,7054 - 0,0036 (Davies, 1970; Barton et al. 1981). The onset of magmatism in the second cycle, therefore, occurred approximately 3,2 b.y. ago and continued for some 300 m.y. Geological, geochemical and isotopic relationships (see Chapter 6) suggests that the batholiths were derived by partial melting of tonalitic or trondhjemitic material related to the first magmatic cycle. Field evidence indicates that the batholiths form relatively thin sheets over much of the earlier-formed crust in the region and are likely, therefore, to immediately overlie residues of material from which they were originally derived. The considerable areal extent over which the components of the second magmatic cycle have been emplaced, suggests that they represent the main event contributing to cratonization, during and subsequent to which a measure of tectonic stability gradually prevailed in the early continental masses.

1.3. Third magmatic cycle

The Archaean granitic terrane occupying the area shown in Figure 97 contains eleven, discrete, granitic (*sensu lato*) plutons which collectively comprise the third magmatic cycle. These plutons are distinguished by their topographic expression, lithology, transgressive mode of emplacement and limited metamorphic effects (Hunter, 1973; Robb. 1978; Viljoen and Viljoen, 1969 f,g). They are commonly homogeneous, coarse-grained and porphyritic with bulk adamellitic or granitic (*sensu stricto*) compositions, although two of the bodies have dominantly syenitic and tonalitic compositions.

The plutons of this cylce can be divided into two categories on the basis of their ages and broad geochemical characteristics. The older plutons fall in the time span 2 927 ± 59 m.y. to 2 784 ± 53 m.y. (Davies, 1970; Barton et al. 1981) and have low K/Na and Rb/Sr ratios, higher K/Rb ratios and a granodioritic bulk compostition, by comparison with their younger equivalents (Condie and Hunter, 1976; Glikson, 1976a) The exception in this category is the tonalitic pluton that occurs east of Bushbuckridge (Figure 97, pluton 3c) which has different chemical attributes, but falls into the above time span (Robb, 1977). The younger plutons range in age from 2 608 ± 123 m.y. to 2 496 ± 176 m.y. (de Gasparis, 1967; Davies, 1970) and typically have adamellitic or granitic compositions with higher K/Na and Rb/Sr ratios and lower K/Rb ratios (Condie and Hunter, 1976).

Little detailed work has been carried out on the various granitic plutons of third magmatic cycle and at this stage nothing more can be said except that they have been derived from the reworking of pre-existing sialic crust of probably variable composition. This cycle, however, represents the terminal event in the evolutionary development of the Archaean granitic crust in this region and it is likely that its various components were emplaced into a largely stabilized crust that was at least as thick then, as it is now.

1.4. The present study in terms of the magmatic cycle concept

In the introduction to this thesis it was stated that the main goal of the Barberton Geodynamics Project was an understanding of the processes responsible for the transformation of large areas underlain by mafic, ensimatic crust into a stable continental sialic environment. The magmatic cycle scheme outlined above represents an attempt to conceptually model the evolutionary processes whereby the sialic crust in the eastern Transvaal and Swaziland has developed in the time period 3,5 - 2,5 b.y. ago. The scheme, however, is restricted in its outlook in that it does not speculate directly on the nature of the global primordial crust, nor does it necessarily attempt to account for the evolution of the sialic crust in Archaean terranes from other regions. The reasons for this stem from the fact that, firstly, geological events that are related to the proto-Archaean era (i.e. > 3,9 b.y.) are no longer preserved on the surface of the Earth and, secondly, Archaean granitic terranes from different regions may quite simply not comply with the above scheme. These shortcomings in the magmatic cycle concept logically suggest that the anticipated goals for the Barberton Geodynamics Project fall short of expectation, at least with regard to the ultimate origins of this cyclical scheme. The inevitable question of the geological relationships between the earliest exposed sial and sima finds itself no closer to a solution, at least in terms of the limited coverage outlined by the magmatic cycle scheme. Thus, one of the major goals of the present study was an attempt to elucidate the primary relationships possibly still preserved between components of the first magmatic cycle and the greenstone belt, or its equivalents exposed as innumerable remnants within the former. The study of migmatitic rocks intimately associated both with the earliest developed sial (i.e. the first magmatic cycle) and original remnants of

sima (i.e. the basal portions of the greenstone successions) was undertaken, therefore, with this view in mind. Thus, with the scheme of magmatic cycles acting as a conceptual framework, the conclusions presented in the remainder of this chapter are offered as a contribution towards a better understanding of the geological processes whereby the initial development of continental crust was accomplished by the progressive transformation of ensimatic material into sialic basement.

2. THE SIGNIFICANCE OF MIGMATITES IN THE BARBERTON MOUNTAIN LAND

2.1. Conceptual significance

During the regional mapping programme that accompanied much of the work undertaken for the Geodynamics Project in the area southwest of the Barberton greenstone belt (Anhaeusser, 1980; Anhaeusser and Robb. 1980a) it became apparent that the distribution of migmatites was not random but restricted to a close spatial relationship with the numerous, scattered greenstone remnants in the region. As pointed out in Robb (1980 this relationship can be interpreted in two possible ways :

(i) in terms of ideas expressed concerning the bimodal gneisses and migmatites of the AGC in Swaziland (Hunter, 1973, 1974) where the latter are regarded as a basement to a succession of *supracrustal* greenstone belts, the migmatites in the study area, which are now juxtaposed and intimately related with vertically dipping greenstone remnants, could represent a pre-greenstone basement complex; or

(ii) if the view is adopted that the lowermost greenstone successions in the Barberton region are ensimatic and pre-date intrusion by the protoliths of younger tonalite and trondhjemite gneisses (Anhaeusser 1973, 1975), the same migmatites could be interpreted as forming in response to the interaction between older mafic crust and younger tonalitic-trondhjemitic magma.

The assessment of migmatites in the present study, which revolved essentially around very detailed mapping of single outcrops, showed that these rocks cannot simply be expressed in terms of one or other of these two

possibilities. In some of the exposures examined it was clear that certain migmatite components were correlatable with a lithological unit represented in a larger greenstone remnant, or in the greenstone belt itself, and formed distinct xenoliths enveloped by tonalitic and trondhjemitic gneisses. Thus, certain outcrops undoubtedly qualify for the second of the two interpretations. On the other hand, other exposures were characterized by mafic material that was clearly intrusive into pre-existing banded trondhjemite gneisses, with the entire outcrop having been subjected to, at least part of, the range of migmatization processes that are described in the following section. In this light it is feasible that these mafic dykes represent an intrusive magmatic event that was coeval with the extrusion of certain younger volcanic successions in the Onverwacht Group. This logically implies the presence of sialic crust during the actual deposition of the greenstone accumulation, suggesting that certain migmatite outcrops might be more profitably interpreted in terms of the first abovementioned possibility.

A number of other complicating features were also documented from the migmatite exposures investigated in the present study. In most of the outcrops examined, anatexis had played a significant role in contributing to the process of migmatization, so that, in some instances, the primary relationships between early sial and sima were either masked, or complicated by palingenetic effects. In addition, a ubiquitous feature of all the migmatite exposures examined was the variable effects of tectonism, the latter being a unifying characteristic of all components of the first magmatic cycle. In spite of the fact that most migmatitic outcrops were selected for examination on the basis of a minimal structural overprint, this feature always contributed towards providing an element of uncertainty in interpretation. Thus, in areas of high strain the distinction between mafic xenoliths and dykes became extremely difficult, as primary discordancies tend towards parallelism. Similarly, the effects of boudinage and the behaviour of closely related components of differing competency also tend to eliminate primary relationships in this type of terrane.

The structural relationships at one of the migmatite outcrops studied, namely the Theeboom outcrop, provided the most tantalizing insight into the possible relationships between early sial and sima in the study area. At this outcrop two distinct phases of trondhjemite gneiss occur, with the older, compositionally banded, phase being clearly intruded by

a younger, more homogeneous variety. In places, the older phase is in direct contact with an amphibolitic body of komatiitic composition, such that discordancies between the gneissocity or compositional banding in the trondhjemite and the amphibolite, are directly exposed (Figure 6 and Plate 2, Chapter 2). Although certain of these relationships may be due to boudinaging (Figure 9) it is argued that the older, banded trondhjemite gness may represent a remnant of pre-greenstone sialic basement. An unequivocal decision on this interpretation awaits the results of U-Pb isotopic studies currently in progress.

The above discussion provides an insight into the conceptual significance of migmatitic rocks in the Barberton Mountain Land. This complex suite of rocks provides a useful tool whereby the relationship between early sial and sima may be gauged, as components representative of both can be observed interacting directly one with another. Furthermore, in addition to the broad interpretations considered above, an understanding of the magmatic and related processes involved in the formation of these rocks, provides a better understanding of the evolution of all components of the first magmatic cycle.

2.2. Migmatization processes

Recognition of the various processes that result in the formation of migmatitic rocks in the Barberton Mountain Land will naturally place constraints on the physio-chemical conditions prevailing in the crust at the time of their formation. Four, largely related, processes are considered to contribute to the mechanisms by which the migmatites in the study area were formed, and these are viewed as being dominantly arteritic in nature. The following sections summarize the main points related to the principal migmatite-forming processes:-

(i) Tonalite and trondhjemite gneisses form an integral part of all migmatitic rocks related to the first magmatic cycle. In many instances the gneiss protoliths intruded pre-existing greenstone remnants with the resultant formation of a distinctly arteritic migmatite. The detailed mapping undertaken led to the recognition of discrete tonalite-trondhjemite gneiss phases suggesting a prolonged history for the origin and emplacement of these rocks. The latter statement is quantified

by geochronological studies which suggest that magmatic and structural activity in the first magmatic cycle continued for approximately 600 m.y. after its inception. In addition, certain trondhjemite gneisses record metamorphic pre-histories (such as a more intense foliation, lineation and compositional banding) not evident in other equivalent rock types from the same broad region of study, indicating a complex continuum of structural and metamorphic evolution. Certain migmatite outcrops also contain quartz-dioritic veins which are considered to be genetically related to the tonalite-trondhjemite gneisses and form an additional component in the migmatization process. The emplacement of tonalitic and trondhjemitic magma into a dominantly ensimatic greenstone crust can, therefore, be viewed as one process which contributed to the formation of migmatites in the Barberton Mountain Land.

(ii) The majority of exposures examined showed evidence of partial melting which, in some instances, has developed to the extent where anatectites form the dominant material contributing to the formation of migmatites. Most of the anatectites examined appear to have been derived by partial melting of either tonalitic or trondhjemitic precursors. This observation suggests that pressures, temperatures and partial pressures of water were such that, at least in localized areas, the tonalite solidus was intersected. This is confirmed, in part, by equilibration temperatures attained for coexisting garnet and biotite in a tonalitic gneiss from the study area (i.e. in the range 700 - 770^{o}C), the latter being above the water-saturated tonalite solidus at pressures in excess of approximately 5 kb. One particular facet of anatexis involves the process of palingenesis where partial melting has been initiated by the intrusion of dykes which themselves have been re-intruded, fragmented and assimilated by the magma which they generated. The contribution of anatexis to the formation of migmatites can be viewed as an arteritic process as the magmas thus generated are intruded into a variety of different rock types probably at some distance away from their source region. A confirmation of this view is found where the effects of localized partial melting are enhanced by structural control (e.g. the Weergevonden outcrop,

see Chapters 2 and 3). At the Weergevonden outcrop the development of heterogeneous gneiss-migmatite textures is considerably more pronounced in areas where the existence of a fold hinge zone appears to have concentrated anatectic material. The recognition of anatexis in most areas of migmatite development effectively eliminates the widespread occurrence of sub-solidus processes such as metamorphic differentiation in the formation of these rocks. Thus, the presence of excess - H_2O is inferred in order to facilitate melting processes, and the source of this medium is probably ultimately derived from the de-watering of greenstone remnants.

(iii) Related to the presence of both tonalitic-trondhjemitic magmas and anatectites are the effects of assimilation or hybridization, the latter having influenced the development of certain migmatite exposures. In certain outcrops, where the presence of mafic dykes intrusive into tonalite and trondhjemite gneisses are recorded, the latter appear assimilated by the prolonged effects of structural deformation and crustal residence contamination. In areas where anatexis or palingenesis has occurred, mafic dyke material has been hybridized by the re-intrusive effects of magma that is probably in equilibrium with an attendant volatile phase. The study of a migmatite outcrop associated with potash-rich magmas of the second magmatic cycle (i.e. the Mara outcrop, see Chapter 2), showed that assimilation of mafic (greenstone) xenoliths was responsible for the formation of the dioritic bodies encountered at this exposure. The ultimate gneissification of the outcrop as a whole (portrayed in Figure 18) might also have occurred as the result of contamination of pre-existing (possibly tonalitic) crust by the passive intrusion of potash-rich magmas, fluids or vapour phases. It is pertinent to remark that assimilation and hybridization processes in general, are most likely facilitated and engendered by the presence of volatile phases. This is inferred in view of the contradistinction that many magmas (in particular the protoliths of tonalite-trondhjemite gneisses) exhibit clearly intrusive relationships but are not accompanied by the effects of assimilation (e.g. the Theeboom outcrop, Figure 7 and Plate 2).

(iv) A fourth process whereby migmatites in the Barberton Mountain Land appear to have formed may be regarded as converse to (i) above and involves the syn-tectonic intrusion of mafic magma into pre-existing tonalite-trondhjemite gneisses. It is important to stress that rocks formed in this way qualify for description as migmatites because the various components have been subjected to deformation, anatexis and contamination to the same extent as other migmatites may have (see Figures 15 and 16). Outcrops of this nature are not, therefore, similar to a situation where, for example, an undeformed Proterozoic dyke intrudes a trondhjemite gneiss. The syn-tectonic nature of the mafic dykes in this migmatite category suggests that they may represent an intrusive magmatic episode that was coeval with the extrusion of mafic volcanics in the greenstone depository. Although chemically altered, the dykes have a tholeiitic composition which indicates that they may be more closely correlated with the upper greenstone successions where komatiitic magmatism is largely subordinate. The intrusion of these mafic dykes is clearly, therefore, one facet in the development of the first magmatic cycle and is closely related to the interactive processes between early sialic plutonism and the broadly synchronous deposition of volcanic rocks in a nearby oceanic environment.

In order to conclude this section it is necessary to re-emphasize the role of structural deformation in the context of the petrologic processes discussed above. Regional dynamo-thermal tectonism is the single unifying characteristic of all components of the first magmatic cycle and must, therefore, have contributed to the various migmatization processes (see below). Not insignificant in these considerations are the conditions necessary for the partial melting of amphibolitic meta-basalts to form tonalites and, subsequently, of tonalites-trondhjemites to form the migmatite-related anatectites. The creation of such an environment would presumably have been the result of an unstable lithosphere and the dominance of tectonic factors in the development and subsequent evolution of the processes envisaged in the preceding discussion.

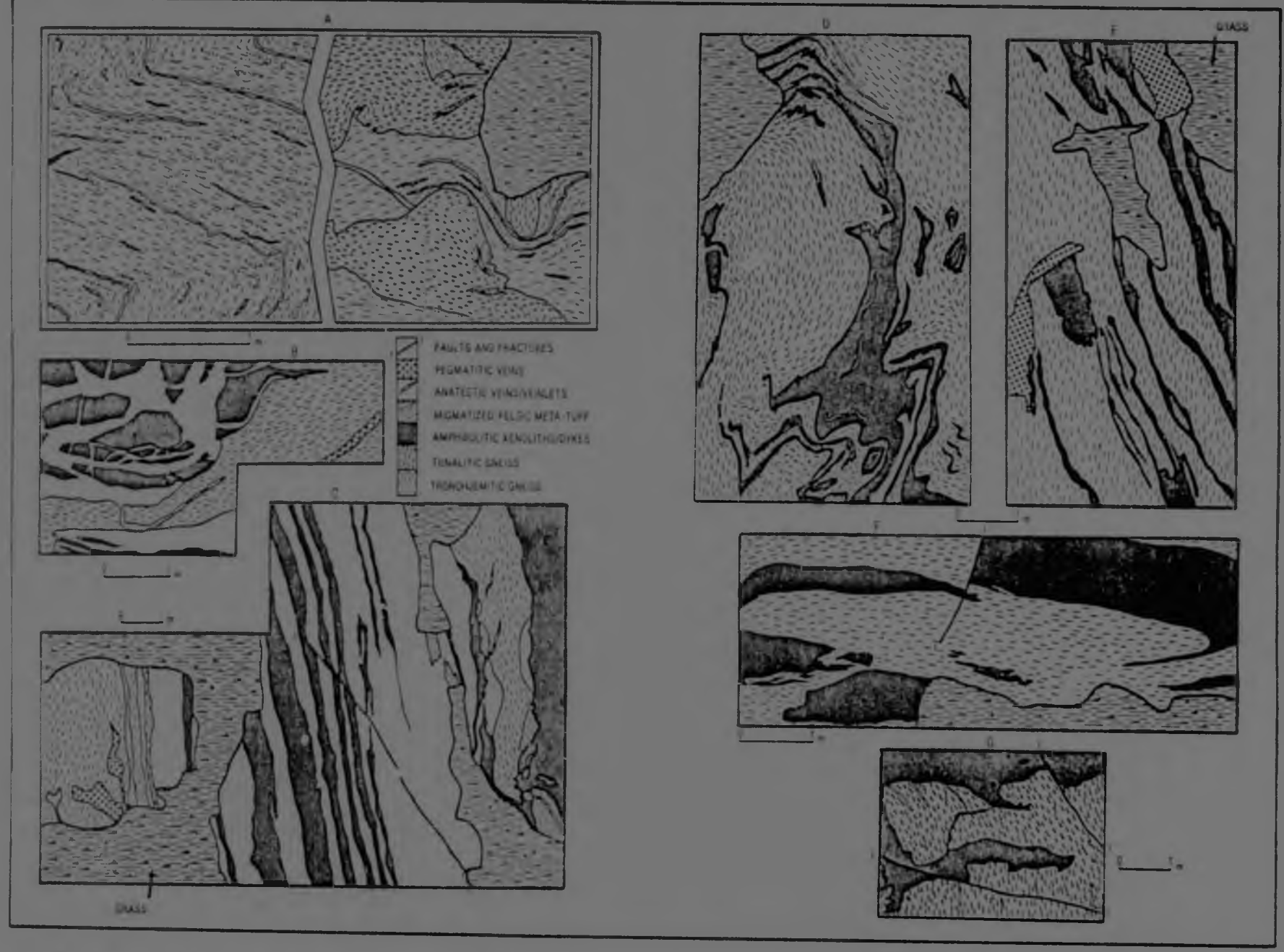

Figure 98 : *Summary of the various migmatitic textures encountered in the study area. Panel A is from the Weergevonden outcrop (Figure 13); B is from the Roothoogte outcrop (Figure 11); C is from the Theeboom outcrop (Figure 6); D, E and G are from the Batavia section (Figures 10, 15 and 16 respectively); and panel F is from the Mooiplaats outcrop (Figure 17).*

2.3. Summary statement

The localities of migmatitic rocks related to the first magmatic cycle are spatially restricted to zones in close proximity to the numerous greenstone remnants that can occur up to 50 km or more away from the Barberton greenstone belt. The existence of these migmatites, within which components of both early simatic and sialic crust occur juxtaposed, provides one of the best means for gaining insight into the early process responsible for the transformation of ensimatic crust into a progressively stabilizing continental sialic environment. In the present study area, this complex suite of rocks did not yield unequivocal evidence for the existence of sialic material predating the developmert of the earliest greenstone successions. However, indications suggest that very early phases of trondhjemitic gneiss were in existence during the on-going volcanism related to the deposition of the Onverwacht Group and, hence, the development of sialic crust occurred coevally with that in adjacent oceanic or ensimatic environments.

The processes whereby these migmatitic rocks formed are regarded as being principally arteritic in nature; these processes are summarized in Figure 98 where pertinent sections from the migmatite maps in Figures 3 - 18, Chapter 2, are compiled. The intrusion of tonalitic and trondhjemitic magmas into components of pre-existing greenstone lithologies is demonstrated in parts A and D of Figure 98. In the former panel, tonalitic gneisses intrude a metamorphosed felsic tuff whereas, in the latter, an amphibolitic xenolith is enveloped by trondhjemitic gneisses. Both exposures are intensely deformed and in panel A the development of migmatitic and gneissic textures is more pronounced in the fold hinge zone (i.e. left hand segment of panel A); in panel D, minor structures reflect superimposed fold increments and a parallelism between foliations in the trondhjemite and amphibolite. The process and effects of anatexis are demonstrated in parts B and C of Figure 98. In the former panel, the intrusion of anatectites has created an agmatitic texture, whereas in the latter, similar material has intruded in a lit-par-lit fashion. Deformational effects are also illustrated in panel C where a compositionally-banded trondhjemite gneiss is apparently truncated by the adjacent amphibolitic meta-basalts; it is not clear whether this reflects a primary discordancy or, is the result of boudinaging. In panel A, again, anatectic veinlets are preferentially concentrated in fold hinge zones. The intrusion of

syn-tectonic mafic dykes is demonstrated in parts E, F and G in Figure 98. In the first mentioned panel, amphibolitic dykes are clearly discordant with respect to a pronounced foliation in the adjacent trondhjemite gneisses; in panel F the interpretation of a dyke-like phase is equivocal as the linear amphibolitic bodies are conformable with trondhjemite gneissocity. The mafic dyke in panel G has been palingenetically intruded by a hybridized anatectite which, itself, has been deformed and faulted. These processes can be viewed as being principally arteritic in nature with sub-solidus processes such as metamorphic differentiation being relatively minor in extent.

Migmatites related to the second magmatic cycle occur mainly in marginal zones related to large, multi-component, potash-rich batholiths that occupy a considerable areal extent both to the north and south of the Barberton greenstone belt Textures in these rocks reflect the passive emplacement and concomitant assimilation and hybridization of pre-existing crust (related to the first magmatic cycle) by magmas and volatile phases related to the second magmatic cycle. In this light, these migmatites also record the secular transformation and evolution of the early continental crust but, in comparison to the genetically earlier migmatites, provide evidence for processes operative at a more advanced stage, where magmatism was related to the subsequent emplacement of the potash-rich batholiths.

The summary presented above and outlined diagrammatically in Figure 98, can be viewed as a model for the development and evolution of the migmatitic suite in the Barberton Mountain Land. Both in terms of primitive sial-sima relationships and from the point of view of the magmatic cycle concept, the migmatitic rocks can be regarded as indicators of transient processes within the overall magmatic and tectonic evolution of the Archaean crust. Migmatitic rocks reflect the complex dynamic and interactive processes involved in the [illegible]ormation of a thin, unstable, mafic ensimatic crust into the stable sial[illegible] masses now represented in the contintental shield areas. Their interp[illegible]tion, even within the confines of the study area, is, therefore, extremely involved and open to a subjective approach. In this light, if the above diagrammatic summary is to be considered as a model, it must be regarded as having limited applicability and should be assessed strictly in terms of the numerous, multi-faceted processes related to the formation of these rocks. As such,

although the model may have a limited uniformitarian applicability, it is quite possible that different geological conditions and/or different levels of present crustal exposure, will preclude these processes from being relevant in other Archaean terranes.

3. TONALITE-TRONDHJEMITE PLUTONS AND CELLS IN THE BARBERTON MOUNTAIN LAND

A second major objective of the present study entailed an examination of tonalite and trondhjemite gneiss bodies in the Barberton Mountain Land. As seen in Figure 97 these are mainly distributed in the region west and southwest of the Barberton greenstone belt (see distribution of 1b and 1c, Figure 97), which can be viewed as the type-area for granitic rocks of the first magmatic cycle in the eastern Transvaal. A variety of geological and geochemical aspects related to these bodies were examined in the preceding chapters, with particular emphasis being placed on the Kaap Valley tonalite pluton, the latter representing the largest individual body of Na-rich gneiss in the study strip.

3.1. The Kaap Valley tonalite pluton

The Kaap Valley tonalite is unique in the Barberton Mountain Land in that it is the only pluton that consists ubiquitously of hornblende, either with, or without biotite, as its main mafic mineral phase. It has been argued in the past that the reason for this may be related to extensive and pervasive assimilation of greenstone material during the emplacement of this body. This view is not in accordance with the present data which suggests that the magmatic protolith from which the pluton was derived was originally more ferromagnesian than the leucocratic biotite trondhjemites which comprise the remainder of the plutons and cells in the study area. Petrographic observations, rare-earth element mixing models, systematic changes in coexisting hornblende and biotite compositions and distinct differences between the composition of hornblendes from the Kaap Valley tonalite and those from a number of greenstone remnants in the region suggest that the amphibole component in this tonalite crystallized directly from the magma.

The more mafic bulk composition of the Kaap Valley tonalite indicates that it should have been derived by a significantly higher

degree of partial melting than that required to form the more leucocratic trondhjemitic equivalents of the first magmatic cycle. This notion is not, however, upheld by data representing the incompatible element concentrations in this body. Elements such as Rb and the LREE should occur in significantly lower concentrations in the Kaap Valley tonalite than the trondhjemites which represent smaller degrees of melting from similar mafic precursors. Instead, the incompatible elements have similar, if not slightly higher, concentrations than the latter. In the present study, therefore, the Kaap Valley tonalite was considered to have been derived by processes akin to zone melting, where existing magma is allowed to continually re-equilibrate with undepleted wall-rock material during its upward ascent in the crust. Such a process may account, both for the more mafic appearance of the body, as well as its slightly enriched incompatible element content, the latter being more efficiently partitioned into a zone-melted phase than into a magma derived by conventional batch melting processes.

Although remarkably homogeneous in appearance, the Kaap Valley tonalite is characterized by variations in its hornblende and biotite content. The most ferromagnesian tonalites are characterized by up to, and in excess of, 20% modal hornblende and no biotite, whilst the progressively more leucocratic tonalites become hornblende-poorer with biotite becoming a prominent phase; all the tonalite samples contain hornblende although a few may have biotite in excess of hornblende. Thus, chemical analyses over the entire body exhibit a pronounced fractionation trend that is also reflected in significant variations in trace and rare-earth element concentrations. This pattern is indicative of crystal fractionation where it is envisaged that hornblende was present on the tonalite liquidus for a significant porportion of the crystallization history of the body prior to the incoming of biotite. Furthermore, the spatial distribution of hornblende and hornblende + biotite tonalites suggests that magma differentiation may have been engendered by the preferential solidification of portions of the magma chamber before others. In this way, variations in trace element concentrations over the body may be explained, although the erratic behaviour of for example, Rb, Sr and Ba may be due to discrepancies in this process and also the presence of "intercumulus" liquid.

The spatial distribution of elements over the Kaap Valley pluton is considered to reflect both the crystal fractionation processes mentioned

bove, as well as regional structural lineaments that may have accompanied the emplacement of the body. Certain of the orthogonally arranged linea-ents outlined in the present study have been noted previously in terms of regional mapping and gravity interpretation. Complementary lineaments are identified on the basis of the contoured distribution of elements over the pluton and the supposition that upwarped lineaments will tend to expose rocks representative of what was, originally, the lowermost portions of the magma chamber. These considerations indicate that crystal fractionation in the Kaap Valley tonalite was sub-horizontally induced, with the more mafic fractions (i.e. the hornblende tonalites) crystallizing towards the bottom of the chamber and subsequently being preferentially exposed in areas of upwarped culmination. The actual development of a pattern of orthogonal structural lineaments over the pluton probably occurred in response to the diapiric emplacement of the body into its present position as the result of gravitational instabilities in the early Archaean crust.

The above discussion summarizes some of the points relating to a detailed study of one of the tonalite-trondhjemite plutons in the study area. Clearly these bodies appear to have been involved in a complex petrogenetic and structural evolution, much of which is masked by apparently homogeneous textures, subtle compositional variations, a regular tectonic fabric and reasonably well-defined outlines. However, the tonalite and trondhjemite plutons represent a turbulent period in the evolution of the Earth's crust and it is to be expected that their mode of formation will be equally complicated. This view is borne out by the following section which considers various, mainly chemical and petrogenetic, factors applicable to other tonalite and trondhjemite bodies in the study area.

3.2. Other tonalite-trondhjemite plutons and cells in the Barberton Mountain Land

In addition to the Kaap Valley tonalite pluton, a total of eleven other tonalite - trondhjemite plutons and cells have been defined in the present study on the basis of existing data and nomenclature, as well as considerable new data generated through the Geodynamics Project in the Barberton area. The plutons that have been described prior to the present

study (e.g. the Theespruit, Kaap Valley and Stolzburg plutons, etc.) owe their early recognition to a well-defined elliptical shape that is generally outlined by either the Barberton greenstone belt or remnants derived therefrom. The newly defined cells (see Figure 82) in the region southwest of the Barberton greenstone belt are not rigidly defined by greenstone remnants (most actually include numerous, small greenstone septa) but have been identified on the basis of regional compositional singularity. Thus, implicit in the definition of new tonalite-trondhjemite cells in the study area is a recognition of the fact that the bodies differ broadly from one another on the basis of both their major and trace element compositions.

Analytical data for each of the twelve tonalite-trondhjemite bodies considered in the study shows that they all exhibit a systematic internal variation in composition which, as suggested for the Kaap Valley tonalite, is probably the result of crystal fractionation. However, as mentioned, the various bodies also tend to differ one from another in having distinctive fractionation trends. Thus, certain bodies are characterized most noticeably by high ferromagnesian and low soda contents whilst others exhibit a converse trend, but with most of them tending to show a similar range in silica content. This data indicates that the individual plutons and cells may be characterized by small, yet nevertheless noticeable, differences in the degree of partial melting required for their derivation. Such differences probably reflect the complex incongruent melting behaviour of hornblende, which produces melt increments of differing compositions as it is progressively dissolved.

The most significant differences in the chemistry of the various tonalite-trondhjemite bodies are found in their Sr contents, which vary by a factor of approximately 5 (i.e. ~ 150 - 750 ppm, see Figure 85) from one body to another. By contrast Rb and, to a lesser extent, Ba contents remain relatively constant, confirming the view that differences in the degree of partial melting necessary to derive the various bodies are likely to be small. It was also noted that plutons with low Sr contents (and, consequently, high Rb/Sr ratios) had many chemical similarities to the bimodal gneisses from the AGC in Swaziland. The latter are characterized by tonalitic-trondhjemitic compositions, high Rb/Sr ratios relative to the typical gneiss plutons and cells and a characteristic REE pattern with lower Ce_N/Yb_N ratios and an enriched ΣREE content.